C.P. No. 1372

PROCUREMENT EXECUTIVE, MINISTRY OF DEFENCE

AERONAUTICAL RESEARCH COUNCIL

CURRENT PAPERS

A Wind-Tunnel Investigation of the Effects of Flap Span and Deflection Angle, Wing Planform and a Body on the High-Lift Performance of a 28° Swept Wing

by

D. A. Lovell

Aerodynamics Dept., R.A.E., Farnborough

ROYAL AIRCRAFT ESTABLISHMENT
BEDFORD.

LONDON: HER MAJESTY'S STATIONERY OFFICE

1977

£8-00 NET

UDC 533.693.1 : 533.695.12 : 533.694.2 : 533.6.013.13 :
533.6.013.644 : 533.6.013.66

*CP No.1372

March 1976

A WIND-TUNNEL INVESTIGATION OF THE EFFECTS OF FLAP SPAN AND DEFLECTION ANGLE, WING PLANFORM AND A BODY ON THE HIGH-LIFT PERFORMANCE OF A 28° SWEPT WING

by

D. A. Lovell

SUMMARY

Lift, drag and pitching moment have been measured over an extensive range of configurations of the high-lift system on a wing of basic aspect ratio 8.35 and with a trailing-edge planform extension and a body added. The results were analysed and compared with two linear-theory prediction methods. The measured increments in lift generated by the various elements of the high-lift system were lower than the predicted levels. An exploratory analysis of the drag results showed that the lift-dependent drag factor was considerably underestimated by linear theory, particularly when the slat was deployed. The limitations of the planar vortex sheet used in the theory and the neglect of viscous effects are suggested as the principal reasons for the differences between experiment and theory.

Deflection of the flap produced a load, which acted at a distance forward of the mean quarter chord of the flap, that was practically independent of incidence and flap span. The wing/body interference effect was insensitive to flap span and there was some evidence of a download being generated on the rear body when the high-lift system was deployed. The performance of the high-lift system was downgraded when the wing planform was extended in the root region and this was attributed to the greater non-uniformity of the spanwise loading.

---

* Replaces RAE Technical Report 76030 - ARC 36936.

CONTENTS

1 INTRODUCTION

The design process for swept-wing/body combinations has been the subject of continuing development for many years. With the application of advanced aerofoils and the associated three-dimensional wing design procedures it has been possible to define wings, for both commercial and military aircraft, which result in substantial economies in the cruise phase of flight. In many cases this has led to a decrease in the size of wing used for a given aircraft, mainly to reduce the drag produced by the wing, but also to improve passenger comfort in commercial aircraft and to provide a steady weapon-aiming platform in military aircraft. As a result of the concomitant rise in wing loadings it is necessary to design more powerful high-lift systems for use during the low-speed phases of flight in order to maintain a good field performance and limit the increase in noise in the vicinity of airports.

The design of a high-lift system usually starts with the development of a suitable two-dimensional multi-element section. As with the wing design for cruise, this involves a mixture of theory and experiment in order to achieve the required performance in viscous, compressible flow. The two-dimensional design of a high-lift section has tended to be based on experiment rather than theory because, although theoretical methods for predicting the inviscid flow about multi-element aerofoils have been available for some time, these methods did not include the effects of the important viscous interactions between the wakes and boundary layers of the various elements of the wing section. However the recent progress in understanding these interactions (Williams[1] and Ashill[2]) which largely determine the optimum relative positions of the elements for a given lift and drag requirement, should eventually lead to a rational two-dimensional section design method.

The incorporation of this two-dimensional aerofoil design into a swept, tapered wing attached to a body relies even more heavily on wind-tunnel experiments as a comprehensive set of theoretical tools is not available for the main design problems, which include:

(1) Finite wing effects (e.g. wing root and tip effects, part-span flaps)
(2) Wing/body interference effects
(3) Three-dimensional viscous effects.

To obtain the best design of high-lift system one might expect that, in an analogous manner to the cruise wing design, an overall design method is

required to determine the optimum spanwise variation of the effective camber and twist of the wing with the high-lift system deflected. However, because of the practical difficulties of manufacturing a twisted slat or flap and the design problems of retracting such a slat or flap into the cruise section, this approach to design is not likely to be pursued. The normal procedure is to apply the two-dimensional multi-element aerofoil design to the three-dimensional wing and optimise the relative positions of the elements by a series of wind-tunnel tests on configurations differing slightly from a datum case. Because of the large number of variables involved (including ideally such practical features as flap tracks, engine pylons and nacelles etc.) a very extensive wind-tunnel test programme involving several models may be necessary in order to achieve a viable configuration.

The aim of the work described in the present Report was twofold. Firstly, to provide data covering several of the major parameters affecting high-lift system performance, including flap span and deflection angle, a detailed set of measurements of the longitudinal force and moment components was made for a range of flap span and deflection angle on a swept-wing model having a basic sweep and aspect ratio of 28^{o} and 8.35 respectively. Similar sets of measurements were also made to quantify the effects of adding a wide-bodied fuselage, making cutouts in the trailing-edge flap, and modifying the basic wing planform to include the type of trailing-edge planform extension commonly required on transport aircraft to accommodate the retracted undercarriage. In this manner it was hoped to extract some general trends that would shorten the design process for high-lift systems. The model used in these tests and the associated test procedure are described in sections 2 and 3.

Secondly, as the data obtained are only directly relevant to a particular wing planform, aerofoil section and type of high-lift system (leading-edge slat and trailing-edge Fowler flap), a major aim of the work was to compare the experimental results with some simple theoretical prediction methods. This process of comparison, which is described in section 5, has been deliberately limited to the examination of linear theory lifting-surface methods (the Weber, Kirby and Kettle method[3] for wing/body combinations and the method of McKie[4] for part-span flaps). By this means any arbitrariness in the definition of the geometry of the flow model (e.g. the position of discrete vortices) has been avoided and the results of the linear theory calculations lend themselves more readily to physical interpretation. As the panel methods currently in use are refined and

become more reliable in their treatment of multi-aerofoil wings the present set of data could provide a useful test case and for this reason the complete set of data is tabulated at the end of the Report.

All the existing prediction methods that can be used for high-lift system design on three-dimensional wings are inviscid although it is possible that some of the two-dimensional methods being developed for handling the viscous layers on multiple-element aerofoils may soon be applied to the design of three-dimensional wings by means of some form of simple strip theory.

The prediction of the drag of high-lift wing/body combinations has not reached such an advanced state as the prediction of lift performance. At the present time the linearised theory proposed by Maskell[5] to relate the profile and vortex drag to the lift of a three-dimensional wing probably represents the best foundation for the analysis of experimental data. Although the measurements made during the experimental work reported here were not aimed towards drag analysis (particularly as regards the effects of model support interference and boundary-layer transition on drag), a simple analysis of the experimental data has been made on the basis of Maskell's theory in view of the importance of drag prediction in the design process.

High-lift systems having highly cambered trailing-edge devices over a large proportion of the span produce a large negative contribution to the overall pitching moment. As the method of trimming this moment may introduce performance penalties it is important to be able to predict the magnitude of these moments. The experimental results have been analysed to find the point of action of the extra load produced by the flap and this has been related to the planform of the flap.

As no tests were made with a tailplane it was not possible to investigate the effects of variations in the high-lift system on the longitudinal stability. One of the effects on stability that is introduced by the high-lift system is its influence on the stalling characteristics of the wing. In order to attain an acceptable variation of pitching moment through the stall it is often necessary to degrade the high-lift system in certain areas of the wing. A short series of measurements and photographs were made on a typical aircraft layout in order to determine the principal flow characterisitcs and to see if there were any gross effects of the support brackets for the high-lift system on the development of the stall. These flow investigations are discussed in section 4. It was not

thought worthwhile making a more extensive investigation as the viscous effects at the high Reynolds number associated with a full scale aircraft, and hence the spanwise load, are likely to be significantly different from those on the model (test Reynolds number 1.35×10^6).

2 DESCRIPTION OF THE MODEL

The aerofoil section chosen for the basic wing was a development of an NPL type having considerable rear loading. Fig.1 shows the thickness and camber distributions and the ordinates are tabulated in Table 1. The maximum thickness of 10.7% occurs at 37.5% chord and the maximum camber of 1.1% occurs at 75% chord.

A straight-tapered planform was chosen for the basic wing in order to eliminate any effects on the high-lift performance that might be associated with a particular cranked planform of the type commonly used on transport aircraft. The aspect ratio (8.35), quarter-chord sweep angle (28°) and taper ratio (0.35) are typical values for the current generation of transport aircraft. The wing had no twist or dihedral. The basic planform is shown in Fig.4 and the leading dimensions are given in Table 2.

The high-lift section comprised a leading-edge slat and a trailing-edge Fowler flap with a hinged tab (Figs.2 and 3). The slat, which could be deflected 15°, 20° or 25°, had a chord of 16% of the basic wing chord and when deflected it produced an extension in chord of between 10% (25° deflection) and 12% (15° deflection). The Fowler flap chord was 34% of the basic wing chord with the flap shroud terminating at 90% chord so that the flap could extend the chord by up to 24%. The tab formed the rear part of the Fowler flap and had a chord of 12.6% of the wing chord. It could be deflected either 15° or 30° relative to the Fowler flap. The geometry of the high-lift section is explained in more detail in Appendix A. The layout of the wing section is shown in Fig.2a and the ordinates of the slat and flap are given in Table 1. When in use the slat was deflected over the full span of the wing. The flap/tab combination was used over a range of spans up to full span (y_F/s = 0.6, 0.8 and 1.0 basically) with a range of filler pieces to ensure that the ends of the flaps were maintained in a streamwise direction for all the flap spans.

In order to compare this constant percentage-chord high-lift section, mounted on a straight-tapered wing, with a more practical layout including an extension of the type commonly found necessary to house the retracted undercarriage, a trailing-edge extension to the basic wing was made inboard of

y/s = 0.355 by sweeping the trailing edge forward 3.2°. The aspect ratio of the extended wing was thus reduced to 7.69 but the wing section and thickness/chord ratio were kept constant. The extended planform is shown in Fig.4 and the leading dimensions are given in Table 2.

A streamwise cut at y/s = 0.355 was made in the slat/flap/tab systems on the basic wing in order to retain the part of the system outboard of this position when the extended planform was fitted. Inboard of y/s = 0.355 the slat was of the same chord as on the basic wing but the thickness distribution of the slat was modified because of the necessity to match the thicker inboard wing section. The Fowler flap/tab was made of constant chord inboard of y/s = 0.355; the chord being equal to the value at y/s = 0.355 on the basic wing. It was necessary to modify the shroud profile inboard of y/s = 0.355, again because of the thicker inboard wing section. These modifications to the constant percentage-chord high-lift section used on the basic wing were made as they were more typical of the arrangements currently in use on transport aircraft and they were terminated at the body side. The slat, flap and tab deflection angles were kept the same as for the basic wing. Details of the modified high-lift section inboard of y/s = 0.355 are given in Fig.2b and Table 1.

The large diameter body tested with both wing planforms was that used in the work reported in Ref.6 and is based on a design for a wide-bodied transport aircraft. In mounting the two wing planforms in the body the wing reference plane was set at an angle of 1.1° to the body axis. In both cases the leading edge was set in the same position in the body, at a mid-low wing position. The body is shown in Fig.4 and the leading dimensions are given in Table 2. No fillet or underbody distortion was used in the junction between the wing and the body.

A streamwise cut was made in the slat/flap/tab systems of both wing planforms at a spanwise distance equal to the body radius (y/s = 0.142) so that the mid-low wing mounting on the body resulted in the appearance of small gaps at the body side when the elements of the high-lift section were deflected.

An additional streamwise cut was made in the flap/tab system at y/s = 0.257 to simulate, when required, the type of spanwise discontinuity in the flap systems that is necessary, for example, behind an underwing-mounted engine to prevent the exhaust impinging on the structure. The flap/tab section in the region $0.257 < y/s < 0.355$ could thus be left retracted while the remaining parts of the flap/tab system were extended.

The design of the high-lift wing and its practical operation are discussed in more detail in Appendix B.

3 EXPERIMENTAL DETAILS

3.1 Test programme

The model was tested in the No.2 11½ft × 8½ft low-speed wind tunnel at Farnborough. It was mounted upright on the lower balance using the standard strut rig. This consists of two slim struts under the wing at y/s = 0.45 and a single strut, which also provides incidence control, connected either to a sting or to a body mounted on the wing.

Tests were made over a range of wing incidence, $-15^{\circ} < \alpha_w < 30^{\circ}$, and windspeed, 46m/s < V < 91m/s, but the majority of the force measurements were made at a windspeed of 76m/s (M = 0.223), which corresponds to a Reynolds number of 1.35×10^6 based on the mean chord of the basic wing planform, using an incidence range of $-5^{\circ} < \alpha_w < 25^{\circ}$ covered in 1° intervals. For these tests it was established that the typical accuracies of measurement, with attached flow on the model, were:

Windspeed, V	±0.05m/s,
Wing incidence, α_w	$\pm 0.05^{\circ}$,
C_L	±0.001,
C_D	±0.0001,
C_m	±0.0003.

The first series of tests was made in November and December 1968 with the basic wing planform. The effects of varying Reynolds number and fixing transition were investigated by means of flow visualisation techniques and force measurements. Transition position was determined by the sublimation of acenapthalene (applied as a solution in petroleum ether) from the model, and surface flow patterns were obtained using a suspension of Dayglow in paraffin. The majority of the force and moment data (lift, drag and pitching moment) for the flap deflected 10° and the slat deflected 25° was obtained in this phase of testing.

The second series of tests was made between June and August 1969. After repeating force measurements for some of the configurations tested in the first phase, the remainder of the force measurements were made for the basic wing planform with and without slats and/or body fitted. The planform extension was

then added by changing the spar covers inboard of y/s = 0.355 and force measurements were made with and without the slats and body. A complete list of the configurations tested is given in Table 3. Finally a short investigation was made of the stalling behaviour of the wing in a typical aircraft condition with the high-lift system extended. The wing was tufted for part of this work and a set of photographs was taken at 1^{o} intervals of wing incidence through the stall using the Dayglow technique for surface flow visualisation.

3.2 Reduction of results

The mechanical balance was operated manually and the force and moment data recorded by hand. This data was subsequently punched onto paper tape and processed by the standard data reduction programme[7]. Corrections were applied for the offset of the balance virtual centre, deflection of the main mounting struts, upwash in the tunnel airflow, and wind-tunnel constraint and blockage effects. No separated wake blockage corrections were applied as extensive regions of separated flow only occurred outside the range of incidence relevant to the present investigation, i.e. at wing incidences above maximum lift and, when the slats were deflected, below the wing incidences at which the flow on the lower surface of the slat separated.

The lift, drag and pitching moment of the strut support system were measured without the model and these tare values were substracted from the forces and moments measured with the model mounted on the struts. No attempt was made to measure the effects on the forces and moments of the interference of the struts on the model or the model on the strut mounting systems. This was because it did not prove possible to include an alternative method for supporting the model in the wind tunnel as the ability to change planform and deploy a range of high-lift devices had resulted in a relatively small main spar. Subsequent measurements of these interference effects on other models[8] suggest that the effect on lift is usually small and that the strut tare lift force provides a reasonable approximation. The interference effects on drag are larger and vary with incidence but, as the present work was concerned with comparisons of drag measurements rather than absolute values, the omission of these interference effects was not considered important.

3.3 Presentation of results

The complete set of force and moment coefficient results are tabulated in Table 4. All these forces are non-dimensionalised with respect to the

planform area of the basic straight-tapered wing (except for the comparisons of planform shown in Figs.85-89 where the particular wing planform area is used) and all the pitching moments are non-dimensionalised using the standard mean chord (rather than the aerodynamic mean chord) of the basic wing and referred to the mean quarter-chord point of the basic wing planform. The angle of incidence is that of the wing reference plane.

The principal results are plotted in Figs.12-56. The coefficients are plotted as C_L versus α_w, C_D versus C_L, and C_m versus C_L and the same scales are used throughout in order to aid the comparison of different figures. The abbreviations 'BC' for a body cutout in the flap span and 'EC' for an engine cutout in the flap span, have been used throughout these figures. The graphs have been arranged to show the effects of flap deflection angle and flap span. As the complete set of coefficients is tabulated it was not felt necessary to include all of the C_D versus C_L and C_m versus C_L curves or alternative presentations of the data to illustrate the effects of changing the planform, adding a body and making cutouts in the flap system. These effects are discussed in detail in the analysis section (see section 5).

4 FLOW INVESTIGATIONS

4.1 Slats and flaps retracted

Before starting the main series of measurements of forces and moments on the range of high-lift configurations, the flow on the basic wing planform without body, slats or flaps was investigated. The chordwise position of transition from laminar to turbulent flow was found by flow visualisation tests at 76m/s. On the upper surface transition occurred within approximately 10% chord of the leading edge. The laminar flow separated at about 5% chord and reattached as a turbulent boundary layer. This pattern was maintained with only small variations in the position of transition over the incidence range 0^o to 10^o. On the lower surface however, there was considerable movement of the position of transition over this incidence range; transition moving aft as incidence was increased.

After some preliminary attempts at fixing transition by means of ballotini, which showed that this technique could not be relied on to produce a turbulent boundary layer over the whole, attached-flow incidence range, it was found that transition of the flow from laminar to turbulent could only be ensured by using a series of 0.5mm diameter wires positioned streamwise round the leading edge from 10% chord on the upper surface to 10% chord on the lower surface. 10 wires

were spaced equally across each half wing. The results of force measurements at a windspeed of 76m/s, with and without the transition device, are shown in Figs.5 and 6 together with the forces measured at three other windspeeds with free transition (46m/s, 61m/s and 91m/s). Only a part of the incidence range has been plotted in order to highlight the differences caused by Reynolds number and the transition device. Over the attached-flow incidence range, $\alpha_w < 10^o$, fixing transition has very little effect on lift coefficient (Fig.5), and produces a small, and practically constant, increment in drag coefficient (Fig.6). Thus fixing transition will not have any significant effects on the conclusions obtained from the analyses of experimental results described in section 5, as these are only applied to the attached flow regime. Above 10^o incidence a large increment in lift coefficient is obtained with the stall being delayed by approximately 3^o. Although some of this lift increase results from fixing transition, a large proportion is probably caused by the tendency of the streamwise wires to act as vortex generators. Increasing the Reynolds number when transition is left free produces an increase in C_L at a given incidence, at the lower Reynolds numbers, and a trend towards a single curve at the highest Reynolds number. The C_D versus α_w graph (Fig.6) again shows that only at the lower Reynolds numbers is there a significant effect of increasing Reynolds number.

4.2 Slats and flaps deflected

A short series of flow visualisation tests was also made on the wing/body combination with slats and flaps deflected. From this work it was apparent that if transition were allowed to occur naturally on the slat, main wing and flap, the only area where there seemed to be any noticeable movement of the position of transition with incidence was on the lower surface of the main wing. The results of some limited force measurements at two Reynolds numbers for a typical configuration again showed no significant effects on the variation of lift and drag with incidence. As a result it was decided to allow transition to occur naturally on the slat, main wing and flap for the remainder of the force and moment measurements without attempting to delay the stall by the introduction of such gross devices as the streamwise wires used on the basic wing with the slats and flaps retracted. The subsequent analysis of the lift and drag results confirmed that a repeatable and consistent set of measurements had been obtained. The small variation in the position of transition with incidence will introduce an additional component to the variation of drag coefficient with lift coefficient and hence the drag analysis was necessarily restricted to a comparison of the configurations tested.

Some typical results of the flow visualisation tests in the pre-stall incidence range, with slats and flaps deflected, are shown in Fig.7. The flow pattern on the upper surface of the extended planform wing, mounted on the body, was photographed for the three flap deflection angles (10°, 25° and 40°), and a fixed flap span ($y_F/s = 0.8$). In each case the slat was deflected 25° and the angle of incidence was about 16°. Regions of laminar flow are visible near the leading edges of the slat, main wing and flap, and laminar separation bubbles are partially visible as white spanwise lines, resulting from an accumulation of the suspended Dayglow powder in these low velocity regions.

Because the principal object of the work was to investigate the effects of flap span and deflection angle on the high-lift performance of the wing it was necessary to fix the slat deflection angle for the main body of the tests. Measurements of forces and flow visualisation tests were made for the three slat deflection angles available (15°, 20° and 25°). The results of the surface flow visualisation showed that there was no gross change of the flow structure as the deflection angle was changed. The laminar-separation/turbulent-reattachment regions were little altered and, at high incidence, the flow on the upper surface first started to separate at the trailing edge of the flap for all three slat angles.

The variation of lift coefficient with wing incidence is shown in Fig.8 for the basic wing planform with the slats retracted, and deflected 15° and 25°. Increasing the slat deflection angle has three effects on lift coefficient. The C_L at a given incidence is decreased slightly (approximately -0.04 on C_L for a 10° increase in slat deflection angle) because the effective chord line of the aerofoil section is reduced in incidence and this more than offsets the increase in camber. The stall is delayed by approximately 3° and a corresponding increment in the maximum lift coefficient is produced (0.2 increase in C_L for a 10° increase in slat deflection angle). There is a tendency for the stall of the under surface of the slat, at negative values of wing incidence, to occur at a more positive value of incidence when the slat deflection angle is increased. However the negative-incidence stall of the slat does not shift over so large an incidence range as the positive-incidence wing stall.

The effect of deflecting the trailing-edge flap for two slat deflection angles (15° and 25°) is shown in Fig.9 for the basic wing with body. Compared with the corresponding flaps-retracted curves, increasing the slat deflection angle with the flaps deflected 10° produces a smaller change in C_L at a given

incidence, and practically the same difference in wing incidence for the onset of flow separation at high incidence. In contrast the onset of flow separation at low incidence, when the flaps are deflected, varies only slightly with the slat deflection angle. Detailed investigation of the flow established that, with both the slat and flap deflected, the separation from the lower surface of the slat, at low incidences, produced a closed separation region on the lower surface of the wing with the flow reattaching near the trailing edge of the flap. Thus the negative incidence stall produced a very large change of the camber line of the effective aerofoil; from a highly-cambered thin aerofoil to a mildly-cambered thick aerofoil, and this change increased with increase of flap deflection angle.

From these tests it was decided to use the 25^{o} slat deflection angle for the remainder of the force measurements as this produced the highest maximum-lift coefficient and the greatest incidence range with attached flow.

The general pattern of the flow on the upper surface of the main wing (as illustrated in Fig.7 for example) shows a spanwise component with the inflow reducing as the trailing edge is approached. This behaviour may be explained by considering the component of the flow normal to the leading edge. This component increases until the suction peak is reached and thereafter it decreases, and the flow direction tends to that of the free stream. The flow pattern does not exhibit this behaviour in three regions:

(i) at the junction of the wing and the body side. This region is complicated by the flow generated by the gap between the end of the slat and the body side. The outflow on the wing immediately adjacent to the body is probably induced by a vortex springing from the root and laying across the upper surface of the wing. There is no evidence of flow separation in the wing/body junction;

(ii) in the region of the wing tip there is a very strong outflow over the rear half of the chord which is induced by the effect of the tip vortex shed from the main wing;

(iii) on the main wing, just outboard of the tip of the flap, there is inflow over the rear third of the chord. This exists because the deflected flap generates a suction at the trailing edge of the main wing, whereas immediately outboard of the deflected flap the trailing-edge pressure is much more positive. The resulting spanwise pressure gradient gives rise to a crossflow.

During the flow visualisation studies on the wing with slats and flaps deflected two other features were noted. From the photographs shown in Fig.7 it

is apparent that there is a large increase in the amount of disorderly flow on the upper surface of the flap when the deflection angle is increased from 25° to 40°. There were indications that only a slight degradation of the upper surface conditions was necessary to cause the flow on the flap to separate when it was deflected 40°. Subsequent force measurements confirmed this tendency.

The investigation of the effect of deflecting the tab mounted on the rear part of the Fowler flap showed a similar surface flow pattern to that on the flap with a 40° deflection angle. The poor performance of the tab was also confirmed by later force measurements. It seemed likely that both these effects were attributable to the relatively low Reynolds number of the wind-tunnel tests, as thick viscous layers would reduce the effectiveness of the gaps between the flap and the shroud and between the tab and the flap. In consequence little detailed analysis was made of the force results obtained with the tabs deflected or with the flaps deflected 40°.

4.3 Stalling behaviour of the extended wing/body combination with slats and flaps deflected

Flow visualisation tests through the stall were made on the extended planform wing/body combination with the slats and flaps deflected 25° ($y_{F/s} = 0.8$). Photographs of the surface flwo patterns are shown in Figs.10 and 11 for intervals of approximately 1° in wing incidence starting at 18.2°. The force and moment results for this configuration are listed as run 81 in Table 4 and the variation of C_L with α_w, and C_D and C_m with C_L are shown in Figs.50, 51 and 52 respectively.

As the angle of incidence, and hence the spanwise and chordwise loadings, was increased it might be expected that the flow would first separate in one of the regions described in section 4.2. Because the inviscid flow over a swept back wing produces a spanwise loading that reaches a peak towards the wing tip it is likely that separation conditions will be first reached in the region of the flap or wing tips. The principal effect of the relatively low Reynolds number of the tests, the reduction of the effectiveness of the high-lift system (because of the thicker viscous layers), will tend to cause the flow to separate at a lower angle of incidence than at high Reynolds number.

The slat brackets are located at y/s = 0.02, 0.12, 0.19, 0.31, 0.39, 0.55, 0.70, 0.84 and 0.96, and the wakes become a major feature in the flow patterns as the angle of incidence is increased. The brackets are in a region of strong outflow and, in addition to the viscous wake, a vortex is shed from each bracket.

It appears that most of this wake passes through the slat gap and over the top surface of the wing, outboard of the slat bracket. The flow patterns on the wing behind the slat brackets show an additional inflow to a separation line. This behaviour is consistent with the presence of a vortex, rotating in the opposite direction to the tip vortex, that is shed by the trailing edge of the bracket in the region where it meets the slat.

These features of the flow have been described in some detail as it is the development of the flow in these areas that leads to the onset of the stall. At an incidence of 18.2° (Fig.10a) there is a slight indication of a flow separation near the trailing edge midway between the two outermost slat brackets. By 19.2° incidence (Fig.10b) this is well established and a further separated flow region has appeared where the wake from the slat bracket nearest the wing tip meets the trailing edge. In addition the crossflow on the main wing in the vicinity of the flap tip has increased and there is some interaction with the flow from the slat bracket in front of this region. The lift is still increasing (Fig.50) but the small regions of separated flow produce an increase in the curvature of the drag polar (Fig.51) and the C_m versus C_L curve (Fig.52).

By 20.2° incidence the flow generated by the second slat bracket inboard from the tip has become a major feature of the flow. There is no evidence to suggest that large parts of the flow are separated in this region but the vortex wake spreads across the span at a much greater rate as the chord is traversed than at 19.2° incidence. A similar broadening of the wake from the third slat bracket from the tip is perceptible at 50% chord. The trailing-edge region of separated flow has grown slightly but the lift is still increasing and the smooth rise of C_D and C_m with C_L suggest that no sudden flow separation has occurred. By 21.2° incidence the wake from the third slat bracket inboard from the tip has enlarged considerably and the trailing-edge separated flow region has also grown. There is a slight fall in lift and a marked divergence of C_D and C_m, which may be attributed to the sudden enlargement of the wake from the third slat bracket inboard from the tip removing the lift contribution of the section of flap downstream.

The remaining photographs in this sequence (Fig.11a-e) show the spread of the stall. In view of the model vibrations, and the associated difficulty of measurement, only approximate values are given for the lift coefficients (which are uncorrected for wake blockage effects). By 22.2° incidence (Fig.11a) the trailing-edge separation has combined with the wake from the second slat bracket inboard from the tip to form one large separated flow region. Another small

separation appears at the trailing edge behind the third slat bracket inboard from the tip. This in turn enlarges and combines with the main separated flow region outboard at 23.2° incidence. Further increase in incidence to 24.2° results in this separation moving inboard so that the section of wing in front of the outer part of the flap span is unloaded, and the outer wing flow becomes fully attached again but with a large amount of crossflow. Finally at 25.2° incidence the separation region reaches the leading edge of the main wing.

Throughout this range of incidence the flow at the extreme tip and over the inboard 35% of the span is virtually unchanged. Thus in order to obtain a more acceptable pitching-moment behaviour at the stall (i.e. a pitch-down rather than a pitch-up tendency) considerable degradation of the high-lift system in the inboard region would be necessary in order to ensure that the onset of flow separation began sufficiently far inboard. The degree of degradation required will depend on Reynolds number and to be effective in aircraft design, wind-tunnel tests at much higher Reynolds number than those described above are necessary.

The last photograph in the series (Fig.11e) shows the body at an incidence of 25.2° and illustrates the complex nature of the flow pattern that results from the interaction of the high circulation produced by the wing high-lift system with the crossflow over the body at high incidence.

5 DISCUSSION AND ANALYSIS OF RESULTS

5.1 General discussion of the effects of varying flap deflection angle and flap span

The results for full-span flaps at the three flap deflection angles are plotted in Figs.12-32. The general trend of the variation of lift, drag and pitching moment coefficients has the same characteristics for all the configurations tested, i.e. with and without slats, a body and a planform change. Changing the flap deflection angle has three principal effects on the variation of lift coefficient with wing incidence (Figs.12, 15, 18, 21, 24 and 27):

(i) There is an increment in the lift coefficient at a given wing incidence which increases as the flap is rotated, thus increasing the camber and the effective incidence of the aerofoil.

(ii) In addition to changing the camber of the aerofoil the Fowler type of flap produces an increase in wing area and this causes an increase in the slope of the lift coefficient curve with incidence. However the lift coefficient

curves for the 40° flap deflection angle do not have an increased slope and this confirms the conclusion drawn from the flow investigations that the flap was not very effective when deflected 40°.

(iii) When the flap deflection angle is increased the angle of incidence at which the stall occurs is decreased. Increasing the deflection of the flap increases the chordwise loading and the adverse pressure gradient at the rear of the upper surface of the shroud and the flap. Thus the flow is likely to separate in these regions at a lower value of wing incidence. Figs.21 and 27 show that variation of the flap deflection angle has little effect on the negative incidence stall of the slat and confirms the results obtained in the flow investigations to determine a suitable slat deflection angle.

The variation of drag coefficient with lift coefficient (Figs.13, 16, 19, 22, 25 and 28) also illustrates these points. The drag polars for the flaps retracted and for the two lower flap deflection angles have the same envelope, but the curve for the 40° flap deflection angle indicates a rise in drag relative to this envelope. The graphs of pitching moment coefficient versus lift coefficient (Figs.14, 17, 20, 23, 26 and 27) show that deflection of the flaps produces a stabilising effect (a decrease in dC_m/dC_L) and a nose-down increment in pitching moment coefficient which increases with flap deflection angle. The results for the 40° flap deflection angle do not follow the same trend as the 10° and 25° flap deflection results. This may be explained by a relative loss of lift towards the trailing edge of the wing and flap leading to a less stable pitching moment coefficient curve (an increase in dC_m/dC_L) and only a slight increase in nose-down pitching moment coefficient relative to the 25° flap results. All the pitching moment coefficient curves show a pitch-up tendency at the stall and confirm the flow visualisation results that the wing first stalled in the region of the wing tip.

A selection of the force and moment results for a range of flap spans, with a given flap deflection angle, are plotted in Figs.30-53. As the flap span is increased some general trends are apparent in the variation of lift coefficient with wing incidence (Figs.30, 31, 34, 35, 36, 39, 40, 41, 44, 45, 48, 49, 50 and 53) for all the arrangements tested:

(i) There is an increase in the lift coefficient at a given incidence which is due to the increase in the proportion of the wing having trailing-edge camber.

(ii) There is an increase in the slope of the lift coefficient curve which is due to the increase in wing area as the flap span is increased.

(iii) There is a decrease in the angle of incidence at which the wing stalls, presumably because the loading in the region of the wing tip is increased at a given incidence and hence separation conditions are reached at a lower incidence.

The graphs of drag coefficient versus lift coefficient (Figs.32, 37, 42, 46 and 51) show that increasing the flap span increases the minimum drag coefficient. This occurs because of the associated increases in wetted area and in the proportion of the wing that is highly cambered. The minimum drag occurs at a lift coefficient which increases with flap span. At higher lift coefficients the larger flap spans produce the lowest values of drag coefficient but there is very little drag reduction to be gained from a flap span greater than $y_F/s = 0.8$.

The pitching moment coefficient figures (Figs.33, 38, 43, 47 and 52) show that increasing the flap span produces a more stable pitching moment coefficient versus lift coefficient curve (dC_m/dC_L is reduced), but this is achieved at the cost of an increased nose-down pitching moment coefficient. These effects are consistent with the additional lift that is generated by the extra flap span on the swept wing acting at a point further aft relative to the moments' centre. For all the configurations tested there is an increase in pitching moment coefficient at the stall for all flap spans.

Figs.54-56 show the results of the tests with the tabs deflected through a range of angles on a part-span flap ($y_F/s = 0.8$), deflected 25° and 40°. The tab produces an increment in lift coefficient for an initial deflection of 15° but further deflection of the tab to 30° results in a decrease in lift coefficient for both flap deflection angles (Fig.54). This suggests that the increase in deflection angle is sufficient to cause the flow over the upper surface of the flap to separate. These results confirm the impression gained during the initial flow investigations that deflecting the slotted tab was not very effective at the test Reynolds numbers. The large increase in drag coefficient (Fig.55) and the increase in pitching moment coefficient (Fig.56), as the tab is deflected from 15° to 30°, are consistent with the flow having separated in the vicinity of the wing and flap trailing edges, and the resultant lift having moved forward.

5.2 Lift coefficient increments due to the variation of slat and flap deflection angles

The lift coefficient increments resulting from the deflection of full-span slats to angles of 15° and 25°, on the basic planform, are shown in Fig.57, plotted against wing incidence. As the wing stalled at a considerably higher wing incidence when the slats were deflected, the increments in lift coefficient, relative to the lift coefficient values with slats retracted, were obtained by extrapolating the lift coefficient versus incidence curve for the slats retracted. As this latter curve was linear over the range of incidence 0° to 10° this provided a reasonable measure of the potential lift-coefficient increments that could be obtained at higher incidences if the flow had remained attached. Also shown in Fig.57 are the lift-coefficient increments predicted by the linear theory method of Mckie[4] for extending-chord flaps. This method is inviscid and takes no account of wing thickness. A flat-plate approximation to the wing is used, with the camber due to the slats and flaps replaced by an equivalent twist of the flat plate. The method of applying this theory to the various configurations of slats and flaps and obtaining the lift-coefficient increments is described in detail in Appendix C. Both the experimental and theoretical lift-coefficient increments are referred to the area of the basic straight-tapered wing with slats and flaps retracted, including the results obtained with the extended planform wing.

The variation of the measured lift-coefficient increments with incidence has a similar slope to that predicted by linear theory over the incidence range 8° to 15° but there is a substantial loss of lift coefficient relative to the predicted levels. Above 15° the difference between the measured and predicted lift-coefficient increments increases with increase of wing incidence. This may be a result of a corresponding increase in the boundary-layer displacement thickness towards the rear of the aerofoil which would tend to reduce the effective camber and, by increasing the effective trailing-edge thickness, reduce the incidence of the chord line. The circulation round the slat reduces the adverse pressure gradient on the upper surface of the wing and prevents the early thickening and separation of the boundary layer in this region as the wing incidence is increased. However this inviscid effect is offset by the interaction of the wake from the slat and the main-wing boundary layer which causes an increase in the thickness of the viscous layer on the wing upper surface and eventually leads to separation of the flow.

At zero wing incidence there is a lift-coefficient decrement as the effect of deflecting a leading-edge slat is to decrease the incidence of the chord line and the resulting reduction in lift coefficient is not offset completely by the increase in lift coefficient due to the increase in camber. In the present case this decrement is also slightly offset by the area extension produced by deploying the slat (approximately 11%). Thus the area extension produced by deflecting the slat 15° is 12.06% of the basic wing area but the increase in the slope of the lift coefficient curve is only 9.84%, as predicted by linear theory. Similarly the 25° slat produces an area extension of 10.45% and a predicted increase of 8.69% in the slope of the lift coefficient curve. The effect of the change in the wing aspect ratio, caused by the extension of chord, has been allowed for in the linear theory predictions by using the extended chord in the calculations and scaling the resultant coefficients to the basic planform area.

The lift coefficient increments obtained by deflecting full-span flaps to the three deflection angles (10°, 25° and 40°) are plotted against wing incidence in Figs.58-63 for the range of combinations of wing planform, wing leading-edge geometry and body that was tested. Also shown in these figures are the lift-coefficient increments predicted by the linear theory of Mckie[4].

In all cases the measured and predicted lift-coefficient increments show a similar variation with wing incidence for the 10° and 25° flap deflection angles. With the slats retracted (Figs.58, 59 and 62) the slope of the measured ΔC_{LF} versus $\alpha_w{}^{\circ}$ curve is the same as the theoretical slope but the experimental results are approximately 20% below the linear theory predictions. This difference may be attributed to two of the principal limitations of the linear theory used. Firstly no account is taken of the effects of viscosity. Thus, as mentioned above in connection with the slat performance, thickening of the upper-surface boundary layer will reduce the effective camber of the wing. The fact that the experimental results differ by a constant decrement from the theoretical results suggests that in this instance the displacement surface effect changes little with incidence. A second limitation of the linear theory is the approximation introduced by the mathematical model that is used to represent the highly-cambered wing. Thus, for example, the twisted flat-plate model incorporates no provision for the shedding of vorticity from the streamwise flap edges which is certain to occur in the physical flow at high angles of incidence of the flap to the airflow. Whether this type of limitation is significant cannot be determined from the present results as the relative magnitude of the above two

factors cannot be assessed. This question is only likely to be resolved when a theoretical method is available for calculating the first approximation to the viscous flow over a wing with a high-lift system, i.e. including the boundary layer displacement thickness in the aerofoil profile as has been done, for example, by Carr-Hill[10] for the cruise wing-design problem. Developments in the more complex lifting-surface theories may also indicate whether the limitations of the linear theory are significant.

When the leading-edge slats are deflected (Figs.60, 61 and 63) there is less similarity in the variation of the measured and predicted lift-coefficient increments with wing incidence. However the minimum difference between the measured and predicted lift-coefficient increments is reduced to a 10% decrement when the flap is deflected 10°. The non-linear variation of the experimental results may be attributed to the interaction of the slat viscous wake with the wing upper-surface boundary layer. The divergence of the measured and predicted lift-coefficient increments above 8° incidence may indicate a more rapid growth in the thickness of this viscous layer.

The minimum difference between the measured and predicted lift-coefficient increments is increased to approximately 20% of the flap lift-coefficient increment when the flap is deflected 25°, i.e. a similar decrement to that obtained with the slats retracted. The increase in wing camber obtained by deflecting the flap further will be partially offset by a decrease in camber due to the increase in thickness of the boundary layer on the upper surface of the wing, arising from the more severe adverse pressure gradient in this region. The non-linearity of the variation of the experimental increments may again be attributed to a slat wake/upper surface boundary-layer interaction.

All these effects are aggravated when the flap is deflected to 40°. There is a large difference between the measured and predicted flap lift-coefficient increments which tends to confirm the qualitative results obtained from the flow investigations discussed in section 4. This flow visualisation work indicated the existence of separated flow regions on the flap and hence the flow was very much more complex than the simple quasi-two-dimensional pictures considered above. Other mechanisms may be responsible for the large losses of lift coefficient relative to the linear theory values.

5.3 Lift coefficient increments due to the variation of flap span

The experimental lift-coefficient increments for each flap span were calculated at constant values of wing incidence. For each combination of wing

planform, wing leading-edge geometry and body, the corresponding configuration having the flaps retracted over the whole span was taken as a datum. The variation of the increments with wing incidence, for a constant flap span and deflection angle, showed the same type of behaviour as the full-span flaps (Figs.58-63) and hence these results have not been plotted. The variation of the lift-coefficient increments with flap span, at a wing incidence of 0°, is shown in Fig.64 for a typical configuration (basic wing with body, leading-edge slats retracted). Also plotted on this figure are the corresponding lift-coefficient increments calculated using linear theory. The increments for this wing/body combination were calculated for the nett exposed portion of the wing; the two half wings being joined to form a reduced-span wing. This is equivalent to assuming that the body side produces a perfect reflection of the type that occurs at the centre line of the equivalent reduced-span nett wing. Thus no mutual interference effects of the body and the wing are included but, to a first order, it is reasonable to assume that the interference effects of the body on the wing are independent of flap span and hence do not affect the lift-coefficient increments. This aspect and the interference effects of the wing on the lift carried by the body are discussed in section 5.6.

Comparing the experimental and predicted lift coefficient increments two trends are noted. Firstly the difference between the two curves increases as the flap deflection angle is increased. This effect has been discussed in the previous section and it is likely that the same mechanisms are responsible for the difference with part-span flaps. The second trend is an increase in the fractional difference between the measured and predicted increments as the flap span is increased. With the flap deflected 25° on the basic wing/body combination (Fig.64) for example, $\left[\Delta C_{L_{theory}} - \Delta C_{expt}\right] \Big/ \Delta C_{L_{theory}}$ increases from 0.085 for $y_F/s = 0.6$ to 0.142 for $y_F/s = 1.0$. This may be caused by the spanwise flow of the boundary layer on a swept-back wing which produces an increase in the boundary-layer thickness on the outer parts of the wing span. On the basis of the two-dimensional arguments, discussed in section 5.2, the deleterious effect of viscosity on the sectional lift coefficient is likely to increase towards the wing tip. As a result of this and other effects there is relatively little increase in lift coefficient to be gained by extending the flap above $y_F/s = 0.8$. The increments obtained for the other configurations tested show a similar behaviour. The relatively poor performance experimentally of the full-span flaps influences the shape of the curves of the part-span flap lift factors plotted against flap span y_F/s in Figs.65-68.

The part-span flap lift factors were obtained from the experimental lift-coefficient increments, at a particular wing incidence, by dividing by the lift-coefficient increment produced by a full-span flap at the same wing incidence. These factors varied with wing incidence (generally within ±0.01) and mean values over the attached-flow incidence range are plotted in Figs.65-68. On each figure a curve of the part-span flap lift factor predicted by linear theory is also shown. A reduced-span nett wing planform was used for calculating the part-span lift factors for the configurations including a body. The differences between the measured and predicted curves emphasize the trends noted above. The linear theory values for the part-span flap lift factors are consistently lower than the measured values at the smaller flap spans. This is because of the relatively poor performance of the full-span flap compared with any of the part-span flaps. Deflecting the slats produces some decrease in this difference (comparing Fig.65a and b and comparing Figs.66a and 67a), presumably because of a beneficial influence of the slat on the chordwise loading on the main wing and flap elements of the high-lift section. There is a large increase in the difference between the predicted and measured factors for the extended planform wing (comparing Fig.67a with Fig.68). The higher taper ratio of this planform will increase the span loading towards the wing tip and hence tend to aggravate the lift losses due to boundary-layer thickening in this area.

In order to test the suggestion that the effects of the body on the part-span flap lift factors do not vary with the flap span, the measured values of the factors for the wing alone are compared (Figs.66b and 67b) with the values measured on th corresponding wing/body combination but with the flap span scaled with respect to the nett wing span. The good agreement between these two sets of data (the error is of the same order of magnitude as the scatter of the experimental results) suggest that values of part-span flap lift factors, measured during a wing alone test may be used to predict the part-span flap lift factors obtainable with the wing mounted on a body. However this result is not likely to hold for wing mounting positions offset from the body centreline by a large fraction of the body radius, as the effective reflection at the body side would be significantly reduced.

5.4 Lift coefficient increments due to cutouts in the flap system

The results of the tests with portions of the flap system retracted are shown in Figs.69-73. The cutouts in the flap span had streamwise ends with the undeflected section of the flap abutting the deflected section so that there were

no spanwise gaps. The increments in lift coefficient are defined as the change in lift coefficient, at constant wing incidence, that occurs when the section of the flap is retracted. In each case the values of the increments obtained from the experimental results are compared with the linear theory predictions obtained using the method described in Appendix C. For the cases in which the wing was mounted on the body the calculations have been made using the nett exposed wing.

Fig.69 shows the effect of a body cutout ($-0.142 < y_F/s < 0.142$) in the flap span, on the basic wing with slats retracted. For the lower flap deflection angles (10^o and 25^o) there is reasonable agreement between theory and experiment in the general levels of the decrements in lift coefficient. However the fact that the variation of the measured lift-coefficient decrement with wing incidence does not resemble the predicted behaviour suggests that the agreement is partly fortuitous. Although the flow in the region of the flap ends at the cutout was not investigated in detail, it was clear that the real flow was considerably more complex than that represented by the simple twisted flat plate used in the linear theory of Mckie. In particular the retraction of a deflected section of flap removes the forward influence of the flap on the pressure distribution at the rear of the upper surface of the main wing. Thus the suction at the trailing edge of the main wing will be replaced by a pressure much closer to the free stream static value. In addition to causing a local adverse pressure gradient this will generate spanwise flow towards the adjacent sections of flapped wing. The streamwise ends of the flap sections at the cutout will contribute to the wake shed from the wing and further increase the three-dimensional nature of the flow in the vicinity of the cutout. The decrements in lift coefficient measured for the lower flap angles are in general slightly greater than the predicted decrements, which is consistent with there being other sources of lift-coefficient loss besides those represented in the linear theory. The decrements produced with a flap deflection of 40^o are not so large as predicted, presumably because the whole flap does not produce the basic lift performance predicted.

Fig.70 shows the corresponding results with the leading-edge slats deflected. The decrements obtained with full-span flaps at the three deflection angles (Fig.70a) behave similarly to those measured with the slats retracted. Fig.70b shows the effect of flap span on the decrement in lift coefficient produced by a body cutout in the flap span when the flaps are deflected 10^o. As the flap span is decreased the measured decrements become closer to the predicted levels.

Turning to a more practical problem, Fig.71 shows the effect of what has been called an 'engine' cutout in the flap span. For $0.257 < y_F/s < 0.355$ the flap section is retracted and the remainder of the flap span is terminated at $y_F/s = 0.8$. In Fig.71a the wing alone results are plotted for the two lower flap deflection angles on the basic wing, with the leading-edge slats deflected to 25^o. For this flap cutout there is very good agreement between the measured and predicted decrements but this may be fortuitous, because of some mutual cancellation of errors. Fig.71b shows the corresponding results for the wing mounted on the body. The agreement is not so good for the lower flap angles and the decrements measured with the 40^o flap deflection are closer to the predicted levels than was the case with the body cutout in the flap system (Fig.70a).

Fig.72 shows the effect of an engine cutout in the flap span ($y_F/s = 0.8$) on the extended wing with the slats deflected 25^o. Comparing these results with the corresponding results on the basic wing planform (Fig.71b), the extended planform produces larger losses relative to the predicted levels.

Finally, Fig.73 shows the lift-coefficient decrement produced by two cutouts in a flap ($y_F/s = 0.8$) deflected 10^o on the basic wing, with the leading-edge slats deflected. Comparing the results for the combination of body and engine cutouts with either cutout alone (Figs.70b and 71a) the difference between the measured and predicted decrements is less than the sum of the differences due to the separate cutouts. Thus there is apparently a beneficial mutual interaction of the flow in the region of these two cutouts. However, in all the comparisons of the effects of cutouts made in this section it should be appreciated that the flow structure, particularly at the flap ends, is very complex and many of its features are not represented in the simple linear theory.

5.5 Pitching moment coefficient increments due to the variation of the geometry of the flap system

When a trailing-edge flap is deflected the pressure distribution over the main wing element is changed because of the forward influence of the flap. If the flow is attached on the main wing the flow over the flap is mainly determined by the geometry of the flap, relative to the main wing, and is largely independent of the incidence of the combination to the freestream. Thus it might be expected that the additional load caused by the deployment of a flap could be related to the flap position and planform geometry alone. In order to examine this possibility the increments in lift, drag and pitching moment coefficients, that were produced by the range of flap deflection angles and spans, have been analysed in the following manner.

The fore and aft position on the wing chord at which the additional normal force acted was first calculated by assuming that the pitching-moment coefficient increment was caused solely by the increment in the normal force coefficient (which was determined by resolving the measured increments in lift and drag coefficients). As the ratio of normal to axial force increments, $(\Delta C_N/\Delta C_A)$, was of the order of 10, and as the vertical movement of the resultant force is likely to be less than 10% of the horizontal movement, this is a reasonable assumption.

The results of these calculations showed that the increment in normal force coefficient due to the flap hardly varied with incidence, and that the point of action of the load due to the flap was practically constant, for each flap span and deflection angle, over the attached-flow incidence range. However, the position of action of this load varied with flap span and deflection angle. In order to relate the point of action of the load to the planform geometry of the flap, the distance of this point forward of the mean quarter-chord point of the deflected flap was calculated and this was divided by the mean chord of the planform with the slats and flaps undeflected. This distance $(x/\bar{c})_{\Delta C_N}$, is plotted in Figs.74-78 for the range of configurations tested. Most of the experimental results lie close to a constant value of $(x/\bar{c})_{\Delta C_N}$ over the attached-flow incidence range. There is a slight variation with flap deflection angle but in general the flap produces a load which acts a distance of about $0.5\bar{c}$ forward of the flap mean quarter chord. If, for a given flap deflection angle, the spanwise loading on the wing were such that there was constant sectional C_L across the flap span, one would expect the data for different flaps spans to collapse onto a single curve when expressed as $(x/\bar{c})_{\Delta C_N}$. In view of the taper and sweepback of the wing planform, both of which tend to increase the spanwise loading towards the wing tip, it might be expected that the method of analysis would not lead to a complete collapse of the data.

Fig.74 shows the variation of the position of the additional load due to flap deflection, $(x/\bar{c})_{\Delta C_N}$, with wing incidence, for the basic wing with slats retracted. The results for the range of flap spans fall within $0.04\bar{c}$ for each flap deflection angle. The scatter of the results for the 10^o flap deflection angle is greater than for the other deflection angles because the size of the increments in the lift, drag and pitching moment coefficients is smaller and the

analysis is correspondingly less accurate. Only the results for the full-span flap with a body cutout differ significantly from the results for the other flap spans. This configuration produces the most abrupt changes in spanwise load (at the junction of the deflected flap and the retracted flap), and hence the implicit assumption of constant sectional C_L across the flap span is most likely to be in error. Changing the flap deflection angle produces a forward shift of about $0.04\bar{c}$ in the position of the load as the angle is increased successively from 10° to 25° and from 25° to 40°.

The corresponding results for the slats deflected on the basic wing (Fig.75) are very similar to those for the slats retracted. The load moves forward approximately $0.03\bar{c}$ on deflecting the slat (the slat itself produces a $0.10\bar{c}$ forward extension of the mean chord).

Adding the body to the basic wing with slats retracted produces results (Fig.76) which do not show such a good collapse with flap span. This is probably due to the flap span being interrupted by the body diameter at the wing root and hence the sectional C_L along the flap is likely to be less uniform than when the flap span is continuous across the wing centre line. The worst deviation from a single curve is produced by the smallest flap span. The body produces a $0.06\bar{c}$ forward shift in the position of the load (comparing Figs.74 and 76).

With the slats deflected (Fig.77) the body again produces a forward shift of the load due to the flap of about $0.06\bar{c}$. Comparing the results for the basic wing with body having the slats retracted and deflected (Figs.76 and 77) the load moves forward by about $0.02\bar{c}$ when the slats are deflected.

The corresponding results for the extended planform wing with body and the slats deflected are shown in Fig.78. There is less agreement between the results for the various flap spans than was obtained with the basic straight-tapered wing (Fig.77). In addition there is a noticeable variation with incidence of the position of the load generated by the flap. It seems likely that both these results are caused by an increase in the non-uniformity of the spanwise loading on the wing. The increase in the root chord (and hence in the taper ratio), and the reduction of the flap chord inboard of the trailing-edge discontinuity, both cause a more non-uniform distribution of the sectional C_L on the wing.

5.6 Body effects

The effects of adding a cylindrical body to the wing are shown in Figs.79-84 for a range of configurations of the high-lift system. The increments

in the lift and pitching moment coefficients were obtained by the process outlined in Appendix C and the results are compared with the predictions of the linear theory method of Weber, Kirby and Kettle[3]. The method of representing the high-lift system for these calculations is also explained in Appendix C.

The variation of the lift-coefficient increment due to the body, with wing incidence, is shown in Fig.79 for the three flap deflection angles, with and without the slats deflected. The total lift-coefficient increments calculated by linear theory, assuming slender body theory predictions for the forebody load and no contribution from the tail section of the body are also shown. The nose load predicted by slender body theory is constant for all the high-lift configurations.

With the slats retracted (Fig.79a) there is a loss of lift coefficient relative to the linear theory predictions that increases as the flaps are deflected to 25°. This loss may be caused in part by the nature of the junction of the wing and body. There was a small gap between the inboard end of the flap (which terminated at a spanwise position equal to the body radius) and the body, which became larger as the flap was deflected. A separation of the flow on the upper surface of the wing near the trailing edge, in the junction region, could also account for some of this lift coefficient loss but flow visualisation tests showed no signs of extensive regions of separated flow in this area. In general the mean slope of the lift-coefficient increment versus incidence is less than that predicted by linear theory, indicating that either the nose does not contribute as much load as predicted by slender body theory, or that the nose load is partially offset by a download on the aft body. The results for the 40° flap deflection angle are inconsistent in that they show a gain in lift coefficient, relative to the linear theory predictions, but this gain is illusory as the basic lift performance of the 40° flap is poor (as discussed in section 5.2), and presumably stems from a very poor performance of the centre section of flap.

The pitching moment coefficient increments (Fig.80a) can be considered in terms of the point of action of the corresponding lift coefficient increments. The pitching moment coefficient increment at zero incidence has three negative contributions. Firstly, with the wing at zero incidence, the body is at -1.1° because of the wing/body setting angle, and hence there will be a download on the nose (negative pitching moment). Secondly, the body is not axisymmetric but has a slight negative camber on the nose and an upswept tail to make it more representative of a transport aircraft fuselage (see Fig.4). This camber produces loads that result in a negative contribution to the pitching moment

coefficient. Thirdly, the decrease in the load on the centre section that occurs when the body is added to the wing, acts in front of the moments centre and hence produces a decrement in the pitching-moment coefficient (although this may be partly offset by the effect of the body-induced upwash on the wing chordwise loading near the body side). Some evidence of the relative magnitudes of these effects can be deduced from Fig.80a. The first two effects will be largely independent of flap deflection and hence account for most of the increment at zero incidence on the flap retracted curve, whereas the third contribution will be strongly dependent on the flap load as this constitutes most of the wing chordwise loading at zero incidence. The pitching-moment coefficient decrement increases in magnitude as the flap deflection angle is increased from 10^{o} to 40^{o}, the larger step between 25^{o} and 40^{o} being associated with the change in lift coefficient referred to above.

As might be expected the variation of the pitching moment coefficient increments with wing incidence shows that the body is destabilising. The progressive deflection of the flaps produces a slight reduction in $dC_m/d\alpha_w$, i.e. more stability, which may be due to a change in the load on the aft body as a result of the modified downwash field.

The corresponding results with the slats deflected are shown in Fig.79b (lift) and Fig.80b (pitching moment). In general these results show similar trends to those for the slats retracted but there is better agreement between the linear theory predictions and experiment. The slat reduces the suction peak on the upper surface of the main wing and hence prevents the early thickening of the viscous layers in this region, so that the interaction between the flow on the wing and body will be reduced. With the flaps retracted the experimental values lie close to the linear-theory curve for the total lift coefficient but as the flap is deflected there is a loss of lift relative to the predicted increments. The progressive deflection of the flap causes an increasingly strong downwash field over the rear body and this may generate a load on the aft body that partially offsets the nose load.

The pitching moment coefficient increments (Fig.80b) show two important differences from those with the slats retracted. Firstly the increments at zero incidence are more positive because the slat causes the overall load on the wing to act further forward. Secondly the body is less destabilising when the slats are deflected, presumably because of the stronger downwash field generated by the slatted wing.

The effect of flap span on the wing/body interference is shown in Figs.81 and 83. The lift-coefficient increments (Fig.81) for four flap spans are very similar although a slight trend for the increments to be more negative as the flap span is reduced can be discerned. The experimental results are compared with the linear theory results for full-span flaps. The results agree closely with the linear theory predictions for the total lift-coefficient increment reduced by the nose load, which suggests that any nose load is offset by a tail load. Unfortunately, the method of Weber, Kirby and Kettle has not been extended to include the discontinuities in chord that occur on a wing having part-span extending chord flaps so the effect of the change in spanwise load cannot be compared with this theory. The corresponding pitching-moment coefficient increments (Fig.83) show an even closer degree of agreement which suggests that the changes in the lift-coefficient increments noted above occur in the wing/body junction area (i.e. close to the pitching moment axis) rather than at the nose or tail of the body.

The effect of changing the wing planform on the wing/body interference is shown in Figs.82 and 84. The experimentally-measured lift-coefficient increments (Fig.82) show the same general trends (magnitude and slope of the curves) as the linear-theory predictions for the total lift coefficient including forebody lift. The body is less destabilising when combined with the extended planform wing compared with the basic wing/body combination (Fig.84). This may be partly explained by the fact that the trailing-edge extension used to form the extended planform resulted in a mean quarter-chord point that was *nearer* to the wing apex (by approximately 2% of the mean chord) than the mean quarter-chord point of the basic planform. (The mean quarter-chord point of the basic planform was used as the moments reference centre for all the force measurements.) Thus the pitching-moment coefficient increment at zero incidence on the extended planform was more positive than that measured on the basic planform. In addition the smaller value of the ratio of the body diameter to the wing chord at the body side, for the extended planform wing, reduces the interference effects.

In view of the number of effects contributing to the interference, between the high-lift wing and the body, which cannot be isolated by the analysis of force measurements, a programme of work, including comprehensive pressure plotting on a range of bodies and a high-lift wing, has been started. Initial analysis of the results[11] indicates that, for wing-mounting positions not far removed from the body centre line, the interference effects of the body on the

wing chordwise and spanwise loadings are small under high-lift conditions (i.e. with slats and flaps deflected). Measurements of body pressure distributions remain to be analysed in order to determine the magnitude of the interference effect of the high-lift wing on the body loads.

5.7 Effects of planform modification

Some comparisons of the basic wing planform and the extended wing planform (10.9% greater area) are shown in Figs.85-89. For these figures only, all the force coefficients are referred to the *gross* area of the wing planform (i.e. of each particular wing). For the wing alone with the slats and flaps retracted (Fig.85) there is practically no difference in the lift coefficient and drag coefficient curves for the two planforms. The variation of lift coefficient with wing incidence (Fig.85a) shows that the slope of the lift-coefficient curve for the extended planform is very slightly lower (0.0738 per degree than that for the basic wing planform (0.0745 per degree). The corresponding linear-theory predictions for the slope of the lift-coefficient curve (neglecting wing thickness and viscous effects) are 0.0778 per degree (extended planform) and 0.0783 per degree (basic planfrom). The minimum drag coefficient of the extended planform (Fig.85b) is identical, 0.0086, with that of the basic planform but the drag coefficient of the extended planform becomes larger than that of the basic planform at higher lift coefficient values indicating an increased vortex drag factor.

Fig.90 shows the spanwise variation of the sectional lift coefficient relative to the overall C_L, calculated by linear theory, for two configurations of the basic and extended planform wings. With the slats and flaps retracted the effect of the decreased aspect ratio of the extended planform is evident in the reduced sectional C_L at the root. The largest increase in the spanwise loading on the extended wing is at the kink, $y/s = 0.355$, but there is a significant increase out to $y/s = 0.6$.

The comparison of planforms for the body mounted on the wing and the slats retracted is shown in Figs.86 and 87. With the flaps retracted, the basic wing planform produces a higher slope of the lift-coefficient curve (0.0788 per degree) than the extended planform (0.0742 per degree). A similar difference in slope is predicted by linear theory[3]; 0.0859 per degree for the basic planform compared with 0.0816 per degree for the extended planform. The principal reason for this difference of approximately 6% in the slope is that, although the increase in the gross planform area is 11%, only 5% of this is outside the body and the lift coefficient carried over onto the body is not directly proportional to the increase in the gross planform area. The corresponding differences in

the drag polars (Fig.87) may be explained in a similar manner. At low values of lift coefficient the drag coefficient of the extended planform is lower than that of the basic planform because of the reduced increase in the wetted area of the wing/body combination. The curvature of the drag polar for the extended planform, and hence the vortex drag factor, is again greater than for the basic planform.

Deflecting the flaps increases the differences between the results for the two planforms. This is partly due to the change of the flap geometry from a simple constant-percentage chord flap on the basic planform to a constant chord flap inboard of y/s = 0.355 on the extended planform. However some of the difference is due to the increased degree of non-uniformity in the spanwise loading on the wing that is caused by the inboard, trailing-edge, extension to the planform. The spanwise loadings calculated by linear theory (Fig.90) show a large increase in the sectional C_L on the extended planform wing for $0.3 < y/s < 0.75$.

The same trends are apparent with the slats deflected 25° on the wing/body combination (Figs.88 and 89). There is again a 6% difference in the slope of the lift-coefficient curves for the two planforms when the flaps are retracted (Fig.88). The losses incurred by the extended planform when the flaps are deflected are not quite as large as those obtained with the slats retracted (comparing Figs.86 and 88), presumably because of the beneficial effect of the slat on the chordwise loading of the main wing.

As some comments on the effects of planform have been made in earlier sections it is worth summarising these and the above results:

(i) The part-span flap lift factors for the extended planform differ from the linear theory predictions considerably more than those for the basic planform - this is attributed to larger lift coefficient losses for the full span flap on the extended planform.

(ii) The engine cutout in the flap span on the extended planform produces a larger lift-coefficient loss than that on the basic planform.

(iii) On the extended planform the point of action of the flap load, relative to the flap, varies considerably over the incidence range whereas it remains practically constant for the basic planform.

(iv) The wing/body interference effects agree with linear theory predictions to a first order.

(v) The additional lift obtained by extending the planform corresponds to the increase in area for the wing alone. For the wing/body combinations an increase in lift of the same order as the increase in wing area external to the body was obtained.

(vi) The drag polars for the extended planform configurations have a higher vortex drag factor than those for the corresponding basic planform configurations.

Most of these results may be attributed to the more extreme spanwise loading that exists on the extended planform. The combination of a higher taper ratio (0.2473), a lower aspect ratio, a reduced sweep inboard, and a poorer trailing-edge flap system inboard lead to a basic spanwise loading distribution that, when added to the incidence loading, results in parts of the wing developing much thicker viscous layers and becoming susceptible to flow separation at lower angles of incidence. In particular the flow in the vicinity of the wing tip separates at a lower incidence so that it would be necessary to degrade the high-lift system on the inner parts of the wing still further in order to obtain stalling characteristics similar to those on the straight-tapered wing planform.

5.8 Drag analysis

The drag polars obtained for a range of configurations have been analysed on the basis of the linear theory of Maskell[5]. The present tests were not conducted specifically for the purpose of drag analysis and consequently no comprehensive measurements of the support interference effects were made, and the effects on drag of allowing transition to occur naturally on the wing elements were not quantified. As a result it was not possible to estimate absolute drag levels. The experimental work reported in Ref.5 was restricted to increments in C_L due to the high-lift system (ΔC_L) of up to 0.8. As the ΔC_L obtained in the present tests were much higher (up to 1.6) and as the slat introduced further lift-dependent viscous effects (a leading-edge droop was used in the work reported in Ref.5) it was thought worthwhile to attempt a comparative drag analysis. No other analyses of the drag of swept wing/body combinations with high-lift devices, and including the effect of flap span, have been published.

The method of analysis of the experimental data is described in detail in Appendix D. The best least-squares-fit parabolae were found for the range of lift coefficient that covers the take-off and landing manoeuvres. The limitations of the method may be appreciated from a consideration of the two drag

polars shown in Figs.91 and 92. When the slats are retracted the method produced a good fit to the experimental data with only minor departures from a parabola at the extremes of the incidence range (Fig.91). These divergences were consistent with the onset of the stall at high incidence and the effect of movement in the position of transition to turbulent flow at low incidences.

When the slats are deflected the parabola obtained by the curve fitting procedure showed a large divergence from the experimental data at low incidence (Fig.92). This difference was too large to be accounted for solely by the effects of a movement in the position of transition, and suggests the occurrence of a gross change in the flow structure at low incidence (perhaps generated by the slat and its brackets). As this peculiarity in the curve-fitting process was limited to the configurations with the slats deflected, and as it occurred at values of lift coefficient below those of interest, this limitation was accepted in the subsequent analysis. However the drag analysis can only be regarded as tentative and as an aid to exploring the effects of flap span.

For the drag polar shown in Fig.91 (a configuration with slats retracted) 11 points lie on a parabola. When the slats were deflected a parabola could be fitted through a larger number of points (14 in Fig.92). It was found that with 10-15 points (at approximately 1° intervals of incidence) the accuracy of the curve fitting was insensitive to changes in the lift-dependent drag factor, k. A change in k of 0.05 produced a typical change in the maximum error in the curve fitting of 0.0001 in C_D, so that it was not possible to determine k to a better accuracy than ±0.05. Once a value of k had been fixed the corresponding values of the drag polar parameters, $\breve{C}_D$ and $\breve{C}_L$ in equation (D-1) could be determined very accurately using a least squares procedure.

Fig.91 also shows the effect of a 0.2 change in the value of k on the accuracy of the curve fitting. The maximum difference in C_D between the fitted curve and the experimental data increases from 0.0006 to 0.0015 as the value of k is reduced from 1.2 to 1.0, the value predicted by linear, inviscid theory. The value of k that gave the best fit with the slats retracted (1.2) produced a very poor fit to the data for the corresponding configuration with slats deflected (Fig.92). The best fit was obtained with k = 1.75, although a change in k of 0.05 to 1.7 again produced a maximum C_D error only 0.0001 greater. This degree of uncertainty in k (±0.05) resulted in an associated uncertainty in the values of $\breve{C}_L$ and $\breve{C}_D$ (typically 0.030 and 0.0020 respectively).

The results of the complete analysis are shown in Figs.93-97 as a variation of the drag polar parameters k, $\breve{C}_D$ and $\breve{C}_L$ with flap span. For each configuration the corresponding values are shown for the vortex drag contribution derived from the part-span flap linear-theory method of Mckie[4]. Any differences between the experimental values and the linear theory values will be due to a combination of the profile drag contribution, any errors inherent in the simple planar-wake model of the linear theory, and the unknown effects of the model support interferences and variations in the position of boundary-layer transition.

For the basic wing with slats retracted (Fig.93) the variation of the parameters k, $\breve{C}_D$ and $\breve{C}_L$ with flap span, has the same form for both the experimental and lineary-theory results. The principal differences are:

(i) a change in level of k which indicates a strong lift dependency of profile drag and/or a large error in the linear theory predictions;

(ii) a change in the lift dependency of profile and/or vortex drag with flap deflection angle;

(iii) a practically constant increment in $\breve{C}_D$ (except for the largest flap spans) relative to the linear-theory predictions. This is of the same order of magnitude (0.01) as the minimum drag of the wing, C_{D_0};

(iv) for the smaller flap spans the variation of $\breve{C}_L$ follows the linear-theory trend but is in general more positive;

(v) for the largest flap span there is a divergence from the linear-theory results which may indicate an increase in the contribution of the viscous effects to drag in the more highly loaded tip region.

Deflecting the slats on the basic wing (Fig.94) produces large divergences from the linear-theory predictions. There are significant changes in the level of k and $\breve{C}_L$, and a considerable variation of k with flap span. This behaviour may be due to interference effects between the slat wake and the viscous layers on the wing upper surface.

Adding the body to the basic wing with the slats retracted (Fig.95) produces similar results to those for the wing alone (Fig.93). The body causes an increment of approximately 0.01 in $\breve{C}_D$ (which is of the same order as the change in C_{D_0}) and changes the form of the variation of $\breve{C}_L$ with flap span. When the slats are deflected there is again a large increase in the level of k and $\breve{C}_L$ (Fig.96).

The analysis for the extended planform wing with the body mounted on the wing and the slats deflected 25° is shown in Fig.97. Comparing these results with those for the corresponding basic wing configuration (Fig.96) the trends for the 10° and 25° flap deflection angles are broadly similar. However the results for the 40° flap deflection angle are very different, presumably because the flap flow is closer to separation in the more highly loaded tip region of the extended planform wing.

6 CONCLUSIONS

An extensive set of measurements of the longitudinal force and moment components on a range of model configurations has been analysed and compared with two linear-theory prediction methods. The principal results of this comparison were:

(i) the experimentally measured increments in lift coefficient due to the leading-edge slats and the trailing-edge flaps were substantially lower than the linear-theory predictions and the fractional difference between experiment and theory increased as the flap deflection angle was increased;

(ii) the experimentally measured increments in lift coefficient due to variation of the flap span were lower than predicted by linear theory and the difference between experiment and theory increased as the flap span was increased;

(iii) for low flap deflection angles, there was reasonable agreement between experiment and theory on the lift coefficient increment produced by making a cutout in the flap span. It was suggested that this agreement was partly fortuitous as errors in the inviscid flow model could counteract the effects of viscosity;

(iv) the body effects measured with the high-lift devices retracted agreed with the linear-theory predictions for the overall load including a contribution from the nose. When the slats and flaps were deployed the experimental results tended to lie closer to the theoretically predicted load reduced by the nose-load, i.e. there may have been some download on the tail section of the body that offset the nose load;

(v) variation of the flap span had practically no influence on the magnitude of the wing/body interference effect;

(vi) changing the planform of the wing by extending the chord of the inboard region at the trailing edge, produced changes in the slope of the lift

coefficient curve, with and without the body, that agreed quite well with linear theory;

(vii) an exploratory drag analysis showed a similar type of variation of the parameters k, $\breve{C}_L$ and $\breve{C}_D$ with flap span, to that predicted by linear theory. However there were large differences of level, particularly in the value of k, the lift-dependent drag factor, which was very much higher than predicted when the slat was deflected.

It is suggested that these differences between experiment and theory may be attributed to two main causes. Firstly the simple planar vortex sheet model of the linear-theory methods is unlikely to give a sufficiently accurate representation of the complicated vortex wake structure that is generated by a wing/body combination having high-lift devices. Secondly no account has been taken of the effects of viscosity and these effects are likely to be large in the highly three-dimensional flow regions that exist on the high-lift wing. It is probable that there will be a significant scale effect on the drag results and hence, in view of the test Reynolds number (1.35×10^6), there may be quite different behaviour at full scale.

Analyses of the force and moment results and some associated flow visualisation tests led to the following conclusions:

(i) the effect of the body on the lift factors for part-span flaps could be predicted quite accurately by assuming that a perfect reflection occurred at the body side and scaling the part-span flap lift factors from the corresponding wing alone tests to the nett exposed wing planform. This scaling is unlikely to hold if the wing is offset appreciably from the body centreline;

(ii) the additional load caused by deflecting a flap was found to act at a constant distance forward of the mean quarter chord point of the deflected flap. This distance was practically independent of wing incidence and flap span, and only slightly affected by change of the flap deflection angle;

(iii) the performance of the high-lift system was downgraded when the wing planform was extended in the root region, and this was attributed to the greater non-uniformity of the spanwise loading;

(iv) the stalling behaviour of the wing was largely controlled by the development of the vortex wakes shed from the slat mounting brackets.

These findings highlight the need for further experimental work to study certain aspects of high-lift system design in depth. A theoretical framework

is needed to predict the viscous effects in the complex three-dimensional flow over a swept wing with high-lift devices deflected and to enable the effects of the non-planar vortex sheets to be estimated.

Appendix A

GEOMETRY OF THE HIGH-LIFT SECTION

A.1 The basic high-lift section

The geometry of the high-lift section used on the basic wing was similar at all *streamwise* sections, apart from some minor modifications to the thickness of the trailing edges of the shroud and the tab, that were necessary to make the wing sufficiently robust. The high-lift section was defined by the characteristic dimensions g and h for the slat, flap and tab (see Fig.3). The values of these dimensions for the basic high-lift section are given in Table 1d.

The deployment of the slat was equivalent to translating it forward and downward until the underside of the trailing edge was at the pivot position, and then rotating it for the 15°, 20° or 25° deflection angle.

The flap was deployed by a combination of translation and rotation to three deflection positions. The translation was defined by a flap gap between the underside of the shroud and the top surface of the flap, measured normal to the underside of the shroud, and a flap overlap of the leading edge of the flap relative to the trailing edge of the flap shroud. Most of the translation was made in the deflection of the flap to 10° (18% chord translation) with the remaining translation (5.5% chord) being added in deflecting the flap to 40°.

The tab was deployed by pivoting about an external hinge so that a gap appeared between the flap and tab as the tab was rotated.

A.2 The high-lift section used on the extended wing

The high-lift section outboard of the kink ($y/s = 0.355$) was left unchanged. No high-lift devices were provided for the region $0 < y/s < 0.142$ (i.e. over the region occupied by the body). The geometry of the high-lift section for the region $0.142 < y/s < 0.355$ was modified from the constant percentage chord section of the basic wing in the following manner.

The slat chord (as measured in the retracted position) was made the same as the slat chord of the corresponding spanwise position on the basic wing. This resulted in slat leading and trailing edges which were colinear with those of the outboard slat when the slat was retracted. The slat tapered linearly from 16% of the local chord at $y/s = 0.355$ to 12.55% of the local chord at $y/s = 0.142$. Because of the larger wing chord, and hence the increased wing

thickness inboard of the kink, the slat thickness was greater than on the basic wing at the same spanwise position. The slat section also depended on the part of the nose of the aerofoil occupied by the slat and thus varied across the spanwise region $0.142 < y/s < 0.355$. The slat undersurface ordinates in this region were determined by distributing the thickness, at a given percentage slat chord, between the slat and the fixed nose in the same ratio as the thickness was distributed between the slat and the fixed nose at the same percentage slat chord outboard of the kink. The fore and aft position of the slat pivot point (i.e the position of the underside of the slat trailing edge) was the same, relative to the corresponding basic wing chord at any spanwise position, as outboard of the kink. The vertical position of the slat pivot point was the same, relative to the actual extended chord at any spanwise position, as outboard of the kink.

The flap and tab chords in the region $0.142 < y/s < 0.355$ were made constant and equal to the flap and tab chords at the kink (0.09667m and 0.03691m respectively). The flap gap and overlap and the tab pivot position were also made constant and equal to the values at the kink. As a consequence of maintaining the constant flap chord inboard, the flap comprised a smaller proportion of the local wing chord and, because of the large camber at the rear of the basic wing section, this resulted in a twist in the flap of 1.33^{o} nose-up at the body side. The shroud thickness that resulted from this geometry was increased, relative to the basic wing, firstly because of the decreased thickness of the flap relative to the local chord and secondly because of the twist in the flap.

The values of the dimensions g and h for the slat, flap and tab geometry at the body side ($y/s = 0.142$) are given in Table 1d. These dimensions varied linearly between the kink ($y/s = 0.355$) and the body side.

Appendix B

DESIGN OF THE HIGH-LIFT WING AND SOME REMARKS ON THE OPERATION OF HIGH-LIFT, COMPLETE AIRCRAFT MODELS

B.1 The design and operation of the high-lift wing

The model design requirements included the following geometric considerations:

(1) variation of the deflection angles for slats, flaps and tabs,

(2) variation of the span of the flap/tab system,

(3) ability to make streamwise cutouts in the flap/tab system.

A full-span slat, flap and tab was designed so that each could be split into spanwise sections. The basic flap corresponded to the full-span flap at 10° deflection as this had the shortest overall length. (The length of the flap required varied with the deflection position because the angle of sweep of the flap changed as it was translated and rotated.) Three separate sets of brackets, one for each deflection position, were used to attach the basic flap to the wing, and filler pieces were secured to the flap to make up the correct span for a particular deflection angle. Two further sets of filler pieces for adding to the flap ends were necessary to ensure:

(1) that the flap ends were streamwise, and

(2) that the flap ends at any cutout in the flap system were at the correct spanwise position for a given deflection angle.

In addition retracted-flap pieces were needed to represent the retracted flap at the engine and body cutout positions, or alternatively, sets of filler pieces were needed to add to the corresponding basic flap sections when retracted.

The basic full-span tab (0° deflection position) corresponded to the basic flap. The tabs were secured to the flap by brackets (one set for each of the three deflection positions). In order to allow for the geometric requirements mentioned above it would have been necessary to provide similar sets of filler pieces for the flap/tab ends for each of the three tab deflection angles. Fortunately the majority of the measurements were made with the 0° tab angle so that a complete set of filler pieces was not required.

The basic slat corresponded to the full-span slat at 25° deflection (as this had the shortest overall length of the deflected slats) and the angle was used for the main body of testing. The change in span that resulted from

changing the deflection of the slat from 25^{o} to 15^{o} was small as no translation was involved in this change of position. A single set of streamwise brackets was used for mounting the slats. The three slat deflection angles were obtained by using a set of wedges for each angle to locate the brackets relative to the landings on the slat.

Detachable leading-edge pieces were used for the nose of the basic aerofoil and for the modified nose when the slat was deflected. A streamwise cut was made in the leading-edge pieces at $y/s = 0.142$ so that, with the body fitted, a step in the leading-edge profile between the nose of the basic wing and the modified nose, used with the deflected slat, could be properly represented. For the same reason a similar cut was made in the flap/tab system at $y/s = 0.142$. Both these features can be seen in the photographs in Fig.7.

This system of a basic slat, flap and tab, with a range of brackets, wedges and filler pieces to make up other slat, flap/tab arrangements as required was found to be satisfactory for model changes in the wind tunnel. A definite advantage of this method of model construction was that small changes in the model (e.g. changing the junction piece between the deflected flap and the body side) could be made without disturbing the remainder of the wing, as it was only necessary to change a filler piece. On the other hand the following disadvantages became apparent during the use of this system:

(i) The large number of small parts resulted in excessive time being used in learning the system and finding the correct pieces for a particular model arrangement. There was also a significant risk of loss of the small parts and attachment screws.

(ii) The surfaces of the resulting high-lift system were broken by many joint lines where the various filler pieces were attached and some care was necessary to ensure that leaks did not occur between the upper and lower surfaces.

(iii) Because of the many joints in the slat, flap and tab assemblies (e.g. for the slat: flat to wedge, wedge to bracket and bracket to main span), there was some concern that the geometry of the high-lift system would not be maintained over a period of assembly and disassembly. This possibility was reduced by keeping the number of model changes to a minimum and choosing a test programme that normally required only one geometric parameter to be varied at a time. The slat setting was checked between the two series of tests and a

slight movement from the design position was detected and corrected. During the second series of tests the slat was only changed once.

An alternative method of designing a model high-lift system would be to use a set of sub-assemblies (e.g. slat and bracket and leading edge) covering a part of the span, that secured to a standard location on the spar. This method would overcome the above disadvantages and have important advantages during manufacture. For the present model a large amount of manufacturing time was spent in ensuring interchangeability between the various combinations of model pieces that might be required for test configurations. Although the alternative method would require many sub-assemblies, each would only need one standard location point on the wing, and the extra time spent in making sub-assemblies should be less than the time spent in ensuring interchangeability on the present model.

B.2 Slat bracket design

The slats were supported by circular arc brackets aligned parallel to the free stream direction (Fig.3a). These were attached to the lower surface of the main wing and to a landing on the slat immediately behind the 'knee' of the slat. The planform was chosen so that the bracket was located in a low velocity region, and the minimum blockage was added to the slat gap. The cross-section of the brackets (normal to their leading edge) was made relatively thick (a thickness/chord ratio in the range $0.3 < t/c < 0.63$) and a semicircular nose profile used, partly in order to accommodate the slat fixing screws, but also to ensure that any cross flow in this region did not cause separation of the flow round the bracket. Examination of the surface flow in this area by the Dayglow flow visualisation technique showed that the brackets produced a turbulent wake which broke through the short laminar separation bubble on the upper surface of the wing but otherwise caused negligible interference to the flow at low incidence, even though cross flow was visible in the path of the portion of the slat wake that passed over the top surface of the wing. Subsequent work[9] using both thick and thin slat brackets of a similar design to those used on the present model has confirmed the advantages of using a relatively thick slat bracket of circular-arc shape.

B.3 Flap bracket design

The design of a flap bracket is less critical than a slat bracket as the local velocities are much closer to the free stream value in the region of the flap gap. The flap was therefore supported by streamwise flat-plate brackets

(Fig.3b) which were fitted to the lower surface of the shroud and the lower surface of the flap (recessed into the flap in order to preserve the flap profile). A semicircular cutout was made in the brackets between the flap leading edge and the shroud so that the flap gap was not blocked.

In order to determine the effect of the flap bracket on the lift and drag characteristics, the inner part of the flap system on the extended wing was arranged so that it could be supported on either two or three brackets. The increments in lift and drag coefficients at constant wing incidence, due to adding the third bracket at y/s = 0.237, are shown in Fig.98a and b respectively, for flap deflection angles of 10°, 25° and 40°. For the 10° flap deflection angle there is an increase in both lift and drag coefficients, while for the 25° and 40° deflection angles (which have similar flap gaps and overlaps, and hence similar brackets) there is a decrease in both lift and drag coefficients which is approximately the same for the two deflection angles. The drag polars for the wing with and without the extra bracket were identical except near the stall and for the 40° flap deflection angle. This would suggest that the effect of the additional bracket was only local in extent, and that any change in lift was offset by a change in drag. This could be explained by an interference between the bracket and the flap flow producing a major change in the local normal force on the flap and hence, after resolution, on the lift and drag forces. The increase in overall wing incidence that would be necessary to collapse the lift and drag coefficient curves versus incidence, when the bracket was added, is shown in Fig.99. It can be seen that there must be a large change (of the order of a few degrees) in the effective camber of the aerofoil in the region of the bracket. A favourable interference was measured with the flap deflected 10° (a reduction in wing incidence being required), but an adverse effect for the flap deflected 25° and 40°.

B.4 Testing of the slatted wing without a body

When testing the wing alone it was mounted on a three strut system. Two main struts were attached to the wing and the third, an aft pitching moment strut, was connected to the wing by a sting. This sting was suitably stressed for the loads anticipated and rigidly attached to the undersurface of the wing. With the slats extended and the flaps deflected 25° or 40° severe pitching oscillations were encountered in the incidence range $-5^{\circ} < \alpha_w < 0^{\circ}$. This behaviour was attributed to the slat stalling at negative incidence and causing

the flow over the majority of the lower surface of the wing to separate. As wing incidence was increased from -5° to 0°, the flow became attached to the lower surface of the slat and the main wing, and caused a sudden increase in the effective camber of the wing section. Consequently there was a sudden increase in lift in the region of the flap (because $dC_L/d\alpha_w \doteq 0.35$ per degree) and a correspondingly large decrease in the pitching moment of the wing (because $dC_m/d\alpha_w \doteq -0.17$ per degree).

The large decrement in pitching moment tended to make the incidence more negative but it was resisted by the bending stiffness of the sting support. Thus at an angle of incidence near where stalling of the lower surface of the slat occurred conditions were such that, unless the sting was very stiff and had a damping effect, large amplitude oscillations of the wing could occur (up to approximately $\pm 3^{\circ}$ incidence change for the sting used on the present model).

For the wing/body combination the pitching moment strut was attached to the rear of the body and no oscillations occurred. As the body was both stiffer and provided more damping than the sting it prevented the growth of any pitch oscillation. The removal of the centre section of the high-lift system ($0 < y/s < 0.142$) may have had some beneficial effect, although the aerodynamic characteristics (C_L versus $\alpha_w{}^{\circ}$ and C_m versus $\alpha_w{}^{\circ}$ curves) were little changed by the addition of the body. It was concluded that any future work which necessitated wing alone testing of high-lift systems in this incidence range (which has some practical importance - for example the investigation of the force and moment characteristics during take-off and landing) would require the use of a sting having much greater stiffness and damping.

Appendix C

LIFT ANALYSIS METHOD

Two linear theory methods were used for calculating the spanwise loading on the various configurations tested. Both methods assumed the flow was inviscid and incompressible, and approximations for thin wings were made throughout.

The method of McKie[4] was used to calculate the effects of changing the flap deflection angle, the flap span, and the planform, and to determine the effect of cutouts in the trailing-edge flap system. To calculate the lift for configurations where the slat or flap extended over the full span, the planform was adjusted to include the area extension caused by the deployment of the slat and/or flap. By this means values for the mid-chord sweep and aspect ratio of the actual extended planform were used in the calculations. All the lift coefficients derived in this manner were factored to refer to the area of the *basic* straight-tapered planform. The slat and slotted flap were represented by extending the slat and flap chord lines until they intersected the chord line of the main wing, and this point of intersection was taken as the hinge line of a simple flap. The area extensions resulting from the translation of the slat and flap systems during their deployment were defined from the projection of the new planform onto a horizontal plane when the wing reference plane was at 0° incidence.

In order to calculate the lift coefficient increments produced by the combined deflection of slats and flaps the increment due to the slat was calculated first with the chord extension included as described above. The slat was then treated as the 'main wing' and the remainder of the wing as the 'flap'. This 'flap' was then deflected through the slat deflection angle and the combination set at the required geometric incidence less the slat deflection angle. McKie defined[4] an equivalent angle of incidence as the angle of incidence that a flat-plate aerofoil would have to be given in order to achieve the same increment in sectional lift coefficient as was produced by the deflection of a simple flap on the flat plate at zero incidence. The spanwise distribution of this equivalent incidence, obtained from the results of the slatted-wing spanwise load calculation, was then applied as a twist distribution to the flat-plate wing in order to replace the slat deflection geometry. For the large flap deflection angles used (typically 25°) the limitations of the linear theory required some slight modifications to the twist distribution in order to obtain

the same C_L with the twisted flat plate as with the slat geometry, at a given incidence, but this was confined to a small constant addition to the twist ($<0.01^{\circ}$). Using this twist distribution to represent the slat, the trailing-edge flap geometry was then added and the lift calculated for the wing with the complete high-lift system.

The method of Weber, Kirby and Kettle[3] was used to calculate the effects of the body on the spanwise loading with the high-lift system deflected. Unfortunately this method does not include provision for the spanwise discontinuities in chord that are required for extending-chord flaps so no calculations were made for part-span flaps. In addition there is no provision for handling a deflected flap in the manner of Mckie[4], but *full-span* slats and flaps were again represented by applying an equivalent twist distribution to the flat-plate wing (thickness effects have been ignored in the calculations). The equivalent twist distribution for the slat deflected alone was determined first and this was used in conjunction with the flaps deflected to obtain an equivalent twist distribution for the wing with slats and flaps deflected. Again a small, constant twist correction was required because of the limitations of the linear-theory approximations. The planform used for the calculations with a body was the nett wing (i.e that part of the wing not covered by the body), with the appropriate chordwise extensions to represent the translations of the deflected slats and flaps. To obtain the lift for the corresponding wing-alone configuration the same procedure was followed using the gross wing.

In view of the degree of approximation in representing the wing geometry a similar degree of approximation could reasonably be accepted for the body. The loads due to the body were calculated for a mid-mounted wing, as the wing was offset below the body centreline by only 0.12 of the body diameter. The nose load was calculated by slender body theory and it was assumed that the tail section produced no lift contribution.

The experimental and theoretical values for the lift coefficients were all referred to the basic straight-tapered wing planform area without the body. The increments in lift coefficient, due to the various changes in the high-lift system, were compared at constant values of wing incidence. Because of the effects of wind-tunnel wall constraint on the corrected model attitude, the wing incidence values for the results from two model configurations were not the same. To obtain the increments from experiment, one of the two configurations was regarded

as a datum and the smoothed α_w versus C_L curve for this datum was used in a simple quadratic interpolation to find the C_L at the values of wing incidence corresponding to the second configuration. All the increments in lift coefficient were referred to the area of the basic straight tapered planform.

Appendix D

DRAG ANALYSIS METHOD

The method of drag analysis proposed by Maskell[5] can be reduced to a simple relation between the overall lift and drag coefficients of a wing. The parabolic variation of the vortex drag coefficient with lift coefficient combines with the parabolic variation of profile drag coefficient with lift coefficient, under the linear approximations used in this theory, to form the relation:

$$C_D = \breve{C}_D + \frac{k}{\pi A} (C_L - \breve{C}_L)^2 \qquad (D-1)$$

where C_D is the measured drag coefficient

$\breve{C}_D$ is the minimum drag coefficient

k is the lift-dependent drag factor (this includes the lift-dependency of both vortex and profile drag)

A is the wing aspect ratio

C_L is the measured lift coefficient

$\breve{C}_L$ is the lift coefficient at which the minimum drag $\breve{C}_D$ occurs.

To obtain the values of k, $\breve{C}_L$ and $\breve{C}_D$ from the experimental results a least-squares fit to equation (D-1) was used. By means of some initial curve fitting an incidence range was determined over which the flow was attached (apart from areas on the underside of the slat and in the front of the flap shroud). The limits of this incidence range were used to determine the effect of discarding successive end points up to a maximum of 5 (i.e. approximately 5^o change in incidence) at each end. In this manner the curve fitting procedure could be used to obtain values of k, $\breve{C}_L$ and $\breve{C}_D$ that were to a large extent insensitive to any variation in the number of points taken from a reduced incidence range.

The initial curve fitting exercise showed that, as might be expected, the values of $\breve{C}_D$ and $\breve{C}_L$ were very sensitive to small changes in k, and furthermore such small changes in k produced no observable change in the accuracy of the curve fitting. The accuracy of the curve fitting over the chosen range of incidence was measured by the largest difference between the measured drag coefficient and the value on the least-squares fit curve at the same lift coefficient. This error was as low as 0.0003 for many configurations, but a more typical value was 0.0006. In order to remove the degree of arbitrariness in $\breve{C}_D$ and $\breve{C}_L$, caused by small changes in the value of k, values of k were estimated to the nearest 0.05 from the initial curve fitting and a second least-squares curve fitting procedure was used for a range of values of k, differing

by 0.05, for each model configuration. $\breve{C}_D$ and $\breve{C}_L$ were allowed to vary to give the best fit to the experimental data for each value of k. By this method values of k and $\breve{C}_D$ (for a particular value of k) could be determined to within 0.05 and 0.0005 respectively. The analyses was completed by applying a third least-squares curve fitting procedure (in which k and $\breve{C}_D$ were assumed to be known) to the experimental data to find $\breve{C}_L$, which could be determined to within 0.005.

The values of the parameters k, $\breve{C}_D$ and $\breve{C}_L$ predicted by the linear, inviscid theory of Mckie[4], were obtained by calculating the lift coefficient and vortex drag coefficient at any three values of wing incidence for each configuration, and fitting the parabola through these three points on the (parabolic) vortex drag polar. The high-lift system of slats and flaps was represented by hinged flat-plate flaps and equivalent twist distributions as described in Appendix C. The nett wing was used for the wing/body combinations, and hence a perfect reflection at the wing root was implied instead of the actual reflection from a cylindrical body. No estimate was made of the contribution of the body to the vortex drag. In view of the lack of experimental information, and the complexity of the three-dimensional viscous flow on the wing, no attempt was made to estimate the profile drag and its variation with lift.

Table 1

ORDINATES OF WING SECTION AND HIGH-LIFT SECTION ELEMENTS

(a) Basic wing section

Ordinates relative to the wing reference plane and camber relative to the chord line

$\frac{x}{c}$	Upper surface $\frac{Z_U}{c}$	Lower surface $\frac{Z_L}{c}$	Thickness $\frac{Z_T}{c}$	Camber $\frac{Z_C}{c}$
0	-0.01015	0.01015	0	0
0.00100	-0.00430	0.01506	0.01076	0.00046
0.00299	0.00122	0.01841	0.01963	0.00152
0.00498	0.00411	0.02012	0.02423	0.00210
0.00736	0.00676	0.02190	0.02866	0.00251
0.01454	0.01200	0.02581	0.03781	0.00310
0.02642	0.01687	0.02995	0.04682	0.00334
0.04284	0.02149	0.03387	0.05536	0.00353
0.06373	0.02573	0.03757	0.06330	0.00358
0.08881	0.02981	0.04080	0.07061	0.00375
0.11791	0.03398	0.04413	0.07811	0.00387
0.15070	0.03793	0.04713	0.08506	0.00402
0.18687	0.04140	0.04991	0.09131	0.00399
0.22607	0.04417	0.05291	0.09708	0.00349
0.26796	0.04618	0.05566	0.10184	0.00269
0.31209	0.04762	0.05732	0.10494	0.00213
0.35806	0.04870	0.05796	0.10666	0.00189
0.40542	0.04913	0.05701	0.10614	0.00210
0.45373	0.04925	0.05403	0.10328	0.00315
0.50249	0.04873	0.04932	0.09805	0.00475
0.55124	0.04740	0.04363	0.09103	0.00643
0.59955	0.04555	0.03734	0.08289	0.00817
0.64692	0.04277	0.03088	0.07365	0.00952
0.69289	0.03909	0.02460	0.06369	0.01036
0.73702	0.03489	0.01870	0.05359	0.01077
0.77891	0.03051	0.01365	0.04416	0.01067
0.81811	0.02622	0.00935	0.03557	0.01029
0.85428	0.02208	0.00590	0.02798	0.00957
0.88707	0.01791	0.00325	0.02116	0.00848
0.90000	0.01620	0.00245	0.01865	0.00790
0.91187	0.01464	0.00156	0.01620	0.00743
0.93705	0.01113	0.00043	0.01156	0.00599
0.96852	0.00616	-0.00026	0.00590	0.00353
1.00000	0	0	0	0

Table 1 (continued)

(b) Slat, flap and tab ordinates of basic high-lift system

Ordinates relative to the wing reference plane

Slat undersurface ordinates
(and nose ordinates with slat deflected)

$\frac{x}{c}$	$\frac{Z}{c}$
0.02543	-0.02746
0.02616	-0.02169
0.02759	-0.01749
0.03035	-0.01243
0.03475	-0.00661
0.03974	-0.00176
0.04817	0.00417
0.05737	0.00894
0.06739	0.01327
0.07820	0.01717
0.08989	0.02089
0.10244	0.02456
0.11574	0.02808
0.13007	0.03154
0.14521	0.03477
0.15758	0.03716
0.16000	0.03775

Flap ordinates

$\frac{x}{c}$	Upper surface $\frac{Z_U}{c}$	Lower surface $\frac{Z_L}{c}$
0.66000	-0.02378	0.02378
0.66226	-0.01876	
0.66452	-0.01610	0.02842
0.66904	-0.01239	
0.67355	-0.00923	
0.67806	-0.00680	
0.68259	-0.00459	0.02595
0.70517	0.00394	
0.72776	0.00897	0.01993
0.75033	0.01174	
0.79550	0.01438	0.01166
0.82550	0.01492	
0.84082		0.00719
0.85422		0.00589
0.85873		0.00528
0.86326		0.00425
0.86777		0.00234
0.87002		0.00061
0.87229		-0.00269
0.87455		-0.00780
0.87680		-0.00988
0.88132		-0.01278
0.88586	0.01542	-0.01460
	Tab ordinates	
0.87410	0.00316	-0.00316
0.87567	0.00719	0.00052
0.87725	0.00875	0.00160
0.88040	0.01097	0.00268
0.88669	0.01374	0.00321
0.89928	0.01555	0.00243
0.91187	0.01464	0.00156
0.93705	0.01113	0.00043
0.96852	0.00616	-0.00026
1.00000	0	0

Table 1 (continued)

(c) Slat, flap and tab ordinates of high-lift system used with extended planform
($y/s = 0.142$, body side)

Ordinates relative to the wing reference plane

Slat undersurface ordinates
(and nose ordinates with slat deflected)

$\frac{x}{c}$	$\frac{Z}{c}$
0.01995	-0.02576
0.02044	-0.02052
0.02164	-0.01671
0.02381	-0.01209
0.02726	-0.00673
0.03118	-0.00231
0.03779	0.00310
0.04501	0.00759
0.05287	0.01158
0.06135	0.01511
0.07052	0.01857
0.08037	0.02186
0.09080	0.02499
0.10204	0.02813
0.11392	0.03111
0.12362	0.03329
0.12552	0.03465

Flap ordinates

$\frac{x}{c}$	Upper surface $\frac{Z_U}{c}$	Lower surface $\frac{Z_L}{c}$
0.77390	-0.01054	0.01054
0.77540	-0.00743	0.01325
0.77690	-0.00582	0.01389
0.77991	-0.00340	0.01354
0.78291	-0.00144	0.01320
0.78592	0.00017	0.01285
0.78892	0.00150	0.01250
0.80394	0.00674	0.01101
0.81891	0.00980	0.00939
0.83397	0.01124	0.00789
0.86401	0.01216	0.00524
0.89414		0.00294
0.90304		0.00236
0.90606		0.00207
0.90907		0.00150
0.91207		0.00035
0.91357		-0.00086
0.91507		-0.00294
0.91658		-0.00622
0.91807		-0.00772
0.92108		-0.00945
0.92410	0.01124	-0.01072
	Tab ordinates	
0.91628	0.00328	-0.00328
0.91733	0.00582	-0.00086
0.91837	0.00697	-0.00012
0.92047	0.00835	0.00063
0.92465	0.01008	0.00104
0.93302	0.01095	0.00063
0.94140	0.01054	0.00035
0.95814	0.00766	-0.00017
0.97907	0.00432	-0.00052
1.00000	0	0

Table 1 (concluded)

(d) Slat, flap and tab deflection geometry

The dimensions g and h are defined in Fig.2

	Basic wing	Extended planform $\frac{y}{s} = 0.142$
Slat chord/local chord	0.16000	0.12552
Slat pivot position (underside of trailing edge):		
g/c	0.00967	0.00967
h/c	0.02248	0.01763
Flap chord/local chord	0.34000	0.22610
Flap gap and overlap:		
10° deflection g/c	0.01300	0.00864
10° deflection h/c	0.06295	0.04189
25° deflection g/c	0.01864	0.01239
25° deflection h/c	0.03530	0.02345
40° deflection g/c	0.01701	0.01129
40° deflection h/c	0.00591	0.00398
Tab chord/local chord	0.12590	0.08372
Tab pivot position:		
g/c	0.01776	0.01181
h/c	0.09495	0.06314
Position of leading edge with slat deflected/ local chord	0.02560	0.02008
Position of flap shroud/ local chord	0.90000	0.92815

Table 2

GEOMETRIC DETAILS OF THE MODEL

Basic wing (straight-tapered planform)

Gross area	$0.5523m^2$
Gross span	2.148m
Standard mean chord	0.2572m
Centre-line chord	0.3810m
Aspect ratio	8.351
Taper ratio	0.3500
Dihedral	0^o
Leading edge sweepback	30.51^o
Quarter-chord sweepback	28^o
Trailing edge sweepback	19.74^o
Position of the mean quarter chord aft of the wing apex	0.3349m
Inclination of wing reference plane to body axis	1.10^o
Slat chord	16% of local chord
Slat deflection angles	15^o, 20^o, 25^o
Flap chord	34% of local chord
Flap deflection angles	10^o, 25^o, 40^o
Tab chord	12.59% of local chord
Tab deflection angles	15^o, 30^o

Extended planform

Gross area		$0.6126m^2$
Gross span		2.148m
Standard mean chord		0.2853m
Centre-line chord		0.5393m
Aspect ratio		7.529
Taper ratio		0.2473
Spanwise position of kink in trailing edge		0.3810m (35.48% span)
Chord at the position of the kink		0.2931m
Trailing edge of extension; sweepforward		3.25^o
Position of the mean quarter chord aft of the wing apex		0.3292m
Inclination of wing reference plane to body axis		1.10^o
Slat, flap and tab deflections unchanged and chords unchanged outboard of the kink		
Inboard:	slat chord unchanged	16% of the corresponding local chord of the basic wing
	flap chord	0.09965m
	tab chord	0.03691m

Table 2 (concluded)

Fuselage

Diameter	0.3048m
Overall length	2.239m
Distance of the wing apex aft of the nose (for both planforms)	0.7161m
Distance of the wing apex below the body centre line (for both planforms)	0.0368m

Table 3

MODEL CONFIGURATIONS TESTED

Transition was left free and the windspeed was 76m/s except where noted. 'Body cutout' signifies that the flap/tab section from the centre line to $y_F/s = 0.142$ is retracted and 'engine cutout' signifies that the flap/tab section from $y_F/s = 0.257$ to $y_F/s = 0.355$ is retracted.

No.	Wing planform	Body on or off	Leading edge slats	Trailing edge				Notes
				Flaps	Tabs	y_F/s	Cutouts	
1	Basic	Off	Retracted	Retracted				Windspeed 46m/s
2								Windspeed 61m/s
3								
4								Windspeed 91m/s
5								Fixed transition
6				10°	0°	1.0		
7						0.8		
8						0.6		
9						0.355		
10						1.0	Body	
11				25°	0°	1.0		
12						0.8		
13						0.6		
14						0.355		
15						1.0	Body	
16				40°	0°	1.0		
17						1.0	Body	
18			15°	Retracted				
19			25°	Retracted				
20				10°	0°	1.0		
21						0.8		
22						0.8	Engine	
23						0.6		
24						0.355		
25						1.0	Body	
26						0.8	Body	
27						0.8	Engine, body	
28						0.6	Body	
29						0.355	Body	
30				25°	0°	1.0		
31						0.8		
32						0.8	Engine	
33						0.6		
34						0.355		
35						1.0	Body	
36				40°	0°	1.0		
37						1.0	Body	
38		On	Retracted	Retracted				
39				10°	0°	1.0		
40						0.8		
41						0.6		
42						0.355		
43				25°	0°	1.0		
44						0.8		
45						0.6		
46						0.355		
47				40°	0°	1.0		
48						0.8		
49						0.6		
50						0.355		

Table 3 (concluded)

No.	Wing planform	Body on or off	Leading edge slats	Trailing edge				Notes
				Flaps	Tabs	y_F/s	Cutouts	
51	Basic	On	15°	Retracted				
52				10°	0°	1.0		
53			25°	Retracted				
54				10°	0°	1.0		
55						0.8		
56						0.8	Engine	
57						0.6		
58						0.355		
59				25°	0°	1.0		
60						0.8		
61						0.8	Engine	
62						0.6		
63				40°	0°	1.0		
64						0.8		
65						0.8	Engine	
66						0.6		
67	Extended	Off	Retracted	Retracted				
68				10°	0°	1.0	Body	
69				25°	0°	1.0	Body	
70				40°	0°	1.0	Body	
71		On	Retracted	Retracted				
72				10°	0°	1.0		
73				25°	0°	1.0		
74				40°	0°	1.0		
75			25°	Retracted				
76				10°	0°	1.0		
77						0.8		
78						0.8	Engine	
79						0.6		
80				25°	0°	1.0		
81						0.8		
82						0.8	Engine	
83						0.6		
84					15°	0.8		
85					30°	0.8		
86				40°	0°	1.0		
87						0.8		
88						0.8	Engine	
89						0.6		
90					15°	0.8		
91					30°	0.8		

Table 4

LONGITUDINAL FORCE AND MOMENT COEFFICIENTS FOR THE CONFIGURATIONS TESTED

All the tabulated coefficients are non-dimensionalised with respect to the planform area of the basic straight-tapered wing. All the pitching moment coefficients are non-dimensionalised using the standard mean chord of the basic wing and are referred to the mean quarter-chord point of the basic wing planform. The incidence is that of the wing reference plane.

The test runs are numbered in the order listed in Table 3.

Table 4 (continued)

1 BASIC WING. SLATS RETRACTED. FLAPS 0, TABS 0. 46 M/S. FREE TRANSITION.

ALPHA	CL	CD	CM
-15.80	-0.734	0.2249	-0.0727
-14.79	-0.724	0.1998	-0.0736
-13.79	-0.717	0.1746	-0.0762
-12.78	-0.699	0.1418	-0.0772
-11.78	-0.697	0.1016	-0.0569
-10.77	-0.660	0.0855	-0.0410
-9.75	-0.622	0.0647	-0.0176
-8.73	-0.566	0.0452	-0.0094
-7.70	-0.495	0.0340	-0.0135
-6.67	-0.423	0.0265	-0.0170
-5.64	-0.342	0.0220	-0.0215
-4.60	-0.254	0.0182	-0.0275
-3.57	-0.165	0.0151	-0.0361
-2.53	-0.083	0.0123	-0.0415
-1.50	0.001	0.0105	-0.0470
-0.47	0.077	0.0103	-0.0498
-0.47	0.073	0.0102	-0.0488
0.56	0.149	0.0106	-0.0503
1.59	0.224	0.0118	-0.0488
2.62	0.290	0.0142	-0.0463
3.65	0.361	0.0168	-0.0458
4.68	0.438	0.0197	-0.0465
5.71	0.515	0.0230	-0.0469
6.74	0.585	0.0267	-0.0472
7.77	0.657	0.0314	-0.0455
8.79	0.727	0.0389	-0.0447
9.82	0.789	0.0553	-0.0414
10.83	0.828	0.0710	-0.0303
11.84	0.841	0.0990	0.0110
12.84	0.841	0.1264	0.0388
13.84	0.850	0.1488	0.0574
14.84	0.838	0.1862	0.0731
15.84	0.836	0.2111	0.0781
16.84	0.833	0.2348	0.0775
17.84	0.835	0.2556	0.0734

2 BASIC WING. SLATS RETRACTED. FLAPS 0, TABS 0. 61 M/S. FREE TRANSITION.

ALPHA	CL	CD	CM
-5.64	-0.352	0.0173	-0.0333
-4.61	-0.262	0.0169	-0.0391
-3.57	-0.175	0.0144	-0.0438
-2.54	-0.093	0.0120	-0.0479
-1.50	-0.010	0.0105	-0.0506
-0.47	0.063	0.0102	-0.0536
0.56	0.144	0.0106	-0.0563
1.59	0.219	0.0122	-0.0547
2.62	0.288	0.0142	-0.0539
3.65	0.363	0.0166	-0.0547
4.68	0.441	0.0195	-0.0564
5.71	0.520	0.0231	-0.0586
6.74	0.592	0.0269	-0.0595
7.77	0.666	0.0317	-0.0589
8.80	0.738	0.0367	-0.0563
9.83	0.807	0.0469	-0.0551
10.84	0.849	0.0673	-0.0439
11.85	0.863	0.0999	-0.0077
12.84	0.853	0.1312	0.0242
13.85	0.872	0.1493	0.0366
14.85	0.866	0.1803	0.0497
15.84	0.839	0.2154	0.0612
16.86	0.901	0.2447	0.0289
17.84	0.842	0.2605	0.0554

Table 4 (continued)

3 BASIC WING. SLATS RETRACTED.
FLAPS 0, TABS 0.
76 M/S. FREE TRANSITION.

ALPHA	CL	CD	CM
-5.12	-0.297	0.0170	-0.0401
-4.09	-0.220	0.0139	-0.0410
-3.05	-0.126	0.0113	-0.0432
-2.02	-0.043	0.0097	-0.0467
-0.98	0.046	0.0086	-0.0487
0.05	0.118	0.0092	-0.0528
1.08	0.197	0.0103	-0.0547
2.11	0.269	0.0126	-0.0517
3.14	0.339	0.0149	-0.0521
4.17	0.431	0.0179	-0.0536
5.20	0.492	0.0203	-0.0547
6.23	0.572	0.0235	-0.0533
7.27	0.660	0.0284	-0.0533
8.29	0.721	0.0323	-0.0523
9.32	0.797	0.0380	-0.0502
10.35	0.867	0.0512	-0.0457
11.37	0.910	0.0621	-0.0359
12.38	0.945	0.0810	-0.0296
13.36	0.896	0.1315	0.0238
14.36	0.898	0.1603	0.0512
15.37	0.918	0.1817	0.0581
16.37	0.918	0.2305	0.0309
17.37	0.924	0.2560	0.0214
18.37	0.919	0.2768	0.0134

4 BASIC WING. SLATS RETRACTED.
FLAPS 0, TABS 0.
91 M/S. FREE TRANSITION.

ALPHA	CL	CD	CM
-5.64	-0.354	0.0192	-0.0362
-4.61	-0.262	0.0152	-0.0392
-3.58	-0.193	0.0130	-0.0427
-2.54	-0.091	0.0109	-0.0454
-1.51	-0.013	0.0095	-0.0473
-0.47	0.066	0.0088	-0.0493
0.56	0.158	0.0094	-0.0507
1.59	0.220	0.0109	-0.0489
2.62	0.306	0.0133	-0.0500
3.65	0.368	0.0150	-0.0513
4.68	0.443	0.0177	-0.0532
5.71	0.531	0.0213	-0.0544
6.74	0.596	0.0248	-0.0541
7.77	0.674	0.0295	-0.0543
8.80	0.744	0.0342	-0.0533
9.83	0.829	0.0426	-0.0512
10.85	0.866	0.0692	-0.0345
11.85	0.875	0.1015	0.0026
12.84	0.855	0.1299	0.0307
13.85	0.873	0.1518	0.0427
14.86	0.893	0.1719	0.0509

Table 4 (continued)

5 BASIC WING. SLATS RETRACTED.
FLAPS 0, TABS 0.
76 M/S. FIXED TRANSITION.

ALPHA	CL	CD	CM
-15.84	-0.842	0.2289	0.0161
-14.84	-0.837	0.1972	0.0028
-13.83	-0.824	0.1673	-0.0083
-12.82	-0.790	0.1324	-0.0187
-11.81	-0.763	0.0925	-0.0253
-10.79	-0.725	0.0677	-0.0235
-9.77	-0.660	0.0498	-0.0230
-8.74	-0.586	0.0367	-0.0241
-7.70	-0.505	0.0285	-0.0245
-6.68	-0.438	0.0239	-0.0263
-5.64	-0.346	0.0197	-0.0297
-4.61	-0.270	0.0164	-0.0319
-3.58	-0.186	0.0137	-0.0343
-2.54	-0.109	0.0119	-0.0378
-1.51	-0.024	0.0103	-0.0406
-0.48	0.058	0.0096	-0.0438
0.55	0.133	0.0101	-0.0459
1.59	0.212	0.0112	-0.0474
2.61	0.284	0.0132	-0.0476
3.65	0.362	0.0157	-0.0492
4.68	0.446	0.0186	-0.0503
5.71	0.526	0.0222	-0.0514
6.74	0.594	0.0259	-0.0515
7.77	0.664	0.0301	-0.0508
8.79	0.727	0.0345	-0.0496
9.83	0.812	0.0425	-0.0480
10.85	0.876	0.0552	-0.0440
11.87	0.922	0.0776	-0.0383
12.90	0.979	0.1039	-0.0304
13.91	1.009	0.1402	-0.0281
14.91	1.021	0.1798	-0.0314
15.92	1.036	0.2201	-0.0455
16.92	1.038	0.2487	-0.0499
17.92	1.034	0.2807	-0.0638

6 BASIC WING. SLATS RETRACTED.
FLAPS 10, TABS 0. 100% SPAN.
76 M/S. FREE TRANSITION.

ALPHA	CL	CD	CM
-4.98	0.046	0.0160	-0.1640
-3.95	0.127	0.0157	-0.1743
-2.90	0.247	0.0165	-0.1920
-1.86	0.344	0.0183	-0.2020
-0.81	0.465	0.0220	-0.2138
0.22	0.557	0.0269	-0.2190
1.26	0.633	0.0311	-0.2260
2.30	0.745	0.0376	-0.2359
3.34	0.845	0.0442	-0.2450
4.38	0.932	0.0507	-0.2525
5.42	1.041	0.0600	-0.2612
6.45	1.108	0.0664	-0.2659
7.48	1.201	0.0777	-0.2707
8.51	1.269	0.0965	-0.2658
9.53	1.310	0.1217	-0.2459
10.51	1.258	0.1804	-0.1867

7 BASIC WING. SLATS RETRACTED.
FLAPS 10, TABS 0. 80% SPAN.
76 M/S. FREE TRANSITION.

ALPHA	CL	CD	CM
-5.00	0.009	0.0162	-0.1264
-3.96	0.105	0.0157	-0.1361
-2.91	0.228	0.0161	-0.1510
-1.87	0.311	0.0176	-0.1583
-0.84	0.400	0.0198	-0.1643
0.20	0.495	0.0240	-0.1683
1.24	0.594	0.0292	-0.1734
2.28	0.682	0.0339	-0.1796
3.31	0.774	0.0392	-0.1863
4.35	0.863	0.0453	-0.1918
5.39	0.958	0.0525	-0.1974
6.43	1.055	0.0609	-0.2025
7.46	1.136	0.0688	-0.2057
8.49	1.210	0.0885	-0.2033
9.51	1.263	0.1157	-0.1856
10.49	1.218	0.1761	-0.1344

Table 4 (continued)

8 BASIC WING. SLATS RETRACTED.
FLAPS 10, TABS 0. 60% SPAN.
76 M/S. FREE TRANSITION.

ALPHA	CL	CD	CM
-5.02	-0.041	0.0165	-0.0627
-3.98	0.050	0.0156	-0.0893
-2.94	0.139	0.0153	-0.0963
-1.90	0.243	0.0162	-0.1023
-0.87	0.332	0.0180	-0.1064
0.17	0.428	0.0214	-0.1100
1.22	0.537	0.0267	-0.1115
2.24	0.593	0.0295	-0.1138
3.28	0.705	0.0356	-0.1193
4.32	0.785	0.0405	-0.1227
5.35	0.870	0.0465	-0.1253
6.40	0.984	0.0557	-0.1288
7.43	1.064	0.0631	-0.1294
8.46	1.132	0.0704	-0.1288
9.47	1.172	0.1006	-0.1154
10.49	1.205	0.1203	-0.1024
11.47	1.164	0.1814	-0.0659

9 BASIC WING. SLATS RETRACTED.
FLAPS 10, TABS 0. 35.5% SPAN.
76 M/S. FREE TRANSITION.

ALPHA	CL	CD	CM
-5.05	-0.131	0.0168	-0.0487
-4.01	-0.035	0.0151	-0.0540
-2.98	0.047	0.0144	-0.0568
-1.94	0.155	0.0142	-0.0601
-0.91	0.235	0.0153	-0.0631
0.13	0.314	0.0170	-0.0651
1.16	0.398	0.0205	-0.0632
2.20	0.505	0.0252	-0.0635
3.23	0.578	0.0286	-0.0652
4.27	0.660	0.0328	-0.0667
5.30	0.736	0.0374	-0.0676
6.33	0.819	0.0431	-0.0681
7.36	0.893	0.0489	-0.0681
8.39	0.975	0.0564	-0.0665
9.42	1.047	0.0654	-0.0639
10.43	1.074	0.1028	-0.0374
11.45	1.105	0.1143	-0.0277
12.43	1.055	0.1775	0.0001

10 BASIC WING. SLATS RETRACTED.
FLAPS 10, TABS 0.
100% SPAN WITH BODY CUTOUT.
76 M/S. FREE TRANSITION.

ALPHA	CL	CD	CM
-5.02	-0.045	0.0172	-0.1633
-3.98	0.041	0.0165	-0.1743
-2.95	0.130	0.0167	-0.1882
-1.91	0.233	0.0177	-0.2002
-0.87	0.323	0.0197	-0.2098
0.17	0.415	0.0229	-0.2172
1.20	0.493	0.0270	-0.2229
2.23	0.582	0.0317	-0.2310
3.27	0.662	0.0361	-0.2389
4.30	0.751	0.0418	-0.2467
5.34	0.847	0.0486	-0.2554
6.38	0.948	0.0568	-0.2635
7.42	1.029	0.0643	-0.2691
8.45	1.117	0.0786	-0.2713
9.47	1.171	0.0972	-0.2627
10.47	1.156	0.1585	-0.1993

11 BASIC WING. SLATS RETRACTED.
FLAPS 25, TABS 0. 100% SPAN.
76 M/S. FREE TRANSITION.

ALPHA	CL	CD	CM
-4.67	0.820	0.0416	-0.4728
-3.64	0.899	0.0477	-0.4792
-2.56	1.033	0.0593	-0.4912
-1.57	1.078	0.0634	-0.4947
-0.51	1.208	0.0762	-0.5078
0.52	1.283	0.0841	-0.5142
1.56	1.397	0.0968	-0.5236
2.61	1.499	0.1096	-0.5328
3.63	1.555	0.1171	-0.5362
4.66	1.640	0.1308	-0.5420
5.69	1.719	0.1484	-0.5389
6.71	1.761	0.1716	-0.5144
7.68	1.680	0.2356	-0.4014

Table 4 (continued)

12 BASIC WING. SLATS RETRACTED.
FLAPS 25, TABS 0. 80% SPAN.
76 M/S. FREE TRANSITION.

ALPHA	CL	CD	CM
-4.73	0.666	0.0361	-0.3395
-3.69	0.772	0.0414	-0.3489
-2.64	0.881	0.0491	-0.3552
-1.61	0.973	0.0574	-0.3589
-0.57	1.061	0.0652	-0.3640
0.47	1.156	0.0737	-0.3704
1.50	1.248	0.0828	-0.3759
2.54	1.337	0.0921	-0.3809
3.58	1.440	0.1042	-0.3859
4.61	1.522	0.1144	-0.3891
5.64	1.594	0.1285	-0.3899
6.66	1.643	0.1494	-0.3779
7.65	1.602	0.2081	-0.3084

13 BASIC WING. SLATS RETRACTED.
FLAPS 25, TABS 0. 60% SPAN.
76 M/S. FREE TRANSITION.

ALPHA	CL	CD	CM
-4.79	0.531	0.0362	-0.1994
-3.77	0.575	0.0379	-0.2016
-2.72	0.693	0.0434	-0.2080
-1.68	0.795	0.0511	-0.2107
-0.64	0.883	0.0583	-0.2126
0.38	0.951	0.0636	-0.2147
1.43	1.058	0.0724	-0.2190
2.45	1.112	0.0773	-0.2206
3.50	1.228	0.0887	-0.2255
4.52	1.296	0.0964	-0.2277
5.56	1.380	0.1068	-0.2302
6.59	1.469	0.1192	-0.2331
7.61	1.513	0.1571	-0.2164
8.63	1.548	0.1798	-0.2038
9.59	1.463	0.2402	-0.1632

14 BASIC WING. SLATS RETRACTED.
FLAPS 25, TABS 0. 35.5% SPAN
76 M/S. FREE TRANSITION.

ALPHA	CL	CD	CM
-4.91	0.232	0.0314	-0.0760
-3.87	0.324	0.0327	-0.0790
-2.83	0.410	0.0347	-0.0814
-1.80	0.494	0.0376	-0.0840
-0.77	0.576	0.0422	-0.0843
0.26	0.656	0.0474	-0.0829
1.30	0.738	0.0527	-0.0824
2.34	0.834	0.0591	-0.0843
3.37	0.916	0.0653	-0.0855
4.40	1.000	0.0724	-0.0864
5.43	1.071	0.0792	-0.0858
6.47	1.157	0.0877	-0.0854
7.50	1.231	0.0962	-0.0831
8.53	1.303	0.1073	-0.0795
9.53	1.305	0.1489	-0.0597
10.54	1.345	0.1736	-0.0533

15 BASIC WING. SLATS RETRACTED.
FLAPS 25, TABS 0.
100% SPAN WITH BODY CUTOUT.
76 M/S. FREE TRANSITION.

ALPHA	CL	CD	CM
-4.81	0.473	0.0422	-0.4660
-3.76	0.595	0.0475	-0.4804
-2.72	0.685	0.0521	-0.4901
-1.69	0.777	0.0592	-0.4968
-0.65	0.865	0.0662	-0.5055
0.39	0.970	0.0734	-0.5109
1.42	1.051	0.0811	-0.5169
2.46	1.148	0.0907	-0.5270
3.49	1.210	0.0973	-0.5314
4.53	1.314	0.1092	-0.5396
5.57	1.411	0.1239	-0.5417
6.59	1.468	0.1356	-0.5377
7.60	1.479	0.1806	-0.4645
8.59	1.468	0.2053	-0.4239

Table 4 (continued)

16 BASIC WING. SLATS RETRACTED.
FLAPS 40, TABS 0. 100% SPAN.
76 M/S. FREE TRANSITION.

ALPHA	CL	CD	CM
-4.52	1.182	0.1158	-0.6011
-3.48	1.280	0.1286	-0.6017
-2.44	1.385	0.1422	-0.6064
-1.41	1.462	0.1525	-0.6083
-0.39	1.517	0.1607	-0.6094
0.65	1.615	0.1754	-0.6109
1.68	1.684	0.1861	-0.6110
2.70	1.741	0.1962	-0.6101
3.73	1.799	0.2079	-0.6075
4.75	1.857	0.2264	-0.5864
5.76	1.887	0.2515	-0.5454
6.75	1.862	0.2996	-0.4894

17 BASIC WING. SLATS RETRACTED.
FLAPS 40, TABS 0.
100% SPAN WITH BODY CUTOUT.
76 M/S. FREE TRANSITION.

ALPHA	CL	CD	CM
-4.63	0.906	0.1023	-0.6638
-3.60	0.985	0.1096	-0.6702
-2.57	1.071	0.1185	-0.6735
-1.53	1.155	0.1274	-0.6781
-0.50	1.233	0.1364	-0.6821
0.54	1.330	0.1485	-0.6897
1.57	1.406	0.1579	-0.6936
2.59	1.472	0.1663	-0.6985
3.63	1.562	0.1806	-0.7004
4.66	1.646	0.1959	-0.6957
5.68	1.682	0.2112	-0.6691
6.67	1.657	0.2556	-0.5759

18 BASIC WING.
SLATS DEFLECTED 15.
FLAPS 0, TABS 0.
76 M/S. FREE TRANSITION.

ALPHA	CL	CD	CM
-5.62	-0.296	0.1315	-0.1526
-4.60	-0.250	0.1172	-0.1443
-3.59	-0.212	0.1029	-0.1337
-2.57	-0.163	0.0893	-0.1206
-1.54	-0.101	0.0768	-0.1136
-0.51	-0.023	0.0652	-0.1125
0.52	0.055	0.0553	-0.1099
1.56	0.139	0.0464	-0.1064
2.59	0.227	0.0392	-0.1015
3.62	0.298	0.0354	-0.0953
4.65	0.374	0.0349	-0.0895
5.68	0.447	0.0366	-0.0840
6.71	0.518	0.0402	-0.0778
7.74	0.593	0.0444	-0.0801
8.78	0.688	0.0478	-0.0871
9.82	0.792	0.0516	-0.0897
10.85	0.880	0.0554	-0.0859
11.89	0.976	0.0615	-0.0799
12.93	1.064	0.0684	-0.0734
13.96	1.144	0.0757	-0.0675
15.00	1.230	0.0842	-0.0605
16.03	1.314	0.0936	-0.0522
17.06	1.398	0.1036	-0.0451
18.09	1.473	0.1136	-0.0370
19.12	1.545	0.1243	-0.0280
20.15	1.608	0.1381	-0.0081
21.18	1.673	0.1512	0.0049
22.19	1.704	0.1703	0.0403
23.20	1.732	0.1946	0.0687
24.19	1.707	0.2178	0.1025

Table 4 (continued)

19 BASIC WING.
SLATS DEFLECTED 25.
FLAPS 0, TABS 0.
76 M/S. FREE TRANSITION.

ALPHA	CL	CD	CM
-5.61	-0.280	0.1458	-0.1601
-4.60	-0.253	0.1325	-0.1494
-3.59	-0.214	0.1178	-0.1413
-2.57	-0.169	0.1033	-0.1353
-1.55	-0.124	0.0890	-0.1239
-0.53	-0.072	0.0773	-0.1154
0.50	0.012	0.0643	-0.1146
1.54	0.092	0.0540	-0.1150
2.57	0.174	0.0468	-0.1133
3.60	0.258	0.0429	-0.1096
4.64	0.336	0.0417	-0.1058
5.66	0.404	0.0426	-0.1013
6.70	0.485	0.0453	-0.0970
7.72	0.553	0.0482	-0.0935
8.76	0.637	0.0524	-0.0939
9.80	0.737	0.0564	-0.0982
9.80	0.739	0.0559	-0.0986
10.84	0.833	0.0600	-0.0996
11.87	0.924	0.0646	-0.0973
12.91	1.016	0.0698	-0.0941
13.95	1.107	0.0761	-0.0898
14.98	1.195	0.0838	-0.0828
16.02	1.282	0.0928	-0.0763
17.05	1.355	0.1012	-0.0689
18.08	1.437	0.1118	-0.0614
19.11	1.513	0.1223	-0.0540
20.14	1.589	0.1335	-0.0470
21.17	1.662	0.1453	-0.0394
22.20	1.733	0.1578	-0.0316
23.23	1.799	0.1708	-0.0236
24.25	1.863	0.1842	-0.0146
25.27	1.914	0.1978	0.0016
26.28	1.936	0.2183	0.0362
27.26	1.889	0.2566	0.0926

20 BASIC WING.
SLATS DEFLECTED 25.
FLAPS 10, TABS 0. 100% SPAN.
76 M/S. FREE TRANSITION.

ALPHA	CL	CD	CM
-5.57	-0.166	0.1253	-0.1575
-4.55	-0.128	0.1125	-0.1479
-3.54	-0.097	0.1035	-0.1412
-2.52	-0.038	0.0938	-0.1441
-1.48	0.053	0.0815	-0.1596
-0.42	0.197	0.0690	-0.2002
0.65	0.367	0.0595	-0.2426
1.70	0.500	0.0571	-0.2673
2.75	0.618	0.0590	-0.2806
3.80	0.735	0.0633	-0.2901
4.84	0.844	0.0690	-0.2966
5.88	0.945	0.0756	-0.3024
6.93	1.059	0.0829	-0.3106
7.97	1.164	0.0905	-0.3173
9.01	1.265	0.0987	-0.3216
10.05	1.364	0.1077	-0.3248
11.10	1.475	0.1186	-0.3266
12.14	1.575	0.1300	-0.3284
13.17	1.672	0.1429	-0.3254
14.21	1.769	0.1566	-0.3235
15.25	1.865	0.1716	-0.3210
16.29	1.946	0.1850	-0.3182
17.32	2.031	0.2006	-0.3153
18.36	2.127	0.2190	-0.3124
19.39	2.209	0.2353	-0.3093
20.42	2.290	0.2523	-0.3030
21.46	2.367	0.2714	-0.2937
22.45	2.342	0.2946	-0.2148

Table 4 (continued)

21 BASIC WING.
SLATS DEFLECTED 25.
FLAPS 10, TABS 0. 80% SPAN.
76 M/S. FREE TRANSITION.

ALPHA	CL	CD	CM
-5.57	-0.175	0.1270	-0.1495
-4.55	-0.135	0.1135	-0.1410
-3.54	-0.107	0.1061	-0.1338
-2.52	-0.042	0.0941	-0.1361
-1.48	0.041	0.0818	-0.1452
-0.43	0.173	0.0695	-0.1728
0.63	0.326	0.0595	-0.2019
1.68	0.459	0.0558	-0.2201
2.73	0.567	0.0565	-0.2266
3.77	0.678	0.0602	-0.2316
4.81	0.780	0.0647	-0.2343
5.86	0.880	0.0704	-0.2361
6.90	0.989	0.0771	-0.2420
7.94	1.098	0.0840	-0.2476
8.98	1.201	0.0919	-0.2509
10.03	1.302	0.1001	-0.2517
11.07	1.406	0.1097	-0.2518
12.11	1.500	0.1195	-0.2502
13.14	1.594	0.1311	-0.2468
14.18	1.688	0.1439	-0.2436
15.22	1.783	0.1578	-0.2389
16.26	1.876	0.1721	-0.2349
17.29	1.959	0.1867	-0.2300
18.32	2.040	0.2013	-0.2257
19.36	2.132	0.2187	-0.2208
20.39	2.204	0.2342	-0.2152
21.42	2.287	0.2520	-0.2096
22.45	2.348	0.2683	-0.1956
22.94	2.317	0.2872	-0.1394

22 BASIC WING.
SLATS DEFLECTED 25.
FLAPS 10, TABS 0.
80% SPAN WITH ENGINE CUTOUT.
76 M/S. FREE TRANSITION.

ALPHA	CL	CD	CM
-5.57	-0.176	0.1268	-0.1561
-4.56	-0.139	0.1144	-0.1451
-3.54	-0.107	0.1054	-0.1357
-2.52	-0.052	0.0944	-0.1349
-1.49	0.023	0.0835	-0.1440
-0.44	0.139	0.0705	-0.1637
0.61	0.270	0.0603	-0.1869
1.65	0.383	0.0553	-0.2020
2.70	0.503	0.0548	-0.2104
3.74	0.594	0.0571	-0.2131
4.78	0.694	0.0607	-0.2152
5.82	0.803	0.0664	-0.2174
6.86	0.891	0.0719	-0.2208
7.90	0.997	0.0779	-0.2259
8.94	1.102	0.0850	-0.2298
9.99	1.207	0.0926	-0.2314
11.02	1.301	0.1006	-0.2313
12.06	1.398	0.1096	-0.2298
13.11	1.505	0.1214	-0.2272
14.14	1.595	0.1329	-0.2234
15.18	1.686	0.1455	-0.2186
16.22	1.773	0.1583	-0.2148
17.25	1.856	0.1716	-0.2099
18.29	1.945	0.1878	-0.2048
19.32	2.029	0.2025	-0.2004
20.35	2.097	0.2160	-0.1951
21.38	2.180	0.2336	-0.1894
22.41	2.251	0.2503	-0.1810
23.42	2.280	0.2690	-0.1479
23.90	2.236	0.2853	-0.0898

Table 4 (continued)

23 BASIC WING.
SLATS DEFLECTED 25.
FLAPS 10, TABS 0. 60% SPAN.
76 M/S. FREE TRANSITION.

ALPHA	CL	CD	CM
-5.57	-0.181	0.1280	-0.1406
-4.56	-0.143	0.1149	-0.1328
-3.55	-0.121	0.1076	-0.1223
-2.53	-0.068	0.0966	-0.1173
-1.50	0.009	0.0834	-0.1176
-0.45	0.129	0.0708	-0.1345
0.61	0.262	0.0603	-0.1506
1.66	0.392	0.0551	-0.1616
2.70	0.499	0.0545	-0.1651
3.74	0.591	0.0566	-0.1647
4.78	0.697	0.0608	-0.1637
5.82	0.791	0.0657	-0.1631
6.86	0.894	0.0717	-0.1658
7.90	0.994	0.0770	-0.1700
8.94	1.093	0.0835	-0.1723
9.98	1.188	0.0901	-0.1716
11.02	1.294	0.0988	-0.1706
12.06	1.387	0.1076	-0.1670
13.10	1.482	0.1181	-0.1617
14.14	1.575	0.1298	-0.1567
15.17	1.668	0.1426	-0.1506
16.21	1.749	0.1546	-0.1443
17.24	1.836	0.1685	-0.1376
18.28	1.930	0.1846	-0.1310
19.31	2.003	0.1984	-0.1241
20.34	2.083	0.2138	-0.1174
21.37	2.158	0.2298	-0.1089
22.40	2.223	0.2461	-0.0994
23.42	2.273	0.2642	-0.0799
24.43	2.305	0.2876	-0.0556
25.42	2.272	0.3318	0.0064

24 BASIC WING.
SLATS DEFLECTED 25.
FLAPS 10, TABS 0. 35.5% SPAN.
76 M/S. FREE TRANSITION.

ALPHA	CL	CD	CM
-5.58	-0.203	0.1328	-0.1387
-4.57	-0.165	0.1207	-0.1267
-3.55	-0.131	0.1088	-0.1255
-2.53	-0.083	0.0971	-0.1151
-1.51	-0.015	0.0842	-0.1110
-0.47	0.073	0.0719	-0.1121
0.57	0.180	0.0607	-0.1164
1.61	0.284	0.0540	-0.1187
2.66	0.386	0.0514	-0.1182
3.69	0.477	0.0515	-0.1150
4.73	0.558	0.0537	-0.1098
5.76	0.653	0.0576	-0.1069
6.80	0.743	0.0624	-0.1032
7.84	0.843	0.0677	-0.1060
8.88	0.937	0.0721	-0.1091
9.92	1.035	0.0778	-0.1091
10.96	1.132	0.0844	-0.1056
11.99	1.219	0.0912	-0.1021
13.03	1.316	0.0999	-0.0975
14.07	1.407	0.1097	-0.0907
15.10	1.495	0.1209	-0.0830
16.13	1.570	0.1311	-0.0757
17.17	1.656	0.1436	-0.0678
18.20	1.741	0.1568	-0.0602
19.23	1.819	0.1702	-0.0520
20.27	1.898	0.1844	-0.0441
21.30	1.973	0.1993	-0.0365
22.32	2.035	0.2133	-0.0269
23.35	2.101	0.2293	-0.0168
24.36	2.134	0.2515	0.0093
25.38	2.174	0.2698	0.0244
26.36	2.120	0.3118	0.0821

Table 4 (continued)

25 BASIC WING.
SLATS DEFLECTED 25.
FLAPS 10, TABS 0.
100% SPAN WITH BODY CUTOUT.
76 M/S. FREE TRANSITION.

ALPHA	CL	CD	CM
-5.59	-0.218	0.1324	-0.1610
-4.58	-0.187	0.1178	-0.1538
-3.56	-0.159	0.1046	-0.1426
-2.55	-0.129	0.0970	-0.1362
-1.52	-0.056	0.0847	-0.1488
-0.48	0.044	0.0728	-0.1779
0.58	0.197	0.0620	-0.2251
1.64	0.336	0.0563	-0.2572
2.69	0.461	0.0556	-0.2760
3.73	0.568	0.0589	-0.2854
4.77	0.667	0.0632	-0.2923
5.81	0.759	0.0683	-0.2976
6.85	0.861	0.0747	-0.3051
7.89	0.959	0.0815	-0.3122
8.92	1.048	0.0879	-0.3169
9.97	1.154	0.0967	-0.3227
11.01	1.262	0.1061	-0.3259
12.05	1.357	0.1157	-0.3273
13.09	1.453	0.1267	-0.3267
14.13	1.550	0.1392	-0.3255
15.16	1.640	0.1521	-0.3234
16.19	1.721	0.1645	-0.3215
17.23	1.805	0.1783	-0.3182
18.27	1.896	0.1941	-0.3160
19.30	1.975	0.2089	-0.3133
20.33	2.052	0.2249	-0.3080
21.36	2.123	0.2410	-0.2792
22.38	2.185	0.2586	-0.2805
23.36	2.128	0.2806	-0.1930

26 BASIC WING.
SLATS DEFLECTED 25.
FLAPS 10, TABS 0.
80% SPAN WITH BODY CUTOUT.
76 M/S. FREE TRANSITION.

ALPHA	CL	CD	CM
-5.59	-0.224	0.1341	-0.1588
-4.58	-0.189	0.1183	-0.1500
-3.57	-0.164	0.1067	-0.1382
-2.55	-0.131	0.0984	-0.1318
-1.53	-0.070	0.0873	-0.1384
-0.49	0.028	0.0735	-0.1566
0.57	0.171	0.0621	-0.1906
1.62	0.304	0.0551	-0.2143
2.67	0.421	0.0530	-0.2276
3.71	0.532	0.0551	-0.2337
4.75	0.630	0.0586	-0.2367
5.79	0.726	0.0632	-0.2392
6.83	0.828	0.0692	-0.2436
7.87	0.928	0.0750	-0.2500
8.91	1.025	0.0814	-0.2544
9.95	1.116	0.0881	-0.2574
10.99	1.222	0.0963	-0.2589
12.03	1.318	0.1047	-0.2588
13.07	1.417	0.1148	-0.2570
14.11	1.515	0.1265	-0.2536
15.15	1.610	0.1388	-0.2506
16.18	1.695	0.1508	-0.2461
17.22	1.786	0.1646	-0.2418
18.26	1.877	0.1793	-0.2383
19.29	1.959	0.1937	-0.2340
20.32	2.037	0.2085	-0.2290
21.35	2.113	0.2236	-0.2231
22.38	2.180	0.2394	-0.2160
23.39	2.212	0.2593	-0.1824
24.37	2.164	0.2922	-0.1072

Table 4 (continued)

27 BASIC WING.
SLATS DEFLECTED 25.
FLAPS 10, TABS 0.
80% SPAN WITH ENGINE CUTOUT.
76 M/S. FREE TRANSITION.

ALPHA	CL	CD	CM
-4.58	-0.202	0.1214	-0.1559
-3.57	-0.172	0.1089	-0.1410
-2.56	-0.140	0.0994	-0.1320
-1.53	-0.082	0.0883	-0.1362
-0.50	0.002	0.0753	-0.1522
0.55	0.130	0.0634	-0.1794
1.60	0.244	0.0552	-0.1983
2.65	0.364	0.0516	-0.2119
3.69	0.467	0.0524	-0.2176
4.73	0.561	0.0549	-0.2196
5.76	0.656	0.0592	-0.2213
6.80	0.751	0.0643	-0.2248
7.84	0.852	0.0703	-0.2304
8.88	0.947	0.0759	-0.2347
9.92	1.042	0.0823	-0.2384
10.96	1.141	0.0894	-0.2396
12.00	1.243	0.0975	-0.2399
13.04	1.343	0.1070	-0.2382
14.08	1.432	0.1166	-0.2343
15.12	1.530	0.1284	-0.2310
16.15	1.608	0.1388	-0.2269
17.18	1.690	0.1507	-0.2228
18.22	1.786	0.1658	-0.2177
19.25	1.868	0.1794	-0.2138
20.29	1.968	0.1941	-0.2122
21.31	2.017	0.2076	-0.2042
22.34	2.091	0.2230	-0.1970
23.36	2.130	0.2424	-0.1660
24.24	2.089	0.2560	-0.0953

28 BASIC WING.
SLATS DEFLECTED 25.
FLAPS 10, TABS 0.
60% SPAN WITH BODY CUTOUT.
76 M/S. FREE TRANSITION.

ALPHA	CL	CD	CM
-5.59	-0.233	0.1337	-0.1491
-4.58	-0.202	0.1203	-0.1396
-3.57	-0.177	0.1098	-0.1305
-2.56	-0.152	0.1013	-0.1196
-1.54	-0.096	0.0889	-0.1171
-0.51	-0.016	0.0756	-0.1244
0.55	0.116	0.0627	-0.1452
1.59	0.235	0.0547	-0.1593
2.64	0.355	0.0511	-0.1673
3.68	0.454	0.0514	-0.1685
4.72	0.546	0.0539	-0.1690
5.76	0.637	0.0582	-0.1684
6.79	0.731	0.0628	-0.1681
7.83	0.829	0.0683	-0.1729
8.87	0.923	0.0734	-0.1760
9.91	1.016	0.0795	-0.1788
10.95	1.119	0.0863	-0.1780
11.99	1.215	0.0937	-0.1764
13.03	1.312	0.1026	-0.1723
14.07	1.403	0.1122	-0.1680
15.10	1.492	0.1234	-0.1617
16.13	1.569	0.1337	-0.1559
17.17	1.658	0.1464	-0.1499
18.20	1.746	0.1597	-0.1438
19.24	1.822	0.1726	-0.1371
20.27	1.909	0.1877	-0.1313
21.30	1.980	0.2016	-0.1233
22.33	2.047	0.2159	-0.1144
23.35	2.110	0.2330	-0.1024
24.37	2.144	0.2546	-0.0751
25.36	2.119	0.2900	-0.0176

Table 4 (continued)

29 BASIC WING.
SLATS DEFLECTED 25.
FLAPS 10, TABS 0.
35.5% SPAN WITH BODY CUTOUT.
76 M/S. FREE TRANSITION.

ALPHA	CL	CD	CM
-5.60	-0.250	0.1385	-0.1476
-4.59	-0.221	0.1248	-0.1392
-3.58	-0.188	0.1123	-0.1279
-2.56	-0.157	0.1002	-0.1205
-1.55	-0.112	0.0895	-0.1129
-0.52	-0.043	0.0760	-0.1133
0.52	0.052	0.0637	-0.1181
1.56	0.150	0.0543	-0.1221
2.60	0.246	0.0488	-0.1231
3.64	0.339	0.0468	-0.1211
4.67	0.429	0.0473	-0.1176
5.71	0.509	0.0496	-0.1138
6.74	0.591	0.0530	-0.1101
7.78	0.682	0.0580	-0.1095
8.81	0.778	0.0625	-0.1139
9.85	0.869	0.0666	-0.1163
10.89	0.967	0.0720	-0.1156
11.92	1.054	0.0775	-0.1126
12.96	1.150	0.0843	-0.1098
14.00	1.241	0.0923	-0.1037
15.04	1.328	0.1014	-0.0968
16.07	1.409	0.1109	-0.0901
17.10	1.496	0.1222	-0.0821
18.14	1.582	0.1341	-0.0751
19.17	1.652	0.1449	-0.0679
20.20	1.732	0.1580	-0.0604
21.23	1.808	0.1716	-0.0518
22.26	1.874	0.1842	-0.0446
23.28	1.939	0.1981	-0.0352
24.31	2.009	0.2151	-0.0255
25.32	2.038	0.2355	0.0021
26.30	1.993	0.2744	0.0644

30 BASIC WING.
SLATS DEFLECTED 25.
FLAPS 25, TABS 0. 100% SPAN.
76 M/S. FREE TRANSITION.

ALPHA	CL	CD	CM
0.42	1.040	0.0911	-0.5145
1.47	1.156	0.0981	-0.5365
2.53	1.325	0.1114	-0.5611
3.58	1.443	0.1203	-0.5725
4.62	1.525	0.1313	-0.5798
5.67	1.660	0.1466	-0.5856
6.72	1.773	0.1616	-0.5892
7.75	1.860	0.1738	-0.5910
8.79	1.958	0.1886	-0.5869
9.84	2.080	0.2083	-0.5850
10.87	2.163	0.2223	-0.5757
11.91	2.261	0.2404	-0.5694
12.94	2.332	0.2538	-0.5637
13.98	2.419	0.2711	-0.5572
15.02	2.513	0.2905	-0.5472
16.04	2.568	0.3039	-0.5364
17.08	2.669	0.3283	-0.5130
18.09	2.709	0.3431	-0.4741
19.10	2.722	0.3622	-0.4157
20.10	2.716	0.3901	-0.3444

Table 4 (continued)

31 BASIC WING.
SLATS DEFLECTED 25.
FLAPS 25, TABS 0. 80% SPAN.
76 M/S. FREE TRANSITION.

ALPHA	CL	CD	CM
0.36	0.901	0.0842	-0.3737
1.42	1.046	0.0912	-0.3915
2.48	1.178	0.0997	-0.3999
3.53	1.317	0.1110	-0.4099
4.57	1.408	0.1191	-0.4143
5.61	1.516	0.1299	-0.4140
6.64	1.586	0.1375	-0.4136
7.69	1.714	0.1537	-0.4155
8.73	1.810	0.1665	-0.4152
9.77	1.895	0.1791	-0.4115
10.81	2.009	0.1960	-0.4052
11.84	2.092	0.2092	-0.3978
12.87	2.163	0.2216	-0.3900
13.91	2.252	0.2375	-0.3770
14.95	2.343	0.2548	-0.3669
15.98	2.428	0.2722	-0.3548
17.01	2.506	0.2885	-0.3448
18.04	2.581	0.3084	-0.3260
19.07	2.639	0.3266	-0.3060
20.08	2.672	0.3432	-0.2804
21.08	2.665	0.3683	-0.2281

32 BASIC WING.
SLATS DEFLECTED 25.
FLAPS 25, TABS 0.
80% SPAN WITH ENGINE CUTOUT.
76 M/S. FREE TRANSITION.

ALPHA	CL	CD	CM
0.27	0.672	0.0819	-0.3213
1.32	0.799	0.0840	-0.3414
2.39	0.974	0.0921	-0.3608
3.44	1.083	0.0991	-0.3689
4.48	1.184	0.1065	-0.3732
5.52	1.288	0.1153	-0.3762
6.56	1.380	0.1234	-0.3804
7.61	1.499	0.1355	-0.3814
8.65	1.600	0.1470	-0.3813
9.67	1.669	0.1556	-0.3777
10.72	1.790	0.1724	-0.3775
11.76	1.883	0.1872	-0.3779
12.78	1.938	0.1966	-0.3735
13.83	2.054	0.2163	-0.3718
14.86	2.127	0.2296	-0.3668
15.90	2.219	0.2468	-0.3577
16.93	2.297	0.2629	-0.3515
17.96	2.387	0.2819	-0.3425
18.99	2.452	0.2990	-0.3287
20.01	2.508	0.3149	-0.3070
21.03	2.547	0.3337	-0.2817
22.02	2.526	0.3553	-0.2209

Table 4 (continued)

33 BASIC WING.
SLATS DEFLECTED 25.
FLAPS 25, TABS 0. 60% SPAN.
76 M/S. FREE TRANSITION.

ALPHA	CL	CD	CM
0.28	0.684	0.0791	-0.2279
1.33	0.811	0.0814	-0.2433
2.37	0.926	0.0865	-0.2499
3.43	1.061	0.0948	-0.2512
4.47	1.170	0.1029	-0.2552
5.52	1.276	0.1116	-0.2572
6.55	1.358	0.1187	-0.2593
7.59	1.469	0.1302	-0.2634
8.63	1.553	0.1399	-0.2628
9.67	1.665	0.1538	-0.2580
10.71	1.765	0.1670	-0.2530
11.75	1.857	0.1802	-0.2420
12.80	1.977	0.1992	-0.2319
13.82	2.027	0.2072	-0.2239
14.85	2.098	0.2201	-0.2155
15.87	2.166	0.2326	-0.2032
16.91	2.257	0.2497	-0.1917
17.94	2.316	0.2625	-0.1809
18.97	2.402	0.2816	-0.1701
19.99	2.454	0.2955	-0.1597
21.01	2.504	0.3227	-0.1231
22.02	2.517	0.3475	-0.0859

34 BASIC WING.
SLATS DEFLECTED 25.
FLAPS 25, TABS 0. 35.5% SPAN.
76 M/S. FREE TRANSITION.

ALPHA	CL	CD	CM
0.17	0.429	0.0760	-0.1244
1.22	0.543	0.0736	-0.1267
2.26	0.653	0.0745	-0.1287
3.31	0.762	0.0779	-0.1254
4.35	0.855	0.0828	-0.1232
5.40	0.986	0.0914	-0.1200
6.43	1.060	0.0965	-0.1195
7.47	1.157	0.1029	-0.1215
8.50	1.248	0.1102	-0.1198
9.54	1.339	0.1186	-0.1172
10.58	1.443	0.1293	-0.1135
11.61	1.520	0.1388	-0.1096
12.66	1.627	0.1533	-0.1034
13.69	1.705	0.1641	-0.0975
14.71	1.760	0.1727	-0.0880
15.75	1.864	0.1889	-0.0779
16.78	1.941	0.2016	-0.0645
17.80	1.991	0.2109	-0.0591
18.84	2.081	0.2276	-0.0466
19.88	2.167	0.2457	-0.0350
20.89	2.203	0.2536	-0.0257
21.91	2.261	0.2695	-0.0112
22.93	2.293	0.2921	0.0218
23.94	2.328	0.3095	0.0499
24.94	2.319	0.3414	0.0844

Table 4 (continued)

35 BASIC WING.
SLATS DEFLECTED 25.
FLAPS 25, TABS 0.
100% SPAN WITH BODY CUTOUT.
76 M/S. FREE TRANSITION.

ALPHA	CL	CD	CM
1.33	0.829	0.0910	-0.5266
2.37	0.923	0.0962	-0.5443
3.44	1.079	0.1072	-0.5627
4.49	1.202	0.1177	-0.5776
5.53	1.307	0.1272	-0.5815
6.56	1.382	0.1349	-0.5849
7.61	1.514	0.1498	-0.5921
8.65	1.618	0.1625	-0.5959
9.69	1.697	0.1731	-0.5934
10.73	1.810	0.1892	-0.5937
11.76	1.890	0.2012	-0.5903
12.81	1.997	0.2189	-0.5858
13.84	2.070	0.2319	-0.5817
14.88	2.170	0.2501	-0.5726
15.91	2.260	0.2671	-0.5687
16.94	2.322	0.2803	-0.5570
17.96	2.388	0.2946	-0.5435
18.98	2.436	0.3100	-0.5006
20.00	2.467	0.3274	-0.4574
21.01	2.492	0.3406	-0.4145
22.00	2.479	0.3642	-0.3462

36 BASIC WING.
SLATS DEFLECTED 25.
FLAPS 40, TABS 0. 100% SPAN.
76 M/S. FREE TRANSITION.

ALPHA	CL	CD	CM
3.74	1.842	0.2033	-0.7197
4.78	1.941	0.2176	-0.7164
5.82	2.026	0.2320	-0.7115
6.86	2.127	0.2488	-0.7066
7.89	2.214	0.2645	-0.7045
8.93	2.292	0.2801	-0.6972
9.95	2.358	0.2936	-0.6852
10.98	2.427	0.3075	-0.6776
12.02	2.514	0.3263	-0.6766
13.04	2.584	0.3424	-0.6711
14.07	2.658	0.3606	-0.6618
15.11	2.734	0.3794	-0.6507
16.12	2.778	0.3938	-0.6300
17.14	2.827	0.4092	-0.6024
18.16	2.879	0.4262	-0.5678
19.16	2.874	0.4435	-0.4972

Table 4 (continued)

37 BASIC WING.
SLATS DEFLECTED 25.
FLAPS 40, TABS 0.
100% SPAN WITH BODY CUTOUT.
76 M/S. FREE TRANSITION.

ALPHA	CL	CD	CM
-5.08	-0.207	0.1383	-0.1267
-4.05	-0.126	0.1276	-0.1416
-2.99	0.017	0.1163	-0.1806
3.60	1.492	0.1867	-0.7409
4.64	1.579	0.1973	-0.7402
5.67	1.661	0.2078	-0.7404
6.71	1.759	0.2212	-0.7394
7.75	1.845	0.2334	-0.7369
8.78	1.926	0.2464	-0.7350
9.81	2.012	0.2611	-0.7312
10.84	2.084	0.2738	-0.7236
11.87	2.157	0.2864	-0.7169
12.90	2.238	0.3018	-0.7086
13.94	2.320	0.3180	-0.7018
14.97	2.404	0.3351	-0.6912
16.01	2.497	0.3552	-0.6821
17.03	2.556	0.3700	-0.6632
18.06	2.612	0.3848	-0.6262
19.07	2.653	0.4058	-0.5614
20.07	2.640	0.4183	-0.5182

38 BASIC WING + BODY.
SLATS RETRACTED.
FLAPS 0, TABS 0.
76 M/S. FREE TRANSITION.

ALPHA	CL	CD	CM
-5.14	-0.347	0.0302	-0.1373
-4.10	-0.255	0.0259	-0.1267
-3.07	-0.169	0.0230	-0.1170
-2.03	-0.082	0.0208	-0.1067
-1.00	0.001	0.0192	-0.0954
0.04	0.088	0.0191	-0.0851
1.07	0.177	0.0199	-0.0727
2.10	0.248	0.0216	-0.0582
3.13	0.327	0.0239	-0.0449
4.16	0.409	0.0265	-0.0337
5.20	0.488	0.0295	-0.0222
6.23	0.574	0.0336	-0.0098
7.27	0.658	0.0383	0.0028
8.30	0.735	0.0436	0.0160
9.33	0.807	0.0492	0.0294
10.35	0.878	0.0578	0.0431
11.37	0.909	0.0881	0.0811
12.38	0.937	0.1072	0.1100
13.36	0.887	0.1679	0.1565
14.36	0.901	0.1869	0.1687
15.35	0.855	0.2320	0.1957

Table 4 (continued)

39 BASIC WING + BODY.
SLATS RETRACTED.
FLAPS 10, TABS 0. 100% SPAN.
76 M/S. FREE TRANSITION.

ALPHA	CL	CD	CM
-5.03	-0.079	0.0298	-0.2637
-3.99	0.021	0.0280	-0.2630
-2.94	0.150	0.0275	-0.2658
-1.90	0.256	0.0285	-0.2655
-0.85	0.363	0.0307	-0.2633
0.18	0.447	0.0339	-0.2589
1.22	0.539	0.0385	-0.2534
2.26	0.648	0.0440	-0.2494
3.30	0.742	0.0495	-0.2463
4.34	0.836	0.0557	-0.2421
5.38	0.930	0.0630	-0.2387
6.41	1.026	0.0715	-0.2352
7.45	1.123	0.0818	-0.2308
8.49	1.206	0.0983	-0.2210
9.51	1.269	0.1286	-0.1865
10.50	1.242	0.1864	-0.1361
11.51	1.265	0.2147	-0.1158
12.51	1.274	0.2479	-0.0967

40 BASIC WING + BODY.
SLATS RETRACTED.
FLAPS 10, TABS 0. 80% SPAN.
76 M/S. FREE TRANSITION.

ALPHA	CL	CD	CM
-5.05	-0.117	0.0299	-0.2253
-4.01	-0.021	0.0279	-0.2223
-2.96	0.095	0.0268	-0.2209
-1.93	0.184	0.0270	-0.2199
-0.89	0.277	0.0282	-0.2158
0.16	0.389	0.0313	-0.2086
1.19	0.470	0.0338	-0.1997
2.23	0.580	0.0400	-0.1924
3.28	0.683	0.0452	-0.1864
4.32	0.783	0.0512	-0.1799
5.35	0.876	0.0577	-0.1739
6.39	0.967	0.0651	-0.1676
7.43	1.061	0.0736	-0.1601
8.46	1.142	0.0883	-0.1500
9.49	1.202	0.1149	-0.1245
10.47	1.165	0.1728	-0.0659

41 BASIC WING + BODY.
SLATS RETRACTED.
FLAPS 10, TABS 0. 60% SPAN.
76 M/S. FREE TRANSITION.

ALPHA	CL	CD	CM
-5.07	-0.168	0.0302	-0.1824
-4.03	-0.078	0.0277	-0.1762
-2.99	0.035	0.0260	-0.1691
-1.94	0.139	0.0257	-0.1636
-0.90	0.240	0.0267	-0.1567
0.13	0.316	0.0283	-0.1512
1.17	0.422	0.0324	-0.1371
2.21	0.509	0.0361	-0.1283
3.24	0.601	0.0404	-0.1201
4.28	0.697	0.0456	-0.1118
5.32	0.789	0.0515	-0.1033
6.35	0.879	0.0580	-0.0944
7.39	0.976	0.0662	-0.0838
8.43	1.054	0.0738	-0.0747
9.45	1.117	0.1040	-0.0503
10.47	1.157	0.1267	-0.0282
11.45	1.114	0.1897	0.0184

Table 4 (continued)

42 BASIC WING + BODY.
SLATS RETRACTED.
FLAPS 10, TABS 0. 35.5% SPAN.
76 M/S. FREE TRANSITION.

ALPHA	CL	CD	CM
-5.10	-0.256	0.0306	-0.1518
-4.07	-0.175	0.0276	-0.1449
-3.02	-0.058	0.0248	-0.1343
-1.99	0.026	0.0234	-0.1255
-0.95	0.120	0.0233	-0.1166
0.08	0.205	0.0241	-0.1085
1.12	0.288	0.0260	-0.0973
2.17	0.377	0.0292	-0.0946
3.19	0.460	0.0325	-0.0712
4.22	0.537	0.0357	-0.0619
5.26	0.636	0.0408	-0.0503
6.29	0.724	0.0461	-0.0392
7.33	0.815	0.0526	-0.0273
8.36	0.891	0.0588	-0.0158
9.40	0.983	0.0679	0.0000
10.40	0.996	0.0994	0.0340
11.42	1.052	0.1205	0.0534
12.40	1.003	0.1855	0.0950

43 BASIC WING + BODY.
SLATS RETRACTED.
FLAPS 25, TABS 0. 100% SPAN.
76 M/S. FREE TRANSITION.

ALPHA	CL	CD	CM
-4.76	0.590	0.0538	-0.5870
-3.72	0.688	0.0578	-0.5867
-2.68	0.784	0.0626	-0.5844
-1.64	0.887	0.0710	-0.5768
-0.60	0.985	0.0788	-0.5720
0.43	1.071	0.0862	-0.5693
1.48	1.182	0.0964	-0.5623
2.51	1.264	0.1047	-0.5585
3.55	1.364	0.1157	-0.5538
4.59	1.456	0.1261	-0.5441
5.62	1.544	0.1400	-0.5339
6.65	1.618	0.1615	-0.5054
7.67	1.658	0.1880	-0.4646
8.63	1.562	0.2461	-0.3492

44 BASIC WING + BODY.
SLATS RETRACTED.
FLAPS 25, TABS 0. 80% SPAN.
76 M/S. FREE TRANSITION.

ALPHA	CL	CD	CM
-4.81	0.465	0.0497	-0.4618
-3.81	0.472	0.0517	-0.4419
-2.73	0.662	0.0563	-0.4538
-1.70	0.755	0.0622	-0.4457
-0.66	0.836	0.0684	-0.4379
0.38	0.936	0.0758	-0.4310
1.42	1.037	0.0837	-0.4233
2.46	1.135	0.0925	-0.4161
3.50	1.232	0.1021	-0.4092
4.53	1.324	0.1122	-0.4012
5.57	1.414	0.1230	-0.3938
6.60	1.491	0.1412	-0.3801
7.62	1.540	0.1665	-0.3461
8.60	1.475	0.2251	-0.2612
9.59	1.451	0.2609	-0.2121

45 BASIC WING + BODY.
SLATS RETRACTED.
FLAPS 25, TABS 0. 60% SPAN.
76 M/S. FREE TRANSITION.

ALPHA	CL	CD	CM
-4.89	0.262	0.0465	-0.3121
-3.86	0.353	0.0473	-0.3078
-2.82	0.457	0.0497	-0.3015
-1.78	0.548	0.0529	-0.2956
-0.74	0.650	0.0588	-0.2830
0.29	0.731	0.0642	-0.2735
1.33	0.826	0.0704	-0.2640
2.37	0.915	0.0768	-0.2558
3.41	1.010	0.0846	-0.2462
4.44	1.098	0.0925	-0.2372
5.48	1.187	0.1014	-0.2266
6.51	1.275	0.1111	-0.2166
7.55	1.363	0.1391	-0.1932
8.56	1.399	0.1619	-0.1720
9.58	1.437	0.1854	-0.1468
10.54	1.339	0.2456	-0.0942

Table 4 (continued)

46 BASIC WING + BODY.
SLATS RETRACTED.
FLAPS 25, TABS 0. 35.5% SPAN.
76 M/S. FREE TRANSITION.

ALPHA	CL	CD	CM
-5.01	-0.023	0.0406	-0.1891
-3.97	0.065	0.0394	-0.1805
-2.94	0.159	0.0390	-0.1709
-1.90	0.257	0.0398	-0.1614
-0.86	0.343	0.0416	-0.1530
0.17	0.421	0.0444	-0.1434
1.21	0.528	0.0499	-0.1254
2.24	0.601	0.0536	-0.1172
3.28	0.690	0.0585	-0.1079
4.31	0.771	0.0637	-0.0998
5.34	0.853	0.0697	-0.0915
6.38	0.941	0.0769	-0.0811
7.41	1.027	0.0848	-0.0709
8.45	1.106	0.0934	-0.0607
9.46	1.142	0.1296	-0.0287
10.48	1.188	0.1516	-0.0088
11.46	1.128	0.2150	0.0245

47 BASIC WING + BODY.
SLATS RETRACTED.
FLAPS 40, TABS 0. 100% SPAN.
76 M/S. FREE TRANSITION.

ALPHA	CL	CD	CM
-4.58	1.052	0.1193	-0.7967
-3.54	1.140	0.1279	-0.7898
-2.51	1.224	0.1366	-0.7803
-1.47	1.317	0.1471	-0.7724
-0.44	1.392	0.1565	-0.7661
0.60	1.478	0.1674	-0.7587
1.63	1.565	0.1788	-0.7494
2.67	1.651	0.1907	-0.7392
3.70	1.731	0.2043	-0.7243
4.73	1.801	0.2208	-0.6934
5.74	1.837	0.2419	-0.6459
6.72	1.769	0.2886	-0.5219

48 BASIC WING + BODY.
SLATS RETRACTED.
FLAPS 40, TABS 0. 80% SPAN.
76 M/S. FREE TRANSITION.

ALPHA	CL	CD	CM
-4.65	0.871	0.1070	-0.6123
-3.61	0.959	0.1126	-0.6038
-2.57	1.054	0.1216	-0.5939
-1.54	1.140	0.1296	-0.5869
-0.50	1.231	0.1385	-0.5790
0.53	1.304	0.1463	-0.5709
1.57	1.401	0.1574	-0.5594
2.60	1.477	0.1672	-0.5506
3.63	1.558	0.1776	-0.5398
4.66	1.638	0.1889	-0.5260
5.69	1.700	0.2116	-0.5012
6.67	1.670	0.2579	-0.4163

49 BASIC WING + BODY.
SLATS RETRACTED.
FLAPS 40, TABS 0. 60% SPAN.
76 M/S. FREE TRANSITION.

ALPHA	CL	CD	CM
-4.75	0.627	0.0918	-0.4030
-3.72	0.687	0.0943	-0.3994
-2.68	0.803	0.1009	-0.3865
-1.64	0.880	0.1069	-0.3758
-0.61	0.969	0.1138	-0.3642
0.42	1.039	0.1196	-0.3552
1.46	1.134	0.1281	-0.3440
2.49	1.217	0.1365	-0.3339
3.52	1.300	0.1458	-0.3218
4.56	1.376	0.1552	-0.3116
5.58	1.448	0.1654	-0.3039
6.61	1.517	0.1917	-0.2832
7.63	1.563	0.2183	-0.2546
8.64	1.585	0.2423	-0.2215
9.59	1.460	0.3047	-0.1620

Table 4 (continued)

50 BASIC WING + BODY.
SLATS RETRACTED.
FLAPS 40, TABS 0. 35.5% SPAN.
76 M/S. FREE TRANSITION.

ALPHA	CL	CD	CM
-4.94	0.153	0.0687	-0.2251
-3.90	0.250	0.0687	-0.2153
-2.86	0.346	0.0697	-0.2052
-1.83	0.418	0.0718	-0.1994
-0.79	0.520	0.0755	-0.1865
0.24	0.593	0.0798	-0.1746
1.28	0.682	0.0849	-0.1601
2.30	0.749	0.0889	-0.1516
3.34	0.835	0.0944	-0.1399
4.37	0.926	0.1011	-0.1273
5.41	1.014	0.1090	-0.1152
6.44	1.097	0.1168	-0.1013
7.47	1.174	0.1251	-0.0874
8.50	1.244	0.1340	-0.0734
9.51	1.261	0.1768	-0.0406
10.53	1.303	0.1962	-0.0221
11.48	1.200	0.2611	0.0069

51 BASIC WING + BODY.
SLATS DEFLECTED 15.
FLAPS 0, TABS 0.
76 M/S. FREE TRANSITION.

ALPHA	CL	CD	CM
-5.65	-0.366	0.1357	-0.2359
-4.63	-0.317	0.1199	-0.2159
-3.60	-0.258	0.1037	-0.1927
-2.58	-0.195	0.0895	-0.1750
-1.55	-0.129	0.0780	-0.1502
-0.52	-0.043	0.0660	-0.1343
0.52	0.047	0.0579	-0.1190
1.56	0.137	0.0501	-0.1018
2.59	0.226	0.0445	-0.0835
3.62	0.305	0.0419	-0.0663
4.65	0.384	0.0418	-0.0491
4.66	0.391	0.0414	-0.0479
5.69	0.473	0.0445	-0.0315
6.72	0.553	0.0491	-0.0141
7.76	0.651	0.0519	-0.0074
8.81	0.760	0.0557	0.0025
9.85	0.868	0.0610	0.0119
10.89	0.963	0.0676	0.0265
11.92	1.052	0.0752	0.0423
12.96	1.141	0.0841	0.0600
14.00	1.233	0.0942	0.0780
15.03	1.320	0.1050	0.0970
16.07	1.409	0.1172	0.1162
17.10	1.492	0.1298	0.1328
18.13	1.569	0.1430	0.1502
19.16	1.642	0.1573	0.1691
20.19	1.700	0.1753	0.1983
21.21	1.766	0.1923	0.1994
22.22	1.782	0.2163	0.2716
23.21	1.762	0.2500	0.3254

Table 4 (continued)

52 BASIC WING + BODY.
SLATS DEFLECTED 15.
FLAPS 10, TABS 0. 100% SPAN.
76 M/S. FREE TRANSITION.

ALPHA	CL	CD	CM
-5.60	-0.257	0.1210	-0.2476
-4.58	-0.203	0.1077	-0.2342
-3.56	-0.147	0.0972	-0.2140
-2.53	-0.068	0.0857	-0.2050
-1.48	0.059	0.0725	-0.2168
-0.42	0.205	0.0633	-0.2332
0.64	0.345	0.0588	-0.2467
1.69	0.477	0.0565	-0.2521
2.74	0.592	0.0586	-0.2507
3.78	0.705	0.0634	-0.2478
4.82	0.803	0.0698	-0.2421
5.87	0.921	0.0760	-0.2393
6.92	1.031	0.0827	-0.2356
7.96	1.151	0.0911	-0.2284
9.01	1.254	0.1005	-0.2207
10.05	1.361	0.1117	-0.2138
11.09	1.469	0.1246	-0.2043
12.13	1.565	0.1375	-0.1934
13.17	1.666	0.1522	-0.1815
14.22	1.776	0.1697	-0.1681
15.25	1.870	0.1863	-0.1562
16.29	1.961	0.2044	-0.1440
17.32	2.029	0.2242	-0.1264
18.35	2.093	0.2452	-0.0836
19.36	2.129	0.2677	-0.0411
20.37	2.154	0.2888	0.0078
21.38	2.187	0.3300	0.0501
22.36	2.129	0.3587	0.1145

53 BASIC WING + BODY.
SLATS DEFLECTED 25.
FLAPS 0, TABS 0.
76 M/S. FREE TRANSITION.

ALPHA	CL	CD	CM
-5.64	-0.338	0.1435	-0.2176
-4.62	-0.299	0.1290	-0.1986
-3.60	-0.252	0.1146	-0.1759
-2.58	-0.198	0.1002	-0.1517
-1.56	-0.139	0.0868	-0.1304
-0.53	-0.075	0.0762	-0.1084
0.50	0.010	0.0654	-0.0932
1.54	0.104	0.0562	-0.0797
2.58	0.195	0.0509	-0.0645
3.61	0.277	0.0481	-0.0484
4.64	0.356	0.0477	-0.0341
5.68	0.439	0.0497	-0.0164
6.71	0.523	0.0526	0.0005
7.75	0.610	0.0568	0.0159
8.79	0.716	0.0608	0.0206
9.83	0.814	0.0645	0.0256
10.87	0.914	0.0696	0.0372
11.91	1.013	0.0760	0.0499
12.95	1.115	0.0841	0.0635
13.99	1.206	0.0931	0.0787
15.02	1.297	0.1036	0.0968
16.06	1.384	0.1152	0.1144
17.09	1.461	0.1266	0.1243
18.12	1.539	0.1387	0.1410
19.15	1.617	0.1525	0.1525
20.19	1.703	0.1684	0.1743
21.22	1.775	0.1838	0.1881
22.25	1.849	0.2005	0.2052
23.27	1.913	0.2176	0.2237
24.29	1.967	0.2371	0.2513
25.31	1.998	0.2608	0.2814
26.30	1.981	0.2941	0.3498

Table 4 (continued)

54 BASIC WING + BODY.
SLATS DEFLECTED 25.
FLAPS 10, TABS 0. 100% SPAN.
76 M/S. FREE TRANSITION.

ALPHA	CL	CD	CM
-5.60	-0.250	0.1295	-0.2651
-4.58	-0.196	0.1149	-0.2525
-3.56	-0.136	0.1006	-0.2319
-2.53	-0.085	0.0920	-0.2096
-1.50	0.002	0.0823	-0.2088
-0.45	0.125	0.0716	-0.2237
0.62	0.292	0.0639	-0.2542
1.68	0.442	0.0613	-0.2696
2.73	0.565	0.0632	-0.2706
3.77	0.679	0.0673	-0.2692
4.82	0.787	0.0728	-0.2639
5.86	0.896	0.0794	-0.2573
6.91	1.011	0.0860	-0.2536
7.95	1.124	0.0935	-0.2490
9.00	1.238	0.1026	-0.2447
10.04	1.343	0.1121	-0.2385
10.04	1.347	0.1137	-0.2379
11.09	1.454	0.1251	-0.2290
12.13	1.557	0.1379	-0.2198
13.17	1.662	0.1521	-0.2068
14.21	1.759	0.1666	-0.1934
15.25	1.858	0.1834	-0.1803
16.29	1.953	0.2009	-0.1676
17.33	2.046	0.2186	-0.1551
18.36	2.127	0.2361	-0.1423
19.39	2.212	0.2554	-0.1299
20.43	2.304	0.2774	-0.1140
21.45	2.356	0.2973	-0.0837
22.45	2.344	0.3251	-0.0137

55 BASIC WING + BODY.
SLATS DEFLECTED 25.
FLAPS 10, TABS 0. 80% SPAN.
76 M/S. FREE TRANSITION.

ALPHA	CL	CD	CM
-5.60	-0.255	0.1305	-0.2484
-4.58	-0.200	0.1156	-0.2355
-3.56	-0.145	0.1026	-0.2108
-2.54	-0.093	0.0931	-0.1899
-1.50	-0.009	0.0826	-0.1839
-0.46	0.107	0.0715	-0.1877
0.60	0.257	0.0634	-0.2055
1.66	0.400	0.0597	-0.2130
2.71	0.521	0.0605	-0.2095
3.75	0.625	0.0635	-0.2035
4.79	0.729	0.0682	-0.1961
4.80	0.733	0.0684	-0.1988
5.84	0.838	0.0743	-0.1892
6.88	0.952	0.0805	-0.1832
7.93	1.061	0.0866	-0.1775
8.97	1.170	0.0946	-0.1698
10.01	1.276	0.1037	-0.1640
11.06	1.386	0.1145	-0.1537
12.10	1.489	0.1264	-0.1429
13.14	1.590	0.1397	-0.1293
14.18	1.684	0.1537	-0.1153
15.22	1.781	0.1694	-0.0996
16.26	1.879	0.1863	-0.0848
17.29	1.965	0.2028	-0.0711
18.33	2.048	0.2196	-0.0567
19.36	2.137	0.2389	-0.0423
20.40	2.220	0.2584	-0.0275
21.43	2.302	0.2792	-0.0122
22.44	2.334	0.3040	0.0242
23.44	2.322	0.3329	0.0930

Table 4 (continued)

56 BASIC WING + BODY.
SLATS DEFLECTED 25.
FLAPS 10, TABS 0.
80% SPAN WITH ENGINE CUTOUT.
76 M/S. FREE TRANSITION.

ALPHA	CL	CD	CM
-5.61	-0.270	0.1341	-0.2575
-4.59	-0.219	0.1188	-0.2421
-3.57	-0.168	0.1049	-0.2204
-2.55	-0.127	0.0949	-0.1906
-1.52	-0.061	0.0848	-0.1741
-0.48	0.041	0.0741	-0.1752
0.57	0.174	0.0644	-0.1862
1.63	0.314	0.0592	-0.1946
2.67	0.431	0.0583	-0.1921
3.71	0.531	0.0599	-0.1855
4.75	0.627	0.0640	-0.1770
5.80	0.733	0.0689	-0.1663
6.84	0.833	0.0744	-0.1590
7.88	0.940	0.0798	-0.1534
8.92	1.052	0.0865	-0.1468
9.97	1.160	0.0944	-0.1416
11.01	1.271	0.1039	-0.1321
12.05	1.375	0.1148	-0.1219
13.09	1.473	0.1265	-0.1081
14.14	1.575	0.1406	-0.0944
15.17	1.672	0.1553	-0.0796
16.21	1.762	0.1700	-0.0645
17.25	1.855	0.1862	-0.0503
18.28	1.937	0.2026	-0.0352
19.32	2.027	0.2207	-0.0206
20.35	2.106	0.2389	-0.0094
21.38	2.190	0.2589	0.0067
22.40	2.227	0.2822	0.0311
23.40	2.228	0.3081	0.1027
24.40	2.219	0.3470	0.1600

57 BASIC WING + BODY.
SLATS DEFLECTED 25.
FLAPS 10, TABS 0. 60% SPAN.
76 M/S. FREE TRANSITION.

ALPHA	CL	CD	CM
-5.61	-0.267	0.1330	-0.2476
-4.58	-0.208	0.1171	-0.2356
-3.56	-0.160	0.1048	-0.2077
-2.55	-0.116	0.0954	-0.1816
-1.52	-0.043	0.0843	-0.1642
-0.48	0.053	0.0734	-0.1558
0.57	0.186	0.0643	-0.1593
1.63	0.316	0.0589	-0.1572
2.68	0.436	0.0580	-0.1486
3.71	0.531	0.0593	-0.1386
4.75	0.630	0.0632	-0.1267
5.79	0.726	0.0677	-0.1154
6.84	0.832	0.0735	-0.1057
7.88	0.939	0.0784	-0.1004
8.92	1.048	0.0851	-0.0910
9.97	1.162	0.0935	-0.0815
11.01	1.263	0.1025	-0.0707
12.05	1.360	0.1124	-0.0581
13.09	1.466	0.1253	-0.0426
14.13	1.562	0.1388	-0.0269
15.17	1.652	0.1528	-0.0094
16.20	1.745	0.1678	0.0073
17.24	1.832	0.1830	0.0233
18.27	1.915	0.1993	0.0375
18.28	1.924	0.2000	0.0318
19.31	1.995	0.2162	0.0532
19.31	2.005	0.2174	0.0484
20.34	2.076	0.2352	0.0694
20.34	2.089	0.2369	0.0664
21.37	2.157	0.2552	0.0866
21.37	2.165	0.2560	0.0847
22.39	2.216	0.2761	0.1100
22.40	2.233	0.2776	0.1059
23.41	2.251	0.3054	0.1498
23.41	2.254	0.3069	0.1482
24.41	2.250	0.3362	0.2036
24.42	2.283	0.3324	0.1834
25.41	2.241	0.3705	0.2462
25.41	2.263	0.3758	0.2412

Table 4 (continued)

58 BASIC WING + BODY.
SLATS DEFLECTED 25.
FLAPS 10, TABS 0. 35.5% SPAN.
76 M/S. FREE TRANSITION.

ALPHA	CL	CD	CM
-5.61	-0.274	0.1348	-0.2510
-4.59	-0.220	0.1201	-0.2289
-3.57	-0.170	0.1077	-0.2068
-2.55	-0.112	0.0950	-0.1828
-1.52	-0.060	0.0855	-0.1609
-0.49	0.020	0.0750	-0.1453
0.55	0.115	0.0656	-0.1321
1.59	0.213	0.0582	-0.1188
2.63	0.315	0.0549	-0.1038
3.66	0.408	0.0543	-0.0893
4.70	0.494	0.0560	-0.0746
5.73	0.581	0.0595	-0.0584
6.78	0.685	0.0644	-0.0420
7.82	0.784	0.0688	-0.0337
8.86	0.894	0.0736	-0.0274
9.90	0.995	0.0795	-0.0188
10.94	1.092	0.0865	-0.0071
11.98	1.196	0.0952	0.0063
13.02	1.295	0.1053	0.0216
14.06	1.383	0.1162	0.0385
15.10	1.477	0.1291	0.0531
16.13	1.564	0.1426	0.0699
17.16	1.646	0.1561	0.0861
18.20	1.733	0.1714	0.1032
19.23	1.813	0.1873	0.1209
20.26	1.887	0.2034	0.1380
21.29	1.964	0.2213	0.1551
22.32	2.030	0.2390	0.1730
23.35	2.099	0.2596	0.1931
24.36	2.128	0.2863	0.2308
25.37	2.156	0.3133	0.2594
26.33	2.052	0.3641	0.3358

59 BASIC WING + BODY.
SLATS DEFLECTED 25.
FLAPS 25, TABS 0. 100% SPAN.
76 M/S. FREE TRANSITION.

ALPHA	CL	CD	CM
-5.05	-0.123	0.1270	-0.2613
-4.01	-0.033	0.1181	-0.2602
-2.94	0.137	0.1049	-0.3031
-1.86	0.348	0.0945	-0.3805
-0.73	0.664	0.0907	-0.4917
0.35	0.860	0.0944	-0.5343
1.41	1.020	0.1032	-0.5542
2.46	1.146	0.1119	-0.5611
3.51	1.272	0.1222	-0.5597
4.55	1.371	0.1313	-0.5557
5.60	1.494	0.1434	-0.5507
6.65	1.598	0.1554	-0.5438
7.69	1.708	0.1695	-0.5370
8.74	1.824	0.1863	-0.5276
9.77	1.914	0.2006	-0.5197
10.81	1.999	0.2156	-0.5114
11.85	2.106	0.2351	-0.4976
12.89	2.200	0.2526	-0.4823
13.92	2.287	0.2702	-0.4653
14.96	2.377	0.2897	-0.4466
15.99	2.452	0.3069	-0.4274
17.02	2.535	0.3267	-0.4040
18.05	2.607	0.3457	-0.3744
19.07	2.653	0.3662	-0.3096
20.06	2.624	0.3878	-0.2163
21.06	2.618	0.4145	-0.1573

Table 4 (continued)

60 BASIC WING + BODY.
SLATS DEFLECTED 25.
FLAPS 25, TABS 0. 80% SPAN.
76 M/S. FREE TRANSITION.

ALPHA	CL	CD	CM
0.29	0.719	0.0885	-0.4079
1.36	0.896	0.0952	-0.4233
2.41	1.020	0.1024	-0.4252
3.46	1.134	0.1102	-0.4193
4.49	1.226	0.1174	-0.4147
5.54	1.346	0.1275	-0.4069
6.59	1.463	0.1389	-0.3979
7.63	1.560	0.1488	-0.3861
8.67	1.660	0.1612	-0.3760
9.72	1.773	0.1768	-0.3619
10.75	1.866	0.1914	-0.3525
11.79	1.961	0.2073	-0.3393
12.83	2.053	0.2234	-0.3257
13.87	2.145	0.2406	-0.3075
14.90	2.231	0.2567	-0.2879
15.94	2.317	0.2747	-0.2635
16.97	2.399	0.2922	-0.2436
18.00	2.473	0.3094	-0.2214
19.03	2.541	0.3284	-0.1947
20.04	2.582	0.3523	-0.1372
21.04	2.571	0.3817	-0.0807
22.04	2.571	0.4037	-0.0286
23.01	2.506	0.4380	0.0569

61 BASIC WING + BODY.
SLATS DEFLECTED 25.
FLAPS 25, TABS 0.
80% SPAN WITH ENGINE CUTOUT.
76 M/S. FREE TRANSITION.

ALPHA	CL	CD	CM
0.19	0.462	0.0856	-0.3408
1.27	0.660	0.0884	-0.3689
2.31	0.768	0.0923	-0.3722
2.31	0.779	0.0923	-0.3725
3.36	0.896	0.0986	-0.3708
4.41	1.008	0.1057	-0.3641
5.45	1.119	0.1136	-0.3567
6.49	1.219	0.1214	-0.3492
7.54	1.332	0.1307	-0.3369
8.58	1.434	0.1407	-0.3269
9.62	1.541	0.1521	-0.3135
10.66	1.634	0.1639	-0.3033
11.71	1.763	0.1795	-0.2943
12.74	1.841	0.1956	-0.2776
13.78	1.928	0.2112	-0.2655
14.81	2.013	0.2266	-0.2516
15.85	2.105	0.2491	-0.2333
16.88	2.184	0.2607	-0.2175
17.92	2.268	0.2789	-0.1991
18.95	2.341	0.2959	-0.1789
19.97	2.404	0.3170	-0.1405
20.98	2.420	0.3383	-0.0846
21.98	2.420	0.3637	-0.0289
22.96	2.370	0.3984	0.0543

Table 4 (continued)

62 BASIC WING + BODY.
SLATS DEFLECTED 25.
FLAPS 25, TABS 0. 60% SPAN.
76 M/S. FREE TRANSITION.

ALPHA	CL	CD	CM
0.20	0.492	0.0843	-0.2587
1.27	0.678	0.0862	-0.2664
2.32	0.793	0.0905	-0.2626
3.36	0.901	0.0964	-0.2535
4.41	1.004	0.1028	-0.2412
5.45	1.109	0.1103	-0.2314
6.49	1.217	0.1179	-0.2223
7.53	1.323	0.1265	-0.2084
8.57	1.423	0.1365	-0.1961
9.62	1.527	0.1484	-0.1832
10.65	1.621	0.1604	-0.1690
11.70	1.723	0.1755	-0.1538
12.74	1.823	0.1913	-0.1385
13.77	1.908	0.2057	-0.1231
14.81	1.993	0.2213	-0.1056
15.84	2.080	0.2383	-0.0869
16.87	2.157	0.2545	-0.0695
17.90	2.234	0.2722	-0.0543
18.93	2.308	0.2904	-0.0374
19.95	2.358	0.3039	-0.0195
19.96	2.377	0.3095	-0.0200
20.98	2.414	0.3278	0.0186
21.98	2.419	0.3612	0.0785
22.99	2.455	0.3833	0.1163
23.92	2.276	0.9999	0.1752

63 BASIC WING + BODY.
SLATS DEFLECTED 25.
FLAPS 40, TABS 0. 100% SPAN.
76 M/S. FREE TRANSITION.

ALPHA	CL	CD	CM
-5.54	-0.109	0.1465	-0.2628
-4.48	0.060	0.1379	-0.3017
-3.37	0.332	0.1317	-0.4208
-2.19	0.761	0.1338	-0.6153
-1.07	1.060	0.1471	-0.7140
0.01	1.264	0.1596	-0.7461
1.07	1.416	0.1730	-0.7562
2.12	1.528	0.1847	-0.7442
3.17	1.648	0.1979	-0.7372
4.21	1.747	0.2100	-0.7259
5.24	1.832	0.2218	-0.7097
6.28	1.923	0.2358	-0.6941
7.31	1.994	0.2498	-0.6752
8.34	2.077	0.2655	-0.6562
9.37	2.152	0.2816	-0.6402
10.40	2.239	0.2983	-0.6251
11.44	2.330	0.3167	-0.6129
12.47	2.410	0.3338	-0.5983
13.51	2.488	0.3529	-0.5790
14.54	2.572	0.3731	-0.5626
15.57	2.655	0.3942	-0.5439
16.60	2.732	0.4152	-0.5219
17.63	2.800	0.4359	-0.4950
18.63	2.799	0.4562	-0.4038
19.64	2.825	0.4815	-0.3340
20.65	2.850	0.5114	-0.2897
21.63	2.796	0.5438	-0.2056

Table 4 (continued)

64 BASIC WING + BODY.
SLATS DEFLECTED 25.
FLAPS 40, TABS 0. 80% SPAN.
76 M/S. FREE TRANSITION.

ALPHA	CL	CD	CM
-0.06	1.082	0.1412	-0.5606
1.00	1.233	0.1532	-0.5746
2.05	1.351	0.1647	-0.5692
3.10	1.483	0.1754	-0.5663
4.14	1.588	0.1863	-0.5525
5.17	1.665	0.1958	-0.5380
6.21	1.749	0.2076	-0.5215
7.24	1.841	0.2212	-0.5049
8.28	1.926	0.2351	-0.4847
9.31	2.012	0.2495	-0.4677
10.35	2.098	0.2647	-0.4531
10.35	2.098	0.2640	-0.4556
11.38	2.173	0.2788	-0.4361
12.41	2.251	0.2942	-0.4200
13.44	2.336	0.3116	-0.4049
14.48	2.418	0.3293	-0.3900
15.51	2.506	0.3498	-0.3739
16.54	2.583	0.3691	-0.3542
17.57	2.657	0.3885	-0.3361
18.60	2.729	0.4115	-0.3153
19.62	2.760	0.4379	-0.2580
20.61	2.757	0.4666	-0.1850
21.61	2.752	0.4952	-0.1200
22.58	2.667	0.5328	-0.0393

65 BASIC WING + BODY.
SLATS DEFLECTED 25.
FLAPS 40, TABS 0.
80% SPAN WITH ENGINE CUTOUT.
76 M/S. FREE TRANSITION.

ALPHA	CL	CD	CM
-0.18	0.793	0.1304	-0.4828
0.88	0.953	0.1396	-0.5028
1.94	1.092	0.1496	-0.5110
2.99	1.204	0.1591	-0.5074
4.03	1.306	0.1674	-0.4996
5.07	1.402	0.1760	-0.4904
6.11	1.499	0.1855	-0.4705
7.14	1.595	0.1959	-0.4642
8.19	1.698	0.2084	-0.4491
9.22	1.794	0.2220	-0.4330
10.26	1.883	0.2355	-0.4195
11.30	1.977	0.2508	-0.4034
12.33	2.067	0.2668	-0.3892
13.37	2.157	0.2836	-0.3742
14.40	2.240	0.3005	-0.3598
15.44	2.331	0.3188	-0.3448
16.47	2.404	0.3365	-0.3261
17.50	2.484	0.3556	-0.3120
18.53	2.559	0.3753	-0.2982
19.56	2.615	0.3960	-0.2676
20.55	2.596	0.4212	-0.1837
21.55	2.599	0.4438	-0.1221
22.53	2.543	0.4696	-0.0460

Table 4 (continued)

66 BASIC WING + BODY.
SLATS DEFLECTED 25.
FLAPS 40, TABS 0. 60% SPAN.
76 M/S. FREE TRANSITION.

ALPHA	CL	CD	CM
0.33	0.817	0.1272	-0.3415
1.40	1.000	0.1373	-0.3467
2.45	1.114	0.1454	-0.3402
3.49	1.222	0.1540	-0.3311
4.53	1.323	0.1623	-0.3192
5.57	1.417	0.1708	-0.3056
6.61	1.507	0.1795	-0.2856
7.65	1.599	0.1910	-0.2689
8.68	1.687	0.2025	-0.2525
9.72	1.778	0.2155	-0.2356
10.75	1.862	0.2285	-0.2205
11.79	1.953	0.2434	-0.2002
12.83	2.046	0.2598	-0.1828
13.86	2.125	0.2748	-0.1666
14.89	2.206	0.2907	-0.1484
15.92	2.287	0.3080	-0.1287
16.95	2.354	0.3233	-0.1095
17.98	2.423	0.3405	-0.0900
19.01	2.487	0.3582	-0.0739
20.04	2.565	0.3837	-0.0533
21.04	2.573	0.4245	0.0084
22.05	2.605	0.4445	0.0423
22.97	2.396	0.4613	0.0915

67 EXTENDED WING.
SLATS RETRACTED.
FLAPS 0, TABS 0.
76 M/S. FREE TRANSITION.

ALPHA	CL	CD	CM
-5.15	-0.326	0.0189	-0.0518
-4.10	-0.223	0.0151	-0.0551
-3.06	-0.134	0.0127	-0.0617
-2.02	-0.045	0.0106	-0.0650
-0.98	0.040	0.0095	-0.0682
0.06	0.132	0.0099	-0.0688
1.09	0.207	0.0108	-0.0706
2.14	0.310	0.0140	-0.0678
3.17	0.373	0.0162	-0.0707
4.21	0.465	0.0194	-0.0732
5.25	0.567	0.0240	-0.0748
6.28	0.630	0.0273	-0.0734
7.33	0.731	0.0335	-0.0739
8.36	0.802	0.0387	-0.0737
9.40	0.883	0.0455	-0.0693
10.42	0.944	0.0670	-0.0583
11.44	0.974	0.0920	-0.0321
12.42	0.936	0.1427	0.0031

Table 4 (continued)

68 EXTENDED WING.
SLATS RETRACTED.
FLAPS 10, TABS 0.
100% SPAN WITH BODY CUTOUT.
76 M/S. FREE TRANSITION.

ALPHA	CL	CD	CM
-5.03	-0.061	0.0178	-0.1839
-3.98	0.053	0.0166	-0.1964
-2.93	0.156	0.0166	-0.2125
-1.88	0.264	0.0175	-0.2285
-0.84	0.365	0.0198	-0.2366
0.20	0.453	0.0230	-0.2442
1.25	0.549	0.0279	-0.2538
2.29	0.651	0.0332	-0.2614
3.34	0.752	0.0392	-0.2716
4.38	0.856	0.0462	-0.2818
5.43	0.965	0.0547	-0.2925
6.47	1.059	0.0630	-0.3000
7.52	1.157	0.0739	-0.3072
8.56	1.242	0.0908	-0.3082
9.58	1.293	0.1171	-0.2899
10.56	1.252	0.1802	-0.2289

69 EXTENDED WING.
SLATS RETRACTED.
FLAPS 25, TABS 0.
100% SPAN WITH BODY CUTOUT.
76 M/S. FREE TRANSITION.

ALPHA	CL	CD	CM
-4.75	0.554	0.0409	-0.5107
-3.71	0.642	0.0446	-0.5217
-2.67	0.743	0.0497	-0.5342
-1.62	0.851	0.0580	-0.5430
-0.57	0.949	0.0658	-0.5525
0.47	1.040	0.0735	-0.5601
1.51	1.133	0.0820	-0.5707
2.56	1.252	0.0940	-0.5836
3.60	1.337	0.1033	-0.5889
4.63	1.413	0.1123	-0.5959
5.69	1.533	0.1303	-0.5991
6.71	1.595	0.1444	-0.5939
7.72	1.600	0.1891	-0.5205

70 EXTENDED WING.
SLATS RETRACTED.
FLAPS 40, TABS 0.
100% SPAN WITH BODY CUTOUT.
76 M/S. FREE TRANSITION.

ALPHA	CL	CD	CM
0.62	1.394	0.1488	-0.7360
1.66	1.474	0.1592	-0.7371
2.69	1.547	0.1695	-0.7434
3.74	1.649	0.1858	-0.7494
4.77	1.708	0.1961	-0.7444
5.79	1.763	0.2165	-0.7154
6.79	1.751	0.2549	-0.6418

71 EXTENDED WING + BODY.
SLATS RETRACTED.
FLAPS 0, TABS 0.
76 M/S. FREE TRANSITION.

ALPHA	CL	CD	CM
-5.17	-0.369	0.0305	-0.1407
-4.13	-0.280	0.0265	-0.1326
-3.08	-0.177	0.0228	-0.1239
-2.04	-0.086	0.0205	-0.1158
-1.00	-0.004	0.0189	-0.1065
0.04	0.086	0.0185	-0.0971
1.08	0.179	0.0191	-0.0889
2.12	0.262	0.0212	-0.0713
3.15	0.345	0.0237	-0.0601
4.19	0.431	0.0266	-0.0511
5.23	0.522	0.0302	-0.0405
6.27	0.599	0.0341	-0.0310
7.31	0.686	0.0392	-0.0175
8.35	0.772	0.0452	-0.0054
9.38	0.855	0.0521	0.0062
10.42	0.932	0.0672	0.0232
11.43	0.952	0.0978	0.0571
12.41	0.921	0.1555	0.1084
13.42	0.928	0.1822	0.1198
14.42	0.935	0.2066	0.1294

Table 4 (continued)

72 EXTENDED WING + BODY.
SLATS RETRACTED.
FLAPS 10, TABS 0. 100% SPAN.
76 M/S. FREE TRANSITION.

ALPHA	CL	CD	CM
-5.03	-0.078	0.0282	-0.2820
-3.99	0.025	0.0265	-0.2846
-2.94	0.141	0.0259	-0.2922
-1.89	0.245	0.0267	-0.2966
-0.84	0.361	0.0289	-0.2974
0.20	0.457	0.0320	-0.2933
1.25	0.557	0.0371	-0.2887
2.30	0.677	0.0434	-0.2868
3.35	0.780	0.0495	-0.2852
4.39	0.878	0.0562	-0.2827
5.44	0.981	0.0643	-0.2829
6.48	1.080	0.0733	-0.2794
7.53	1.179	0.0840	-0.2754
8.57	1.272	0.1024	-0.2623
9.59	1.324	0.1295	-0.2358
10.57	1.275	0.1958	-0.1620

73 EXTENDED WING + BODY.
SLATS RETRACTED.
FLAPS 25, TABS 0. 100% SPAN.
76 M/S. FREE TRANSITION.

ALPHA	CL	CD	CM
-4.72	0.621	0.0527	-0.6382
-3.69	0.697	0.0561	-0.6404
-2.65	0.790	0.0610	-0.6406
-1.60	0.892	0.0691	-0.6353
-0.56	0.986	0.0769	-0.6323
0.49	1.086	0.0855	-0.6322
1.54	1.198	0.0960	-0.6274
2.58	1.302	0.1066	-0.6268
3.62	1.395	0.1171	-0.6204
4.67	1.502	0.1304	-0.6119
5.71	1.594	0.1452	-0.6042
6.75	1.668	0.1652	-0.5833
7.75	1.663	0.2117	-0.5018
8.74	1.642	0.2465	-0.4395

74 EXTENDED WING + BODY.
SLATS RETRACTED.
FLAPS 40, TABS 0. 100% SPAN.
76 M/S. FREE TRANSITION.

ALPHA	CL	CD	CM
-4.56	0.984	0.1128	-0.8345
-3.51	1.085	0.1216	-0.8301
-2.48	1.172	0.1307	-0.8217
-1.43	1.279	0.1419	-0.8160
-0.39	1.363	0.1517	-0.8099
0.65	1.444	0.1619	-0.8006
1.69	1.535	0.1739	-0.7919
2.73	1.620	0.1862	-0.7840
3.77	1.712	0.2017	-0.7768
4.80	1.784	0.2154	-0.7664
5.83	1.841	0.2402	-0.7207
6.81	1.808	0.2897	-0.6128
7.81	1.801	0.3085	-0.5807

Table 4 (continued)

75 EXTENDED WING + BODY.
SLATS DEFLECTED 25.
FLAPS 0, TABS 0.
76 M/S. FREE TRANSITION.

ALPHA	CL	CD	CM
-5.14	-0.322	0.1405	-0.2049
-4.12	-0.270	0.1237	-0.1807
-3.10	-0.224	0.1098	-0.1452
-2.08	-0.168	0.0963	-0.1235
-1.05	-0.102	0.0827	-0.1046
-0.02	-0.040	0.0741	-0.0866
1.03	0.070	0.0622	-0.0717
2.07	0.153	0.0553	-0.0615
3.11	0.253	0.0500	-0.0465
4.15	0.343	0.0482	-0.0307
5.19	0.421	0.0484	-0.0187
6.23	0.519	0.0508	-0.0047
7.27	0.605	0.0539	0.0056
8.31	0.703	0.0583	0.0184
9.36	0.810	0.0631	0.0237
10.41	0.907	0.0680	0.0309
11.45	1.005	0.0743	0.0412
12.50	1.111	0.0825	0.0554
13.55	1.222	0.0931	0.0722
14.59	1.315	0.1036	0.0850
15.63	1.407	0.1154	0.1019
16.67	1.492	0.1284	0.1165
17.71	1.576	0.1425	0.1366
18.75	1.667	0.1584	0.1558
19.78	1.745	0.1732	0.1724
20.82	1.823	0.1897	0.1755
21.84	1.884	0.2048	0.1802
22.87	1.946	0.2238	0.1950
23.90	1.996	0.2501	0.2298
24.91	2.039	0.2683	0.2575
25.90	2.014	0.3081	0.2905
26.87	1.945	0.3394	0.3397

76 EXTENDED WING + BODY.
SLATS DEFLECTED 25.
FLAPS 10, TABS 0. 100% SPAN.
76 M/S. FREE TRANSITION.

ALPHA	CL	CD	CM
-0.96	0.086	0.0778	-0.2316
0.10	0.222	0.0696	-0.2585
1.17	0.390	0.0630	-0.2857
2.25	0.547	0.0621	-0.3020
3.29	0.647	0.0640	-0.3028
4.34	0.761	0.0686	-0.3037
5.39	0.879	0.0749	-0.3021
6.44	0.990	0.0819	-0.3018
7.49	1.101	0.0894	-0.3012
8.54	1.203	0.0970	-0.2963
9.59	1.324	0.1077	-0.2917
10.66	1.464	0.1222	-0.2847
11.71	1.580	0.1364	-0.2792
12.75	1.674	0.1496	-0.2692
13.80	1.776	0.1655	-0.2594
14.85	1.895	0.1869	-0.2458
15.89	1.986	0.2036	-0.2331
16.93	2.080	0.2222	-0.2229
17.97	2.159	0.2387	-0.2096
19.01	2.242	0.2577	-0.2004
20.05	2.333	0.2799	-0.1826
21.07	2.395	0.3015	-0.1618
22.09	2.433	0.3311	-0.1480
23.09	2.424	0.3566	-0.0950

Table 4 (continued)

77 EXTENDED WING + BODY.
SLATS DEFLECTED 25.
FLAPS 10, TABS 0. 80% SPAN.
76 M/S. FREE TRANSITION.

ALPHA	CL	CD	CM
-0.97	0.058	0.0795	-0.2140
0.09	0.207	0.0689	-0.2305
1.16	0.353	0.0624	-0.2415
2.22	0.486	0.0602	-0.2487
3.28	0.618	0.0619	-0.2462
4.33	0.729	0.0658	-0.2390
5.38	0.838	0.0713	-0.2339
6.42	0.940	0.0773	-0.2272
7.48	1.065	0.0852	-0.2231
8.53	1.189	0.0940	-0.2171
9.59	1.313	0.1049	-0.2111
10.63	1.412	0.1150	-0.2037
11.68	1.517	0.1271	-0.1921
12.72	1.618	0.1406	-0.1821
13.78	1.733	0.1581	-0.1713
14.81	1.813	0.1719	-0.1590
15.86	1.919	0.1904	-0.1406
16.90	2.002	0.2064	-0.1286
17.94	2.101	0.2260	-0.1108
18.98	2.195	0.2463	-0.0982
20.02	2.272	0.2644	-0.0794
21.04	2.319	0.2896	-0.0468
22.07	2.376	0.3147	-0.0157
23.09	2.422	0.3366	0.0205
24.06	2.354	0.3740	0.0692

78 EXTENDED WING + BODY.
SLATS DEFLECTED 25.
FLAPS 10, TABS 0.
80% SPAN WITH ENGINE CUTOUT.
76 M/S. FREE TRANSITION.

ALPHA	CL	CD	CM
-1.01	-0.023	0.0824	-0.1886
0.05	0.111	0.0723	-0.2018
1.11	0.239	0.0639	-0.2121
2.17	0.379	0.0597	-0.2183
3.23	0.508	0.0593	-0.2142
4.28	0.618	0.0620	-0.2104
5.32	0.710	0.0655	-0.2050
6.38	0.841	0.0722	-0.1952
7.43	0.951	0.0792	-0.1932
8.47	1.050	0.0849	-0.1889
9.52	1.160	0.0928	-0.1798
10.57	1.280	0.1031	-0.1721
11.62	1.391	0.1145	-0.1610
12.67	1.490	0.1263	-0.1506
13.71	1.585	0.1389	-0.1397
14.76	1.702	0.1569	-0.1271
15.81	1.799	0.1738	-0.1122
16.85	1.891	0.1905	-0.0966
17.88	1.973	0.2063	-0.0832
18.93	2.074	0.2265	-0.0659
19.96	2.150	0.2438	-0.0504
20.99	2.209	0.2676	-0.0256
22.01	2.246	0.2856	0.0029
23.04	2.316	0.3136	0.0383
24.02	2.265	0.3431	0.1027

Table 4 (continued)

79 EXTENDED WING + BODY.
SLATS DEFLECTED 25.
FLAPS 10, TABS 0. 60% SPAN.
76 M/S. FREE TRANSITION.

ALPHA	CL	CD	CM
-1.00	0.010	0.0824	-0.1923
0.06	0.138	0.0718	-0.1899
1.12	0.274	0.0631	-0.1910
2.18	0.400	0.0592	-0.1900
3.23	0.516	0.0590	-0.1819
4.28	0.627	0.0614	-0.1733
5.33	0.731	0.0658	-0.1657
6.37	0.835	0.0712	-0.1559
7.42	0.944	0.0776	-0.1492
8.48	1.064	0.0847	-0.1442
9.53	1.185	0.0940	-0.1346
10.58	1.301	0.1045	-0.1240
11.63	1.403	0.1151	-0.1117
12.67	1.489	0.1258	-0.1005
13.72	1.604	0.1423	-0.0849
14.76	1.698	0.1573	-0.0701
15.80	1.787	0.1730	-0.0536
16.84	1.882	0.1902	-0.0338
17.88	1.971	0.2071	-0.0185
18.92	2.056	0.2252	-0.0036
19.96	2.140	0.2443	0.0127
20.99	2.212	0.2634	0.0353
22.01	2.258	0.2924	0.0664
23.03	2.297	0.3158	0.0916
24.05	2.335	0.3428	0.1393
25.01	2.247	0.3725	0.1732

80 EXTENDED WING + BODY.
SLATS DEFLECTED 25.
FLAPS 25. TABS 0.
76 M/S. FREE TRANSITION.

ALPHA	CL	CD	CM
-5.05	-0.108	0.1295	-0.3012
-4.00	0.005	0.1164	-0.3021
-2.94	0.130	0.1061	-0.3267
-1.84	0.359	0.0948	-0.4135
-0.70	0.673	0.0893	-0.5333
0.40	0.894	0.0941	-0.5908
1.47	1.048	0.1021	-0.6132
2.54	1.212	0.1138	-0.6270
3.59	1.327	0.1237	-0.6260
4.65	1.448	0.1352	-0.6277
5.70	1.563	0.1469	-0.6220
6.75	1.679	0.1605	-0.6166
7.79	1.770	0.1723	-0.6105
8.85	1.900	0.1912	-0.6039
9.90	1.999	0.2075	-0.5933
10.95	2.109	0.2273	-0.5817
11.98	2.194	0.2435	-0.5698
13.03	2.299	0.2647	-0.5525
14.07	2.395	0.2853	-0.5367
15.11	2.484	0.3056	-0.5150
16.15	2.573	0.3269	-0.4982
17.19	2.651	0.3473	-0.4728
18.22	2.709	0.3674	-0.4295
19.23	2.749	0.3873	-0.3774
20.24	2.752	0.4091	-0.2985
21.23	2.746	0.4355	-0.2486

Table 4 (continued)

81 EXTENDED WING + BODY.
SLATS DEFLECTED 25.
FLAPS 25, TABS 0. 80% SPAN.
76 M/S. FREE TRANSITION.

ALPHA	CL	CD	CM
0.34	0.749	0.0869	-0.4641
1.41	0.917	0.0927	-0.4835
2.47	1.056	0.1007	-0.4890
3.53	1.183	0.1100	-0.4892
4.59	1.312	0.1210	-0.4843
5.64	1.419	0.1306	-0.4790
6.69	1.539	0.1425	-0.4743
7.74	1.643	0.1543	-0.4643
8.78	1.747	0.1678	-0.4566
9.83	1.857	0.1842	-0.4409
10.88	1.968	0.2025	-0.4325
11.93	2.067	0.2199	-0.4181
12.97	2.153	0.2363	-0.4051
14.01	2.249	0.2556	-0.3883
15.05	2.337	0.2743	-0.3739
16.08	2.414	0.2915	-0.3561
17.12	2.503	0.3121	-0.3370
18.16	2.592	0.3339	-0.3183
19.19	2.653	0.3574	-0.2812
20.22	2.708	0.3801	-0.2371
21.21	2.695	0.4087	-0.1766

82 EXTENDED WING + BODY.
SLATS DEFLECTED 25.
FLAPS 25, TABS 0.
80% SPAN WITH ENGINE CUTOUT.
76 M/S. FREE TRANSITION.

ALPHA	CL	CD	CM
0.21	0.464	0.0836	-0.3706
1.30	0.659	0.0858	-0.4036
2.36	0.797	0.0904	-0.4151
3.41	0.923	0.0973	-0.4123
4.46	1.036	0.1047	-0.4100
5.51	1.150	0.1131	-0.4069
6.56	1.259	0.1220	-0.4013
7.62	1.374	0.1320	-0.3939
8.67	1.486	0.1435	-0.3835
9.71	1.577	0.1541	-0.3773
10.76	1.693	0.1694	-0.3618
11.80	1.792	0.1842	-0.3493
12.85	1.889	0.2004	-0.3364
13.89	1.986	0.2181	-0.3192
14.93	2.072	0.2346	-0.3037
15.97	2.167	0.2534	-0.2832
17.01	2.256	0.2719	-0.2690
18.05	2.331	0.2888	-0.2502
19.09	2.420	0.3119	-0.2287
20.11	2.477	0.3328	-0.1951
21.13	2.528	0.3557	-0.1456
22.13	2.510	0.3800	-0.1037

Table 4 (continued)

83 EXTENDED WING + BODY.
SLATS DEFLECTED 25.
FLAPS 25, TABS 0. 60% SPAN.
76 M/S. FREE TRANSITION.

ALPHA	CL	CD	CM
0.24	0.546	0.0832	-0.3192
1.32	0.707	0.0850	-0.3266
2.37	0.835	0.0897	-0.3281
3.43	0.958	0.0970	-0.3240
4.48	1.063	0.1043	-0.3175
5.54	1.195	0.1144	-0.3071
6.59	1.307	0.1234	-0.3033
7.63	1.416	0.1337	-0.2934
8.68	1.517	0.1448	-0.2819
9.72	1.618	0.1577	-0.2731
10.77	1.714	0.1721	-0.2578
11.82	1.819	0.1887	-0.2417
12.86	1.909	0.2040	-0.2251
13.90	2.000	0.2203	-0.2091
14.93	2.085	0.2365	-0.1922
15.97	2.170	0.2540	-0.1710
17.01	2.259	0.2727	-0.1487
18.05	2.340	0.2909	-0.1249
19.08	2.407	0.3076	-0.1006
20.11	2.480	0.3290	-0.0519
21.12	2.501	0.3644	-0.0386
22.14	2.533	0.3942	0.0094
23.15	2.567	0.4132	0.0427
24.09	2.429	0.4408	0.0896

84 EXTENDED WING + BODY.
SLATS DEFLECTED 25.
FLAPS 25, TABS 15. 80% SPAN.
76 M/S. FREE TRANSITION.

ALPHA	CL	CD	CM
0.46	1.026	0.1141	-0.5868
1.53	1.176	0.1243	-0.5965
2.59	1.317	0.1360	-0.6026
3.65	1.449	0.1485	-0.6017
4.69	1.549	0.1585	-0.5952
5.74	1.662	0.1685	-0.5906
6.79	1.766	0.1839	-0.5796
7.84	1.873	0.1992	-0.5669
8.88	1.971	0.2143	-0.5552
9.93	2.072	0.2316	-0.5362
10.97	2.170	0.2488	-0.5207
12.02	2.267	0.2667	-0.4985
13.06	2.356	0.2844	-0.4835
14.09	2.440	0.3023	-0.4612
15.14	2.535	0.3234	-0.4438
16.17	2.613	0.3412	-0.4228
17.21	2.701	0.3635	-0.4000
18.24	2.764	0.3874	-0.3670
19.26	2.818	0.4080	-0.3263
20.26	2.812	0.4337	-0.2539

Table 4 (continued)

85 EXTENDED WING + BODY.
SLATS DEFLECTED 25.
FLAPS 25, TABS 30. 80% SPAN.
76 M/S. FREE TRANSITION.

ALPHA	CL	CD	CM
0.46	1.022	0.1317	-0.5288
1.52	1.168	0.1427	-0.5706
2.58	1.297	0.1540	-0.5674
3.63	1.405	0.1642	-0.5632
4.68	1.513	0.1741	-0.5530
5.72	1.613	0.1844	-0.5404
6.77	1.716	0.1967	-0.5332
7.82	1.823	0.2112	-0.5200
8.86	1.914	0.2247	-0.5060
9.91	2.020	0.2417	-0.4948
10.95	2.113	0.2573	-0.4791
11.99	2.202	0.2735	-0.4633
13.03	2.296	0.2917	-0.4450
14.07	2.396	0.3119	-0.4283
15.11	2.482	0.3307	-0.4082
16.15	2.571	0.3520	-0.3889
17.19	2.657	0.3731	-0.3661
18.22	2.719	0.3948	-0.3440
19.25	2.776	0.4187	-0.2973
20.26	2.809	0.4452	-0.2517
21.25	2.778	0.4791	-0.1810

86 EXTENDED WING + BODY.
SLATS DEFLECTED 25.
FLAPS 40, TABS 0. 100% SPAN.
76 M/S. FREE TRANSITION.

ALPHA	CL	CD	CM
0.63	1.413	0.1648	-0.8481
1.69	1.543	0.1774	-0.8575
2.74	1.652	0.1904	-0.8511
3.79	1.771	0.2062	-0.8356
4.83	1.853	0.2187	-0.8240
5.87	1.937	0.2317	-0.8102
6.90	2.015	0.2460	-0.7941
7.95	2.114	0.2641	-0.7755
8.99	2.211	0.2825	-0.7594
10.03	2.303	0.3000	-0.7381
11.08	2.404	0.3198	-0.7197
12.12	2.502	0.3402	-0.7047
13.16	2.592	0.3602	-0.6855
14.21	2.687	0.3816	-0.6570
15.25	2.794	0.4039	-0.6375
16.28	2.842	0.4230	-0.5945
17.30	2.888	0.4416	-0.5344
18.30	2.898	0.4632	-0.4567
19.31	2.917	0.4897	-0.3920
20.32	2.934	0.5154	-0.3412
21.28	2.857	0.5630	-0.2723

Table 4 (continued)

87 EXTENDED WING + BODY.
SLATS DEFLECTED 25.
FLAPS 40, TABS 0. 80% SPAN.
76 M/S. FREE TRANSITION.

ALPHA	CL	CD	CM
0.53	1.191	0.1435	-0.6454
1.60	1.344	0.1559	-0.6543
2.65	1.454	0.1673	-0.6558
3.70	1.571	0.1803	-0.6454
4.75	1.676	0.1931	-0.6353
5.79	1.755	0.2038	-0.6269
6.83	1.857	0.2195	-0.6166
7.87	1.947	0.2344	-0.5940
8.91	2.028	0.2483	-0.5765
9.95	2.127	0.2652	-0.5555
10.99	2.218	0.2817	-0.5260
12.04	2.317	0.3011	-0.5128
13.08	2.409	0.3199	-0.4954
14.12	2.494	0.3378	-0.4738
14.12	2.492	0.3355	-0.4790
15.16	2.586	0.3563	-0.4569
16.19	2.661	0.3738	-0.4293
17.23	2.745	0.3971	-0.3967
18.26	2.805	0.4205	-0.3629
19.29	2.868	0.4414	-0.3321
20.27	2.826	0.4701	-0.2387

88 EXTENDED WING + BODY.
SLATS DEFLECTED 25.
FLAPS 40, TABS 0.
80% SPAN WITH ENGINE CUTOUT.
76 M/S. FREE TRANSITION.

ALPHA	CL	CD	CM
0.40	0.898	0.1323	-0.5669
1.46	1.037	0.1404	-0.5799
2.52	1.170	0.1497	-0.5817
3.58	1.293	0.1607	-0.5806
4.63	1.398	0.1710	-0.5692
5.68	1.507	0.1815	-0.5573
6.72	1.605	0.1916	-0.5481
7.77	1.709	0.2039	-0.5327
8.82	1.828	0.2197	-0.5168
9.85	1.905	0.2315	-0.5009
10.90	2.009	0.2490	-0.4835
11.94	2.095	0.2646	-0.4603
12.98	2.182	0.2815	-0.4390
14.01	2.262	0.2971	-0.4185
15.06	2.359	0.3171	-0.3968
16.09	2.437	0.3327	-0.3695
17.13	2.518	0.3512	-0.3496
18.16	2.577	0.3676	-0.3246
19.19	2.652	0.3920	-0.2792
20.21	2.700	0.4095	-0.2402
21.18	2.635	0.4422	-0.1584

Table 4 (continued)

89 EXTENDED WING + BODY.
SLATS DEFLECTED 25.
FLAPS 40, TABS 0. 60% SPAN.
76 M/S. FREE TRANSITION.

ALPHA	CL	CD	CM
0.40	0.884	0.1251	-0.4262
1.46	1.024	0.1332	-0.4311
2.52	1.155	0.1439	-0.4305
3.57	1.264	0.1539	-0.4236
4.62	1.380	0.1655	-0.4128
5.66	1.476	0.1753	-0.4041
6.70	1.563	0.1862	-0.3914
7.74	1.651	0.1980	-0.3798
8.78	1.751	0.2118	-0.3596
9.82	1.832	0.2243	-0.3463
10.87	1.930	0.2401	-0.3288
11.91	2.040	0.2591	-0.3078
12.95	2.116	0.2729	-0.2929
13.99	2.207	0.2904	-0.2719
15.03	2.297	0.3088	-0.2496
16.06	2.371	0.3255	-0.2302
17.10	2.446	0.3434	-0.2066
18.13	2.520	0.3633	-0.1832
19.15	2.569	0.3790	-0.1762
20.18	2.619	0.4115	-0.1267
21.19	2.644	0.4452	-0.0772
22.15	2.562	0.4729	-0.0397

90 EXTENDED WING + BODY.
SLATS DEFLECTED 25.
FLAPS 40, TABS 15. 80% SPAN.
76 M/S. FREE TRANSITION.

ALPHA	CL	CD	CM
0.65	1.457	0.1835	-0.7623
1.72	1.598	0.1994	-0.7660
2.76	1.699	0.2118	-0.7551
3.80	1.795	0.2242	-0.7405
4.85	1.896	0.2397	-0.7302
5.88	1.971	0.2525	-0.7147
6.92	2.040	0.2663	-0.6984
7.95	2.124	0.2816	-0.6751
9.00	2.219	0.2987	-0.6535
10.04	2.309	0.3152	-0.6320
11.08	2.405	0.3329	-0.6141
12.12	2.499	0.3522	-0.5908
13.16	2.577	0.3681	-0.5710
14.20	2.670	0.3889	-0.5448
15.23	2.750	0.4079	-0.5186
16.26	2.815	0.4253	-0.4928
17.29	2.873	0.4464	-0.4651
18.32	2.943	0.4700	-0.4303
19.31	2.910	0.4932	-0.3228

Table 4 (concluded)

91 EXTENDED WING + BODY.
SLATS DEFLECTED 25.
FLAPS 40, TABS 30. 80% SPAN.
76 M/S. FREE TRANSITION.

ALPHA	CL	CD	CM
0.61	1.368	0.1919	-0.7038
1.66	1.479	0.2029	-0.7006
2.72	1.600	0.2161	-0.6965
3.76	1.704	0.2280	-0.6821
4.80	1.793	0.2407	-0.6747
5.84	1.871	0.2510	-0.6500
6.88	1.959	0.2654	-0.6370
7.92	2.051	0.2807	-0.6202
8.96	2.143	0.2959	-0.6026
10.00	2.239	0.3125	-0.5808
11.05	2.330	0.3289	-0.5637
12.08	2.414	0.3450	-0.5475
13.12	2.502	0.3631	-0.5236
14.17	2.600	0.3866	-0.5126
15.20	2.668	0.4010	-0.4870
16.24	2.769	0.4287	-0.4643
17.27	2.828	0.4493	-0.4279
18.30	2.884	0.4693	-0.3989
19.29	2.877	0.4971	-0.3091

REFERENCES

No.	Author	Title, etc.
1	B.R. Williams D.S. Woodward	Multiple-aerofoil viscous iterative system (MAVIS) - the initial structure and possible extensions. Unpublished MOD(PE) work
2	P.R. Ashill	A study of the effect of the wake of the main aerofoil of a Fowler-flap configuration on the lift of the flap. ARC CP No.1257 (1972)
3	J. Weber D.A. Kirby D.J. Kettle	An extension of Multhopp's method of calculating the spanwise loading of wing-fuselage combinations. ARC R & M 2872 (1956)
4	J. Mckie	The estimation of the loading on swept wings with extending chord flaps at subsonic speeds. ARC CP No.1110 (1969)
5	E.C. Maskell D.A. Kirby J.Y.G. Evans	Aerodynamic research to improve the low-speed performance of transport aircraft for short and medium ranges. Unpublished MOD(PE) work
6	D.A. Lovell	A low-speed wing-tunnel investigation of the tailplane effectiveness of a model representing the airbus type of aircraft. ARC R & M 3642 (1970)
7	D.A. Lovell	A generalised programme for the processing of low-speed wind-tunnel mechanical-balance force and moment data. RAE Technical Report 70174 (1970)
8	D.J. Kettle	Low-speed wind-tunnel measurements of wing-strut mutual interference effects on tare loads and moments. RAE Technical Report 74055 (1974)
9	I.R.M. Moir D.S. Woodward D.E. Leam	National high lift programme - the optimisation of a 12.5% chord slat and a 33% single-slotted flap on a half model with a tapered planform of 30° sweep. RAE Technical Report to be published
10	E.A. Carr-Hill	Unpublished MOD(PE) work.
11	D.A. Lovell	Unpublished MOD(PE) work.

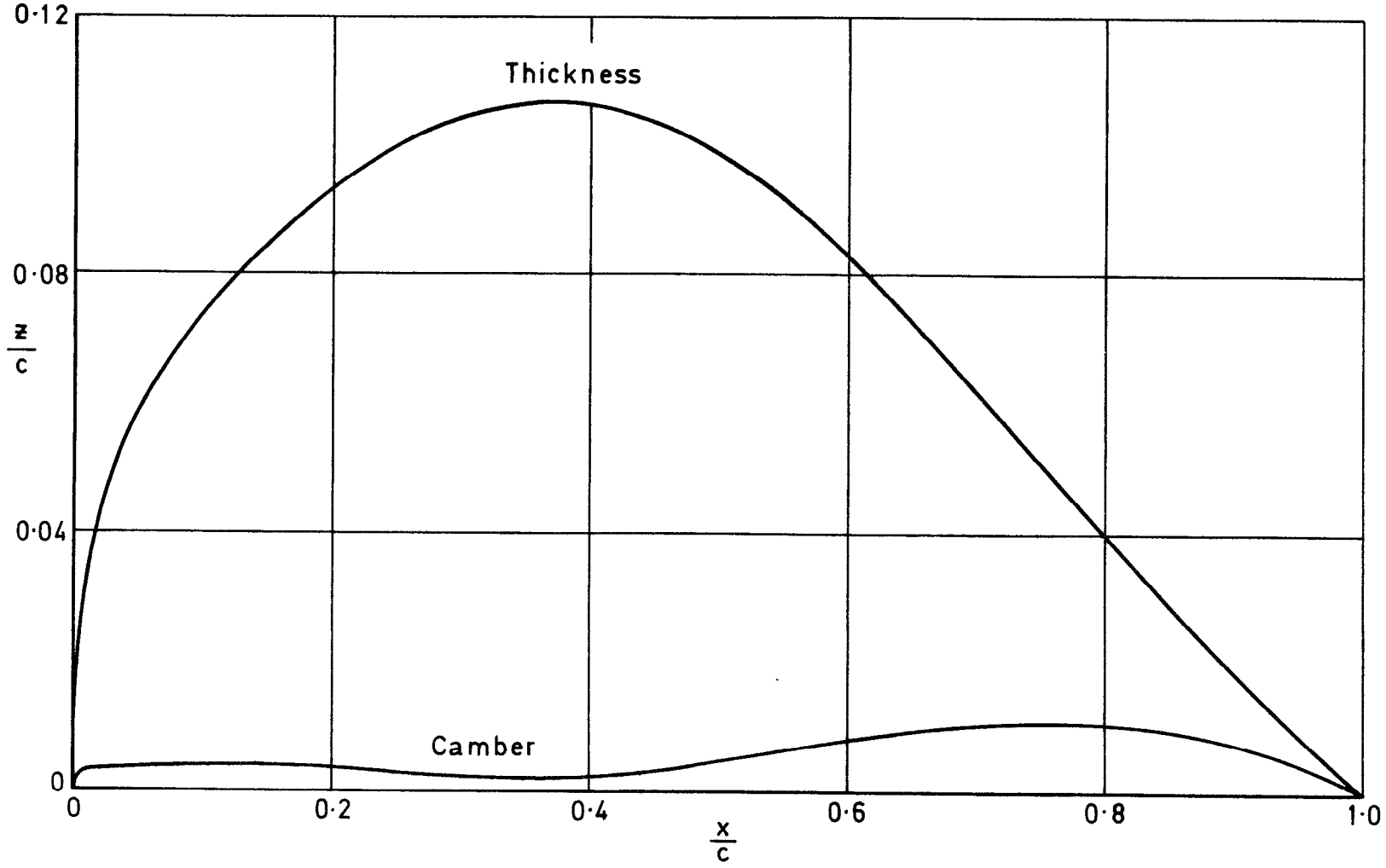

Fig.1 Thickness and camber distributions of the wing section

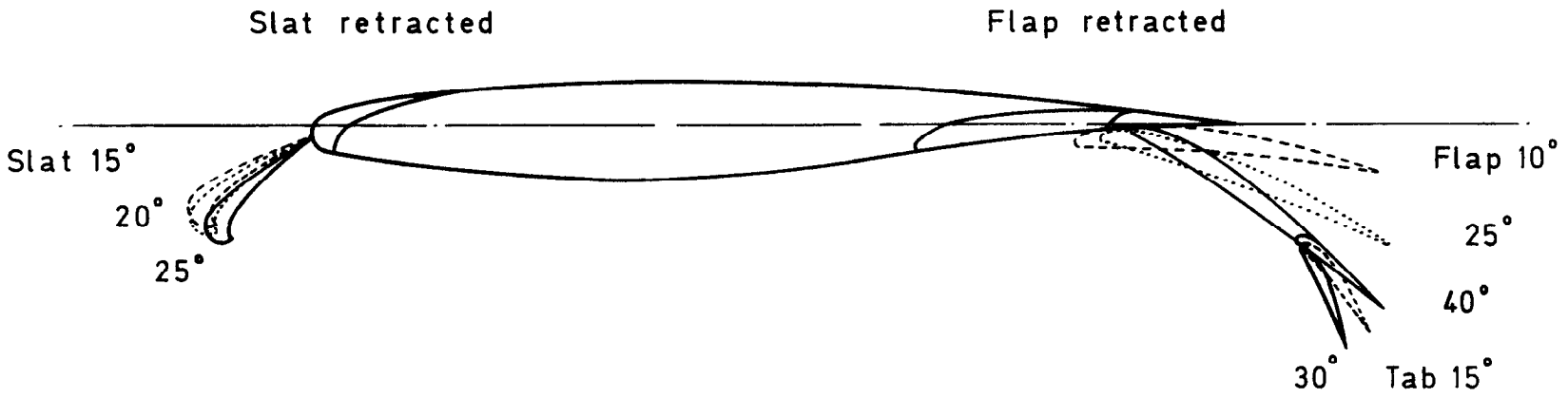

a Basic high-lift section. (Constant percentage chord slat, flap and tab)

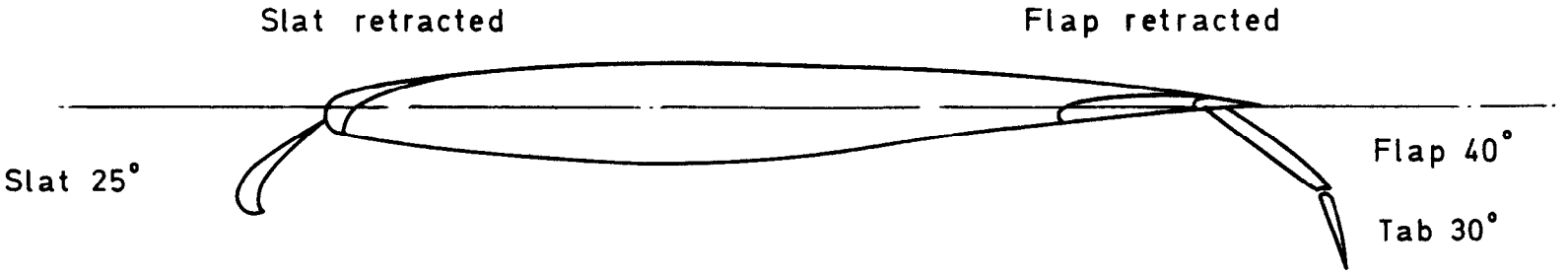

b Modified high-lift section used on extended planform. Section at body side

Fig. 2a & b The high-lift section of the basic and extended planform wings

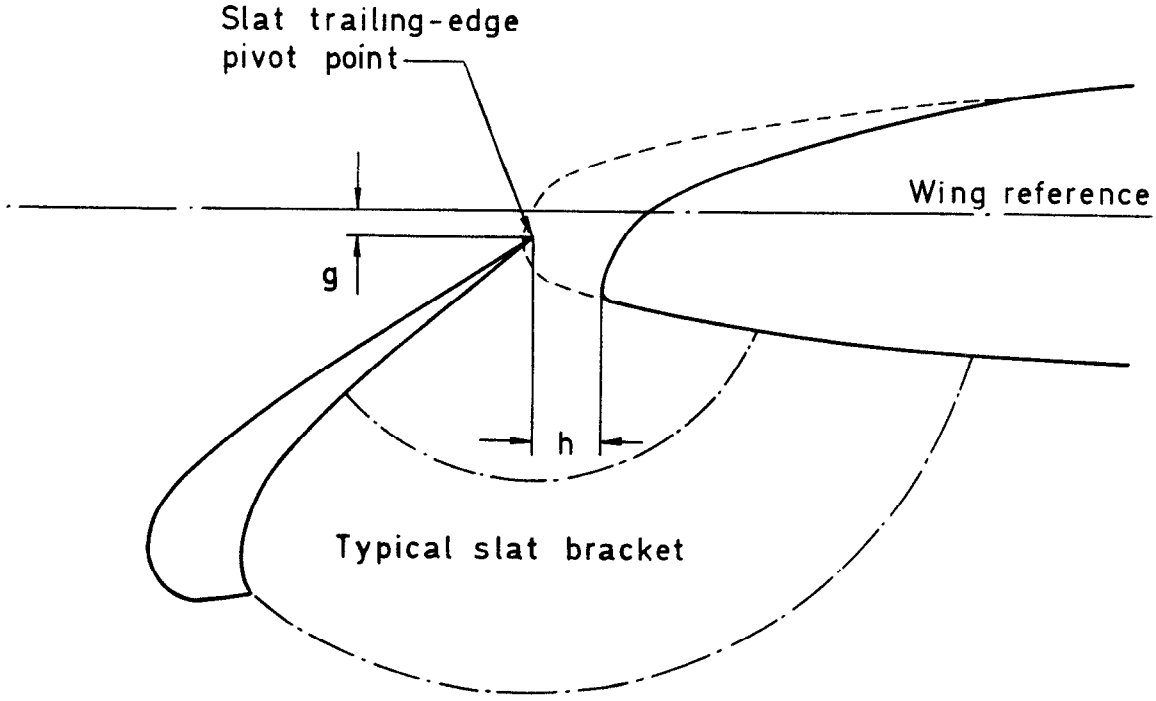

a Slat

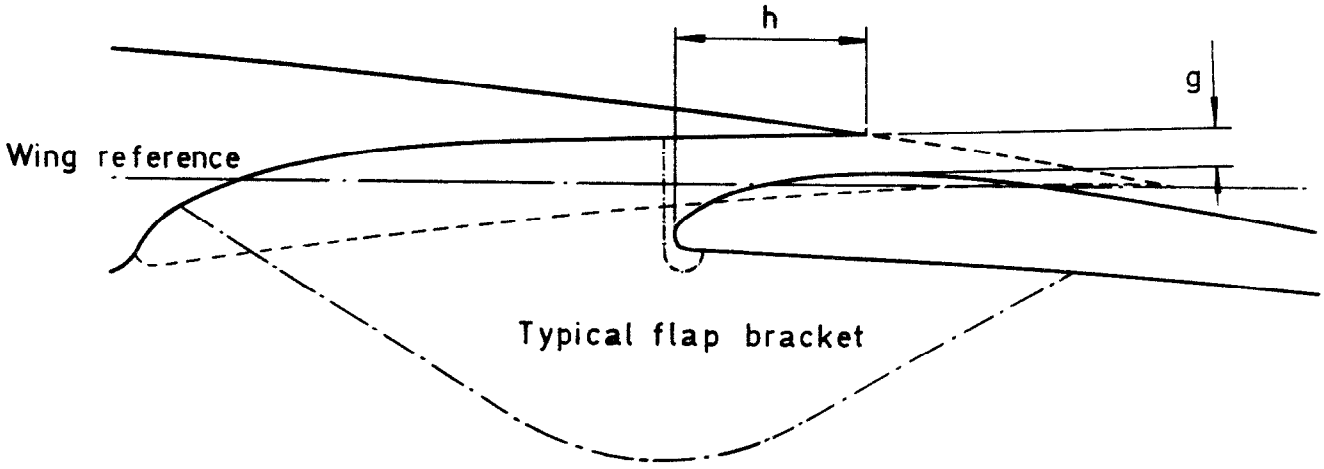

b Flap

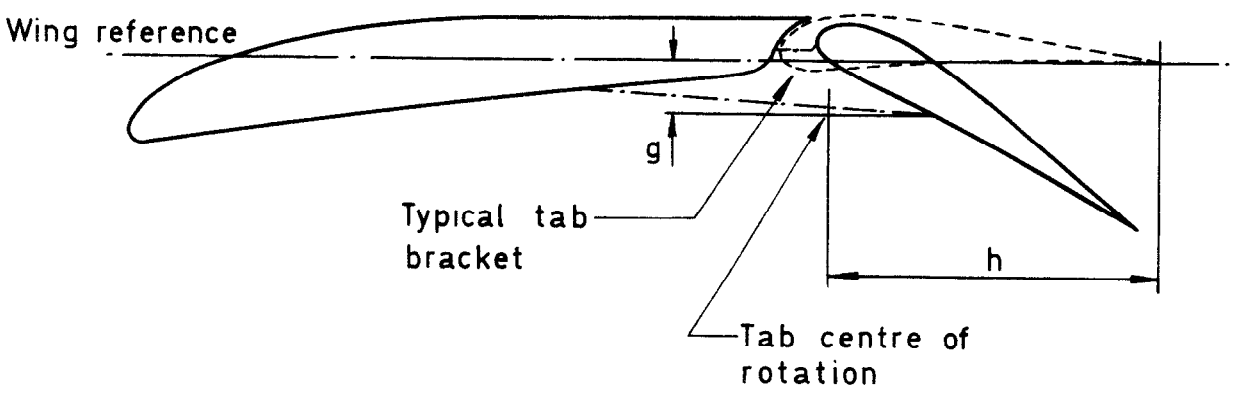

c Tab

Fig.3a-c Deflection geometry for the high-lift section

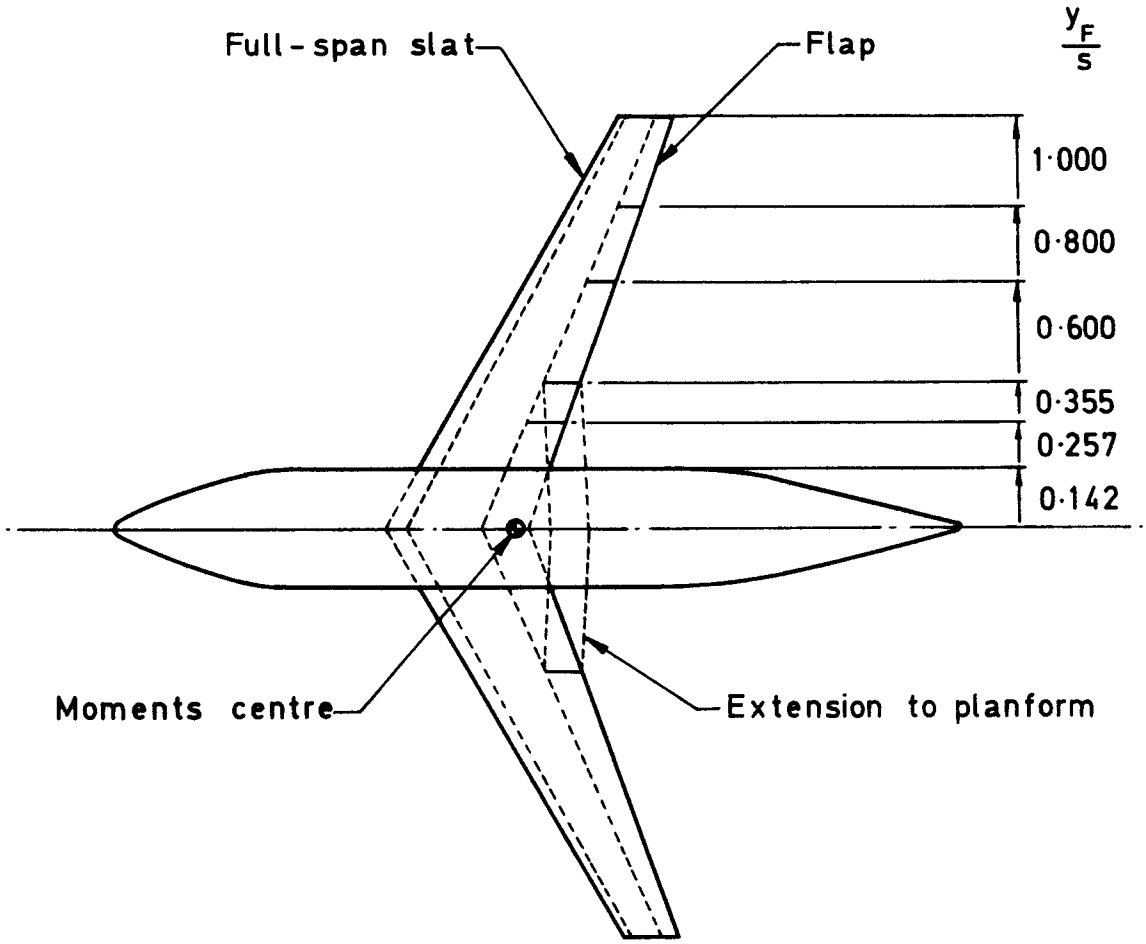

The slats and flaps are shown in the retracted position

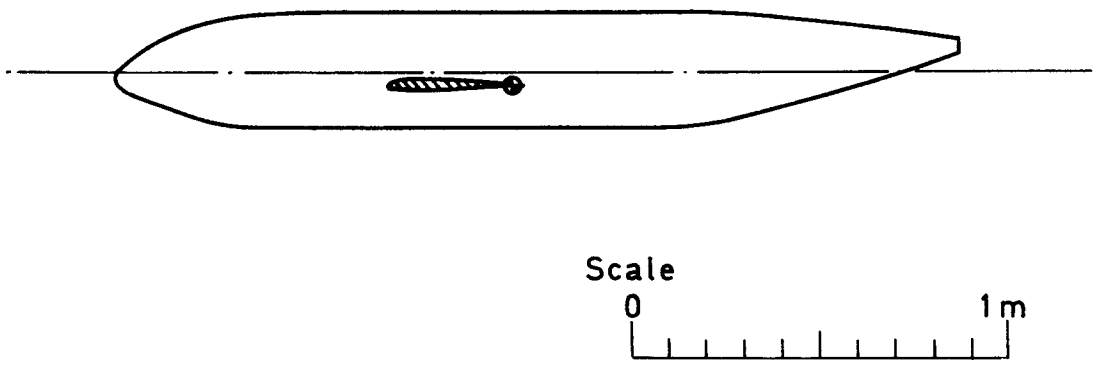

Fig.4 General arrangement sketch of the model

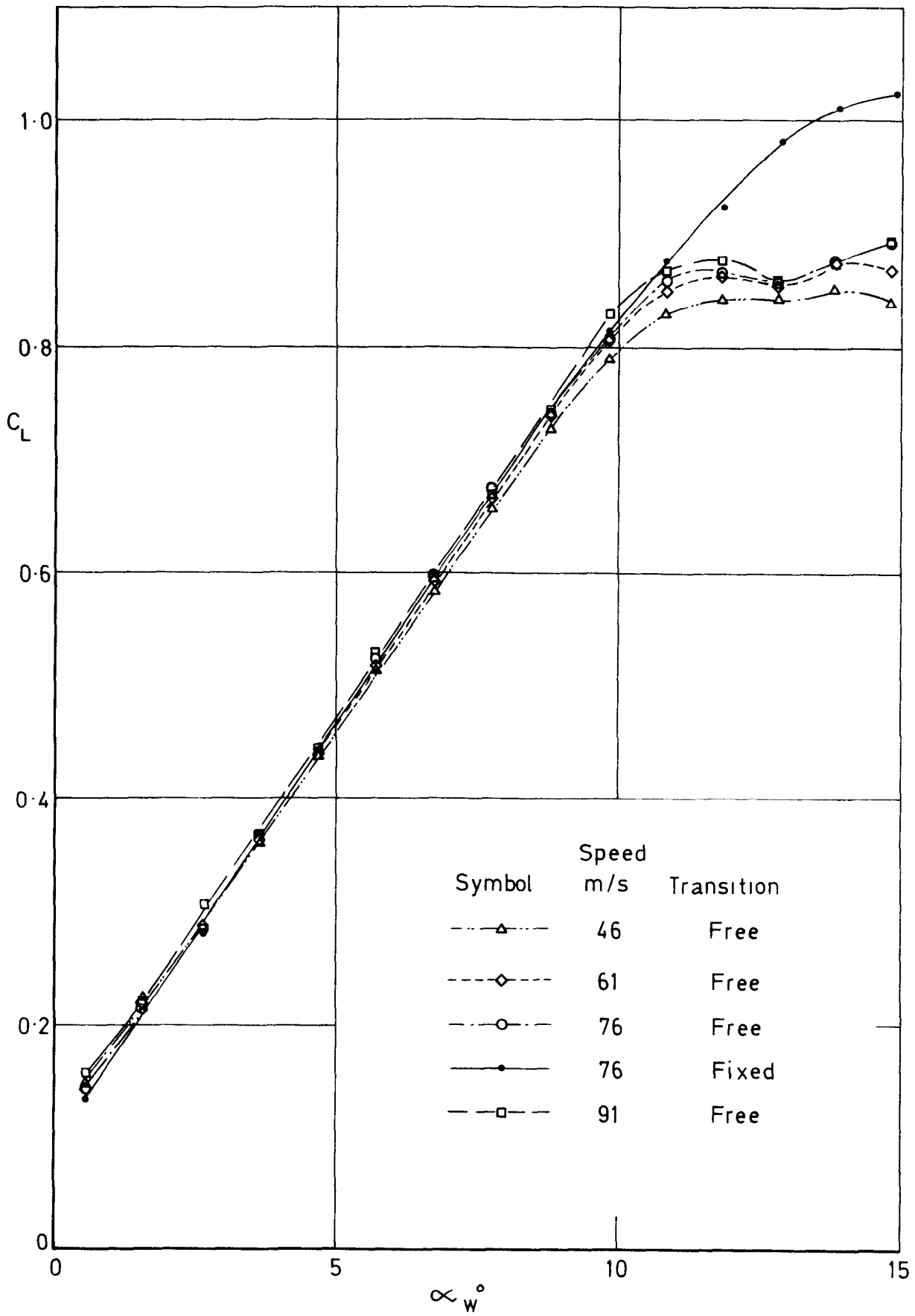

Fig. 5 Effect of transition and varying Reynolds number. Basic wing, slats and flaps retracted, C_L vs $\alpha_w°$

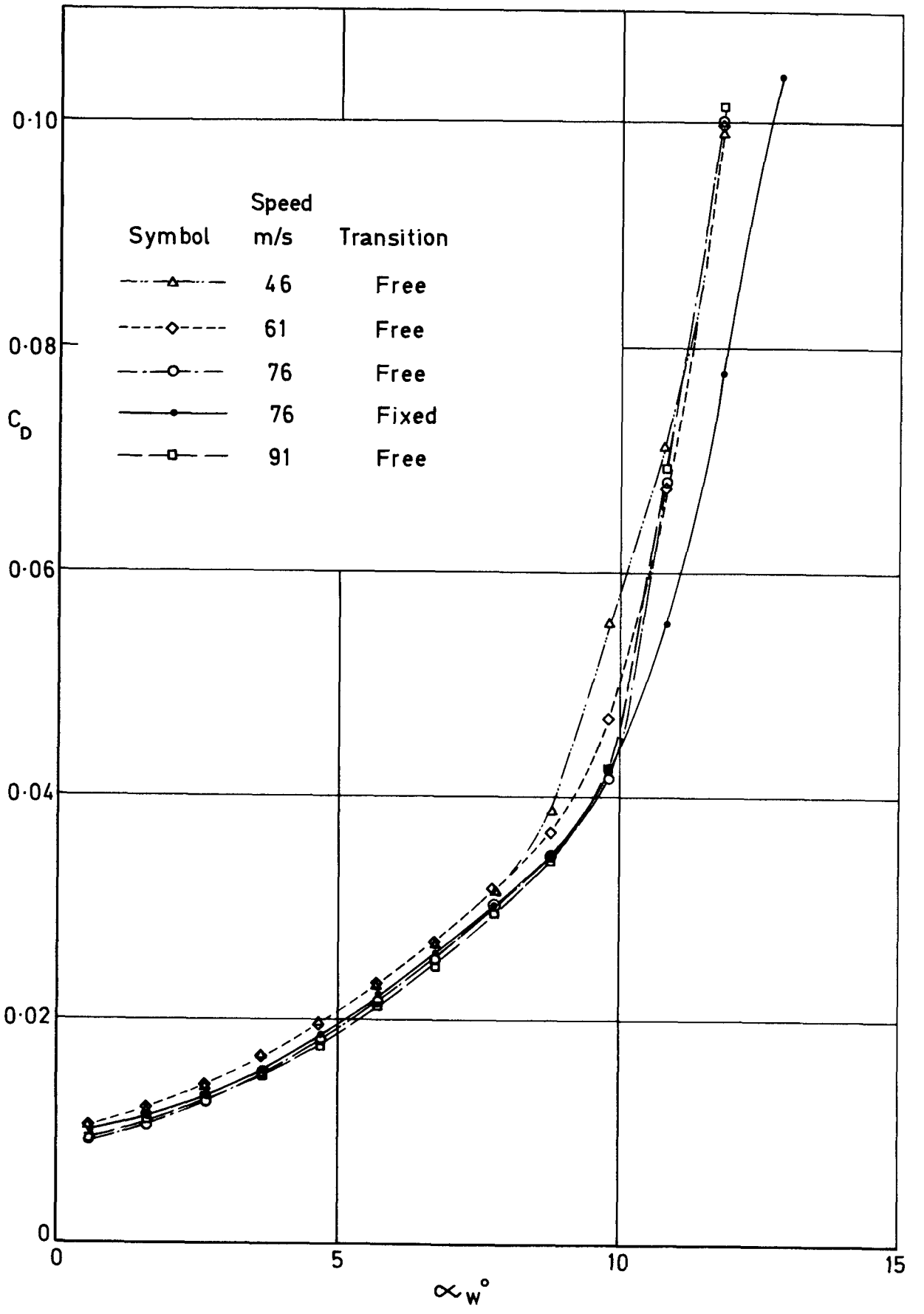

Fig. 6 Effect of transition and varying Reynolds number. Basic wing, slats and flaps retracted, C_D vs $\alpha_w°$

a. Flaps deflected 10°, $\frac{y_F}{s} = 0.8$, $\alpha_w = 15.8°$

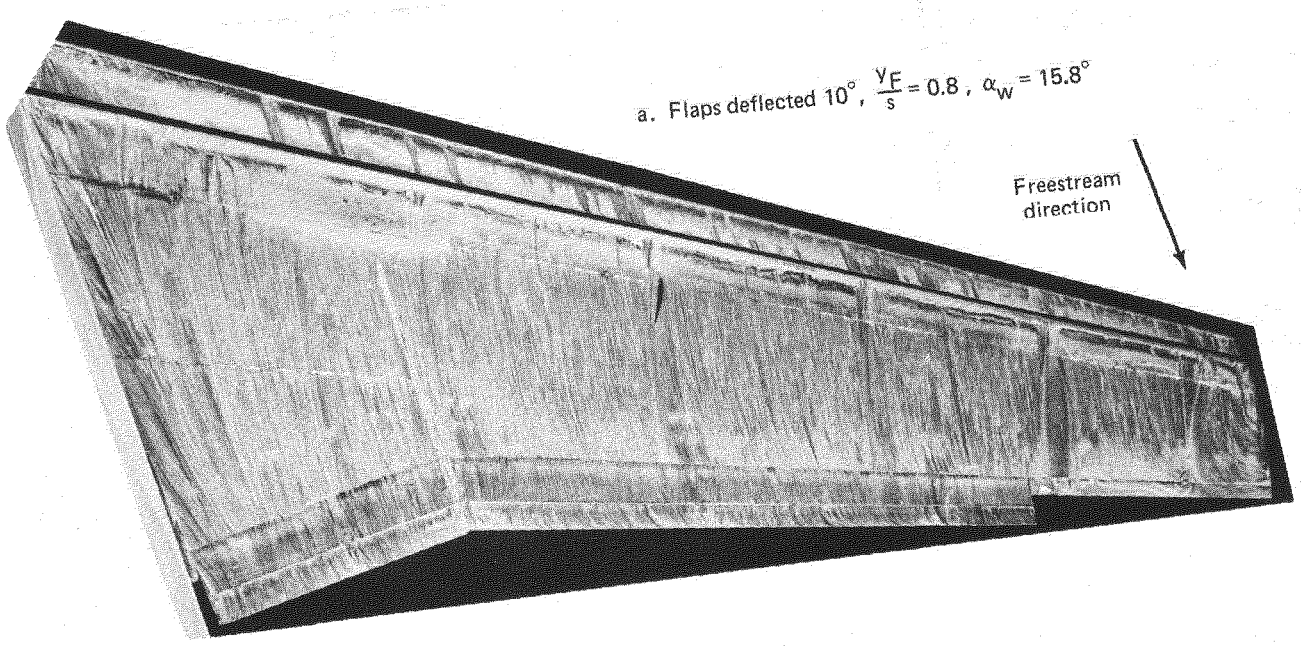

b. Flaps deflected 25°, $\frac{y_F}{s} = 0.8$, $\alpha_w = 16.0°$

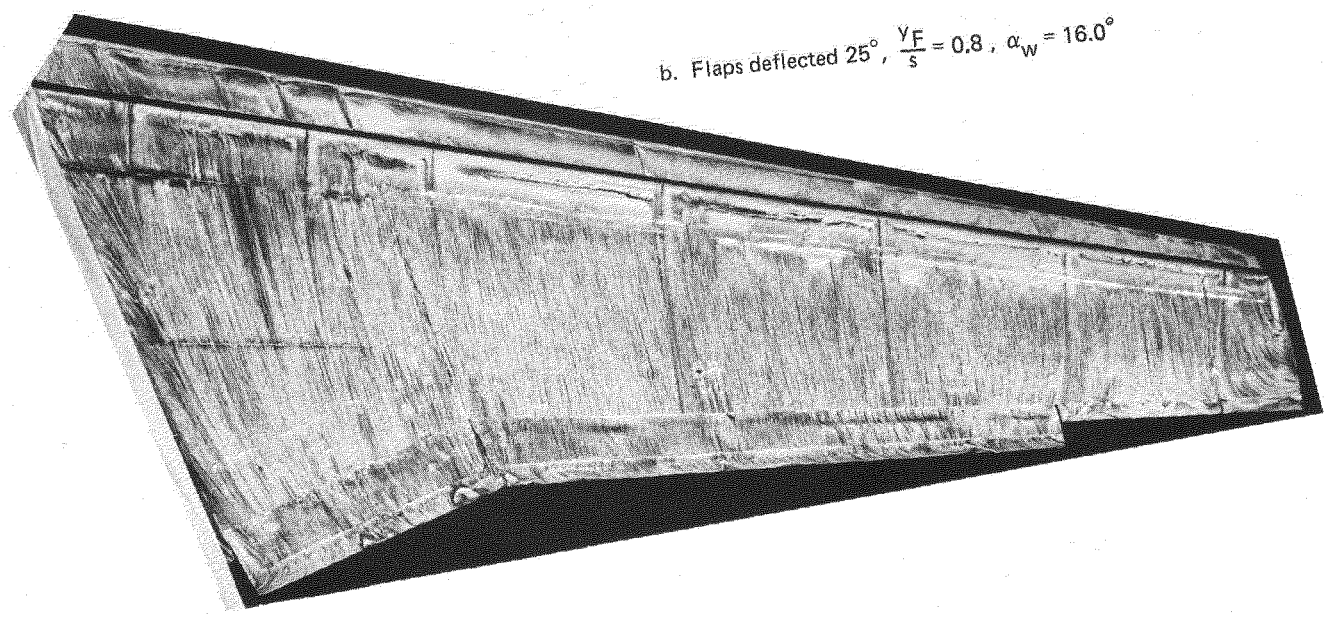

c. Flaps deflected 40°, $\frac{y_F}{s} = 0.8$, $\alpha_w = 16.1°$

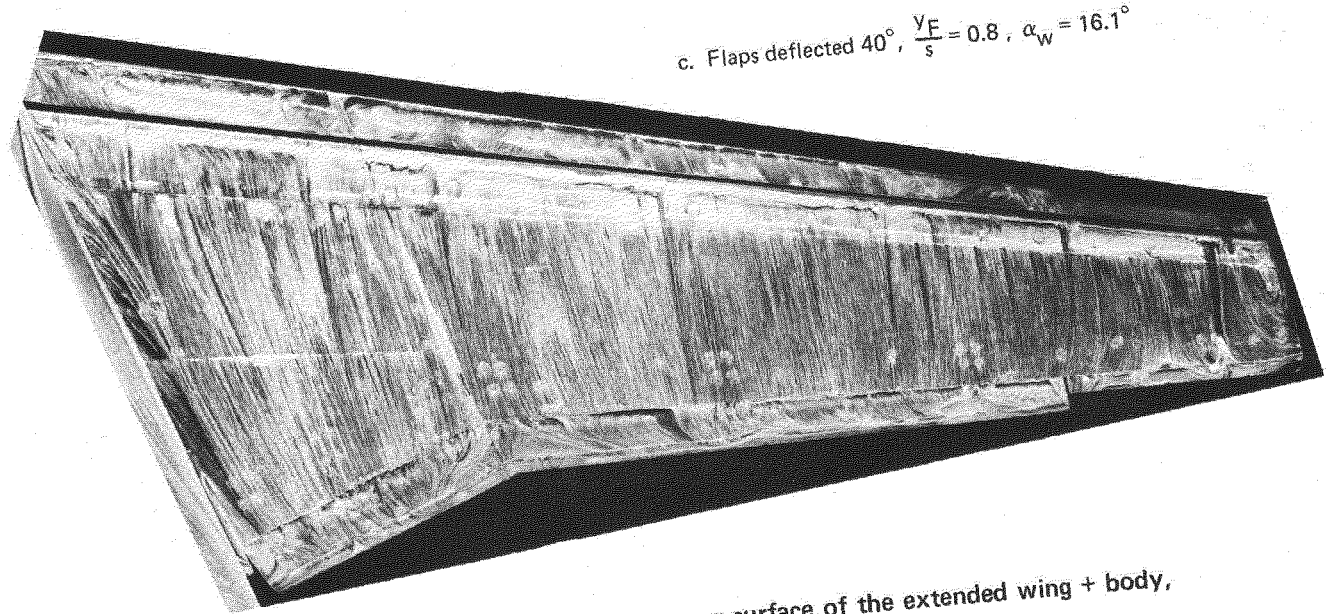

Fig.7 Flow visualisation on the upper surface of the extended wing + body, slats deflected 25°

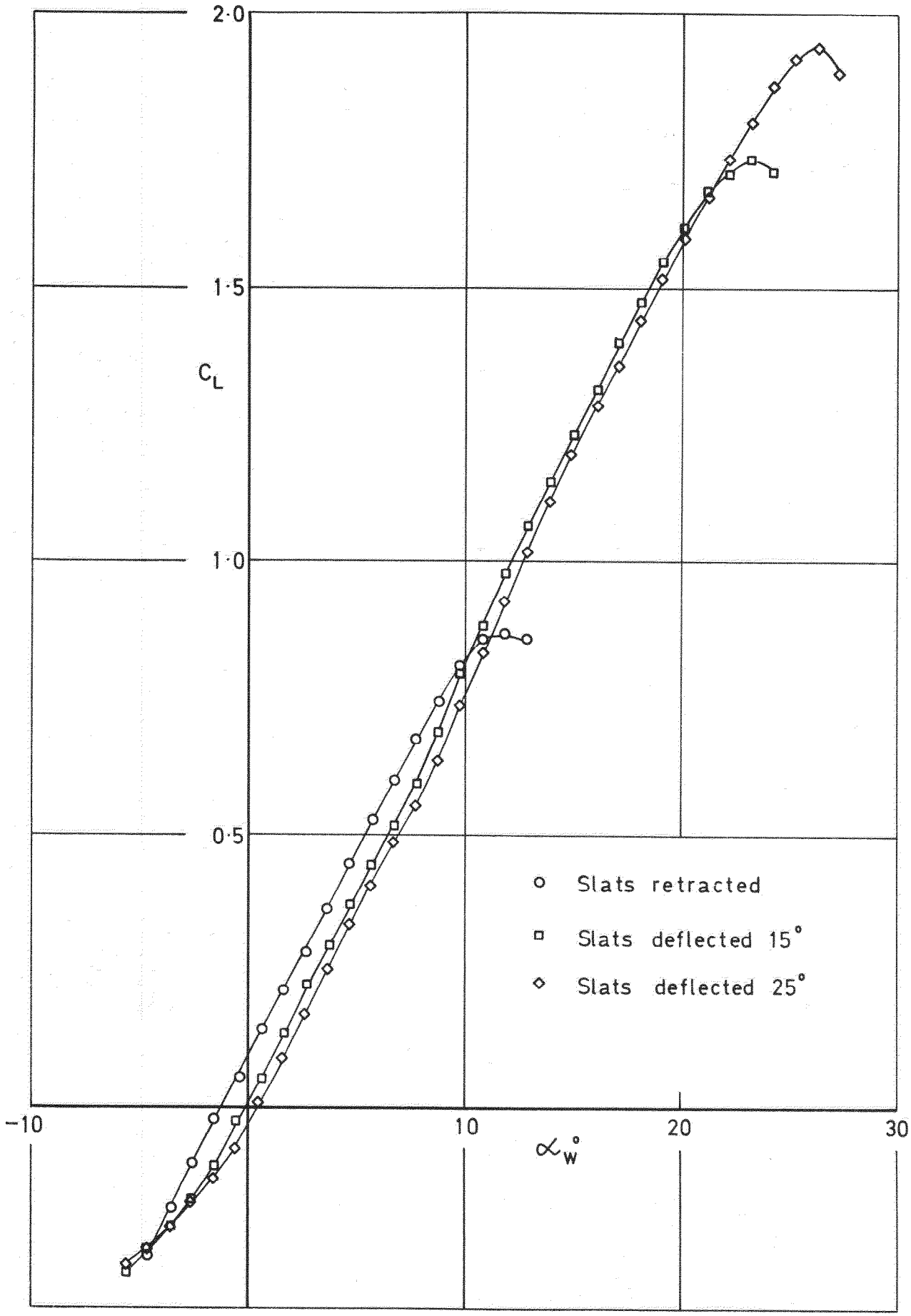

Fig.8 Effect of deflecting the leading-edge slats. Basic wing, flaps retracted, C_L vs $\alpha_w°$

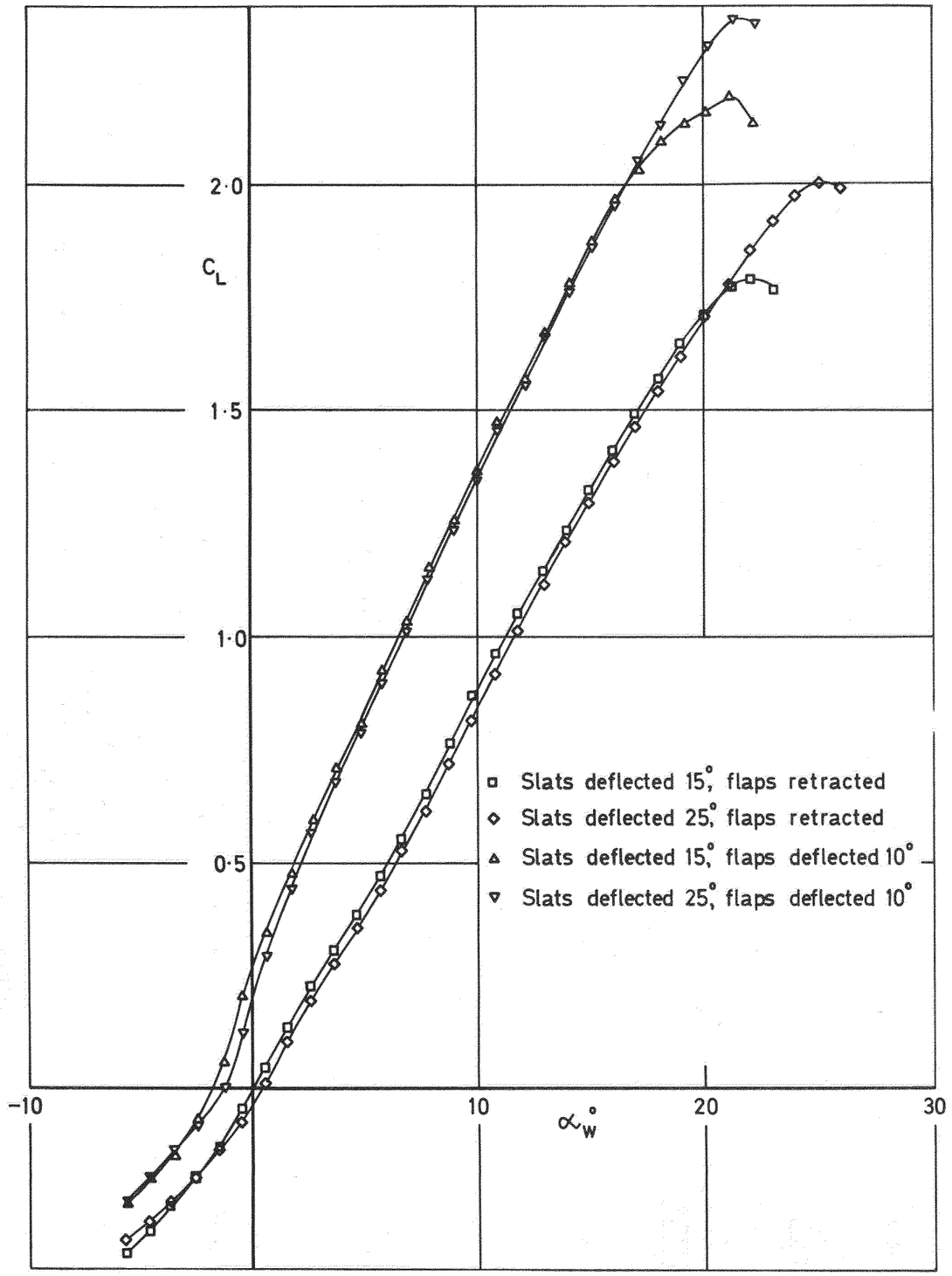

Fig. 9 Effect of deflecting the leading-edge slats. C_L vs $\alpha_w°$
Basic wing+body, flaps retracted and deflected 10° (full span)

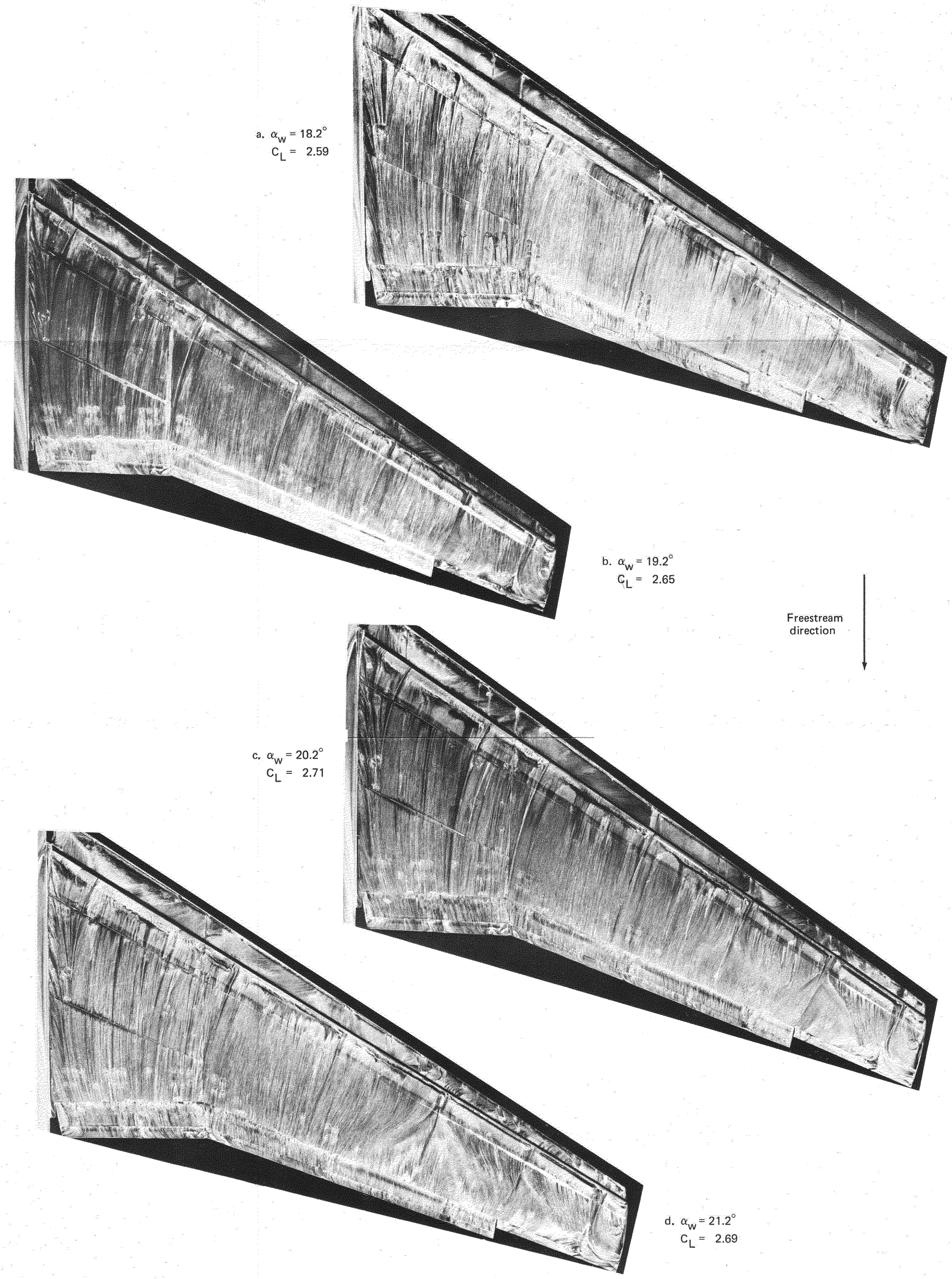

Fig.10 Flow visualisation on the upper surface of the extended planform wing with body. Slats deflected 25°, flaps deflected 25°, $\frac{y_F}{s} = 0.8$

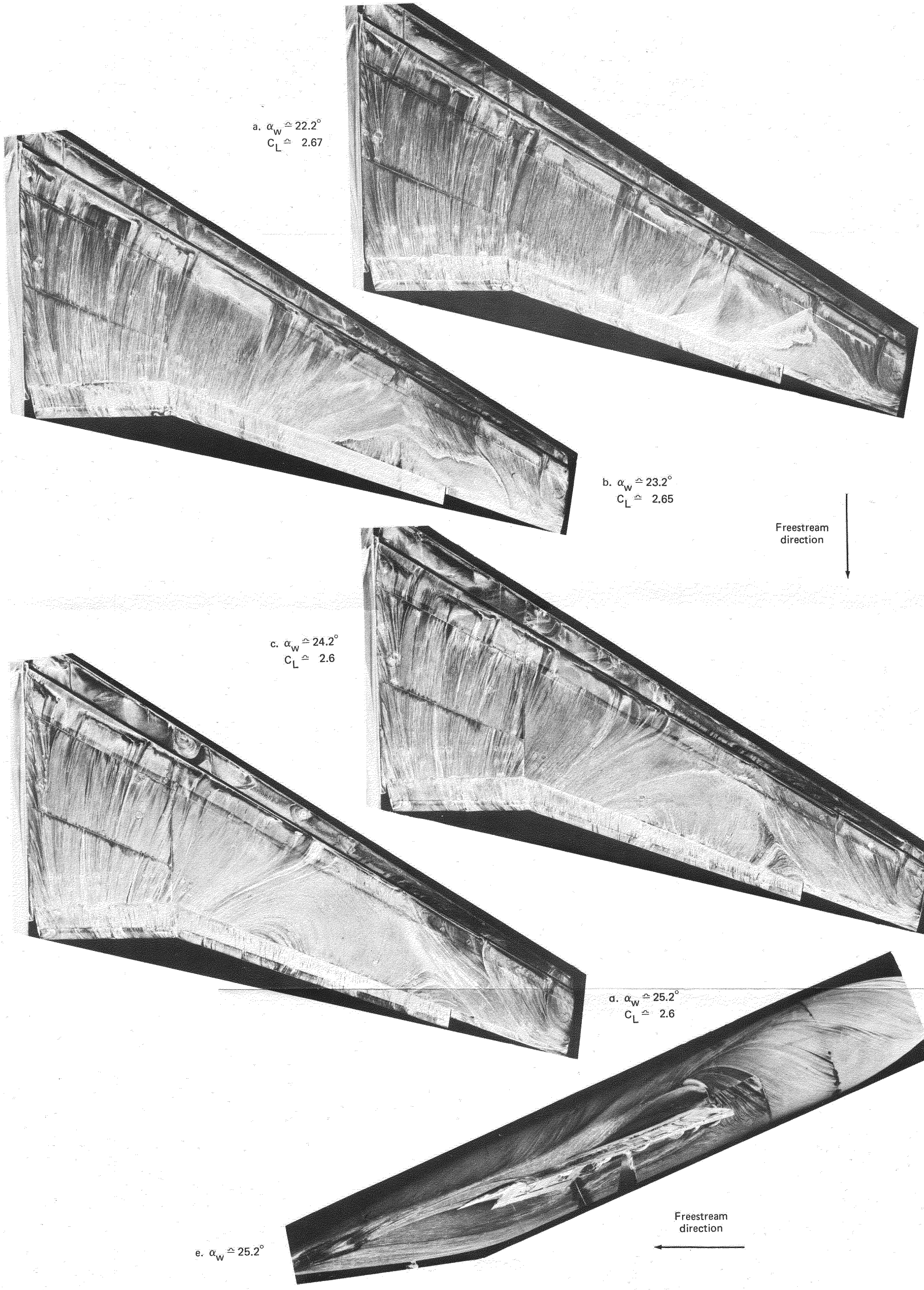

Fig.11 Flow visualisation on the wing upper surface and body. Extended planform with body. Slats deflected 25°, flaps deflected 25°, $\frac{y_F}{s} = 0.8$

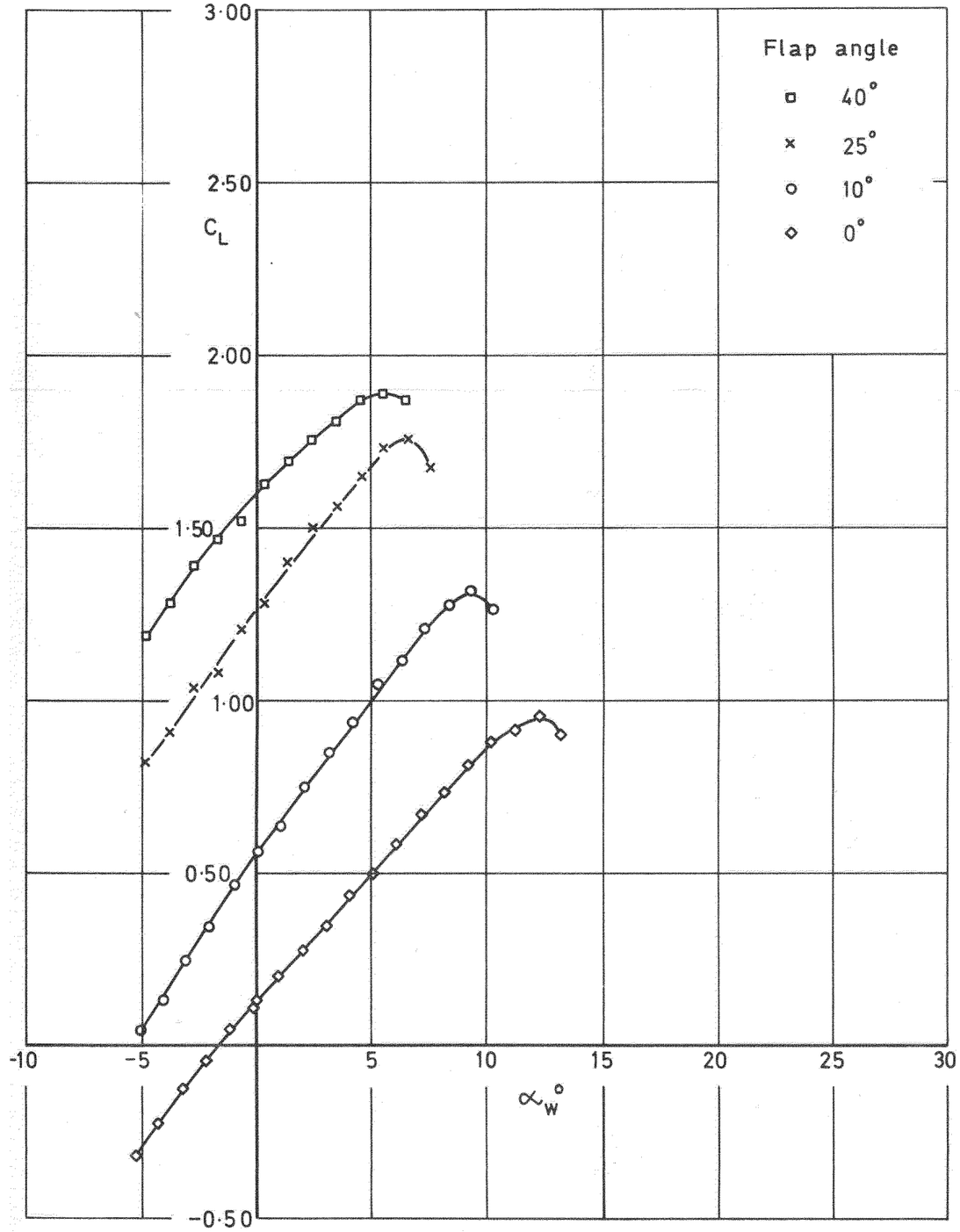

Fig.12 Basic wing, slats retracted, $\frac{y_F}{s}$ = 1·0.
Effect of flap deflection angle, C_L vs $\alpha_w°$

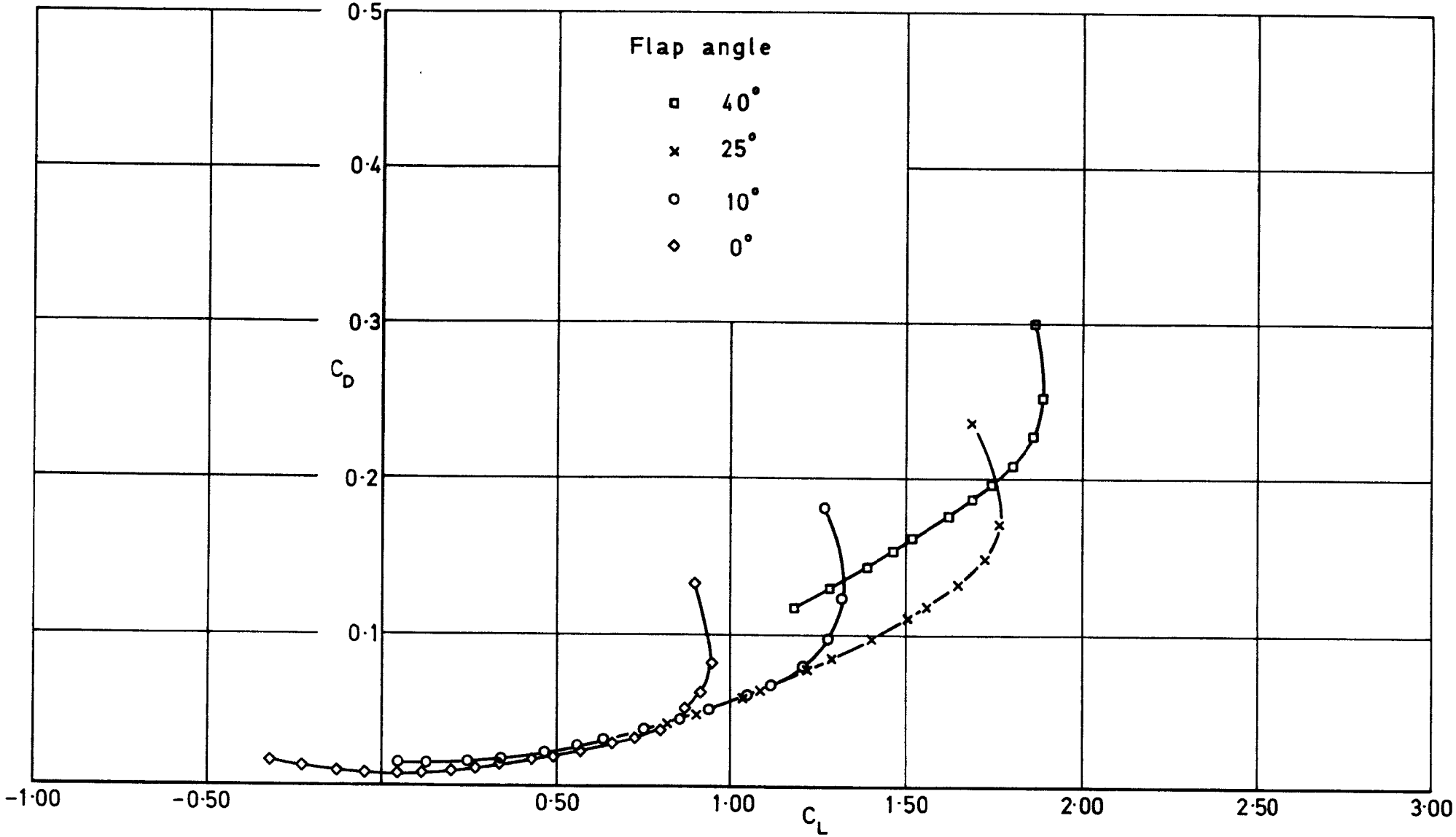

Fig.13 Basic wing, slats retracted, $\frac{y_F}{s}$ = 1·0.
Effect of flap deflection angle, C_D vs C_L

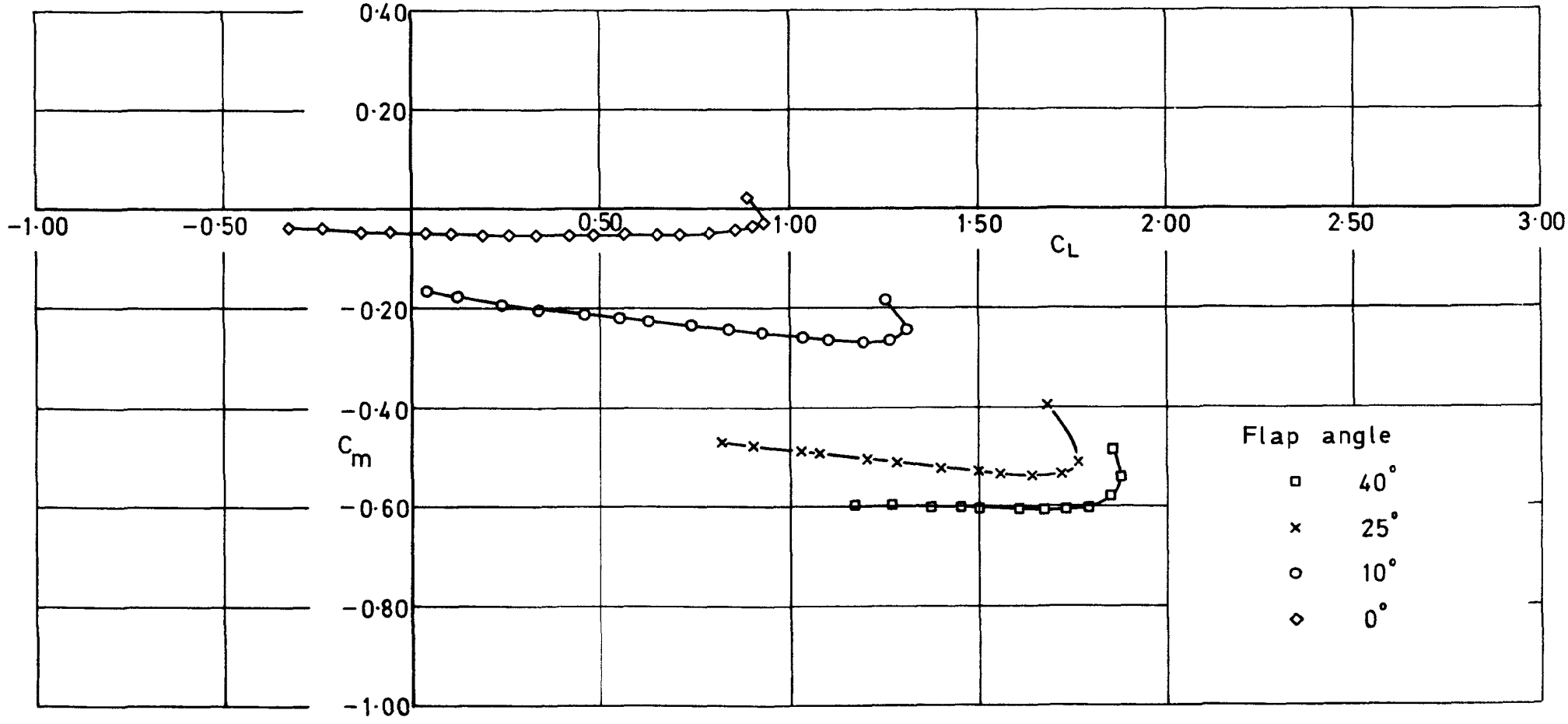

Fig. 14 Basic wing, slats retracted, $\frac{y_F}{s} = 1{\cdot}0$.
Effect of flap deflection angle, C_m vs C_L

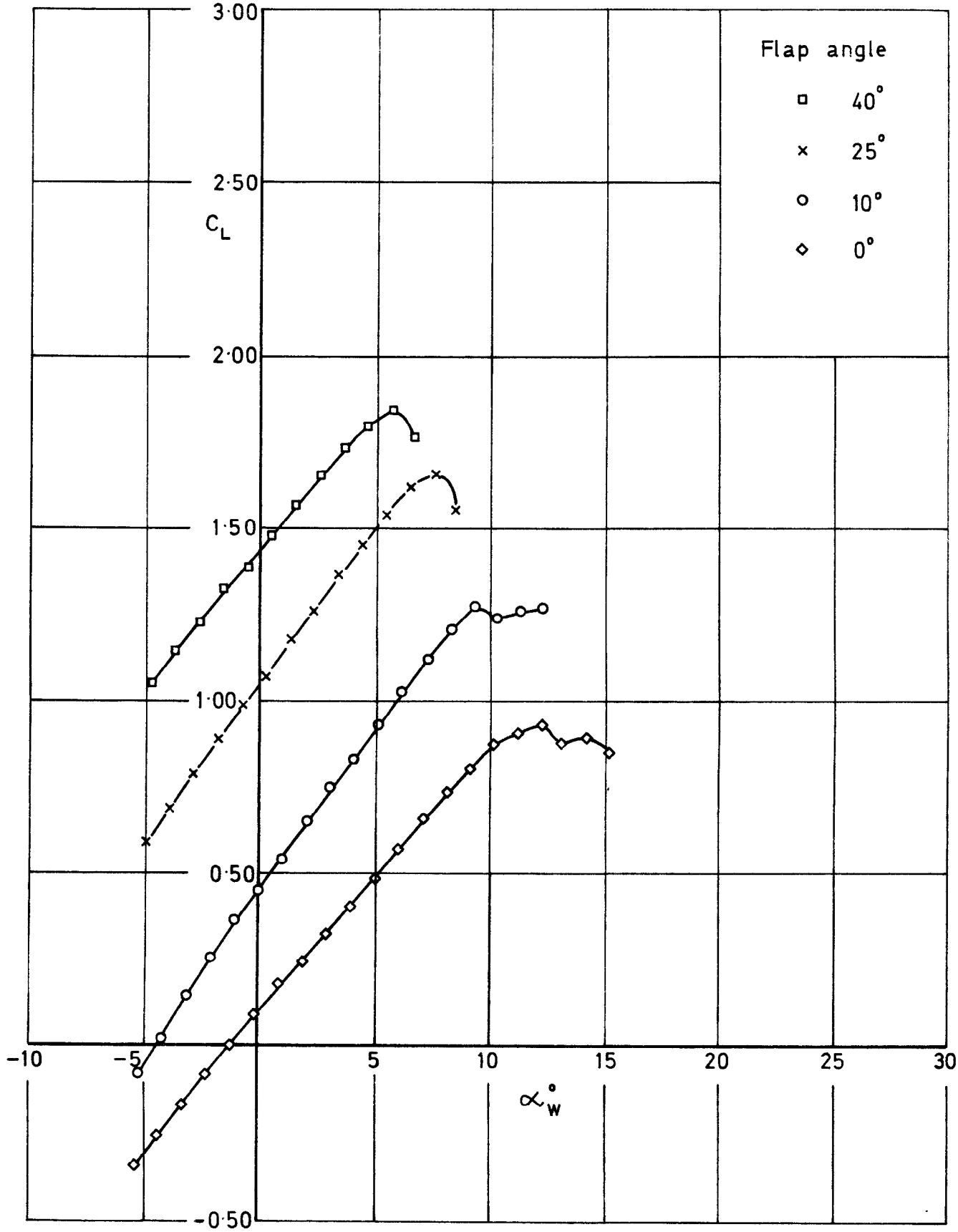

Fig.15 Basic wing + body, slats retracted, $\frac{y_F}{s}$ =1·0.
Effect of flap deflection angle, C_L vs α_w°

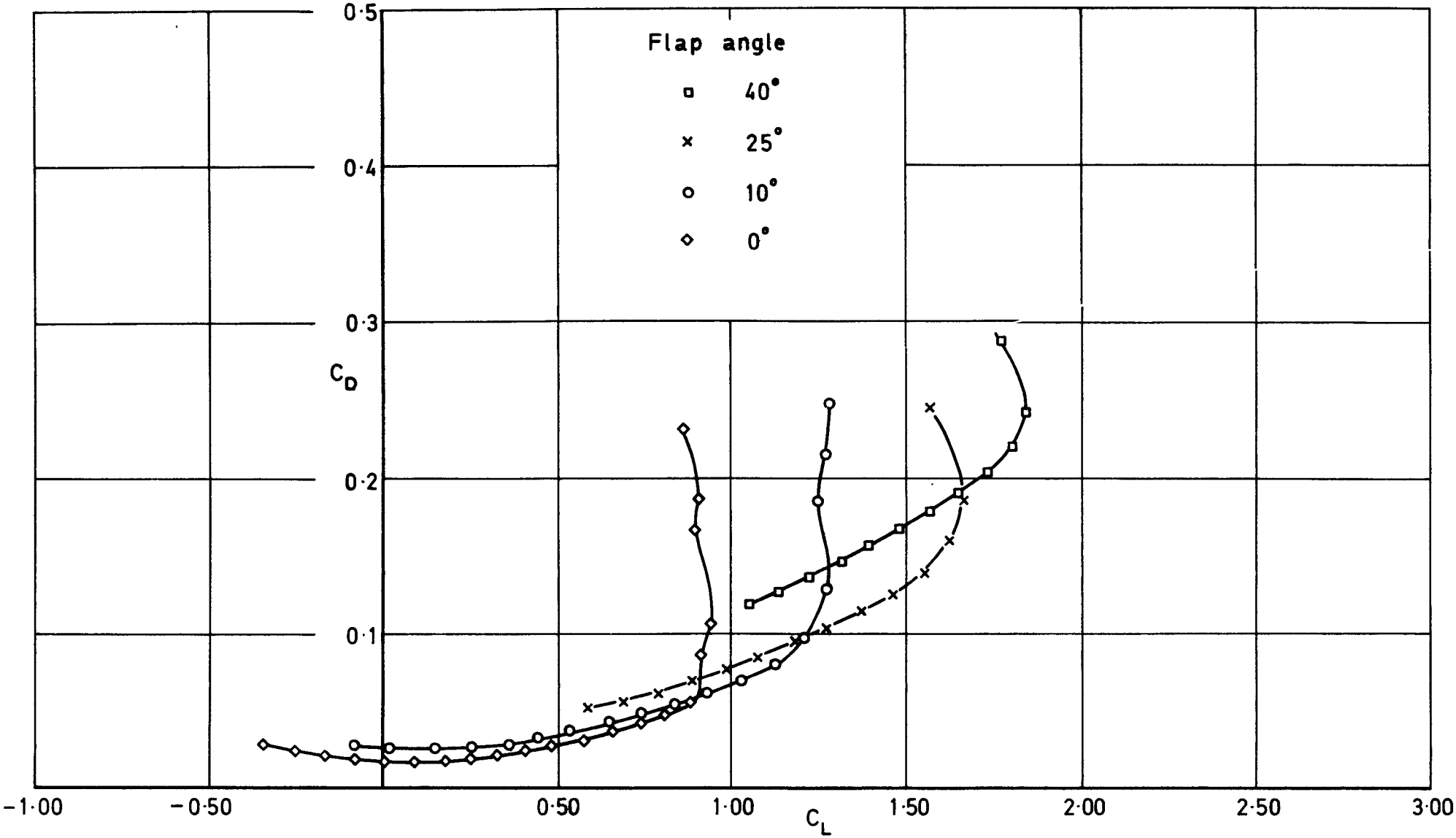

Fig.16 Basic wing + body, slats retracted, $\frac{y_F}{S} = 1{\cdot}0$.
Effect of flap deflection angle, C_D vs C_L

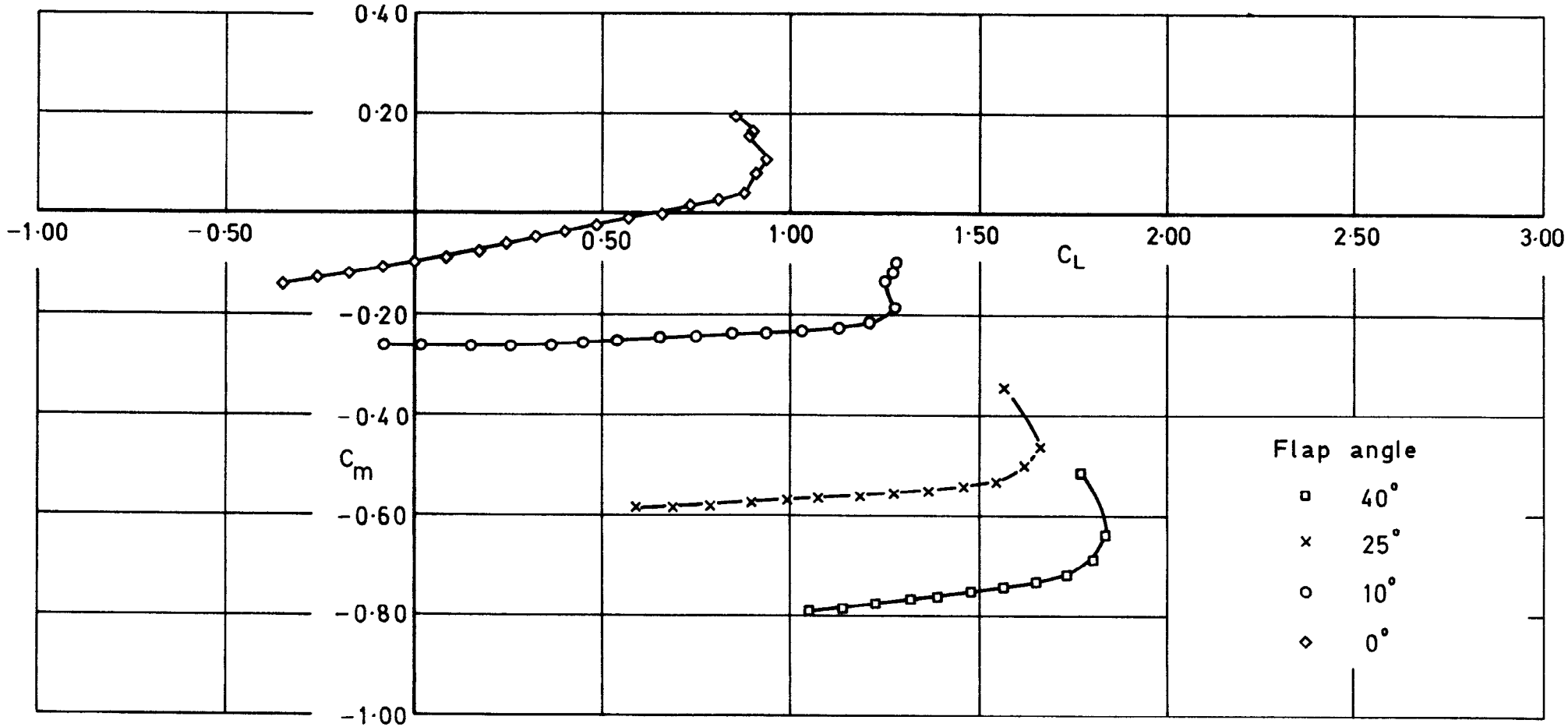

Fig. 17 Basic wing + body, slats retracted, $\frac{y_F}{s} = 1{\cdot}0$.
Effect of flap deflection angle, C_m vs C_L

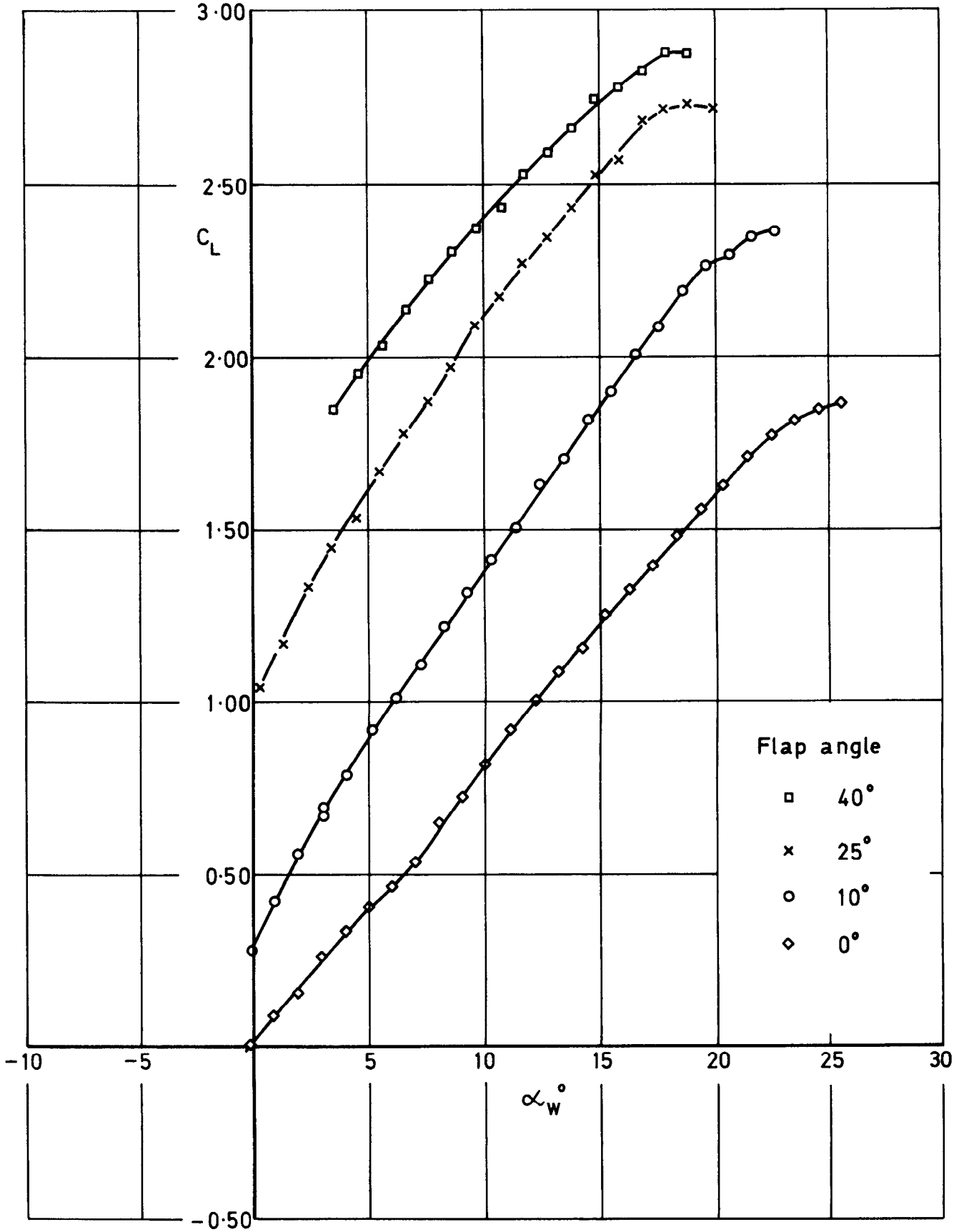

Fig. 18 Basic wing, slats deflected 25°, $\frac{y_F}{s} = 1{\cdot}0$.
Effect of flap deflection angle, C_L vs α_w°

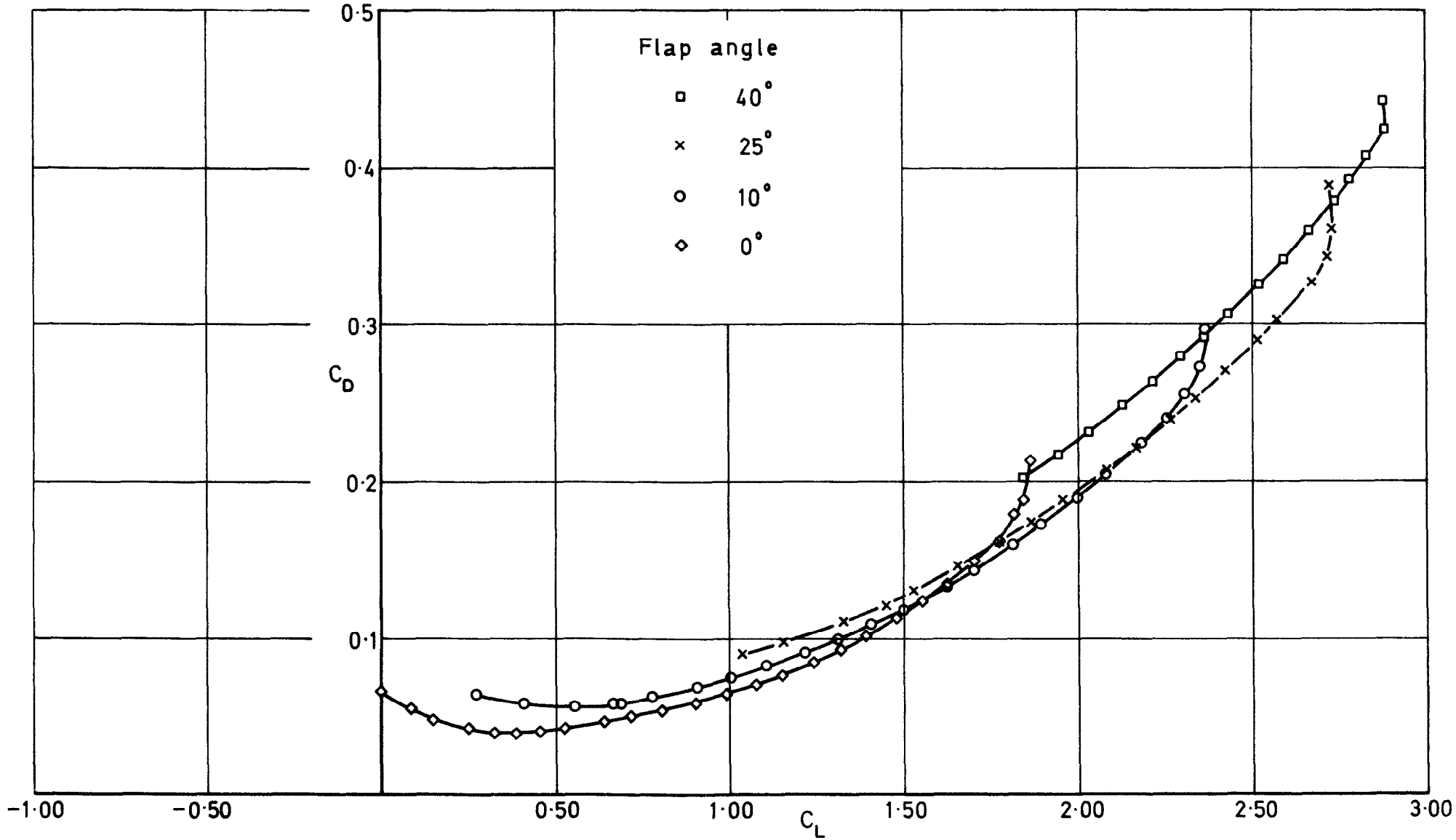

Fig.19 Basic wing, slats deflected 25°, $\frac{y_F}{s} = 1{\cdot}0$.
Effect of flap deflection angle, C_D vs C_L

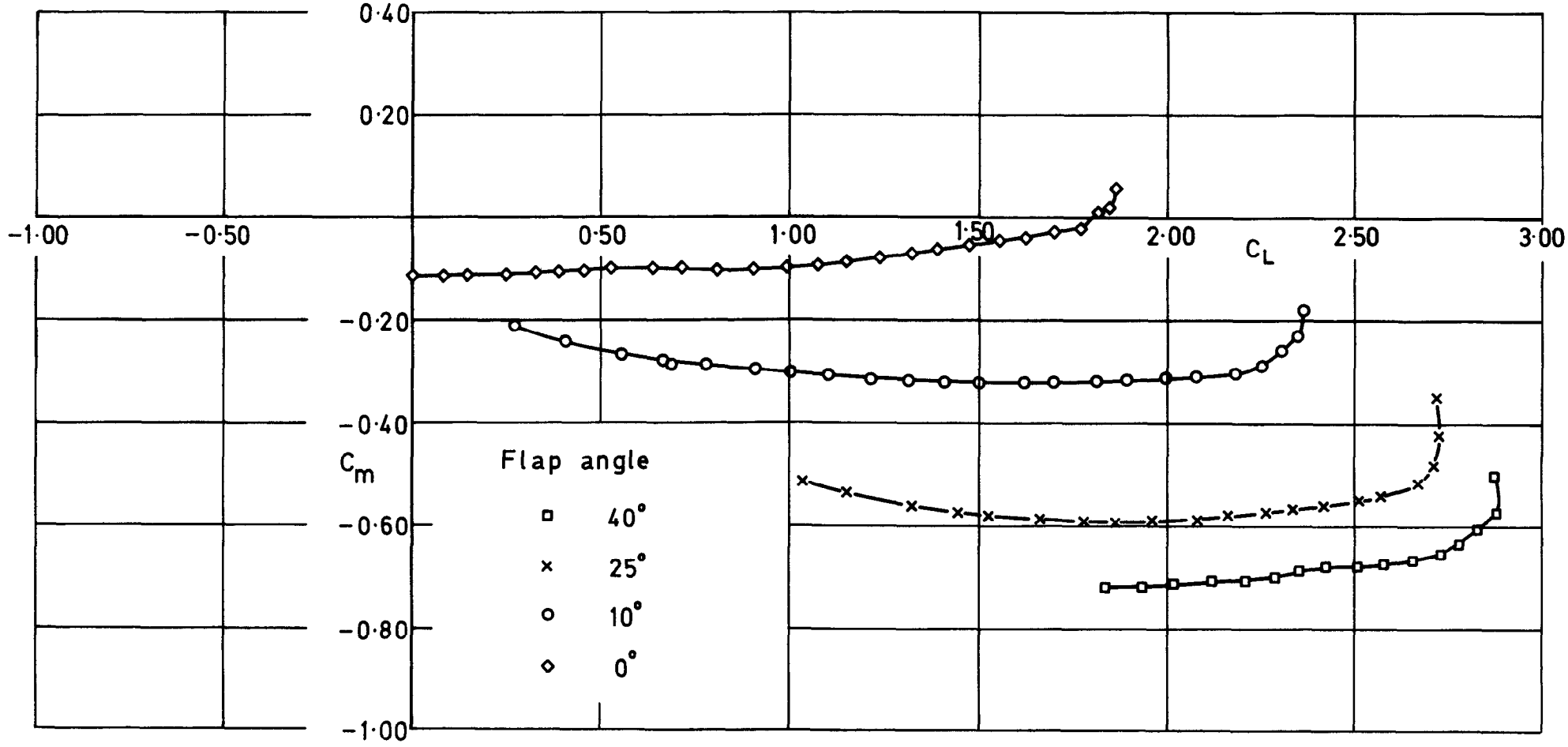

Fig. 20 Basic wing, slats deflected 25°, $\frac{y_F}{s} = 1{\cdot}0$.
Effect of flap deflection angle, C_m vs C_L

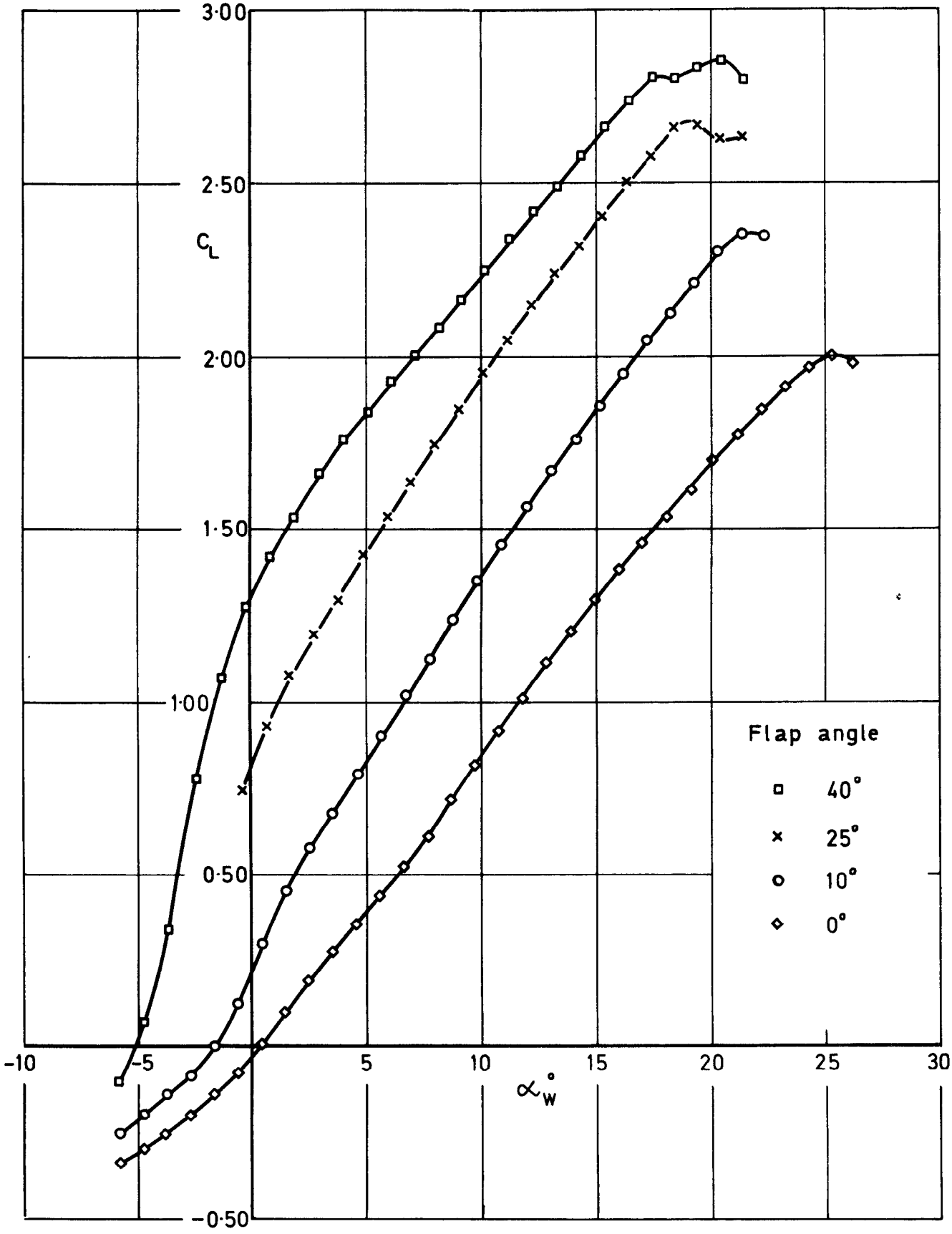

Fig.21 Basic wing + body, slats deflected 25°, $\frac{y_F}{s} = 1 \cdot 0$.
Effect of flap deflection angle, C_L vs α_W°

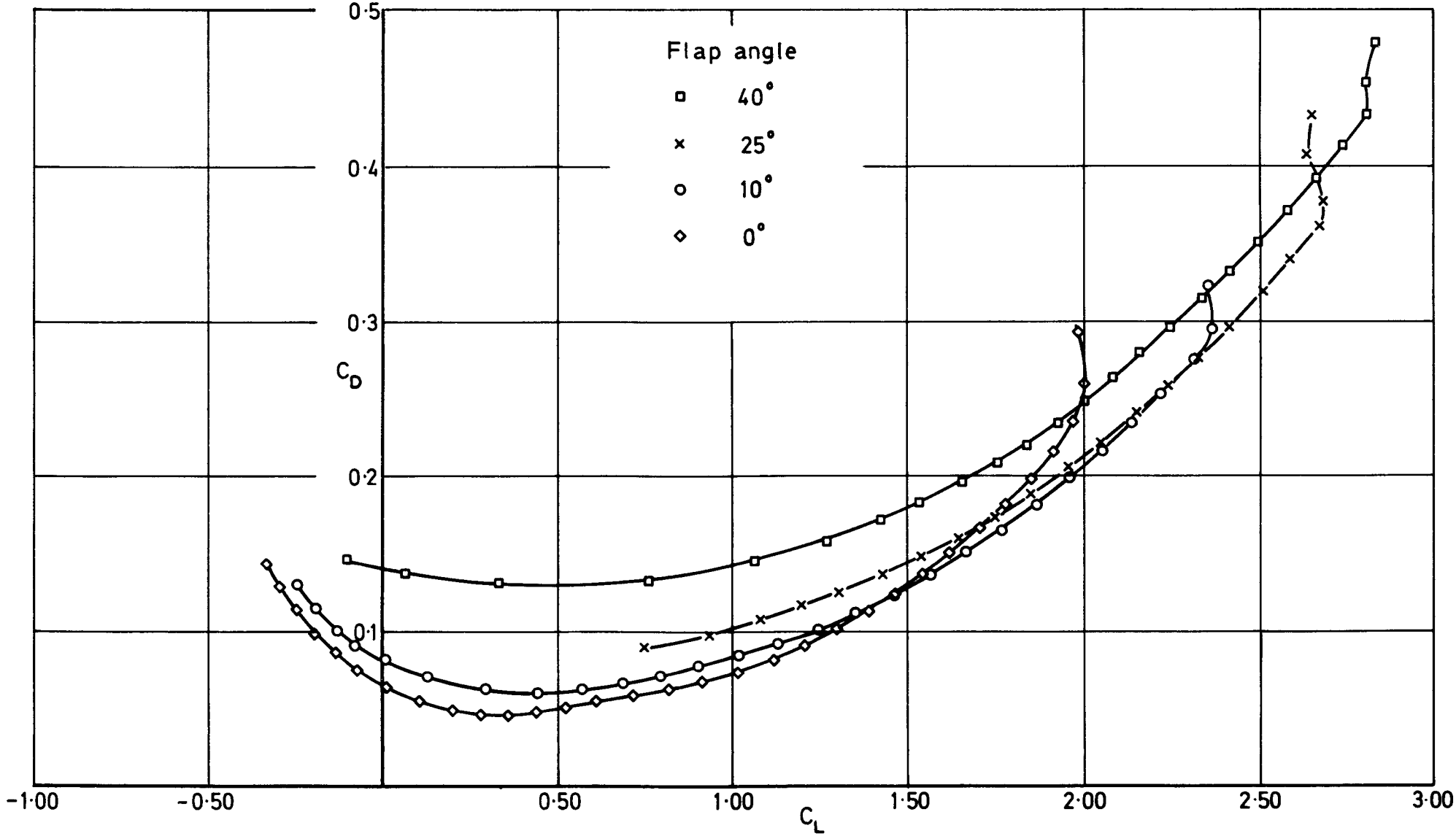

Fig.22 Basic wing + body, slats deflected 25°, $\frac{y_F}{s} = 1{\cdot}0$.
Effect of flap deflection angle, C_D vs C_L

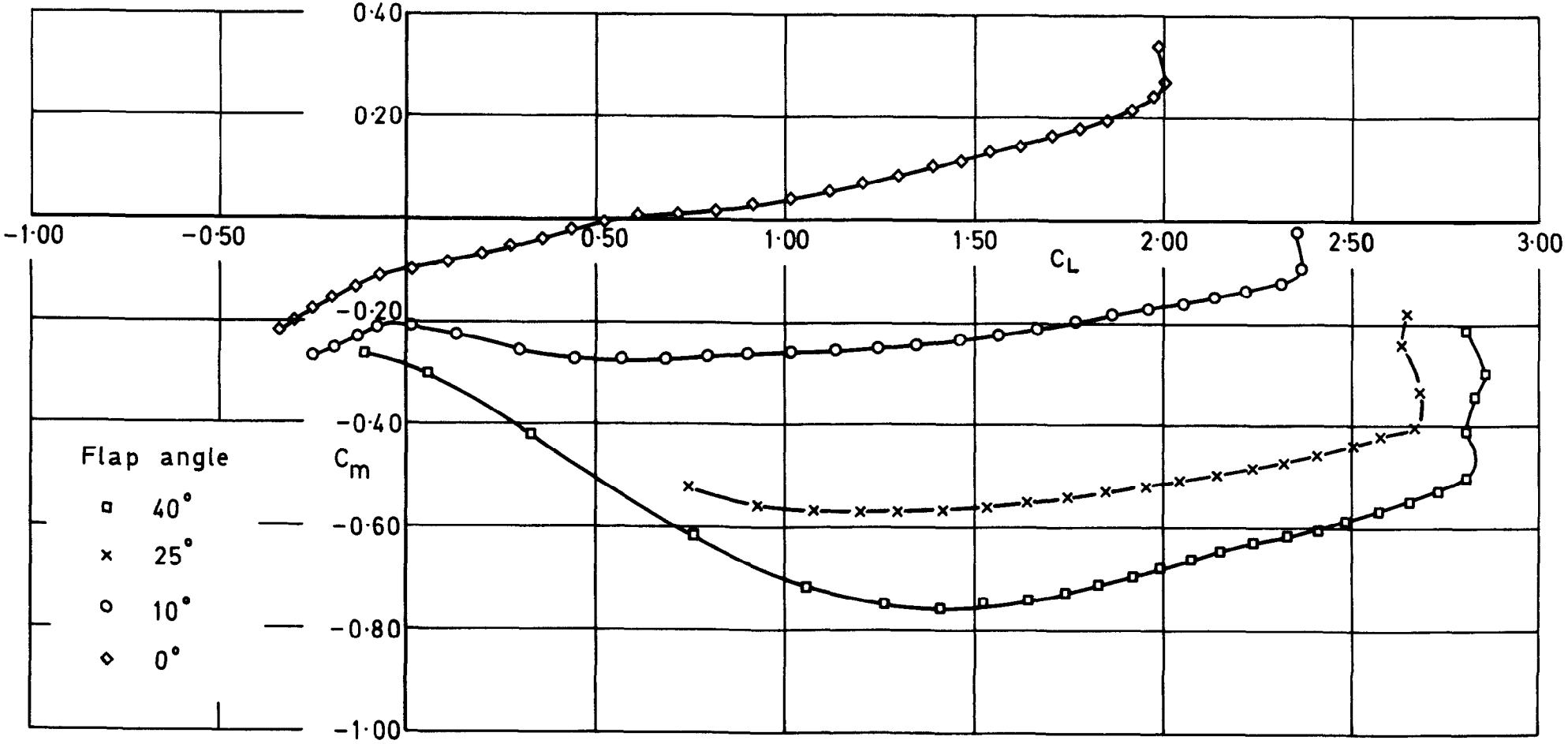

Fig.23 Basic wing + body, slats deflected 25°, $\frac{y_F}{s}$ = 1·0.
Effect of flap deflection angle, C_m vs C_L

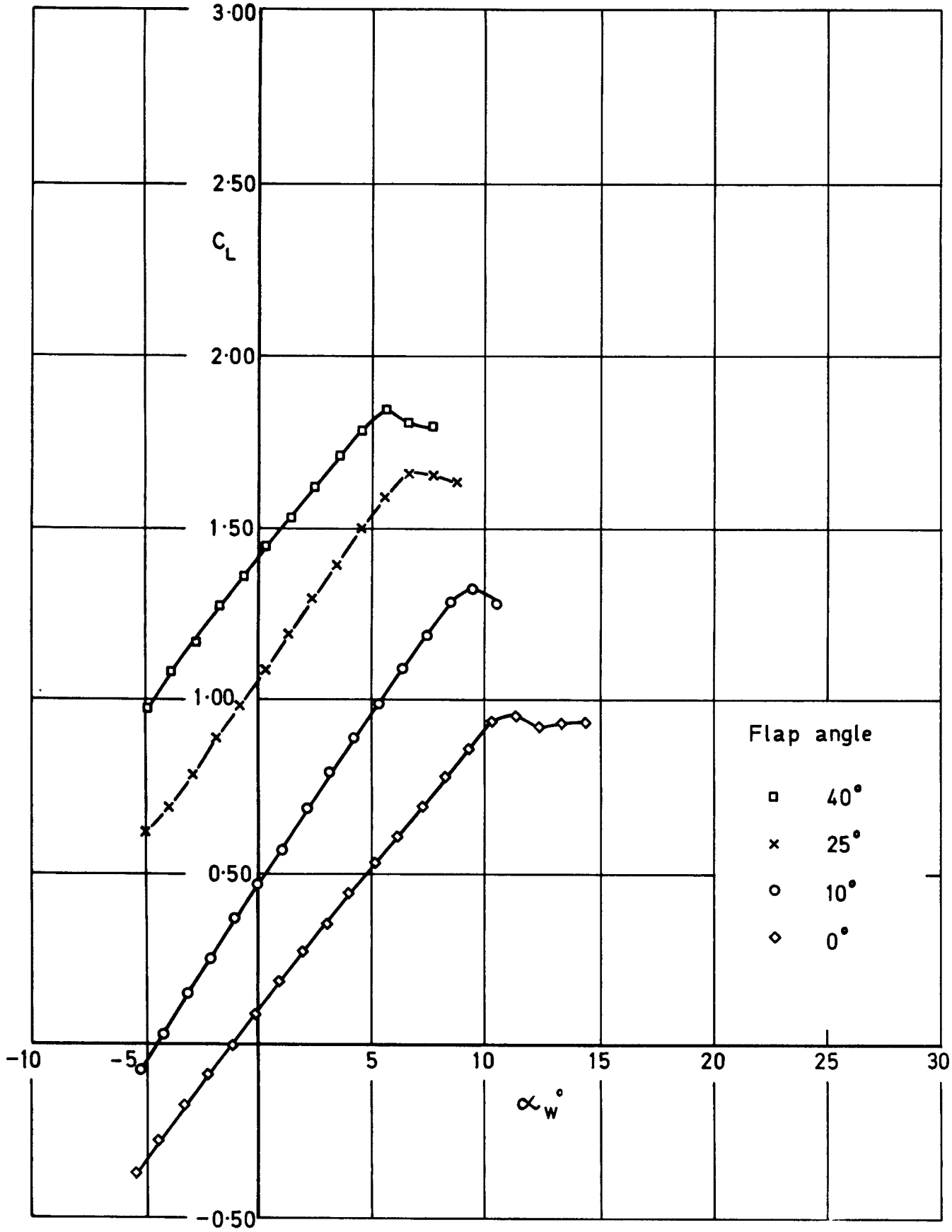

Fig. 24 Extended wing + body, slats retracted, $\frac{y_F}{s} = 1{\cdot}0$.
Effect of flap deflection angle, C_L vs $\alpha_w°$

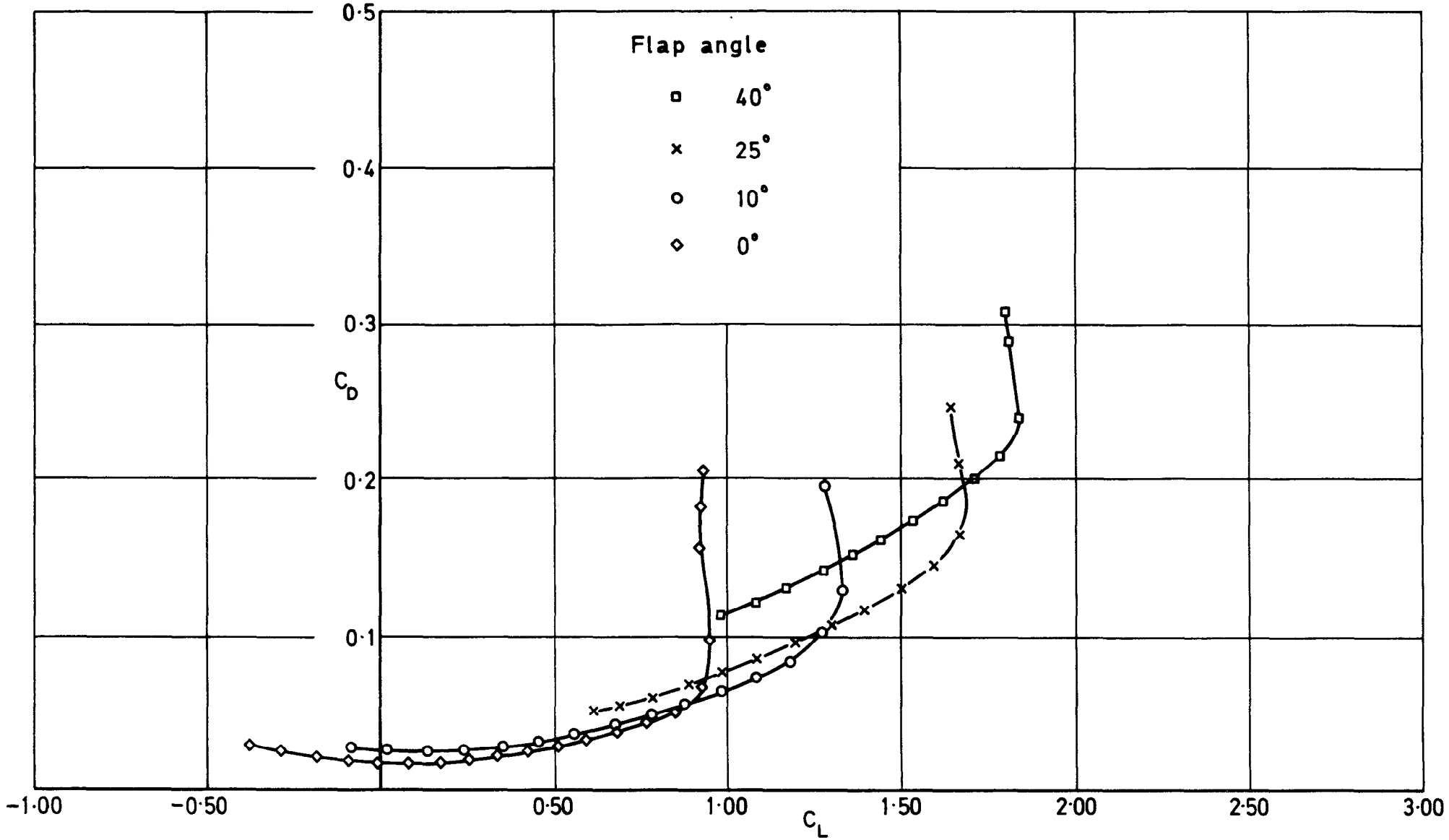

Fig. 25 Extended wing + body, slats retracted, $\frac{y_F}{s}$=1·0.
Effect of flap deflection angle, C_D vs C_L

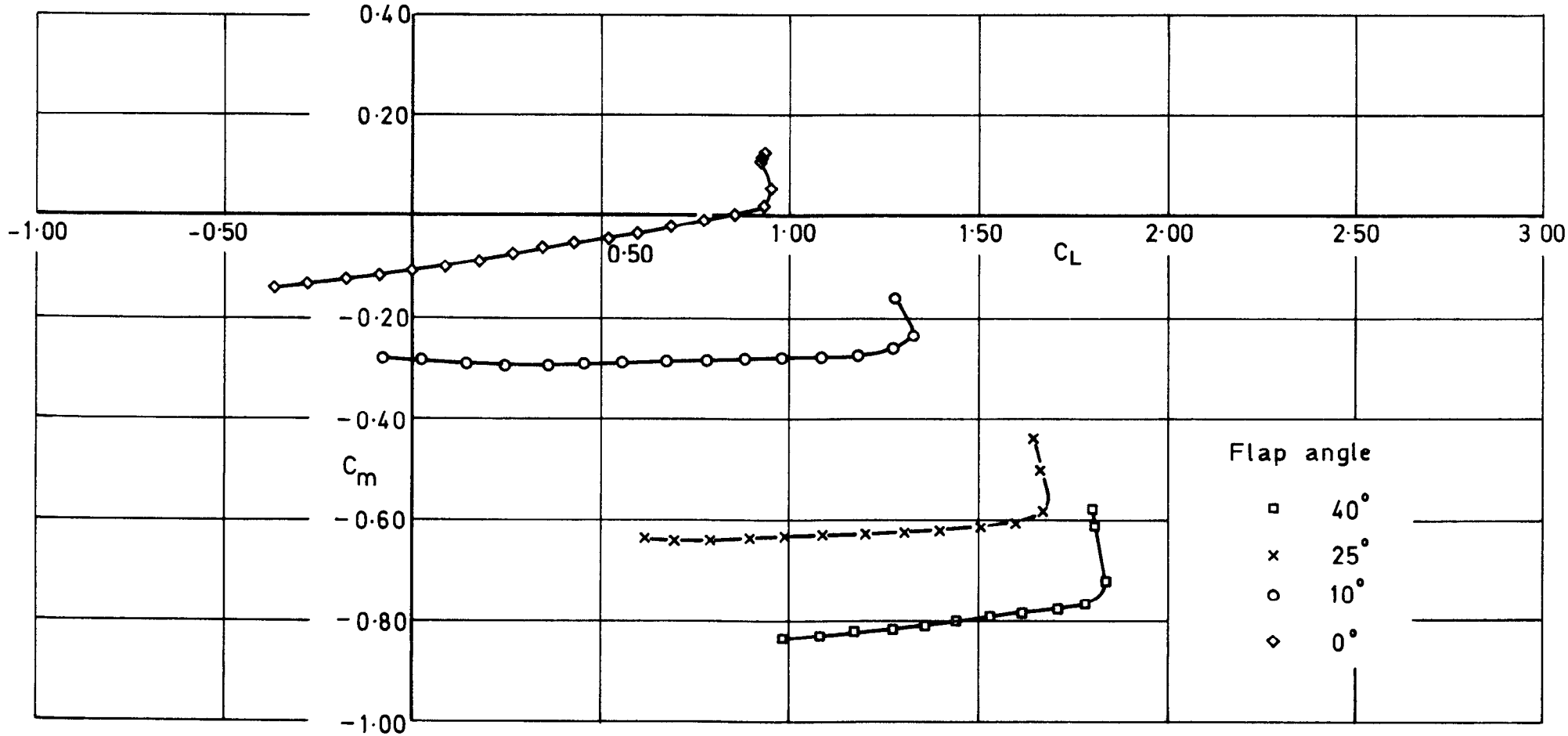

Fig. 26 Extended wing + body, slats retracted, $\frac{y_F}{s}$=1·0.
Effect of flap deflection angle, C_m vs C_L

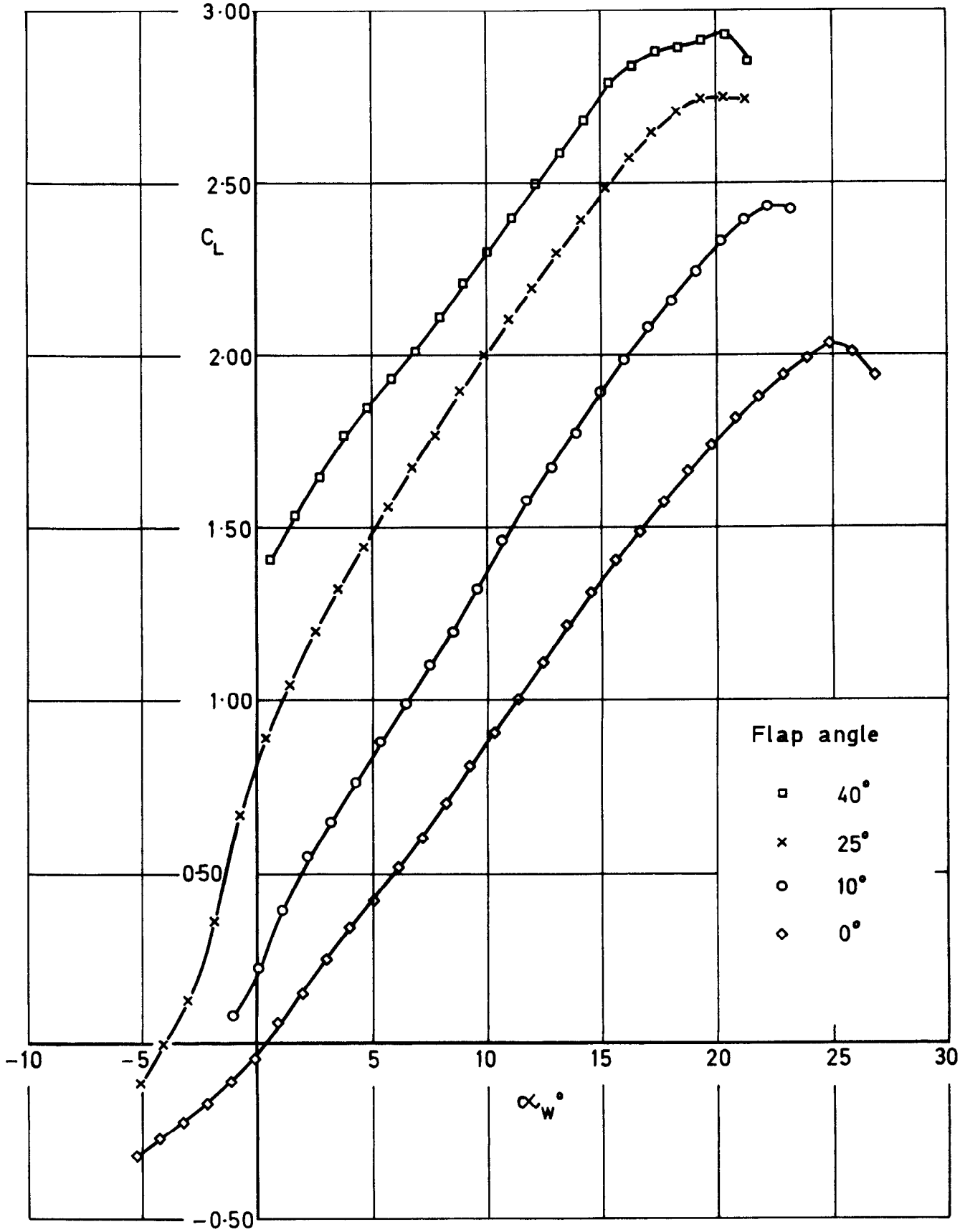

Fig. 27 Extended wing + body, slats deflected 25°, $\frac{y_F}{S}$ = 1·0.
Effect of flap deflection angle, C_L vs $\alpha_w°$

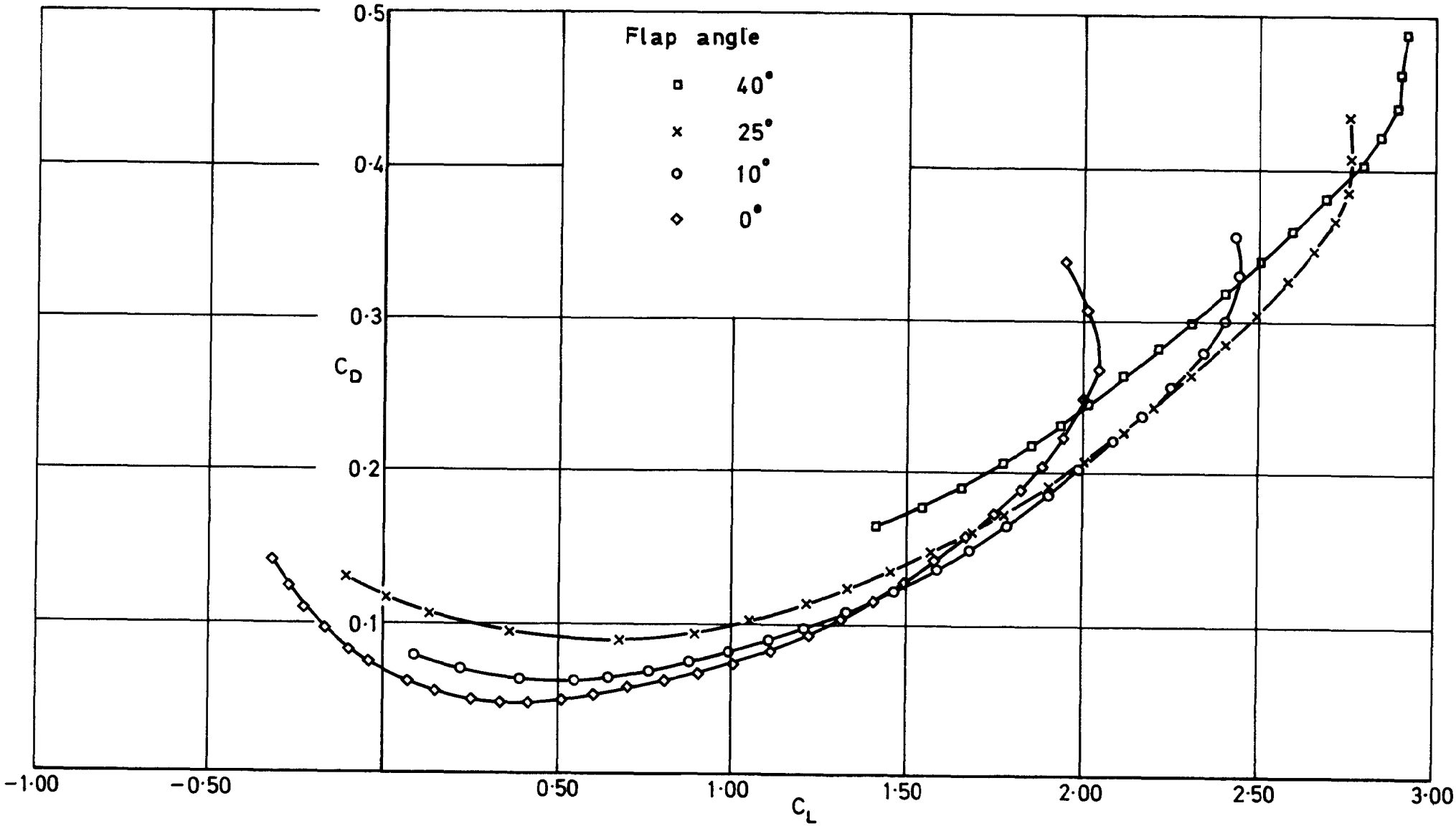

Fig. 28 Extended wing + body, slats deflected 25°; $\frac{y_F}{s} = 1{\cdot}0$.
Effect of flap deflection angle, C_D vs C_L

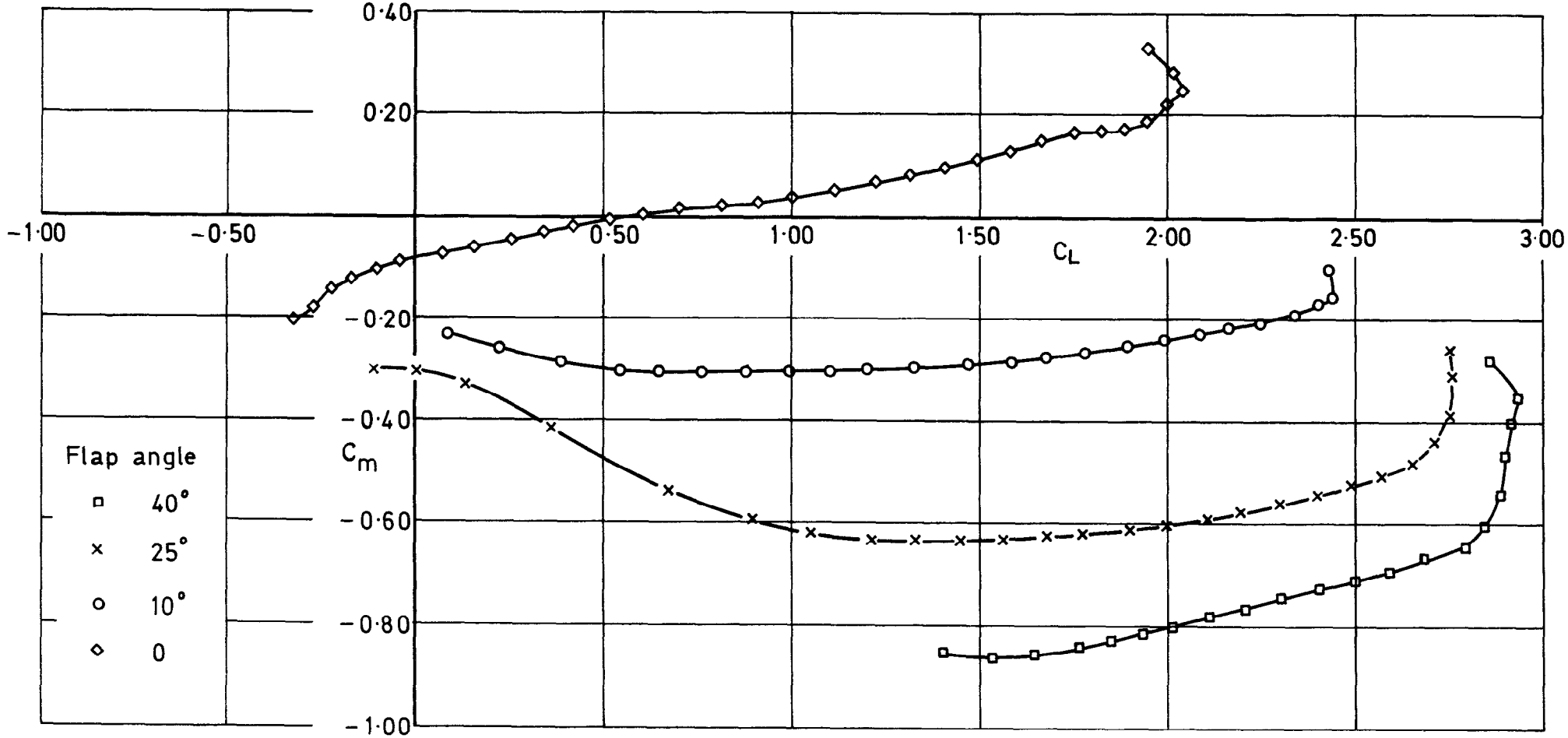

Fig. 29 Extended wing + body, slats deflected 25°, $\frac{y_F}{S} = 1{\cdot}0$.
Effect of flap deflection angle, C_m vs C_L

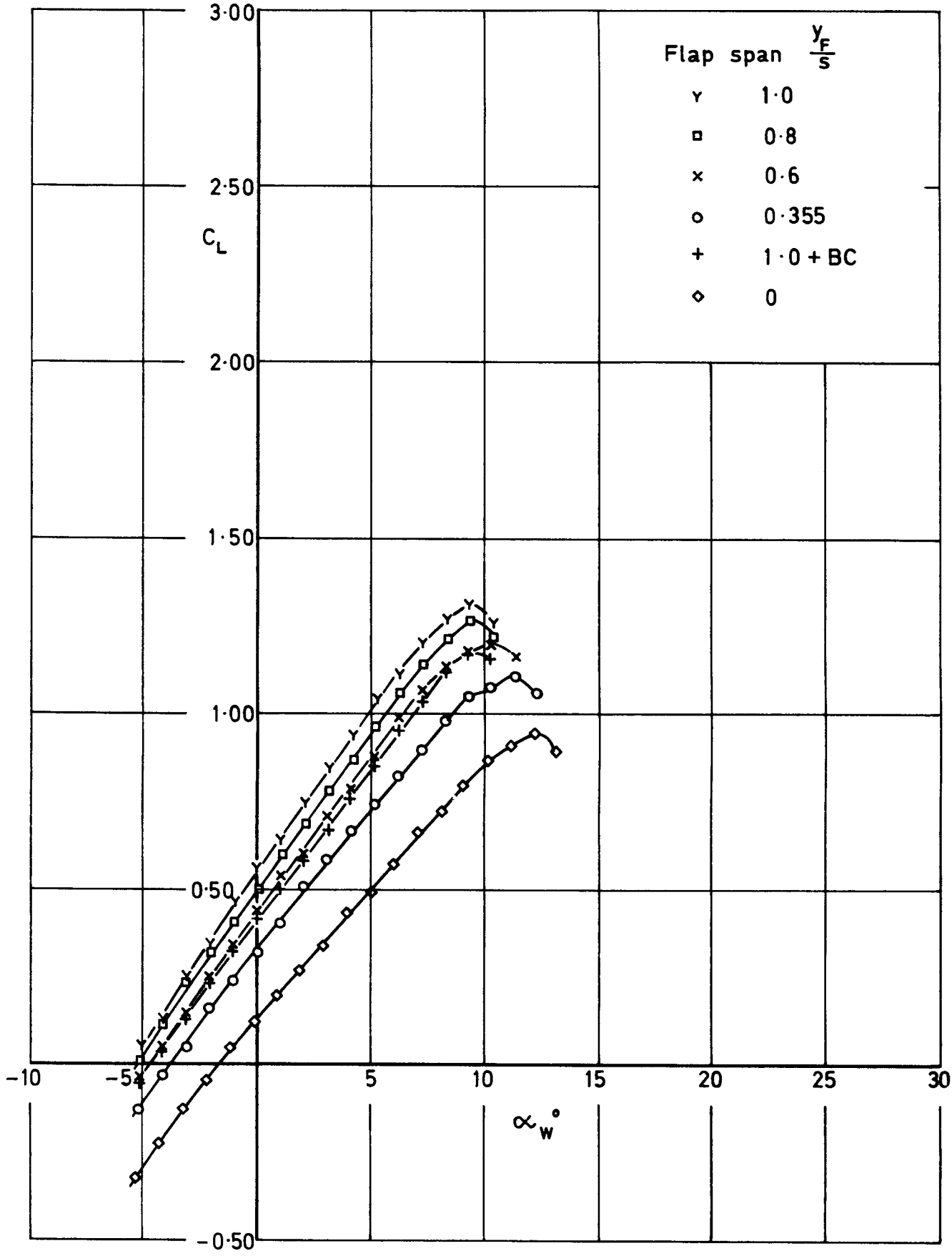

Fig.30 Basic wing, slats retracted, flaps deflected 10°. Effect of flap span, C_L vs $\alpha_w°$

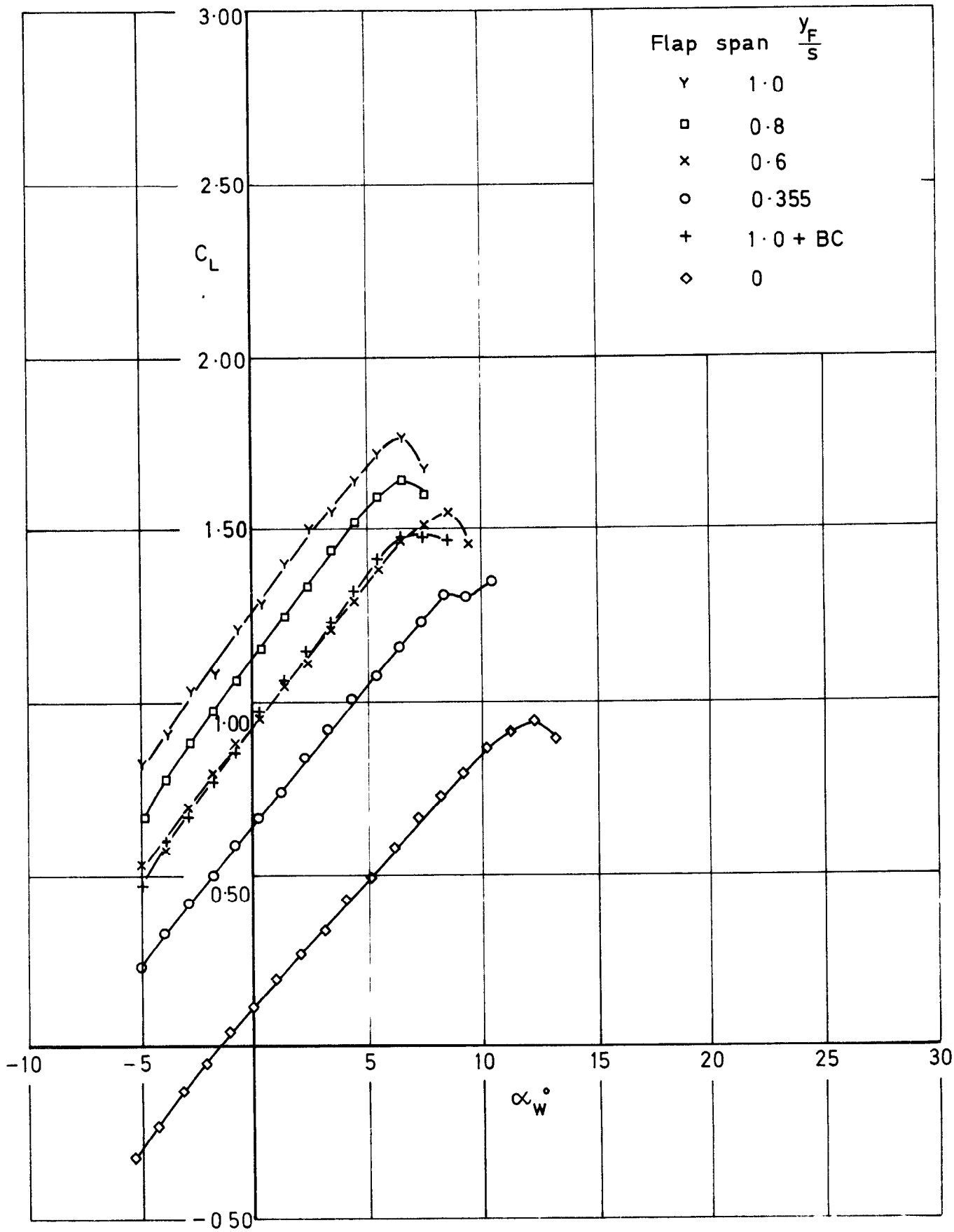

Fig. 31 Basic wing, slats retracted, flaps deflected 25°.
Effect of flap span, C_L vs $\alpha_w°$

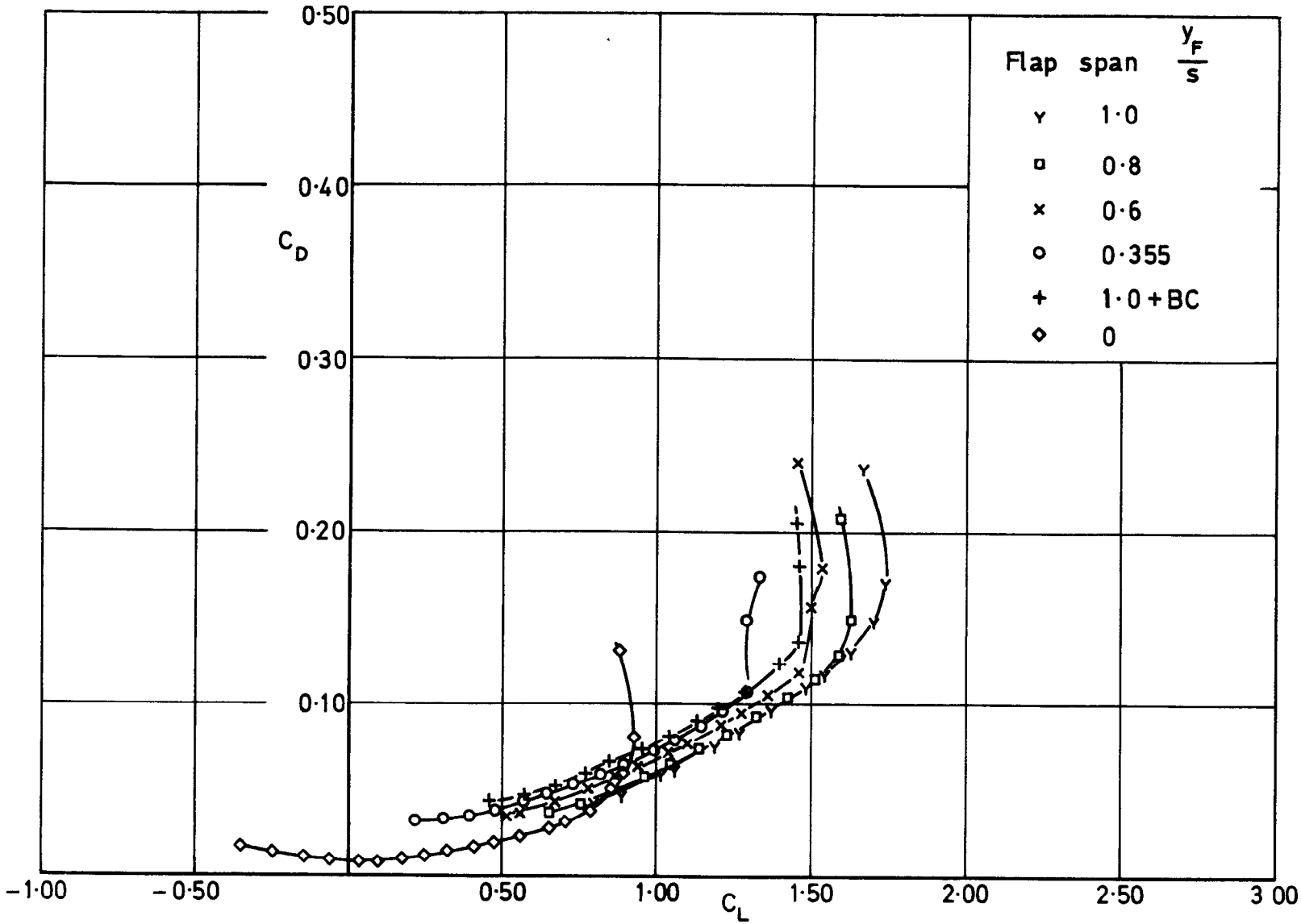

Fig. 32 Basic wing, slats retracted, flaps deflected 25°.
Effect of flap span, C_D vs C_L

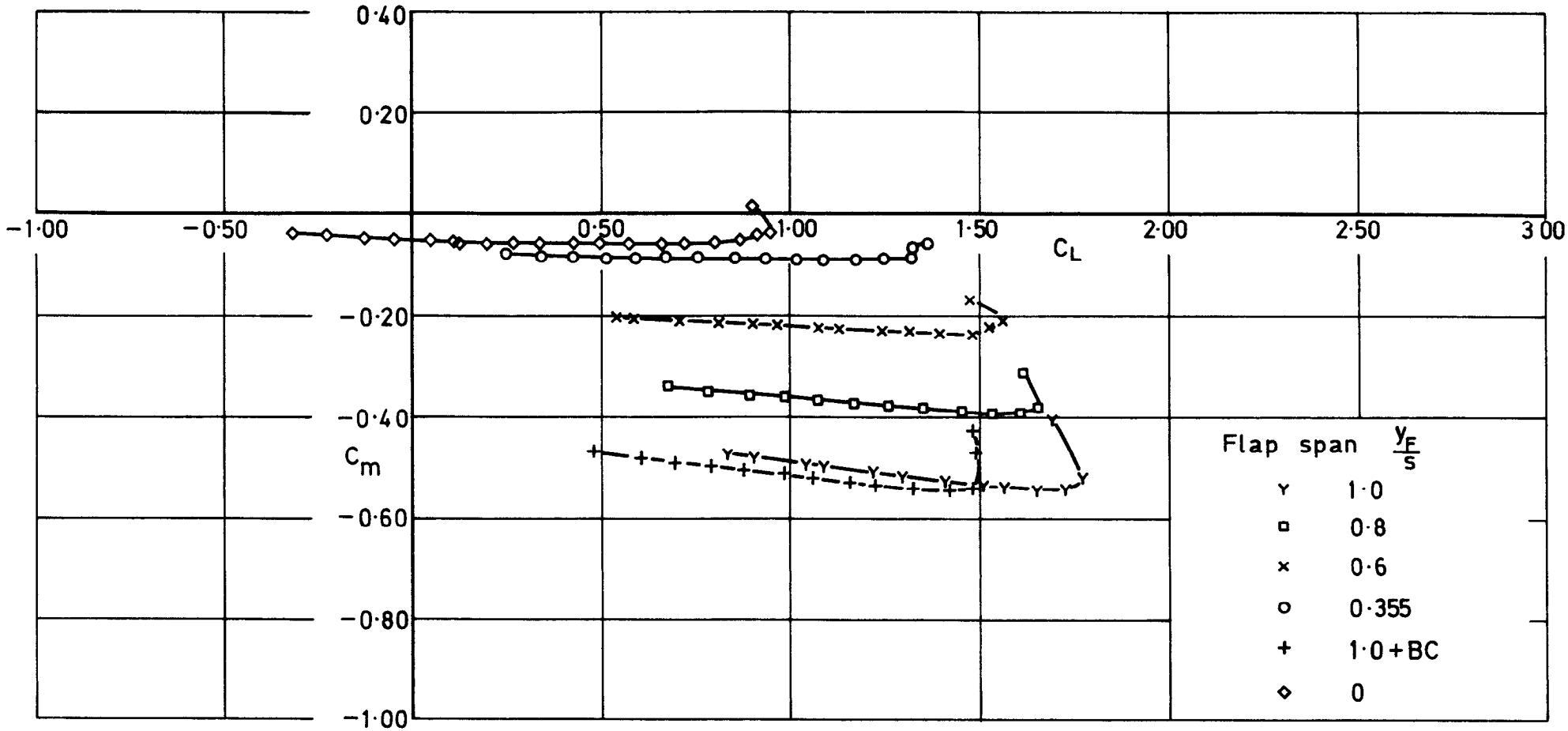

Fig. 33 Basic wing, slats retracted, flaps deflected 25°.
Effect of flap span, C_m vs C_L

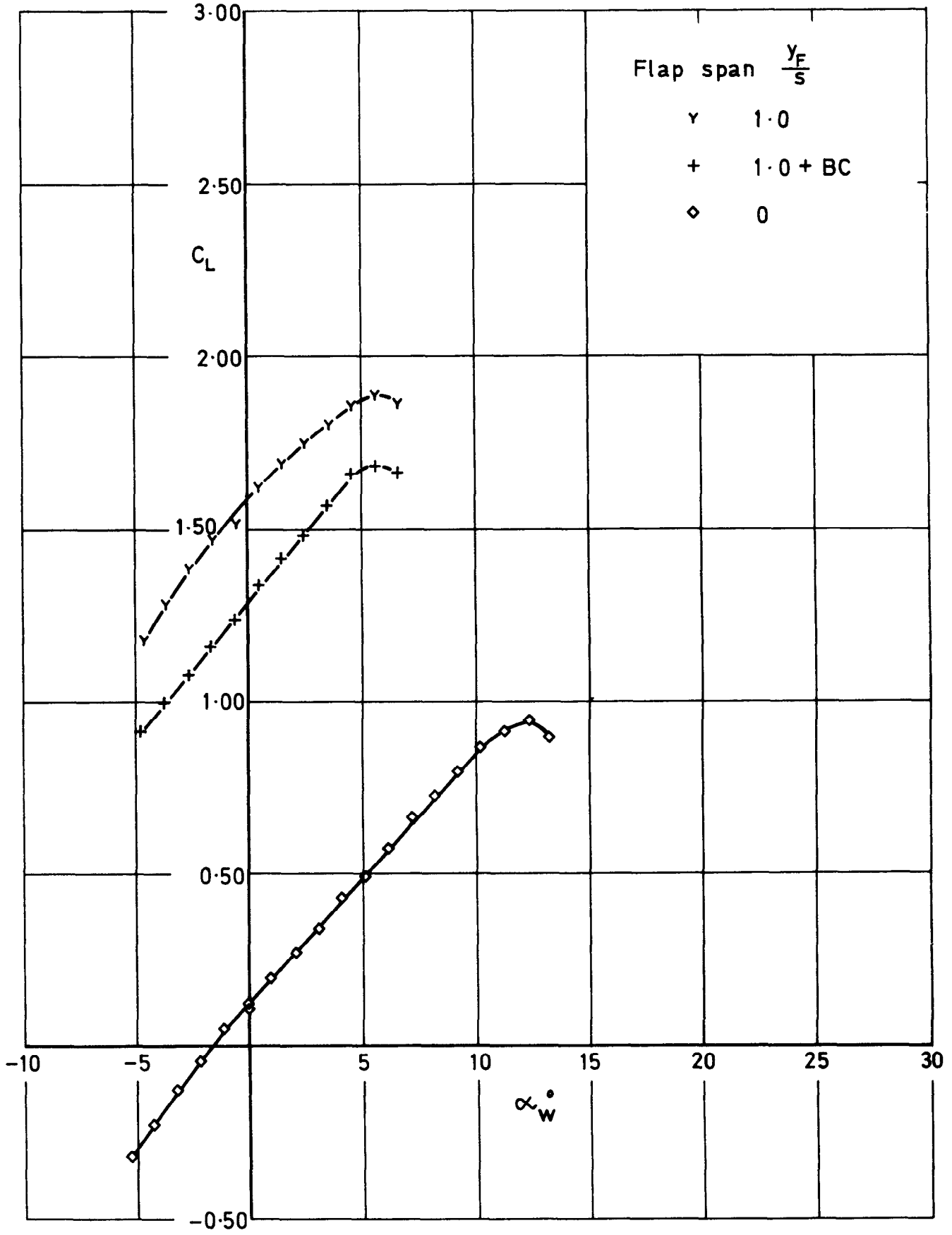

Fig. 34 Basic wing, slats retracted, flaps deflected 40°. Effect of flap span, C_L vs $\alpha_w°$

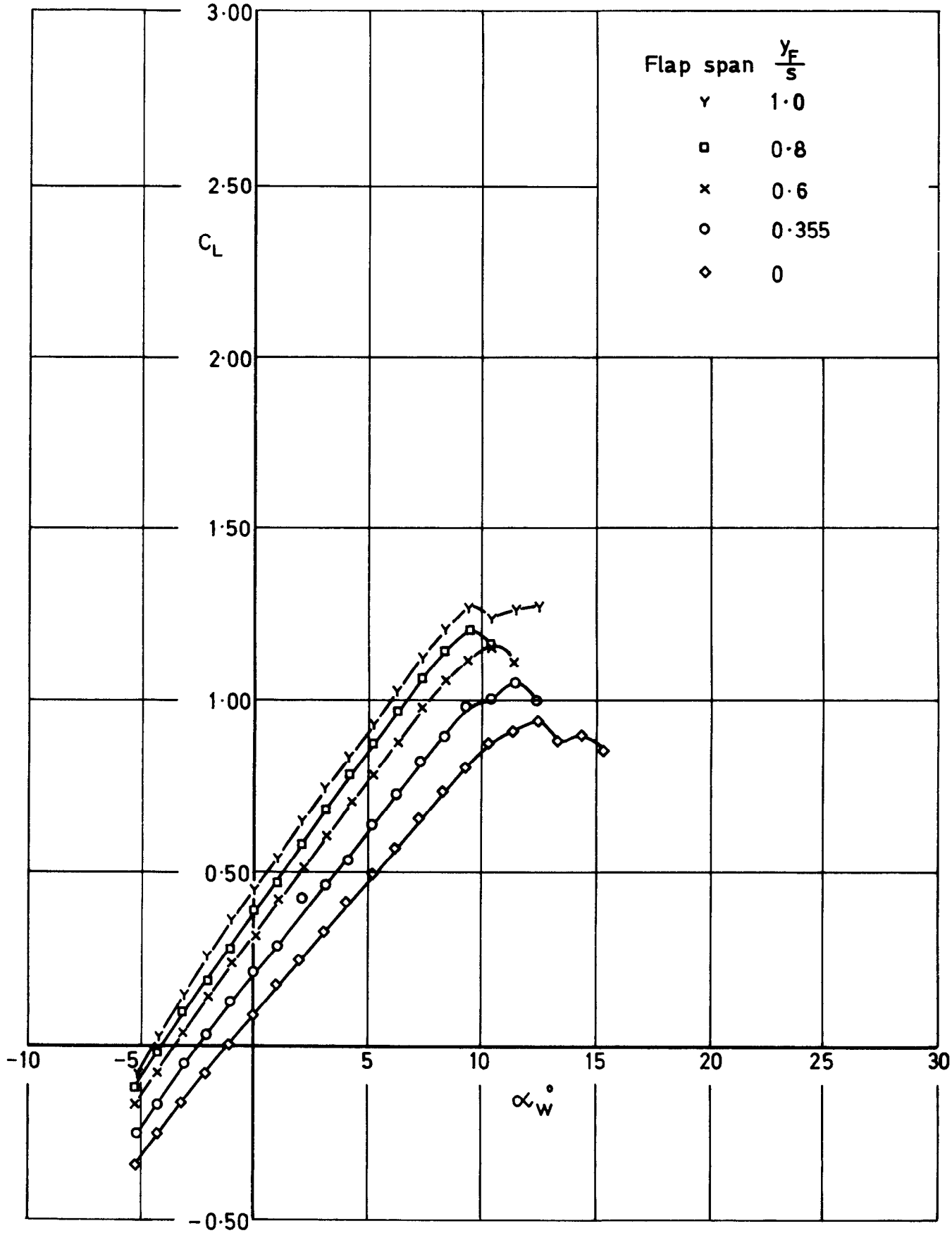

Fig.35 Basic wing + body, slats retracted, flaps deflected 10°.
Effect of flap span, C_L vs $\alpha_w°$

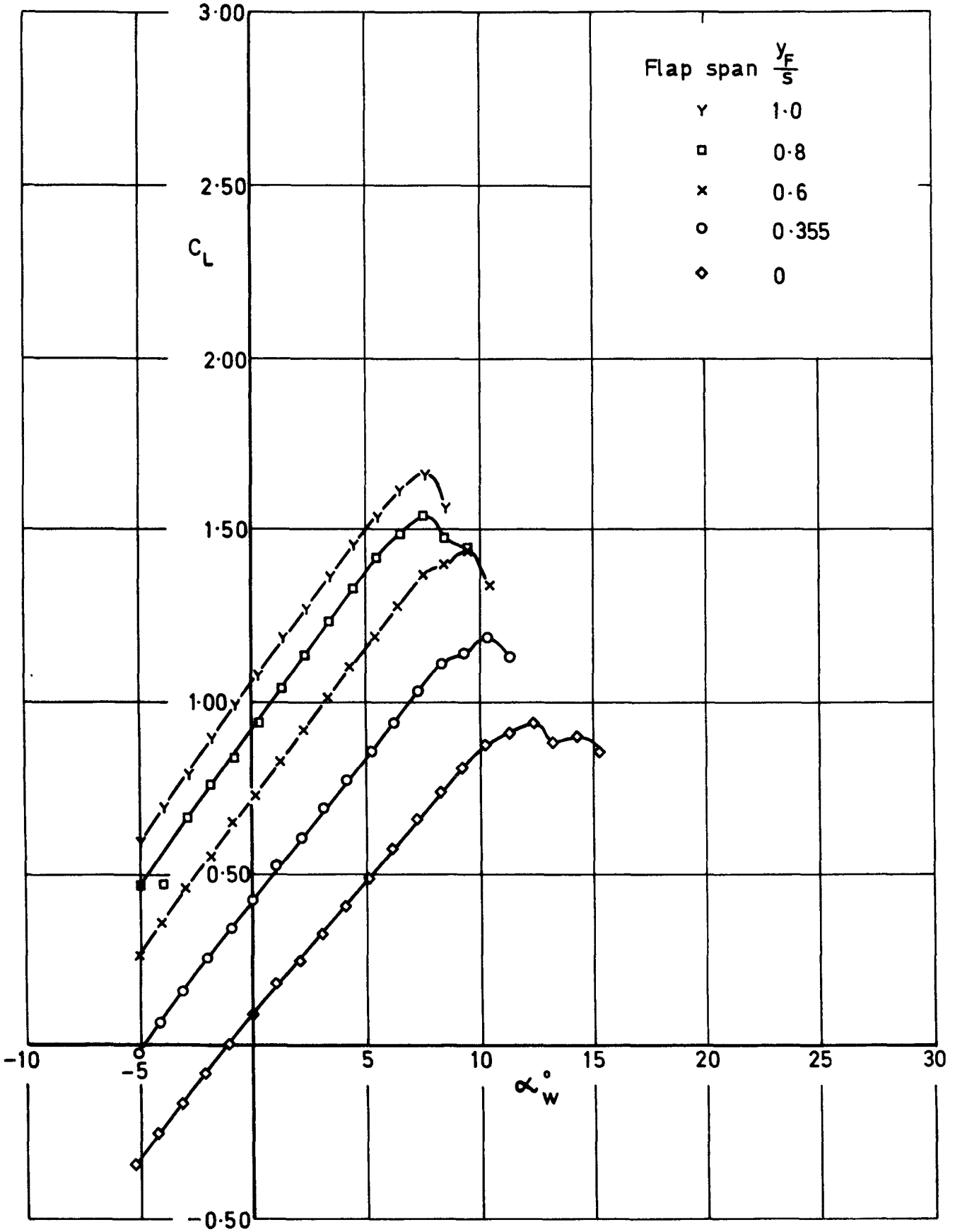

Fig. 36 Basic wing + body, slats retracted, flaps deflected 25°.
Effect of flap span, C_L vs α_w°

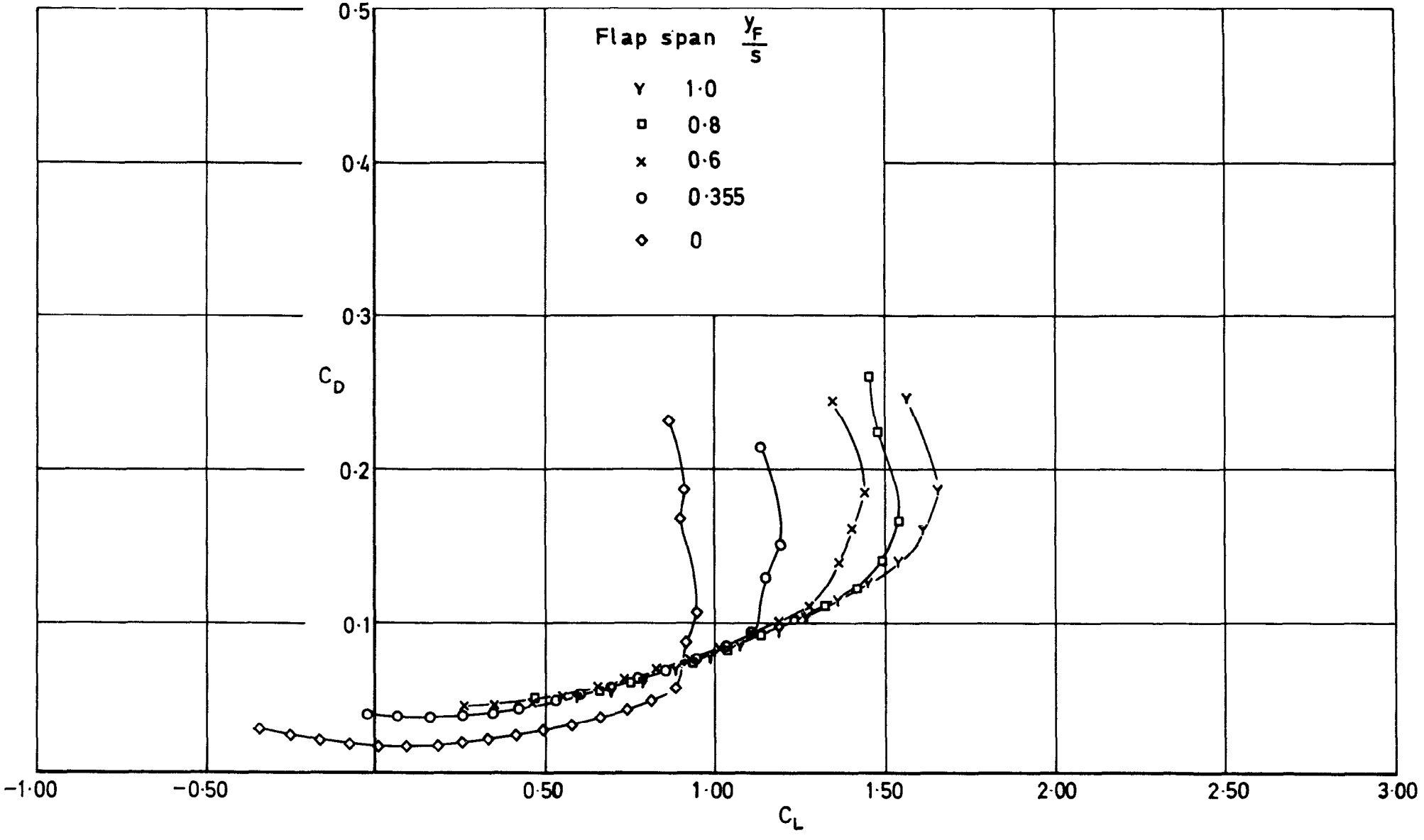

Fig.37 Basic wing + body, slats retracted, flaps deflected 25°.
Effect of flap span, C_D vs C_L

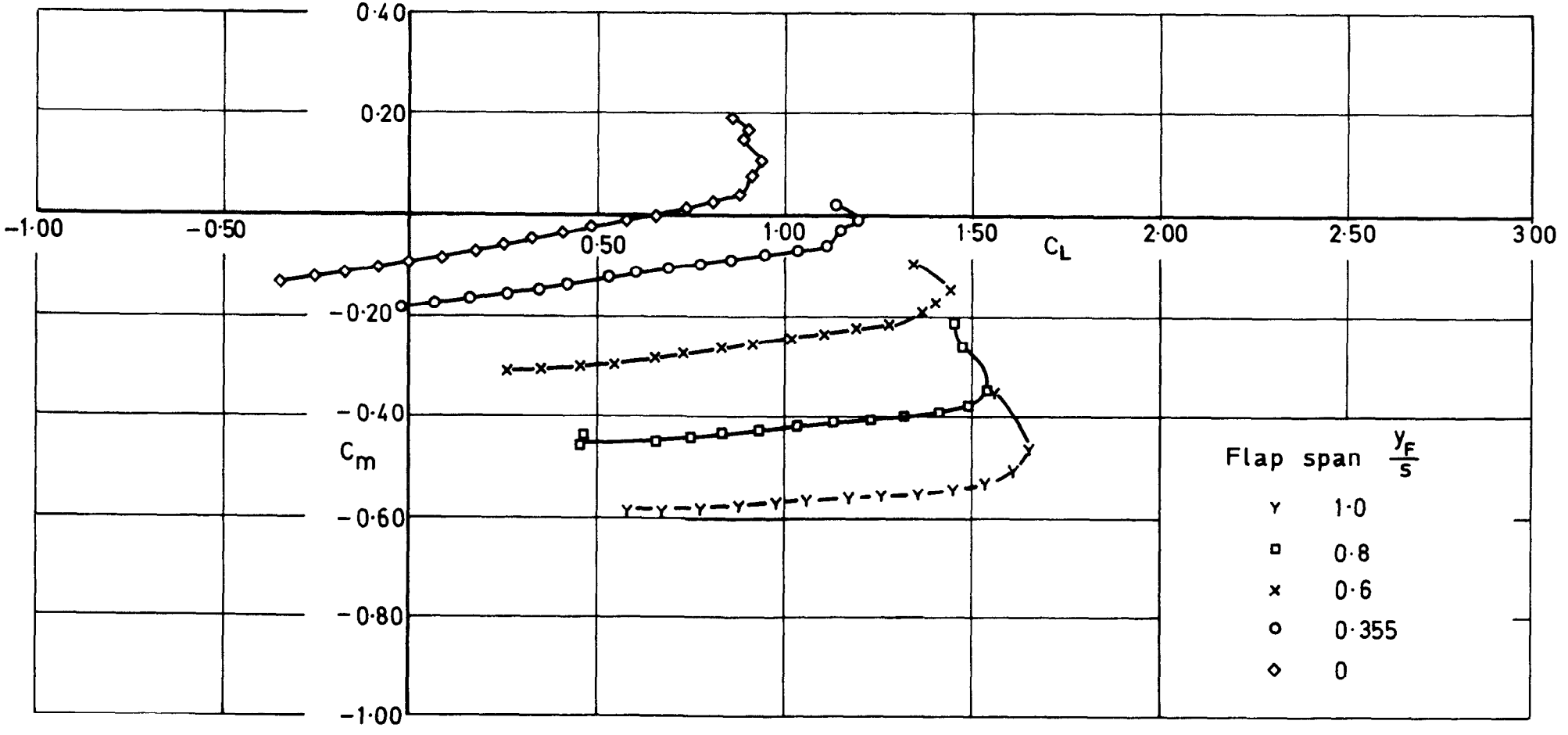

Fig. 38 Basic wing + body, slats retracted, flaps deflected 25°
Effect of flap span, C_m vs C_L

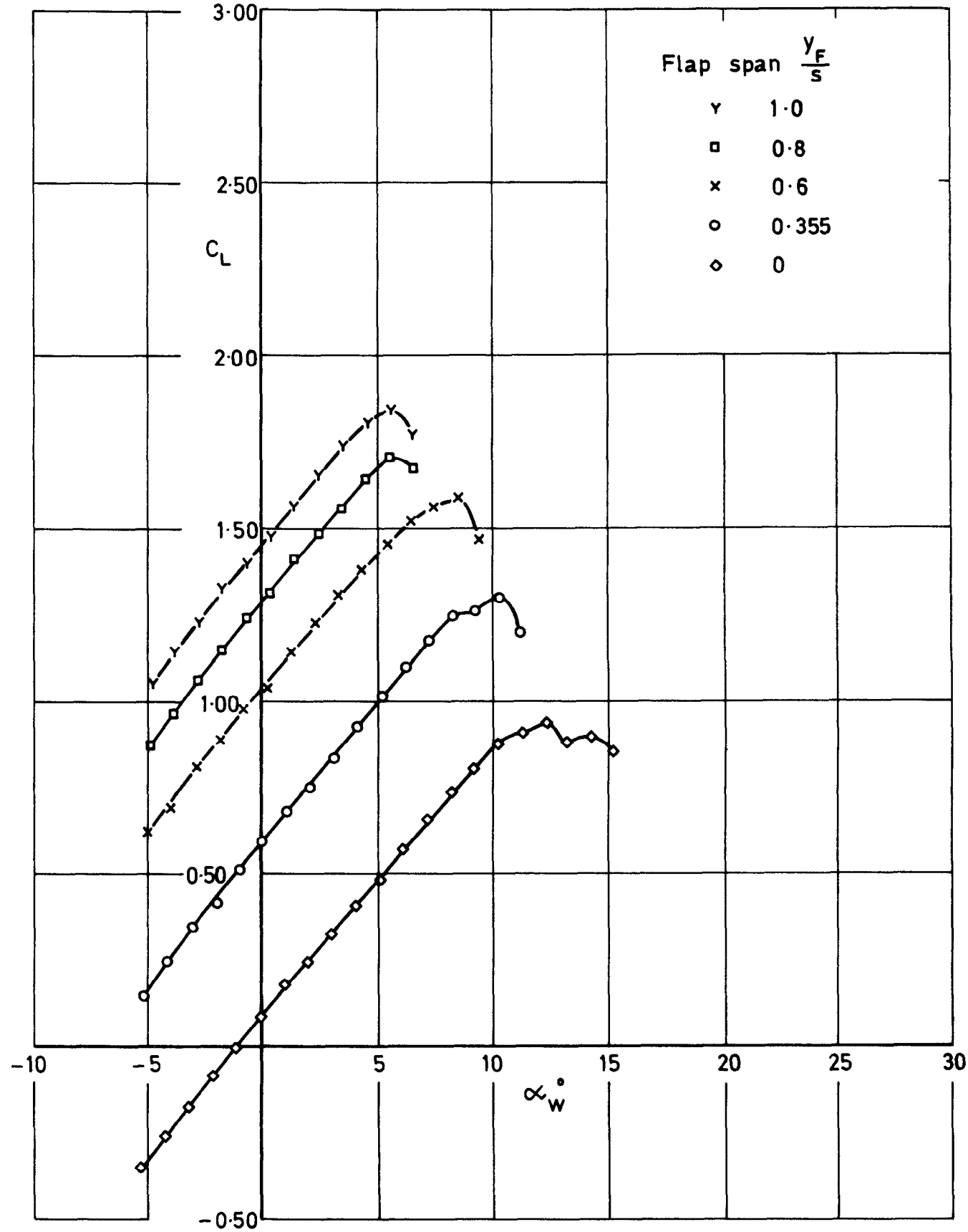

Fig.39 Basic wing+body, slats retracted, flaps deflected 40°.
Effect of flap span, C_L vs $\alpha_w°$

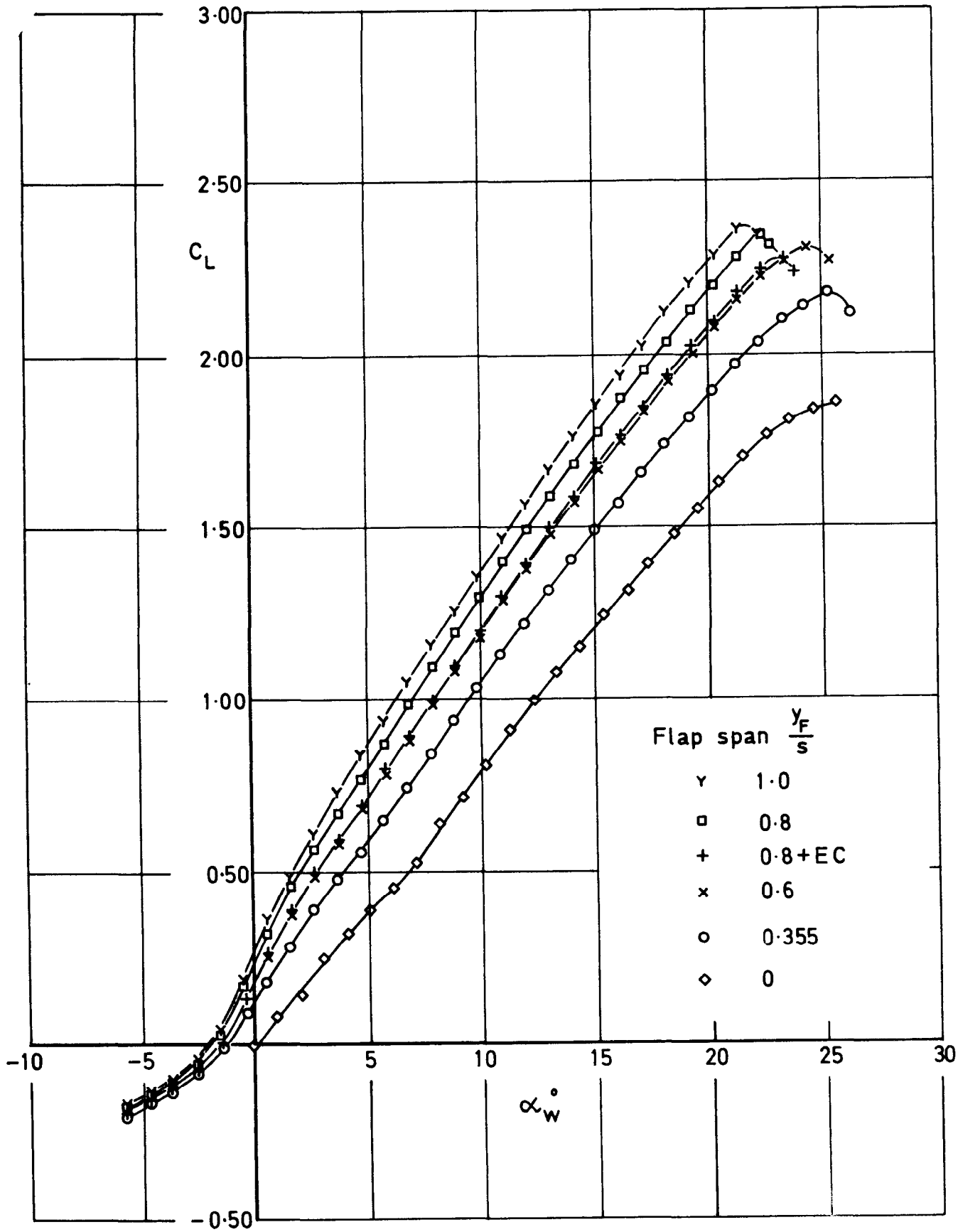

Fig. 40 Basic wing, slats deflected 25°, flaps deflected 10°.
Effect of flap span, C_L vs $\alpha_w°$

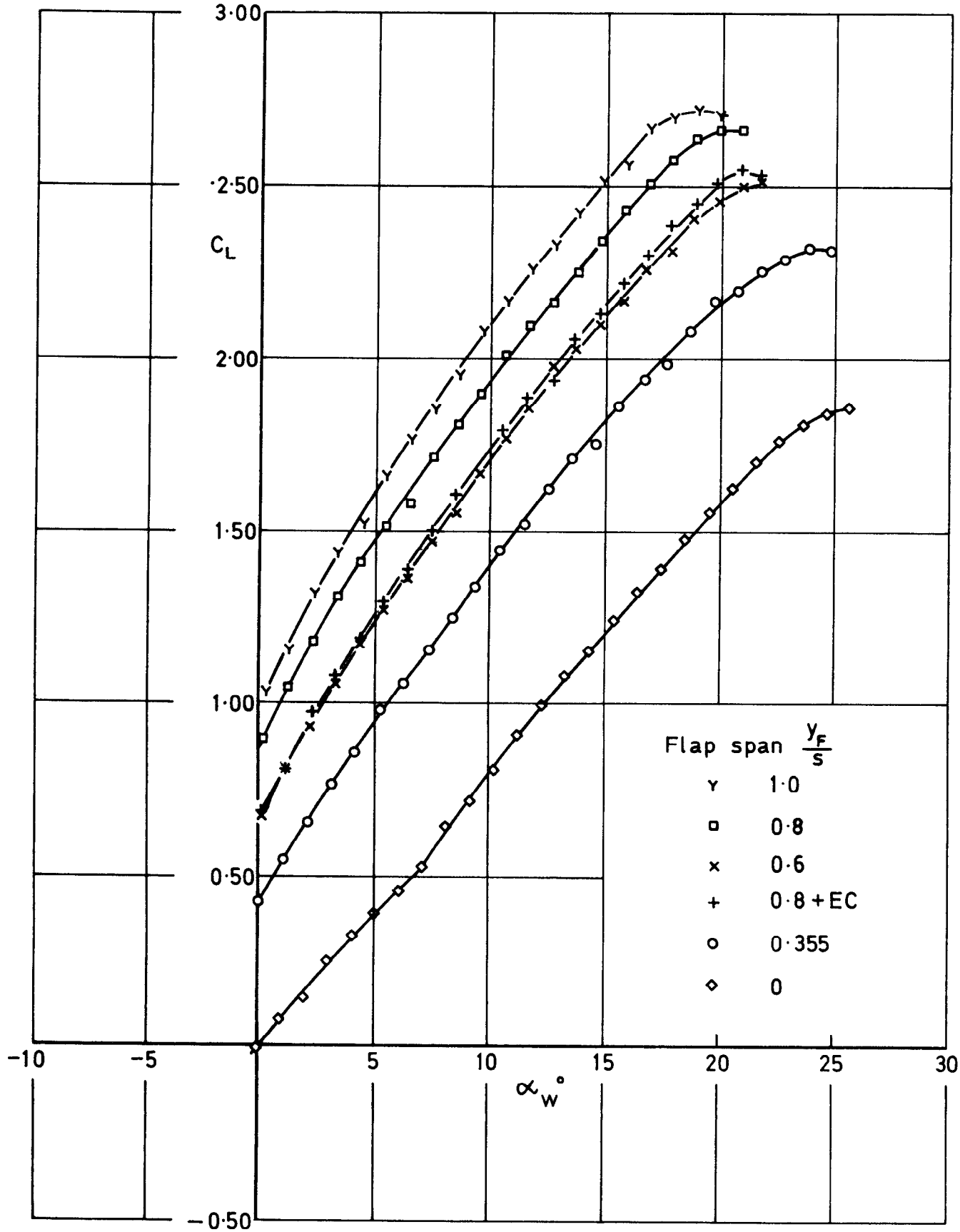

Fig.41 Basic wing, slats deflected 25°, flaps deflected 25°. Effect of flap span, C_L vs $\alpha_w°$

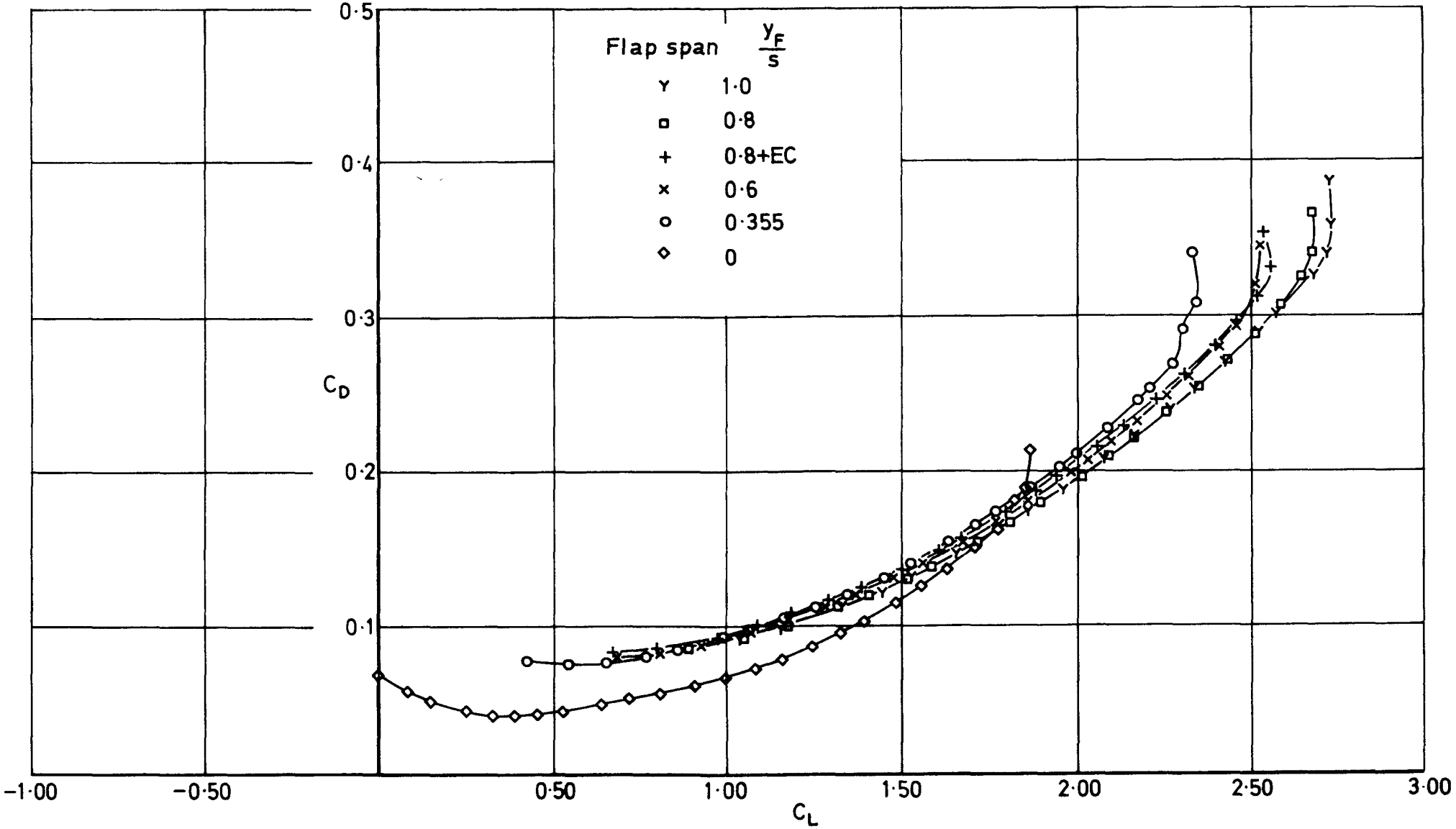

Fig. 42 Basic wing, slats deflected 25°, flaps deflected 25°.
Effect of flap span, C_D vs C_L

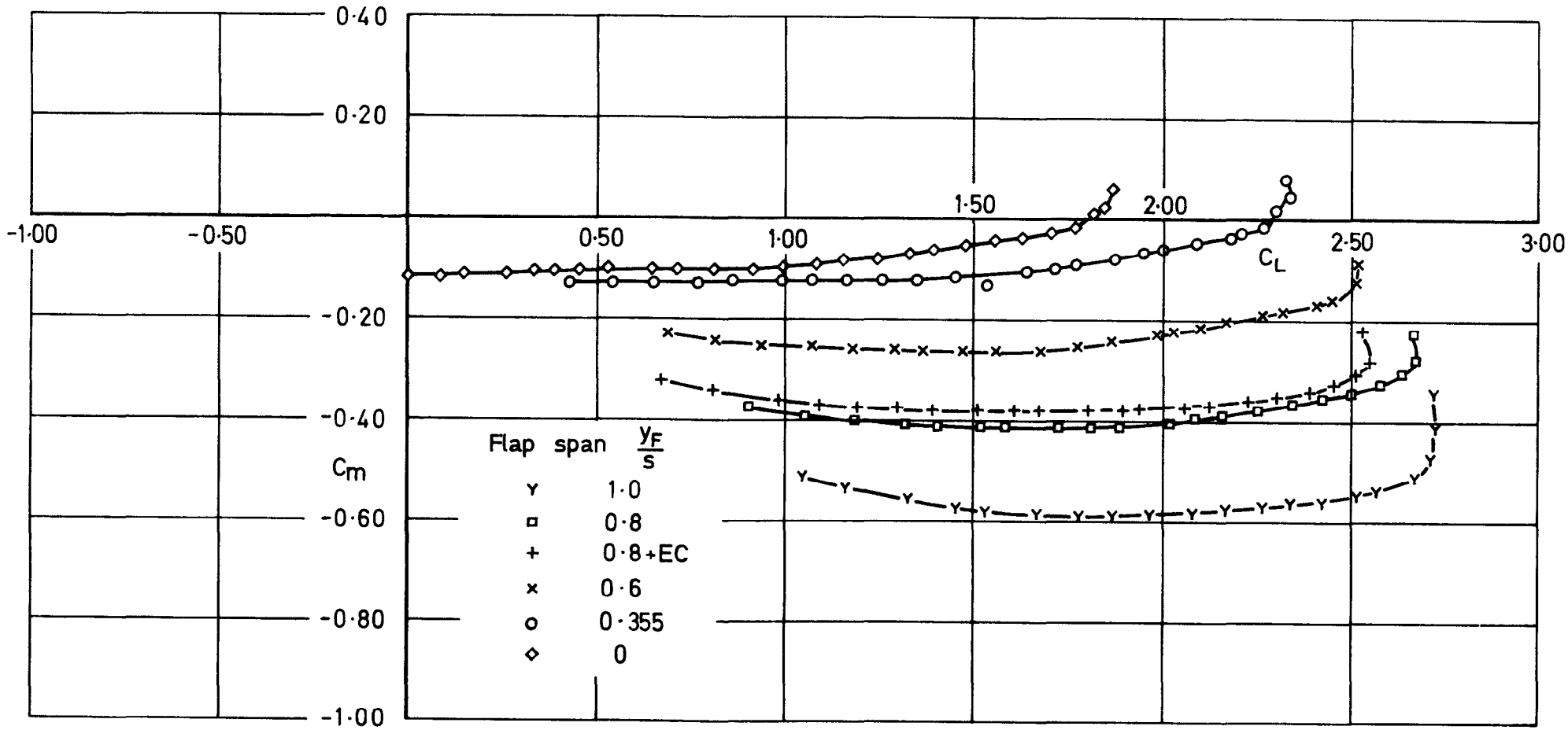

Fig. 43 Basic wing, slats deflected 25°, flaps deflected 25°.
Effect of flap span, C_m vs C_L

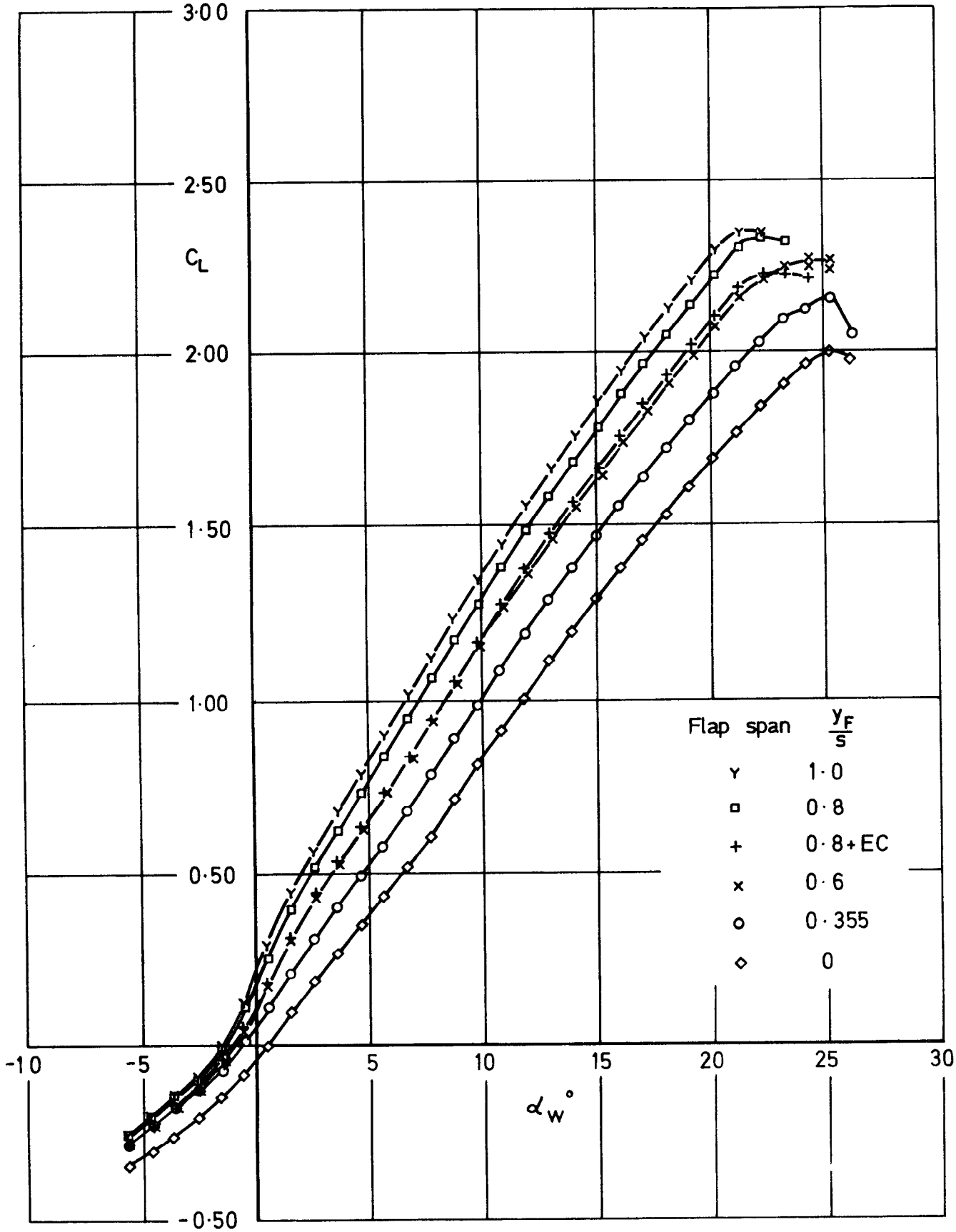

Fig.44 Basic wing+ body, slats deflected 25°, flaps deflected 10°. Effect of flap span, C_L vs $\alpha_w°$

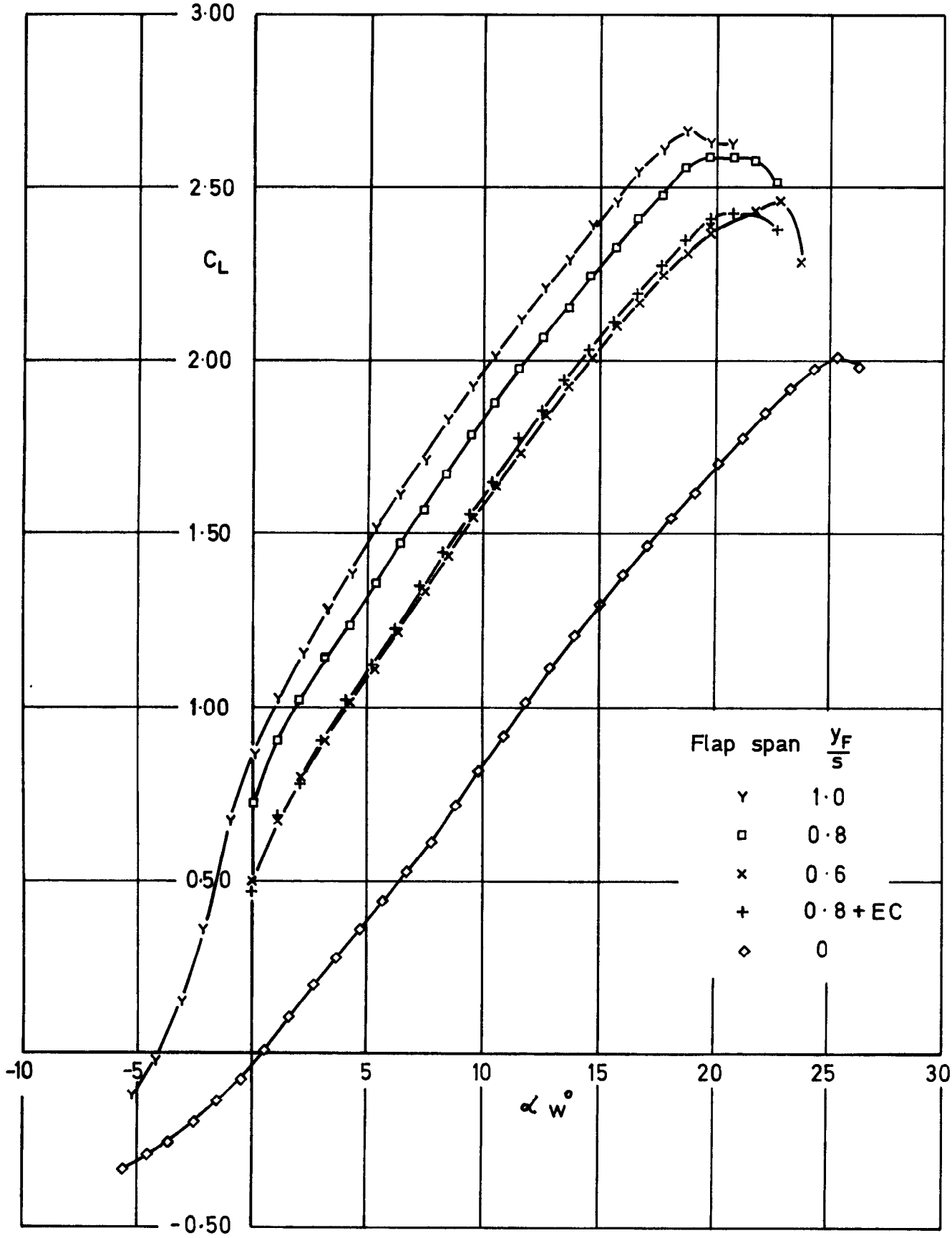

Fig.45 Basic wing + body, slats deflected 25°, flaps deflected 25°. Effect of flap span, C_L vs $\alpha_w°$

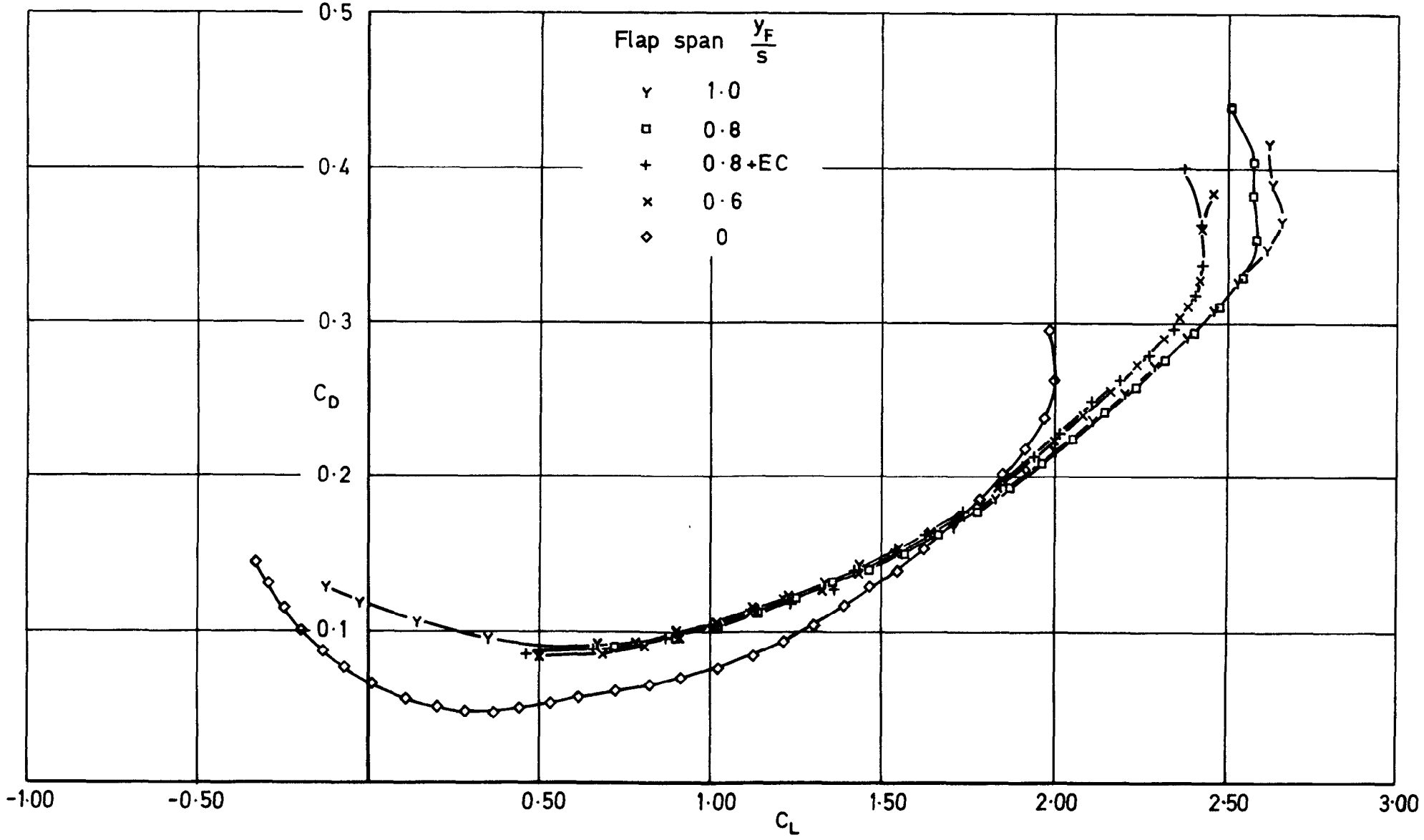

Fig.46 Basic wing + body, slats deflected 25°, flaps deflected 25°.
Effect of flap span, C_D vs C_L

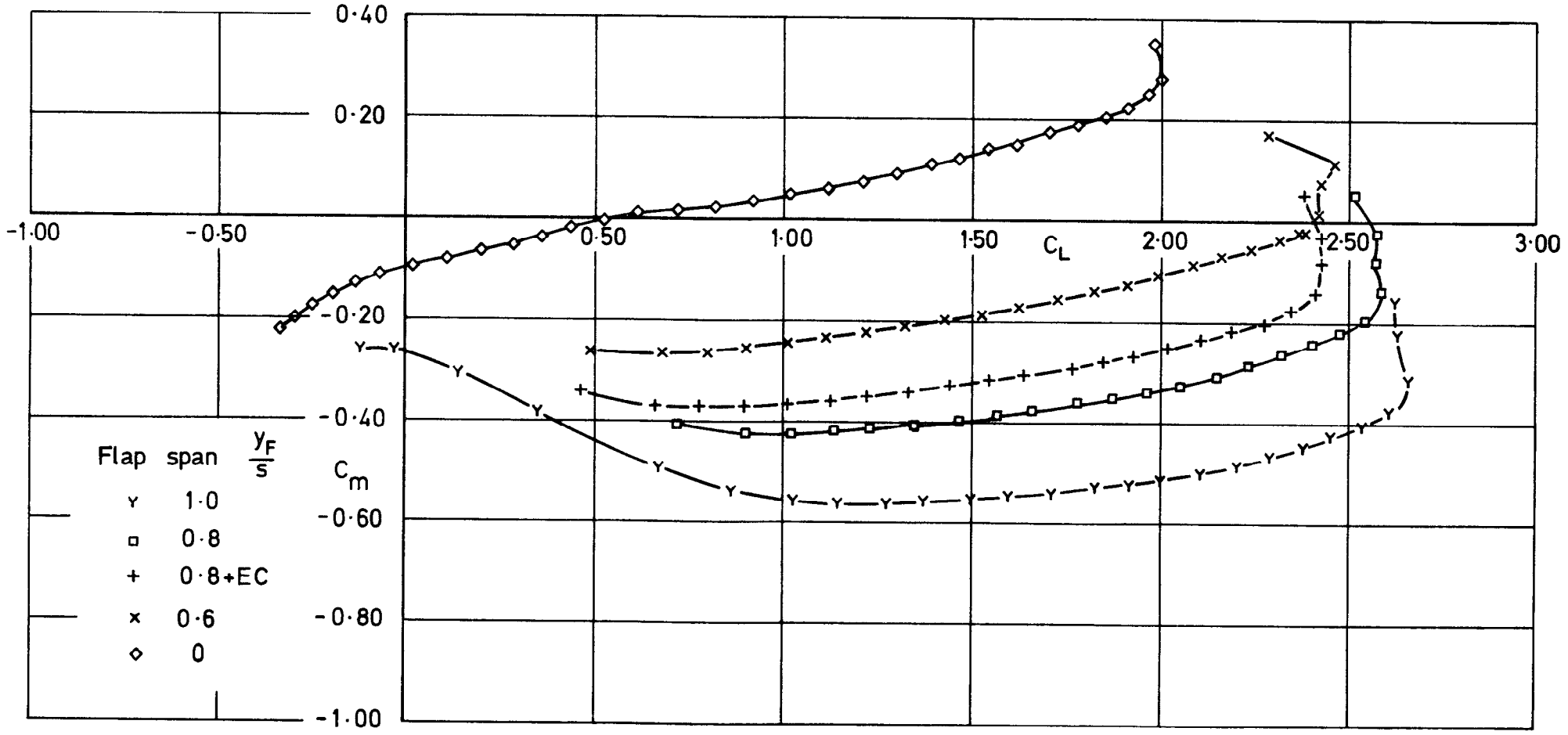

Fig. 47 Basic wing + body, slats deflected 25°, flaps deflected 25°.
Effect of flap span, C_m vs C_L

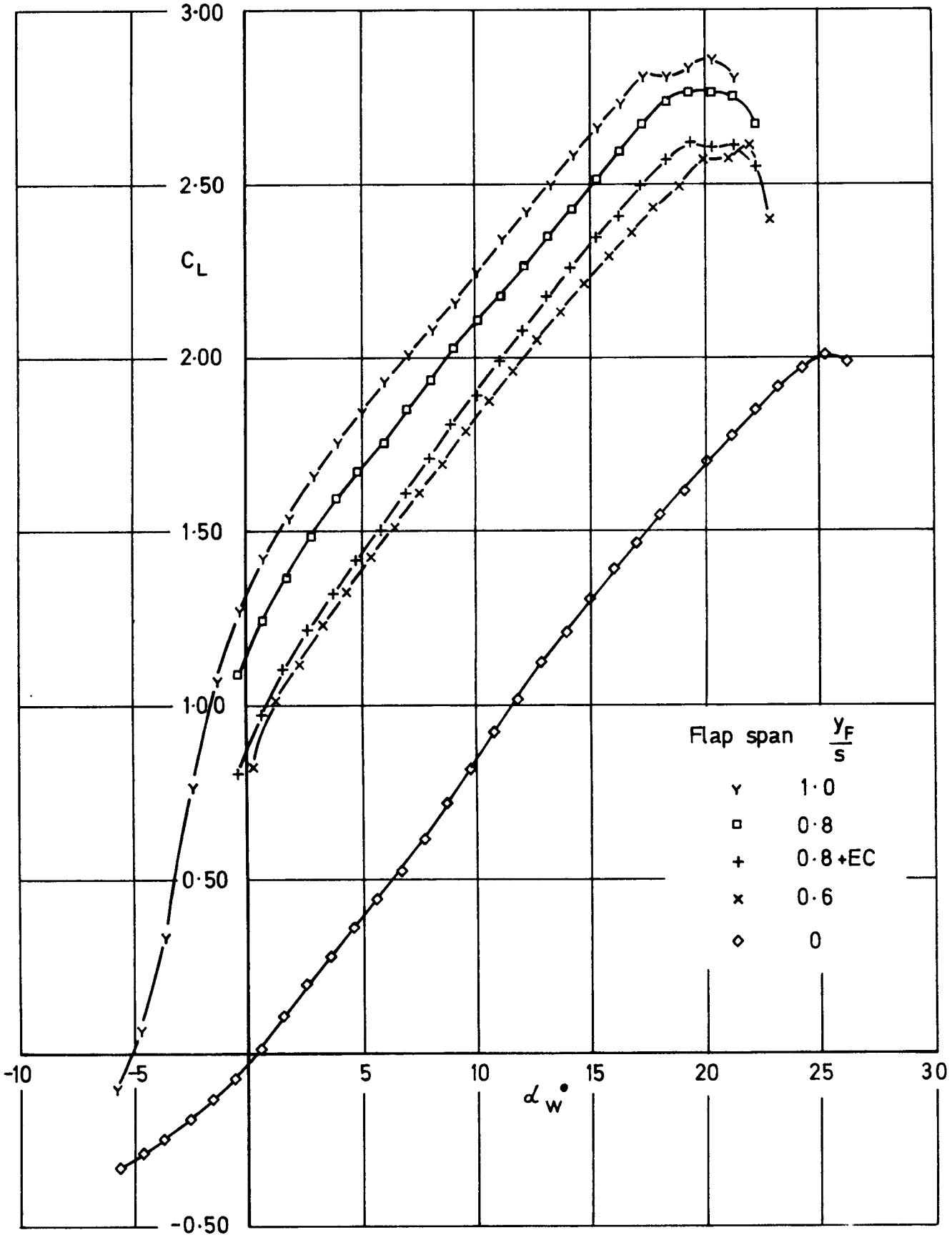

Fig.48 Basic wing+ body, slats deflected 25°, flaps deflected 40°. Effect of flap span, C_L vs $\alpha_w°$

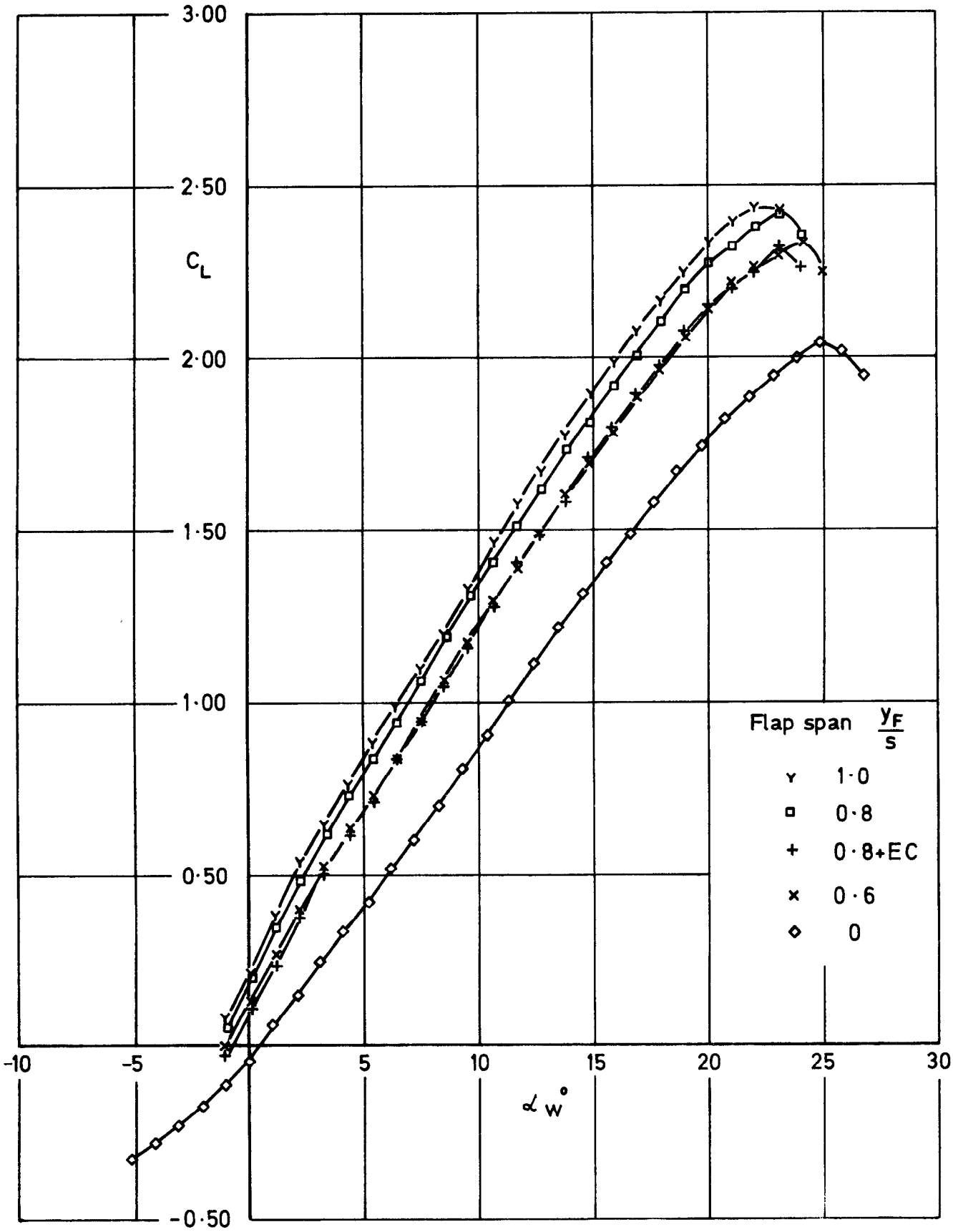

Fig.49 Extended wing+ body, slats deflected 25°, flaps deflected 10°. Effect of flap span, C_L vs $\alpha_w°$

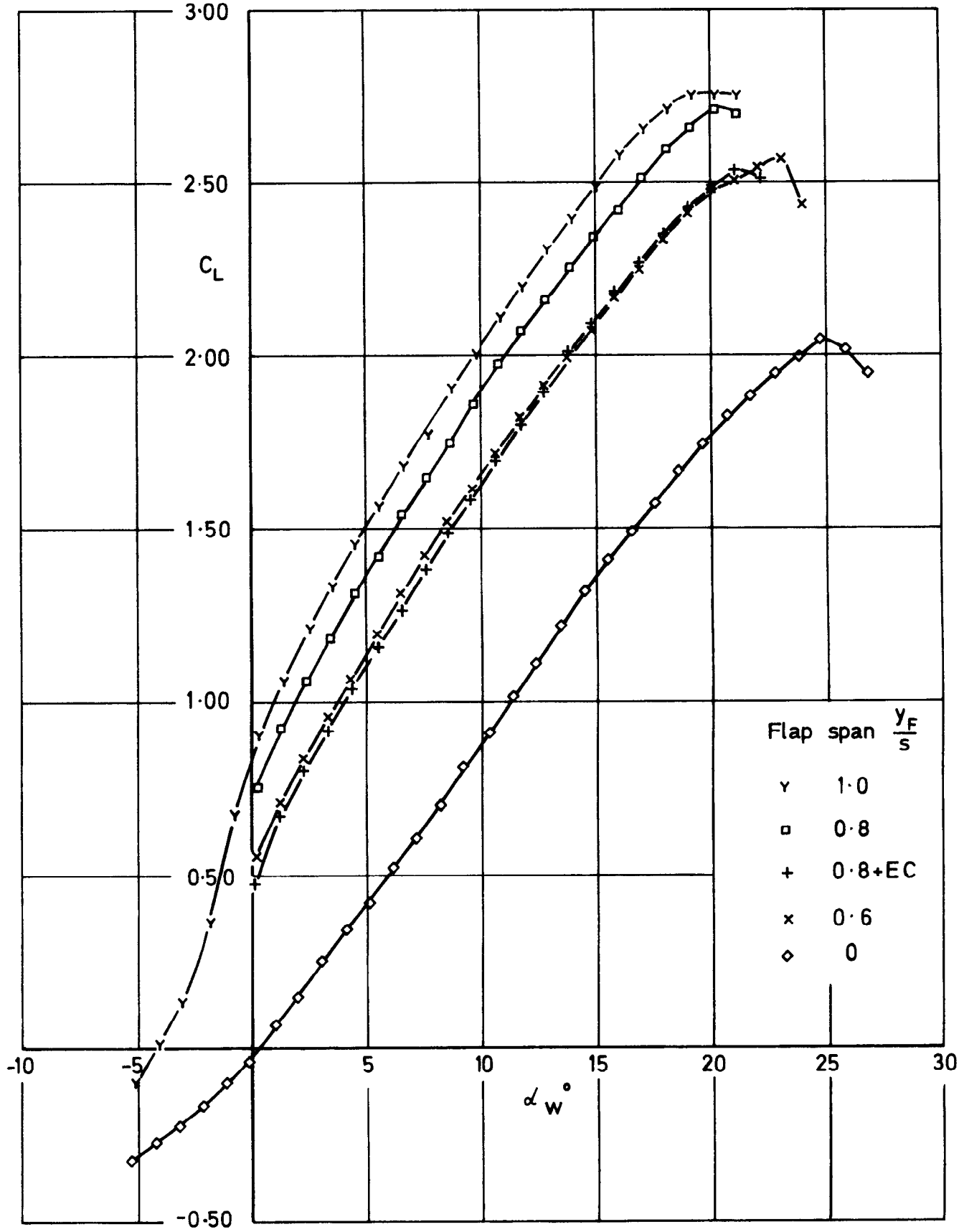

Fig. 50 Extended wing+ body, slats deflected 25°, flaps deflected 25°. Effect of flap span, C_L vs $\alpha_w°$

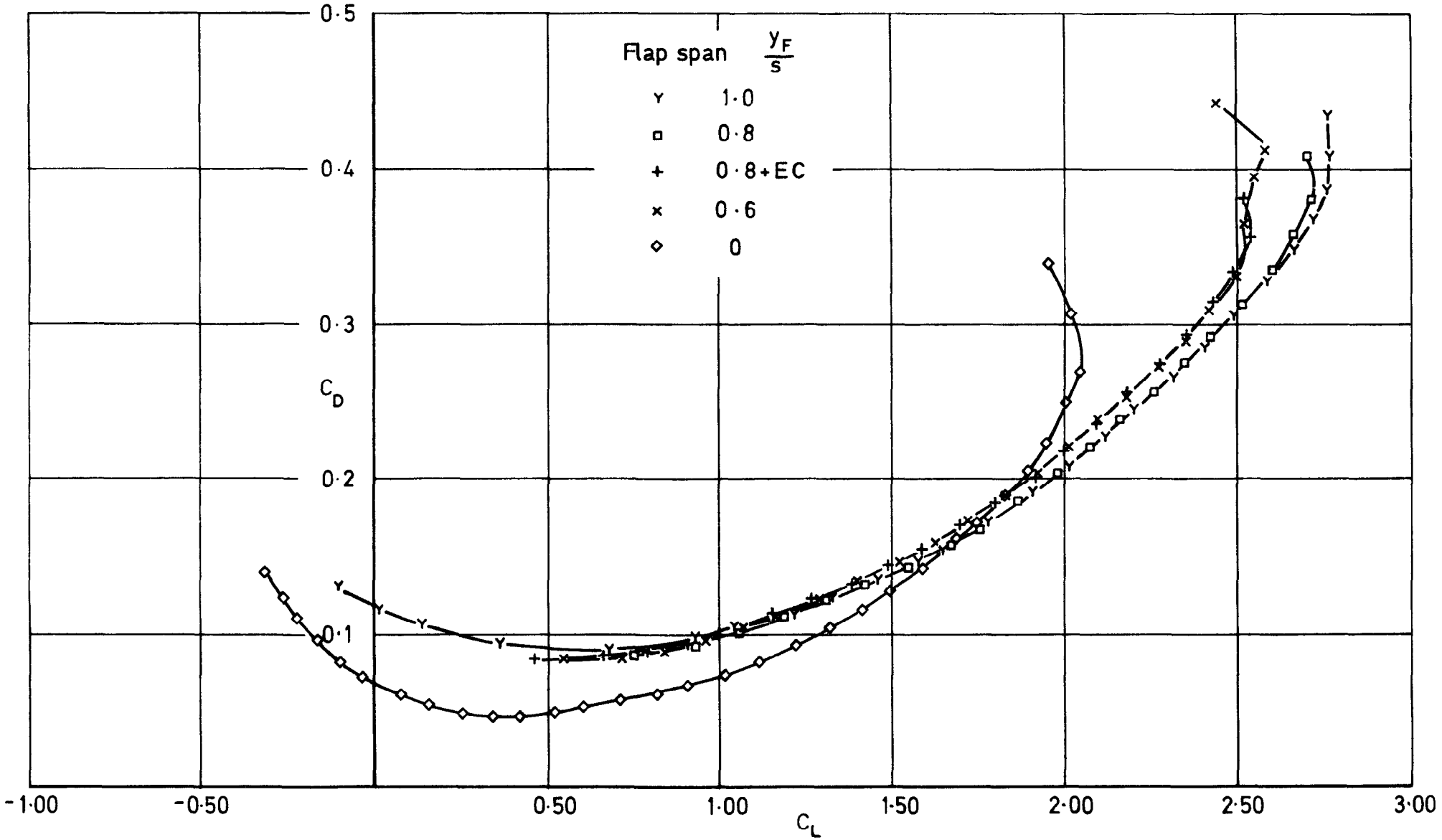

Fig.51 Extended wing + body, slats deflected 25°, flaps deflected 25°.
Effect of flap span, C_D vs C_L

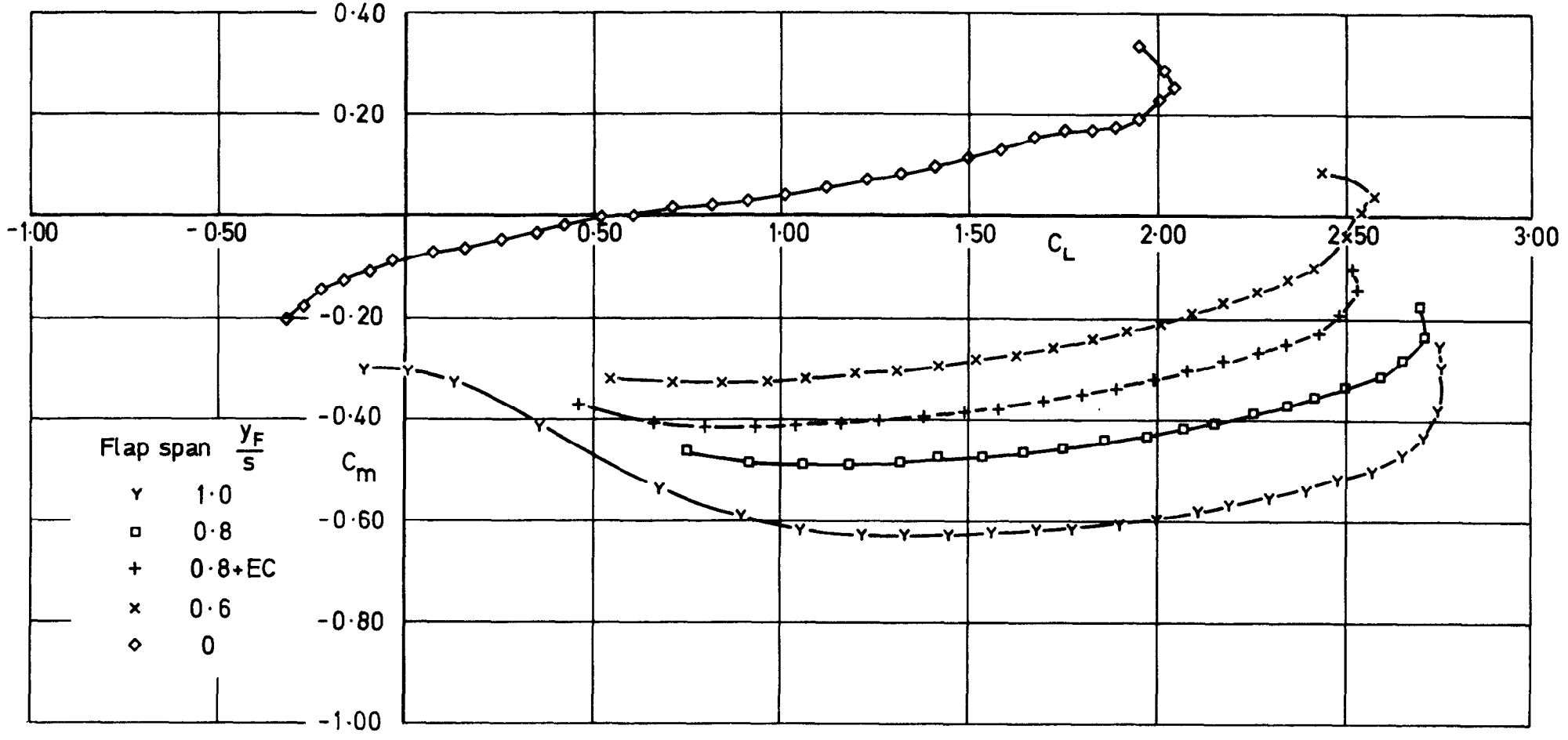

Fig. 52 Extended wing + body, slats deflected 25°, flaps deflected 25°.
Effect of flap span, C_m vs C_L

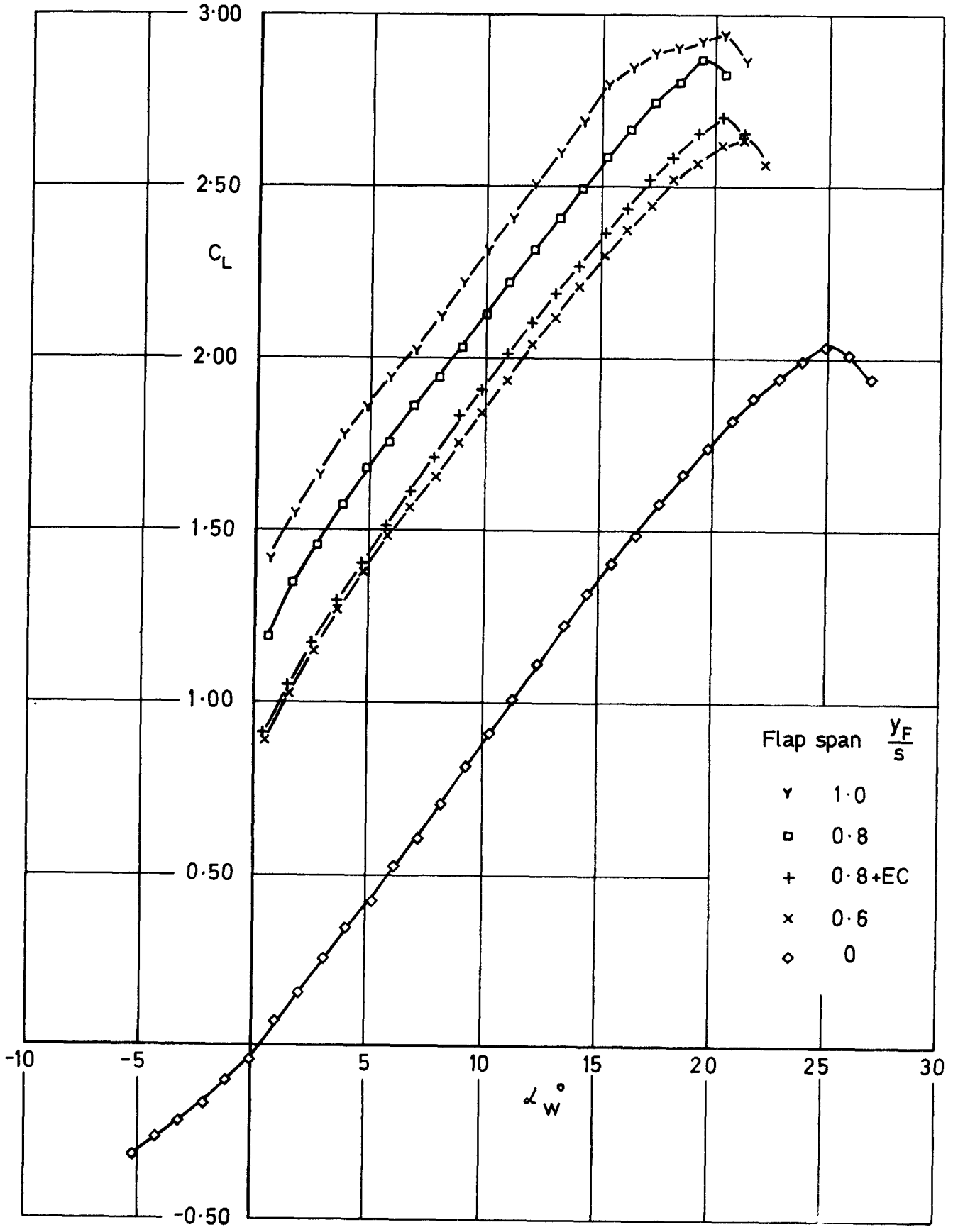

Fig.53 Extended wing+ body, slats deflected 25°, flaps deflected 40°. Effect of flap span, C_L vs $\alpha_W°$

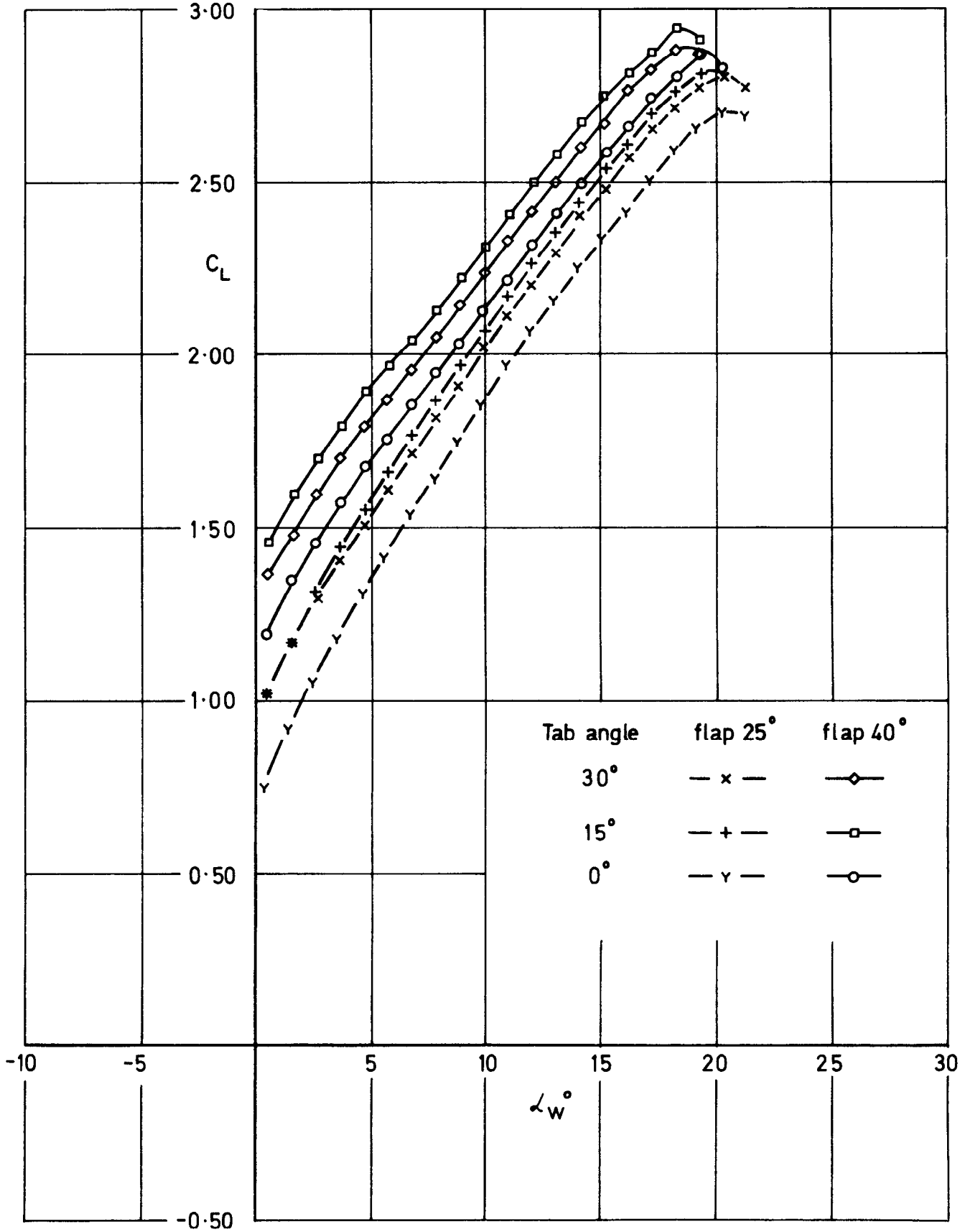

Fig.54 Extended wing + body, slats deflected 25°, $\frac{y_F}{s}$ = 0·8.
Flaps deflected 25° and 40°.
Effect of tab deflection angle, C_L vs $\alpha_w°$

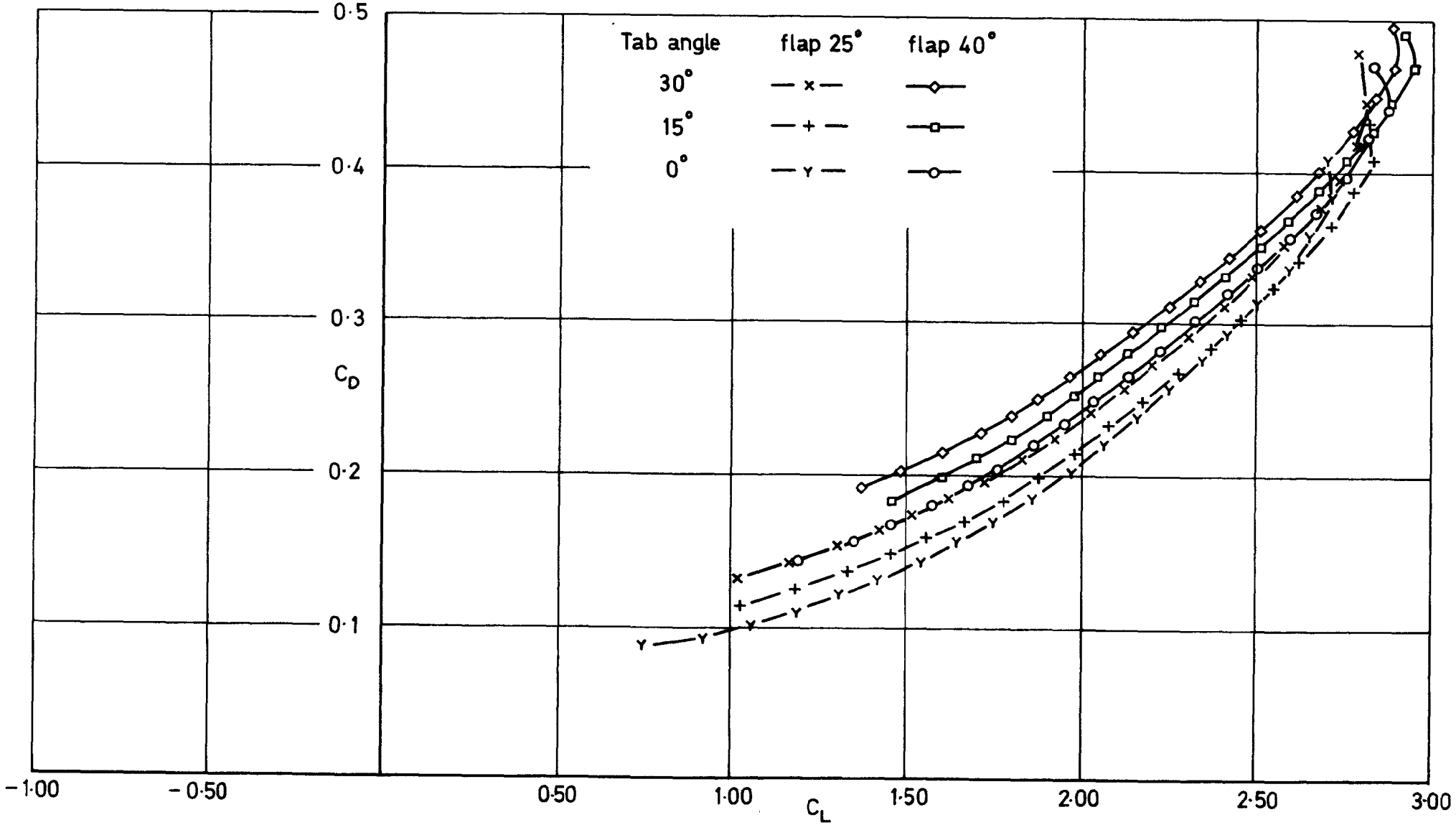

Fig.55 Extended wing + body, slats deflected 25°, $\frac{y_F}{s} = 0{\cdot}8$.
Flaps deflected 25° and 40°.
Effect of tab deflection angle, C_D vs C_L

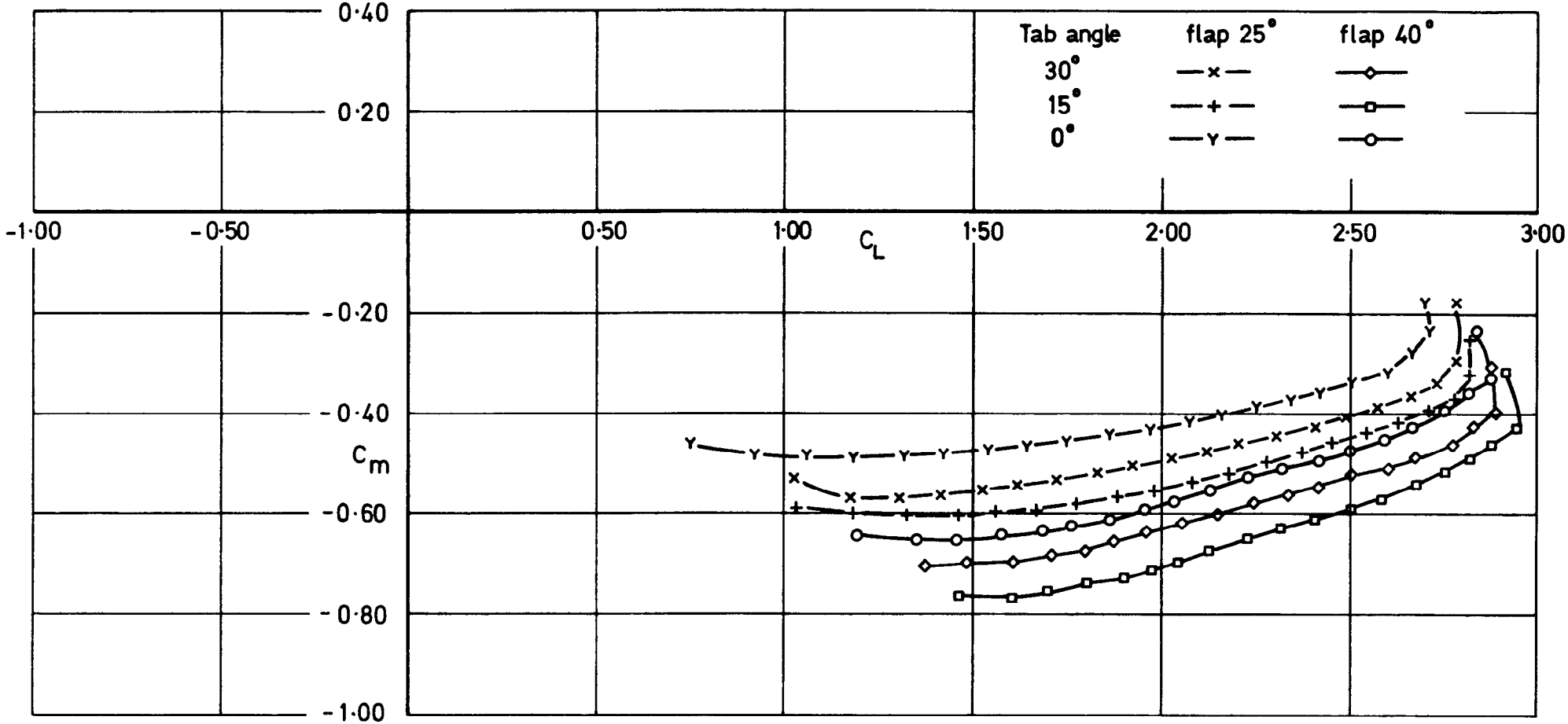

Fig.56 Extended wing + body, slats deflected 25°, $\frac{y_F}{s} = 0{\cdot}8$.
Flaps deflected 25° and 40°.
Effect of tab deflection angle, C_m vs C_L

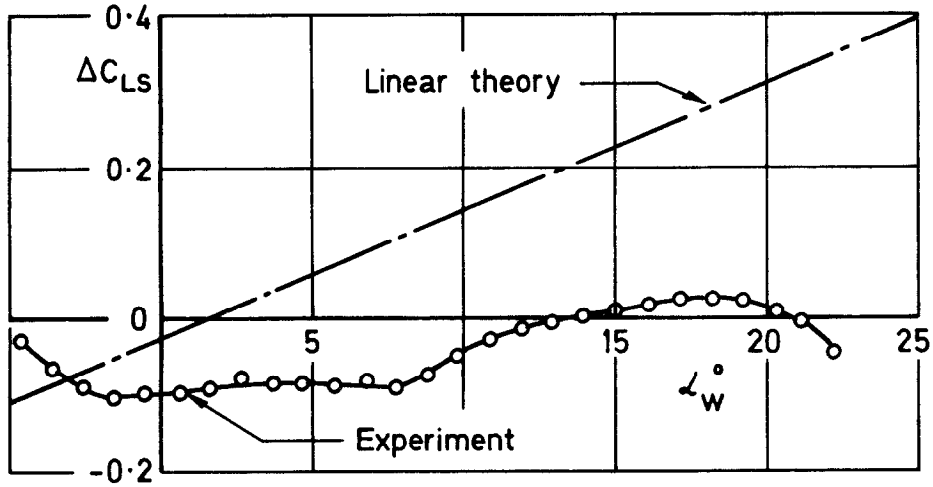

a Slats deflected 15°

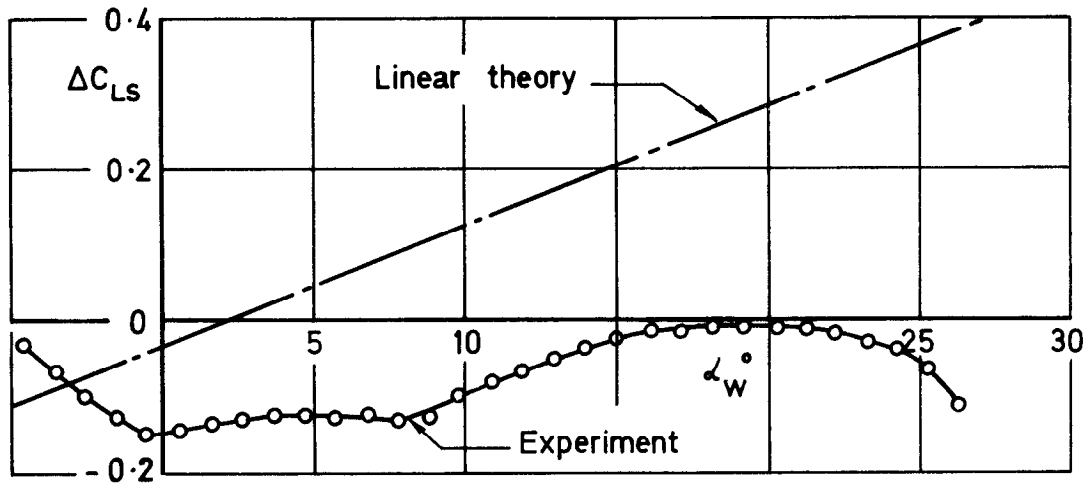

b Slats deflected 25°

$\Delta C_{LS} = C_L$ full-span slat $- C_L$ no slat

Fig.57a & b Lift increments for full-span slats. Basic wing, flaps retracted

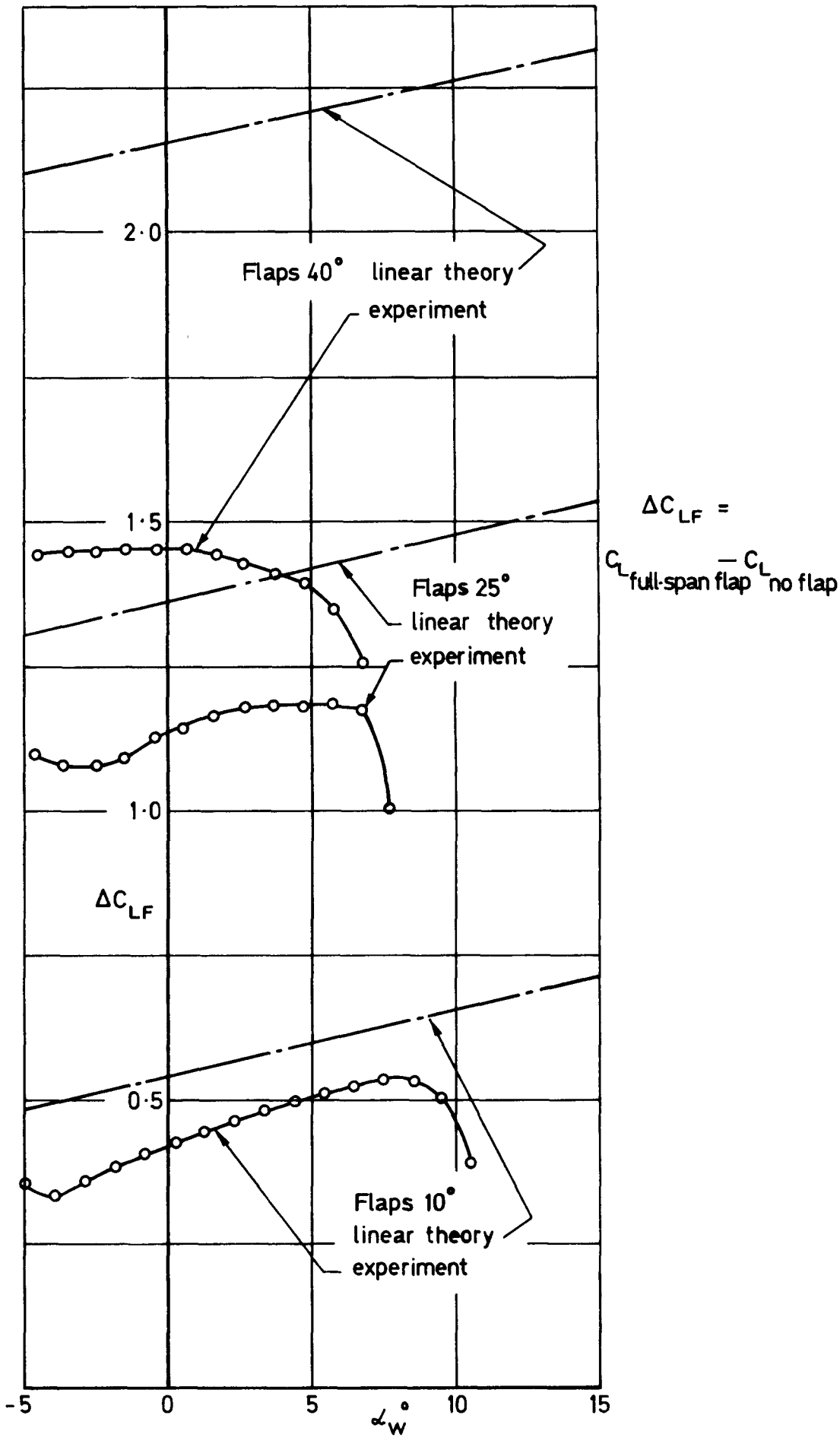

Fig.58 Lift increments for full-span flaps. Basic wing with slats retracted

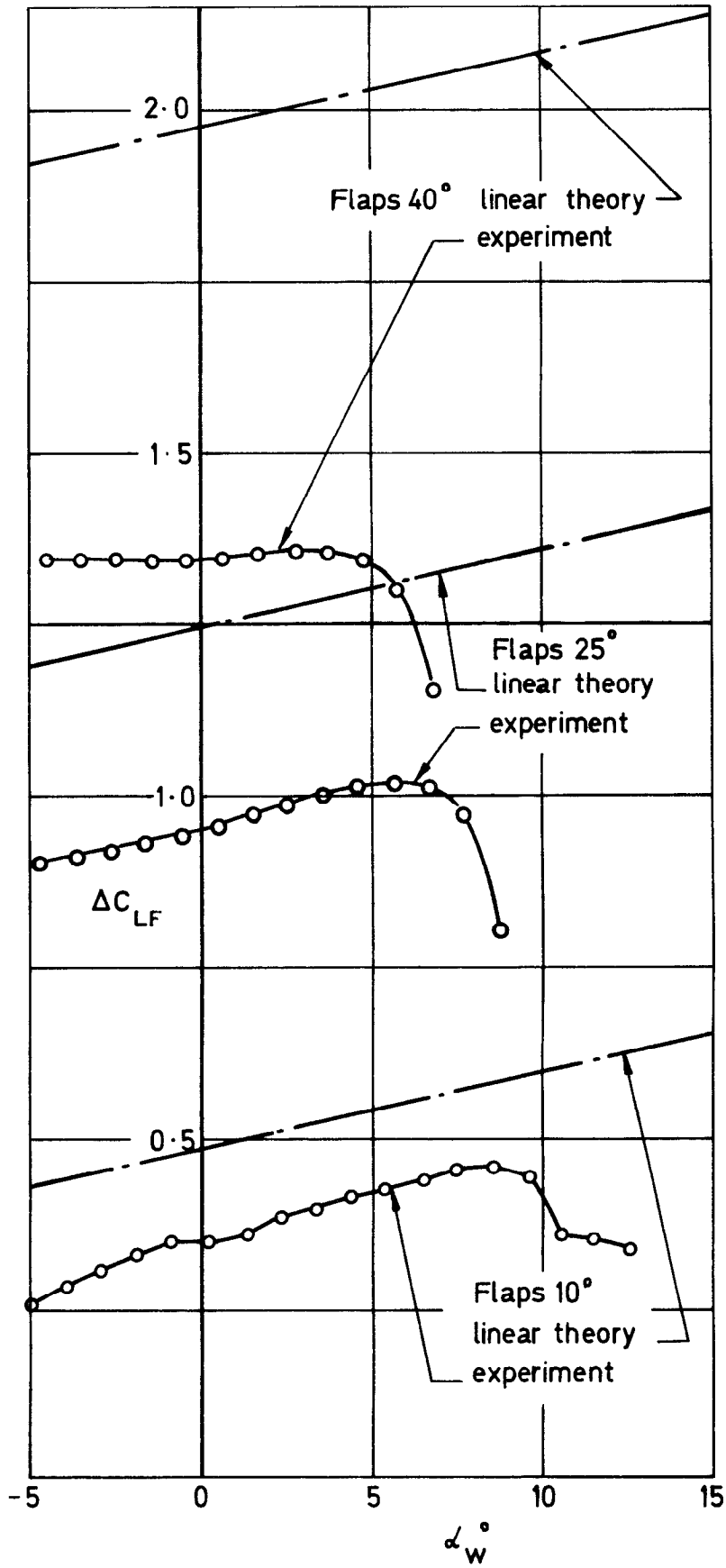

$$\Delta C_{LF} = C_{L\,\text{full-span flap}} - C_{L\,\text{no flap}}$$

Fig.59 Lift increments for full-span flaps. Basic wing+body, slats retracted

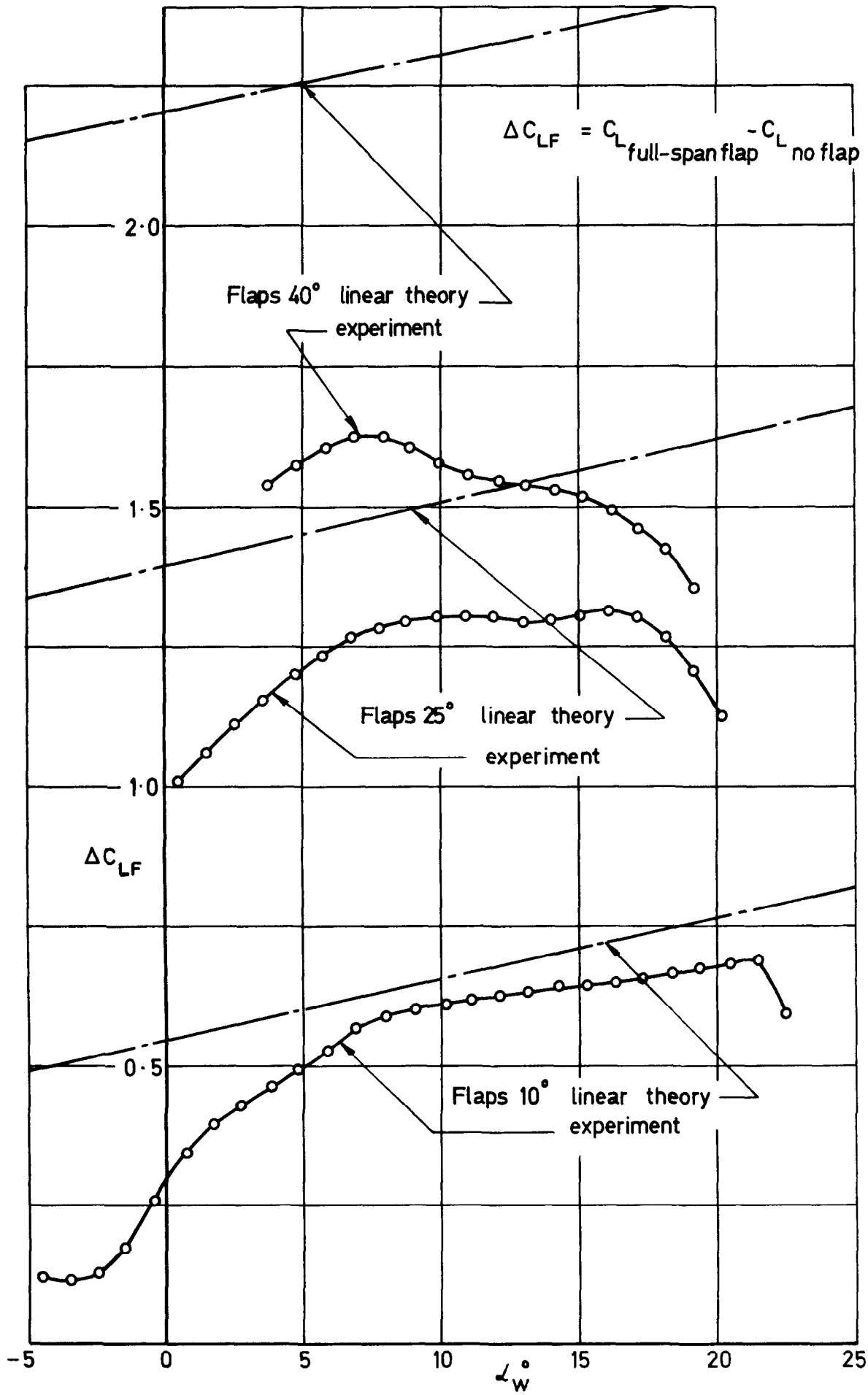

Fig.60 Lift increments for full-span flaps.
Basic wing with slats deflected 25°

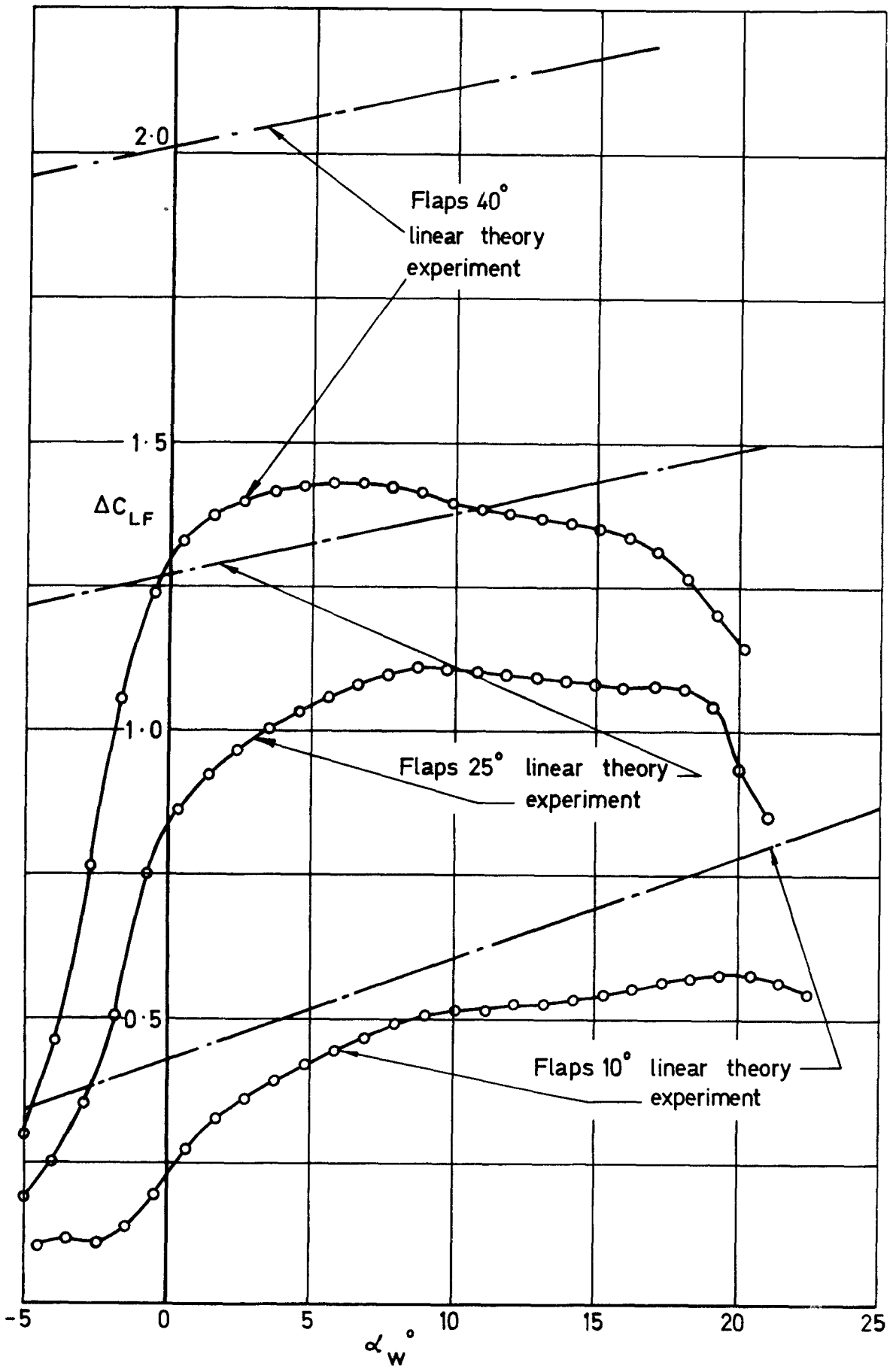

$\Delta C_{LF} = C_{L\,\text{full-span flap}} - C_{L\,\text{no flap}}$

Fig.61 Lift increments for full-span flaps.
Basic wing+body, slats deflected 25°

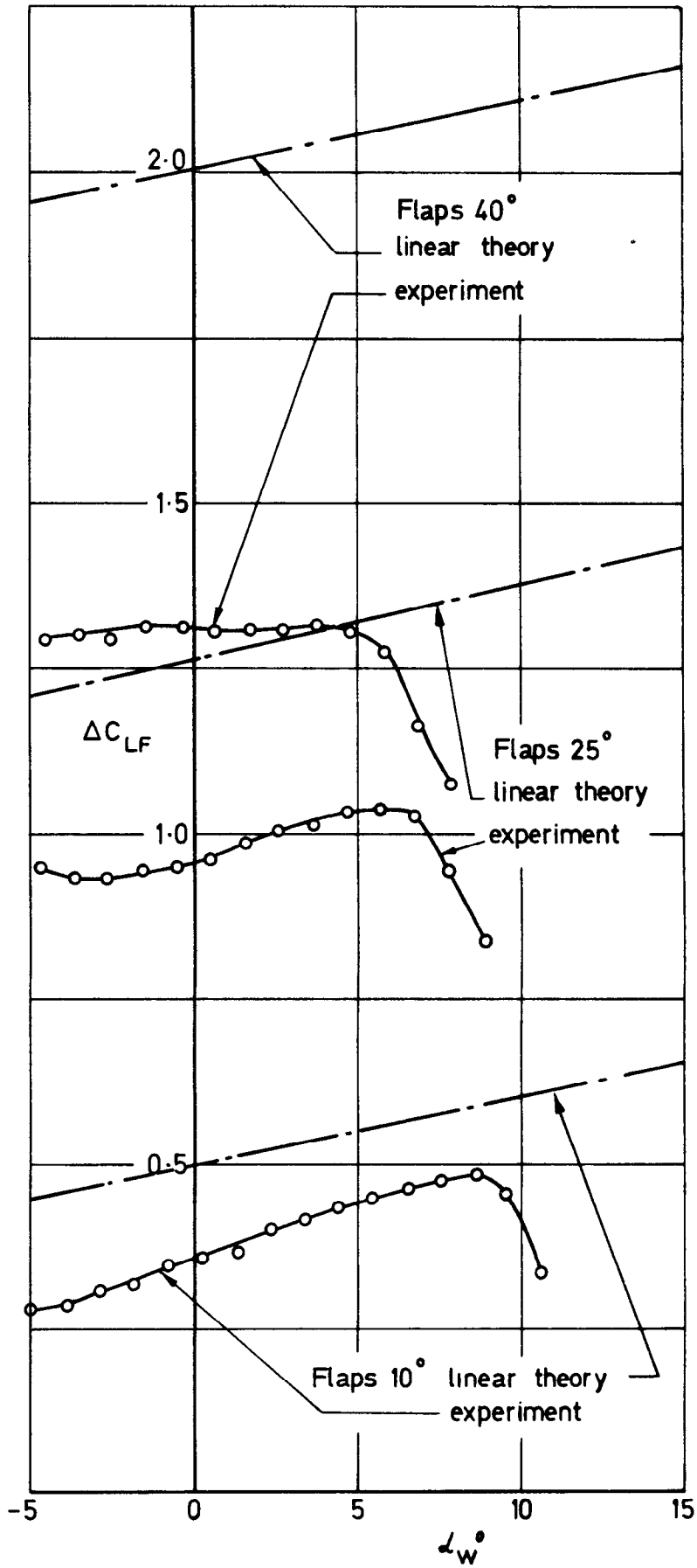

$$\Delta C_{LF} = C_{L\,\text{full-span flap}} - C_{L\,\text{no flap}}$$

Fig.62 Lift increments for full-span flaps. Extended wing + body, slats retracted

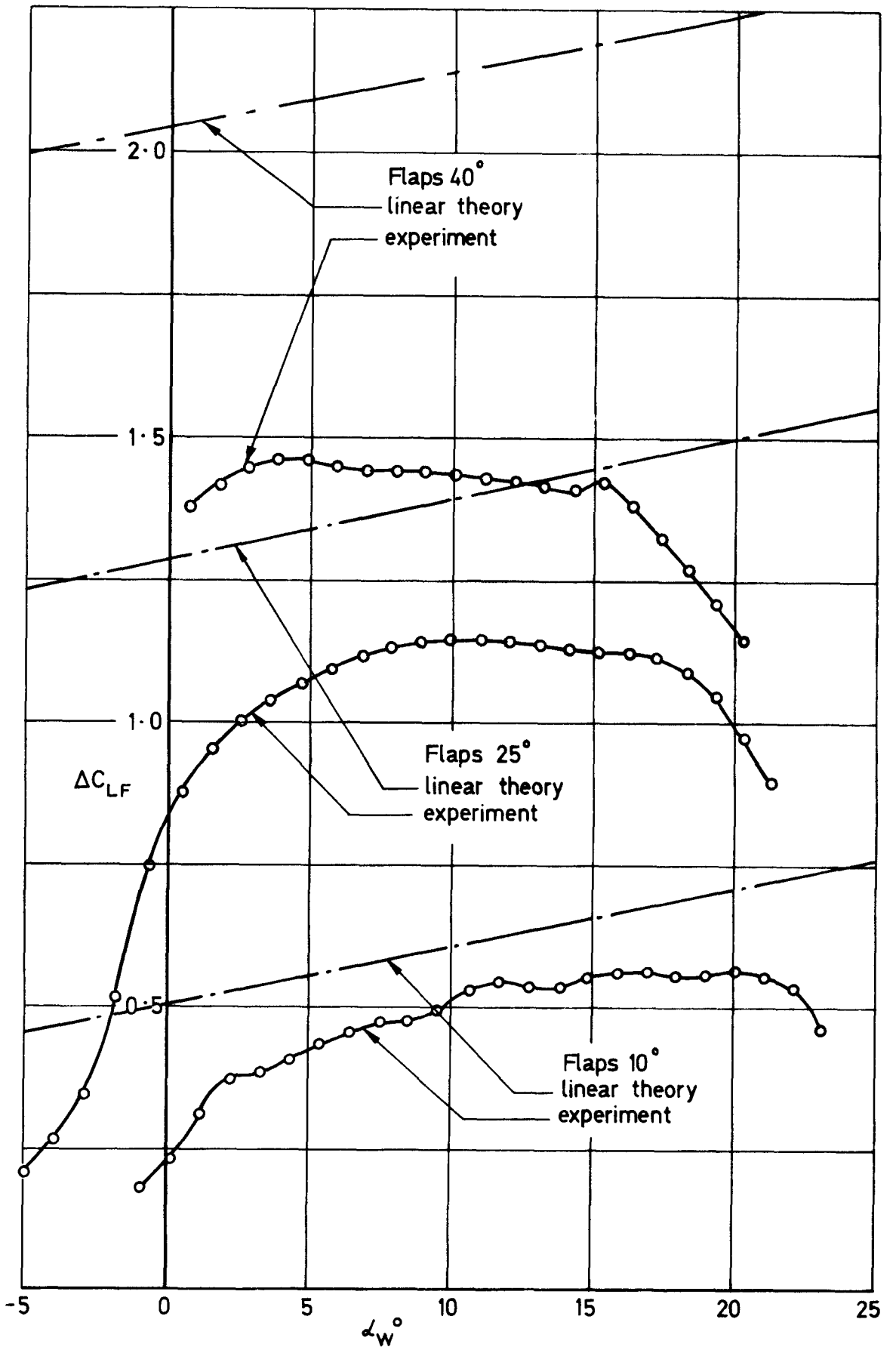

$$\Delta C_{LF} = C_{L\,\text{full-span flap}} - C_{L\,\text{no flap}}$$

Fig.63 Lift increments for full-span flaps. Extended wing + body, slats deflected 25°

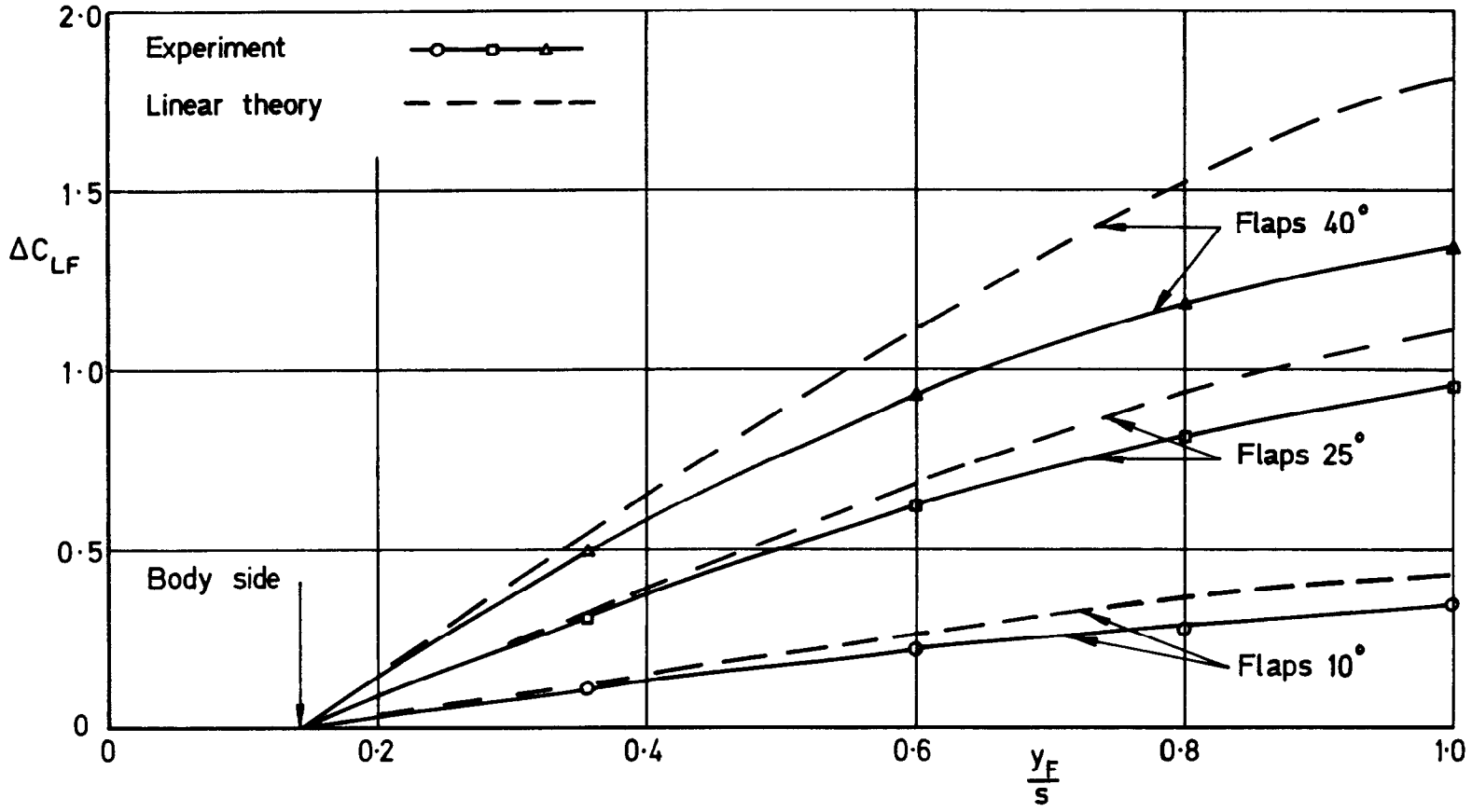

$$\Delta C_{LF} = C_{L\ \text{flap span } y_F} - C_{L\ \text{no flap}}$$

Fig. 64 Effect of flap span on flap lift increments.
Basic wing + body, slats retracted, $\alpha_W^\circ = 0$

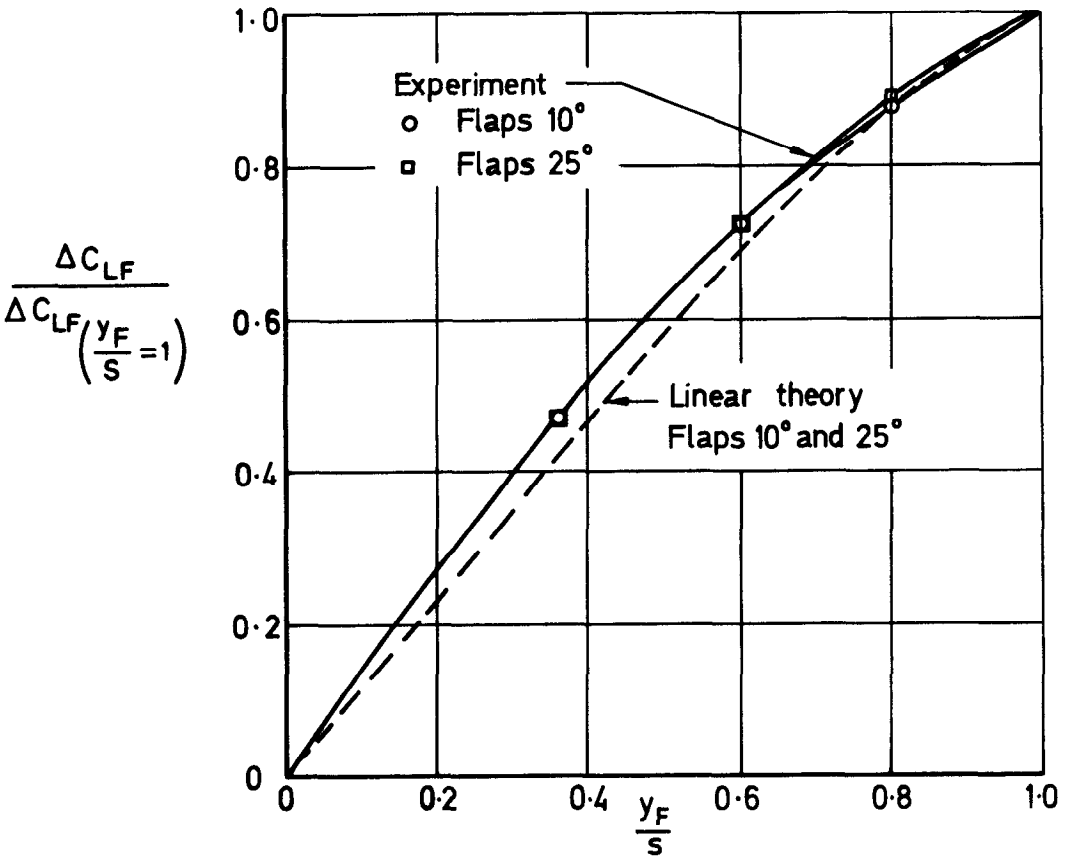

a Slats retracted

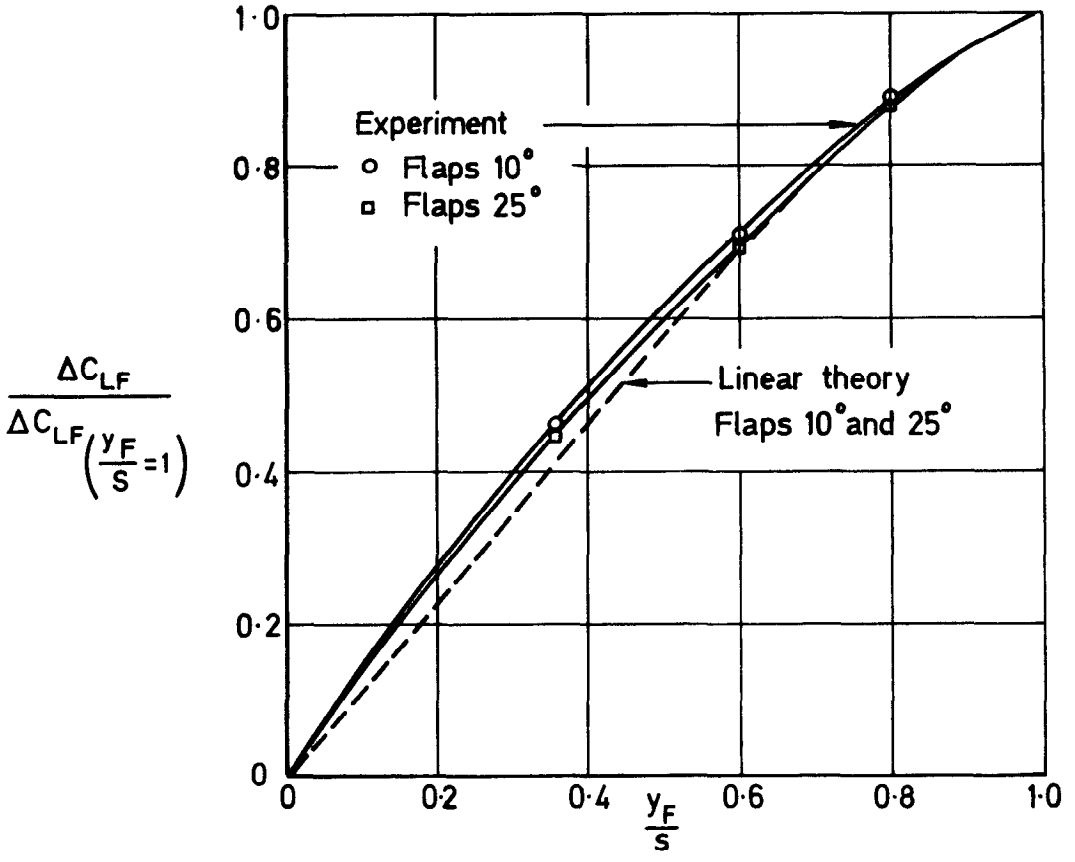

b Slats deflected 25°

Fig.65 a & b Part-span flap lift factors. Basic wing alone

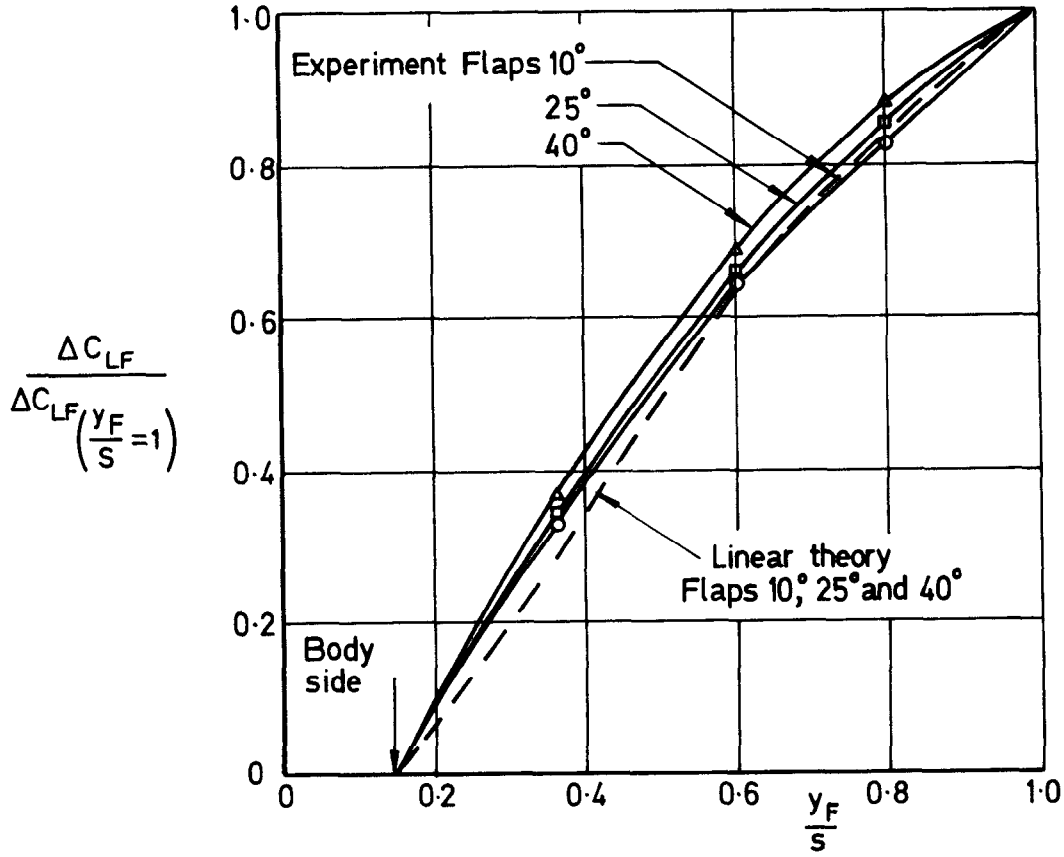

a Referred to gross wing

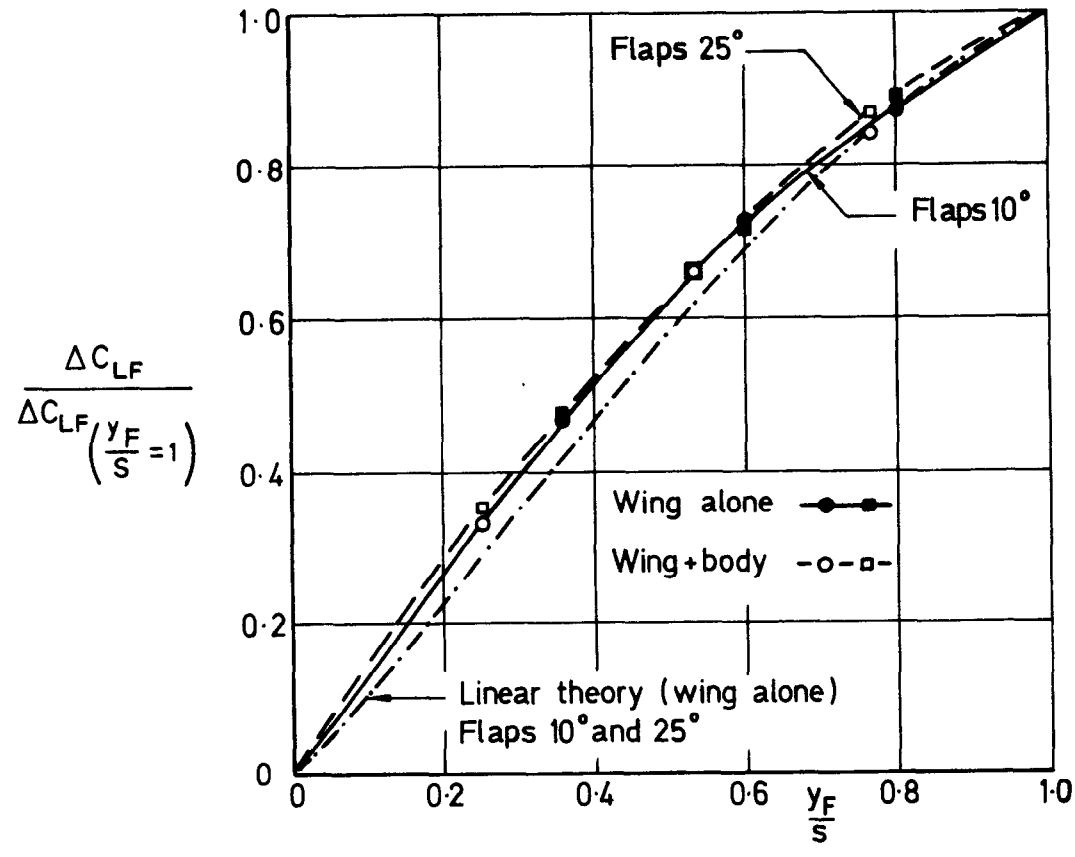

b Comparison of nett wing with wing alone

Fig.66 a & b Part-span flap lift factors.
Basic wing+body, slats retracted

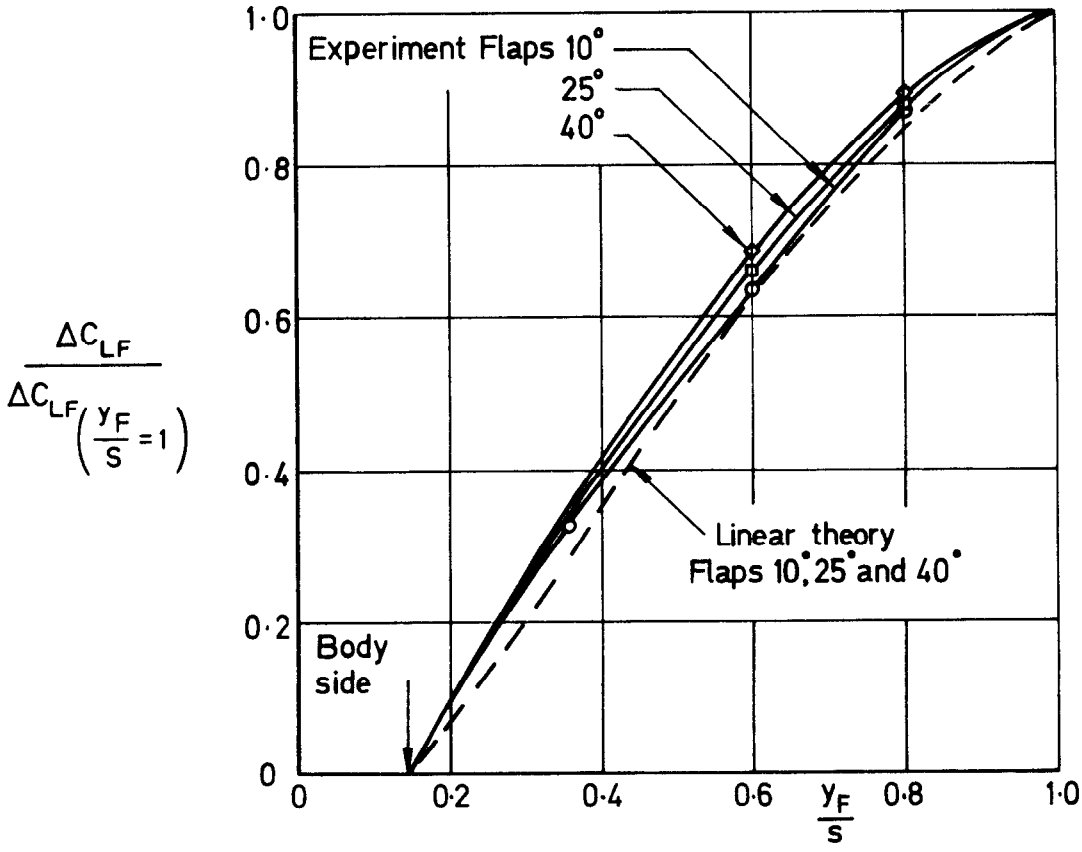

a Referred to gross wing

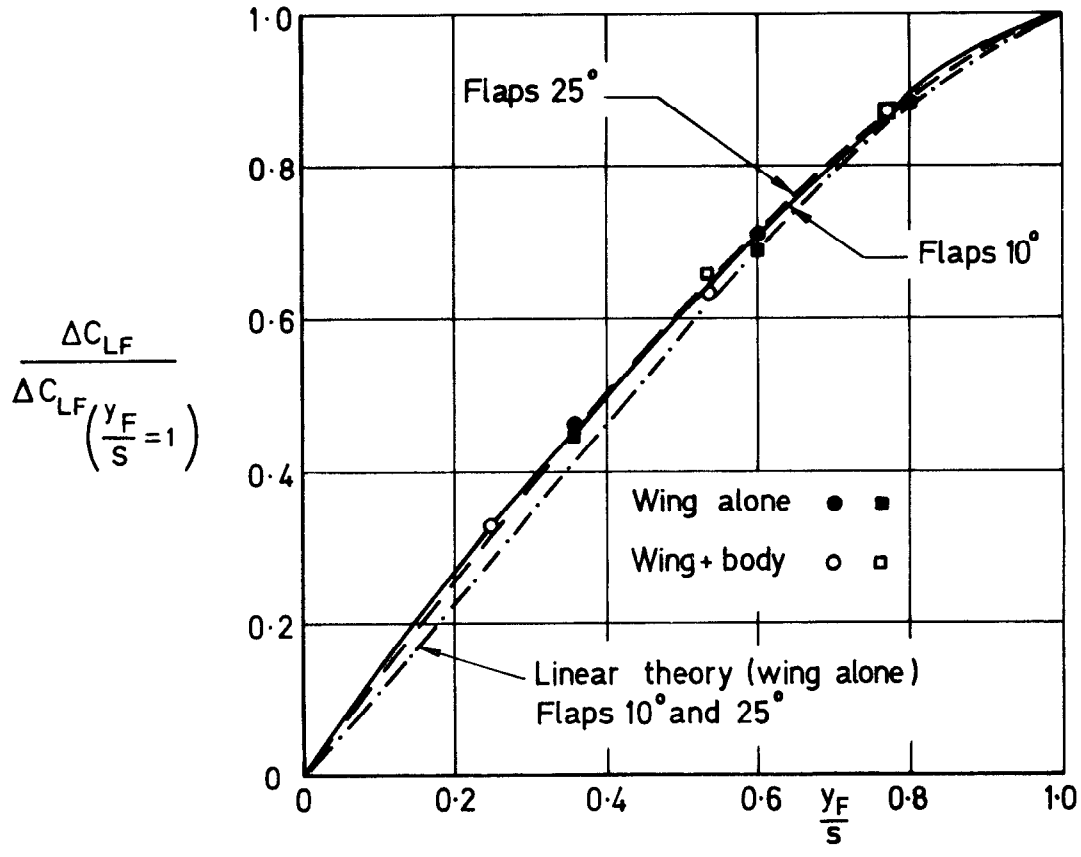

b Comparison of nett wing with wing alone

Fig. 67 a & b Part-span flap lift factors.
Basic wing + body, slats deflected 25°

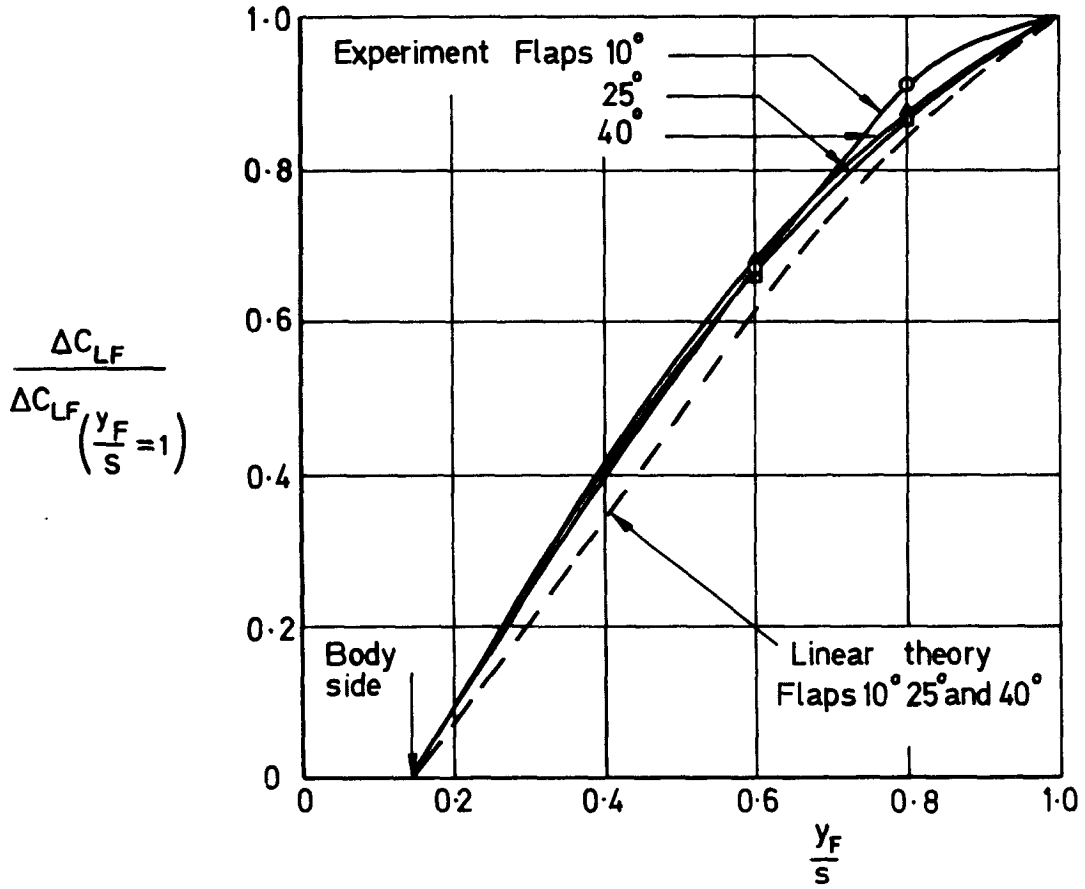

Fig.68 Part-span flap lift factors.
Extended wing+body. slats deflected 25°

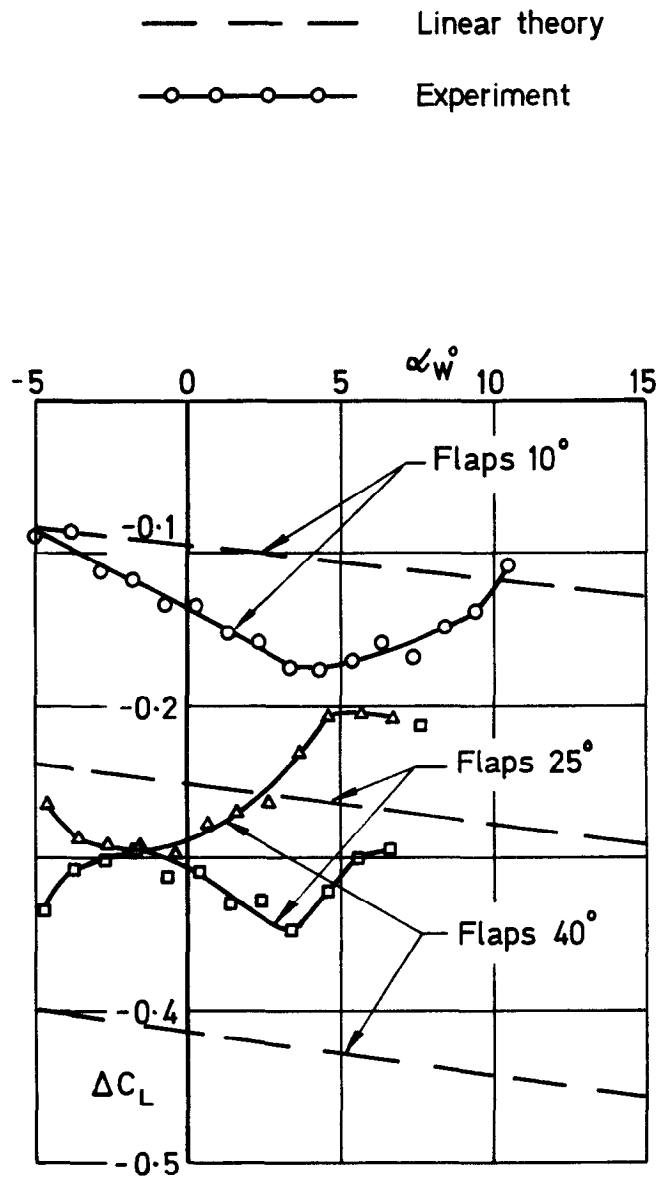

$$\Delta C_L = C_{L\,(\frac{y_F}{s}=1)\ \text{Body cutout}} - C_{L\,(\frac{y_F}{s}=1)}$$

Fig.69 Lift increments produced by a body cutout in the flap span. Basic wing, slats retracted, full-span flaps

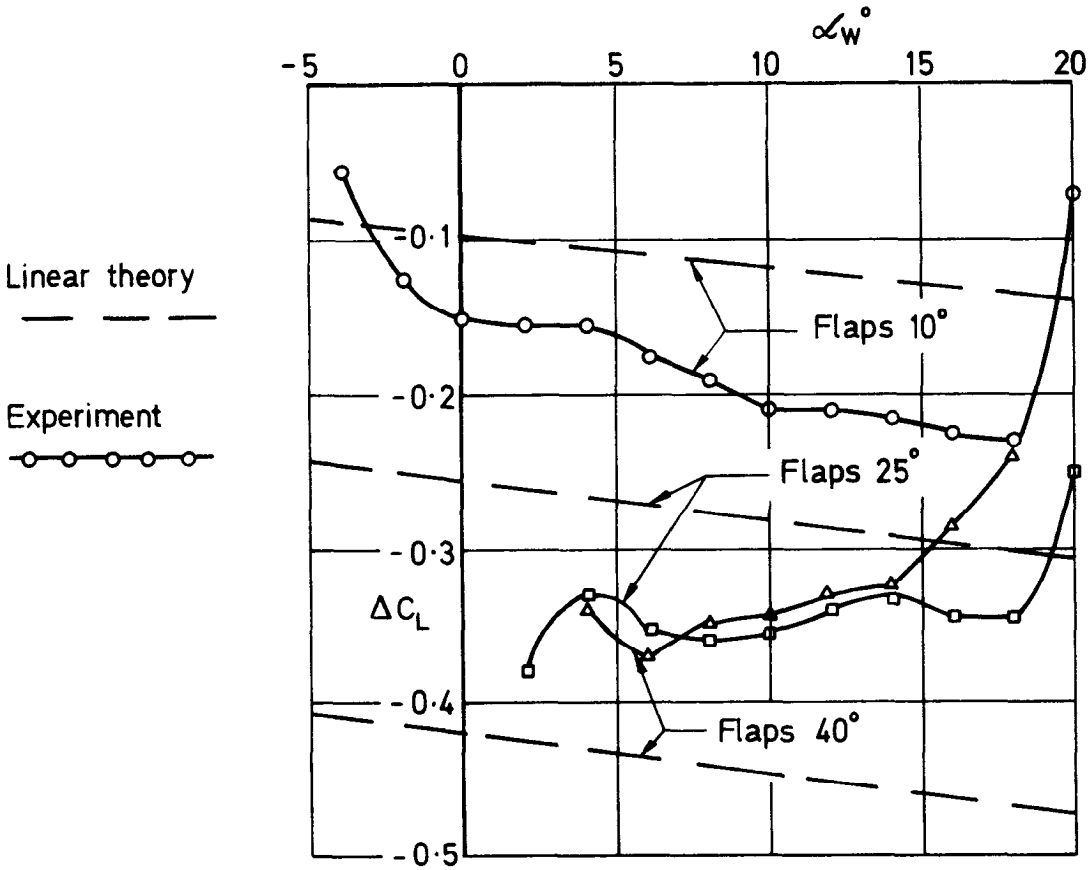

a Effect of flap deflection angle with full - span flaps

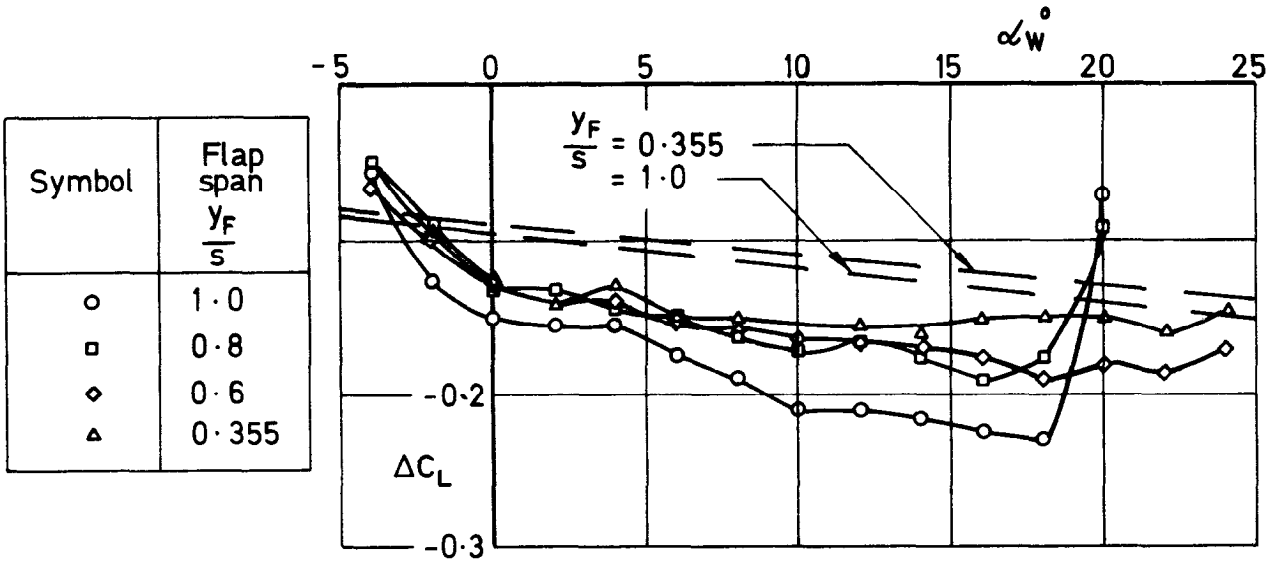

b Effect of flap span. Flaps deflected 10°

$$\Delta C_L = C_{L_{(\frac{y_F}{s})\text{ with cutout}}} - C_{L_{(\frac{y_F}{s})}}$$

Fig.70 a & b Lift increments produced by a body cutout in the flap span. Basic wing with slats deflected 25°

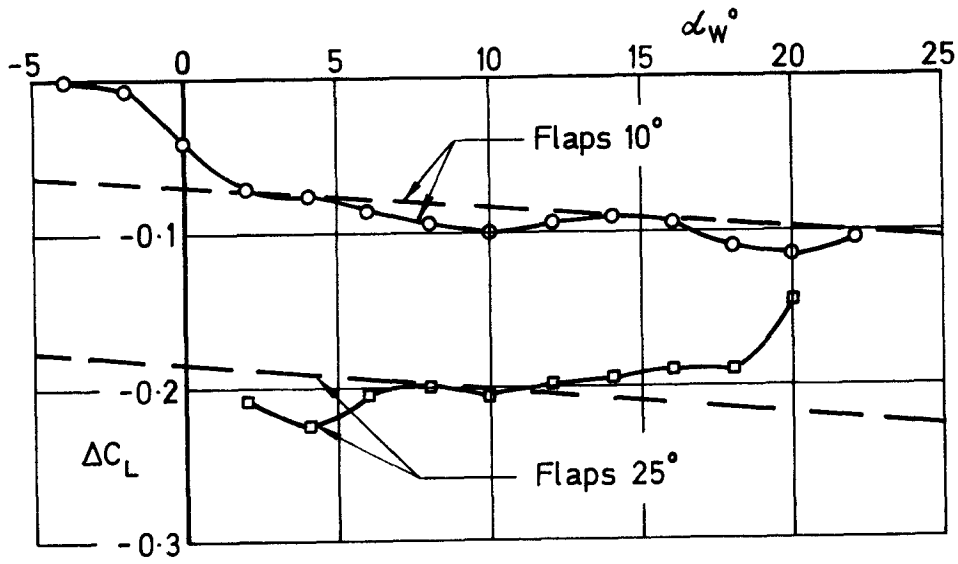

a Wing alone

Linear theory

Experiment

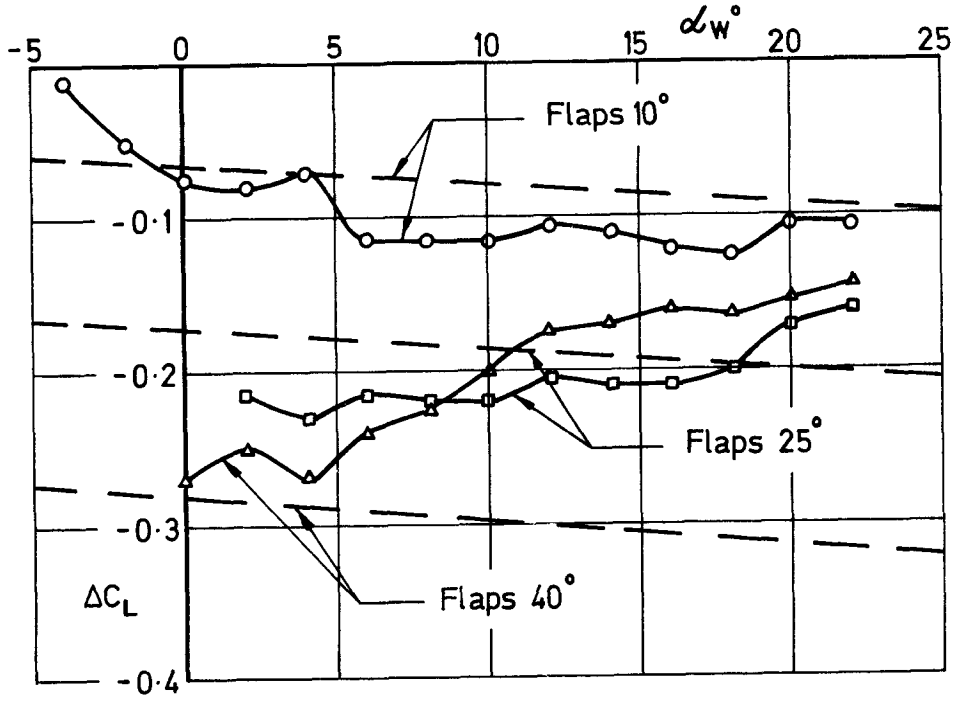

b Wing + body

$$\Delta C_L = C_L\left(\frac{y_F}{s} = 0{\cdot}8\right)^{\text{with cutout}} - C_L\left(\frac{y_F}{s} = 0{\cdot}8\right)$$

Fig.71 a & b Lift increments produced by a cutout in the flap span: $0{\cdot}257 < \frac{y}{s} < 0{\cdot}355$. Basic wing with slats deflected 25°

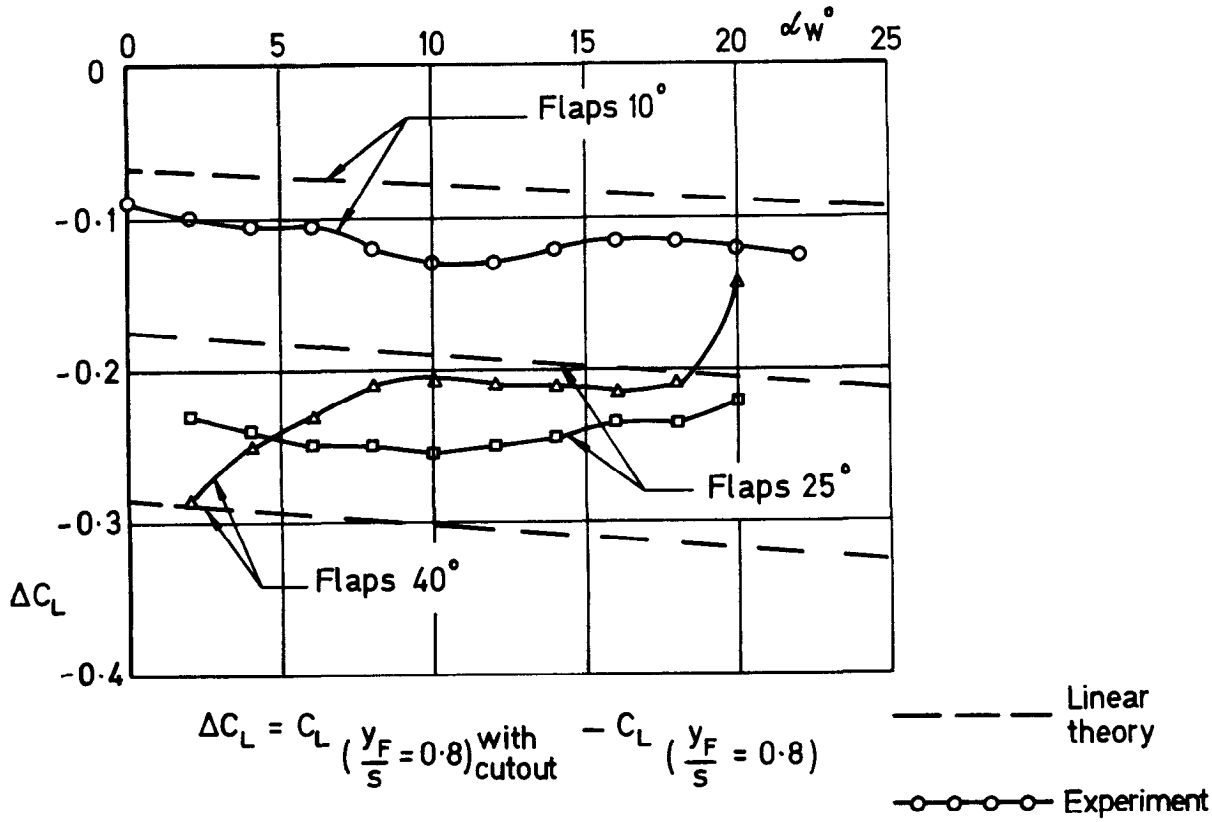

Fig. 72 Extended wing + body, slats deflected 25°
$0{\cdot}257 < y < 0{\cdot}355$ cutout in flaps

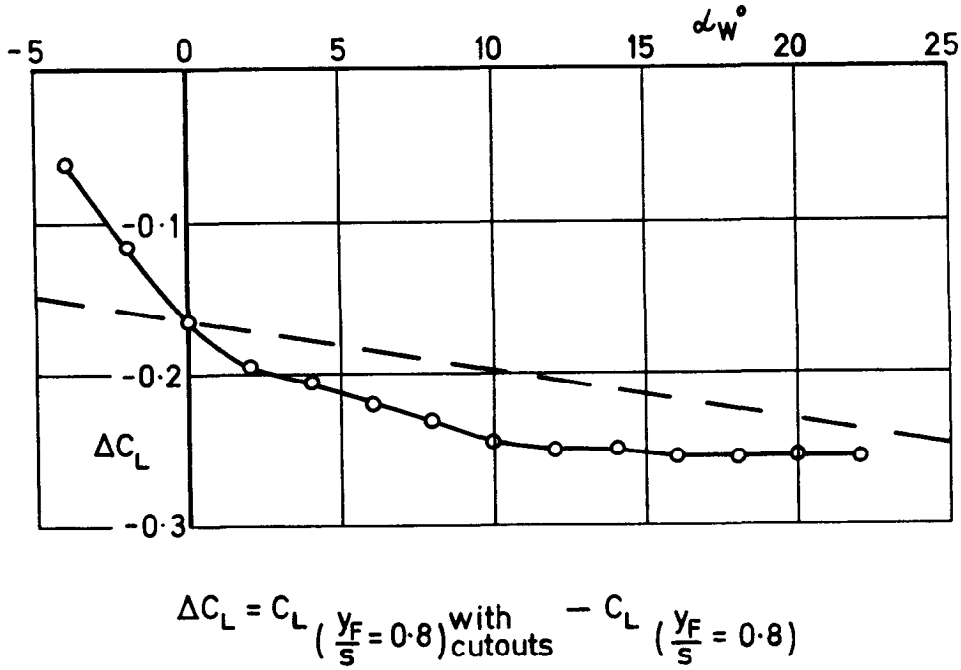

Fig. 73 Basic wing, slats deflected 25°, flaps deflected 10°
$0 < y < 0{\cdot}142$ and $0{\cdot}257 < y < 0{\cdot}355$ cutouts in flaps

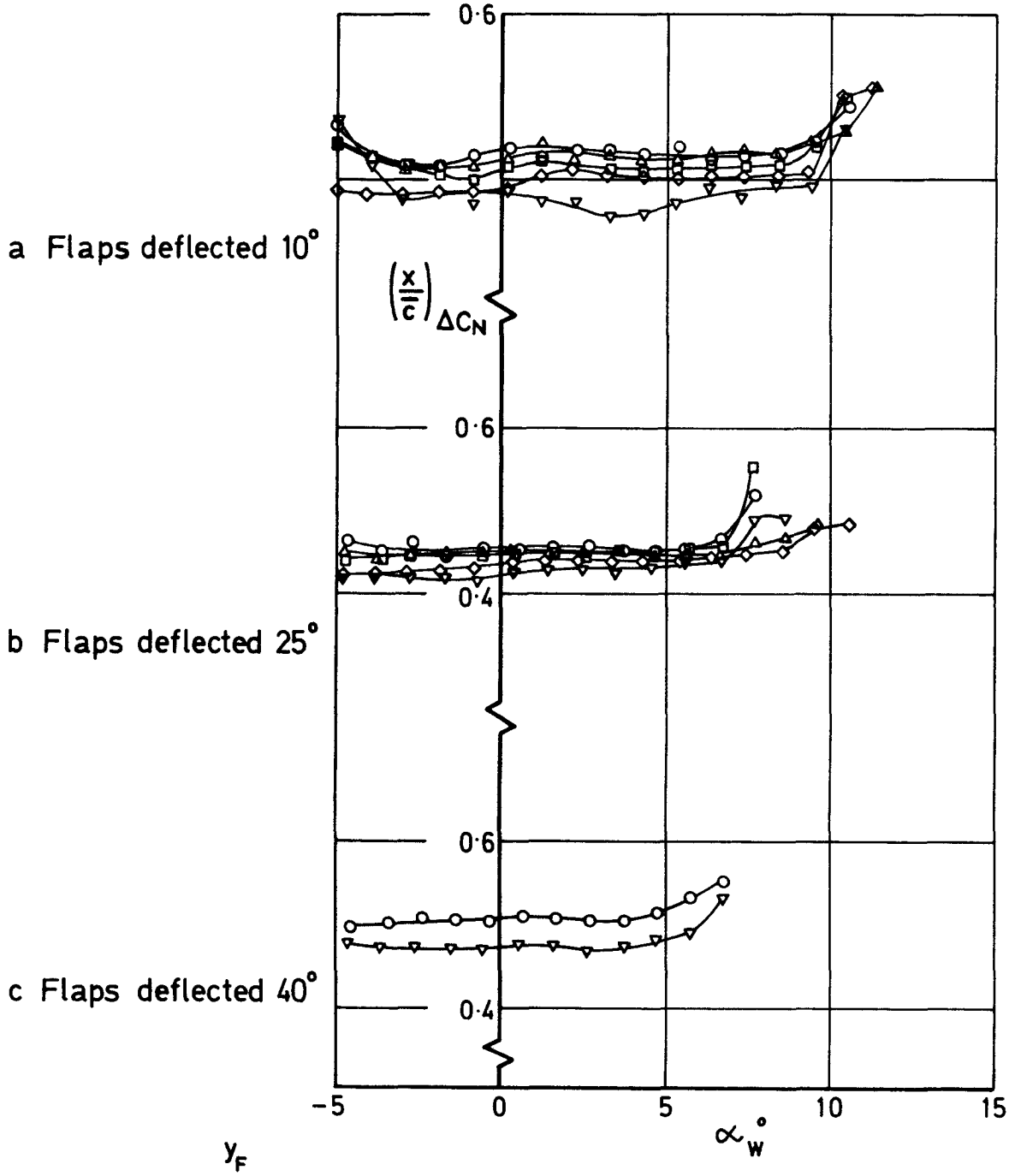

Flap span	$\frac{y_F}{s}$
○	1·0
□	0·8
△	0·6
◇	0·355
▽	1·0 Body cutout in flaps

$\left(\frac{x}{\bar{c}}\right)_{\Delta C_N}$ = Distance forward of the flap mean $\frac{1}{4}$ chord at which the flap load acts

Fig. 74 a - c Variation of the position of the load due to flap deflection with incidence.
Basic wing, slats retracted

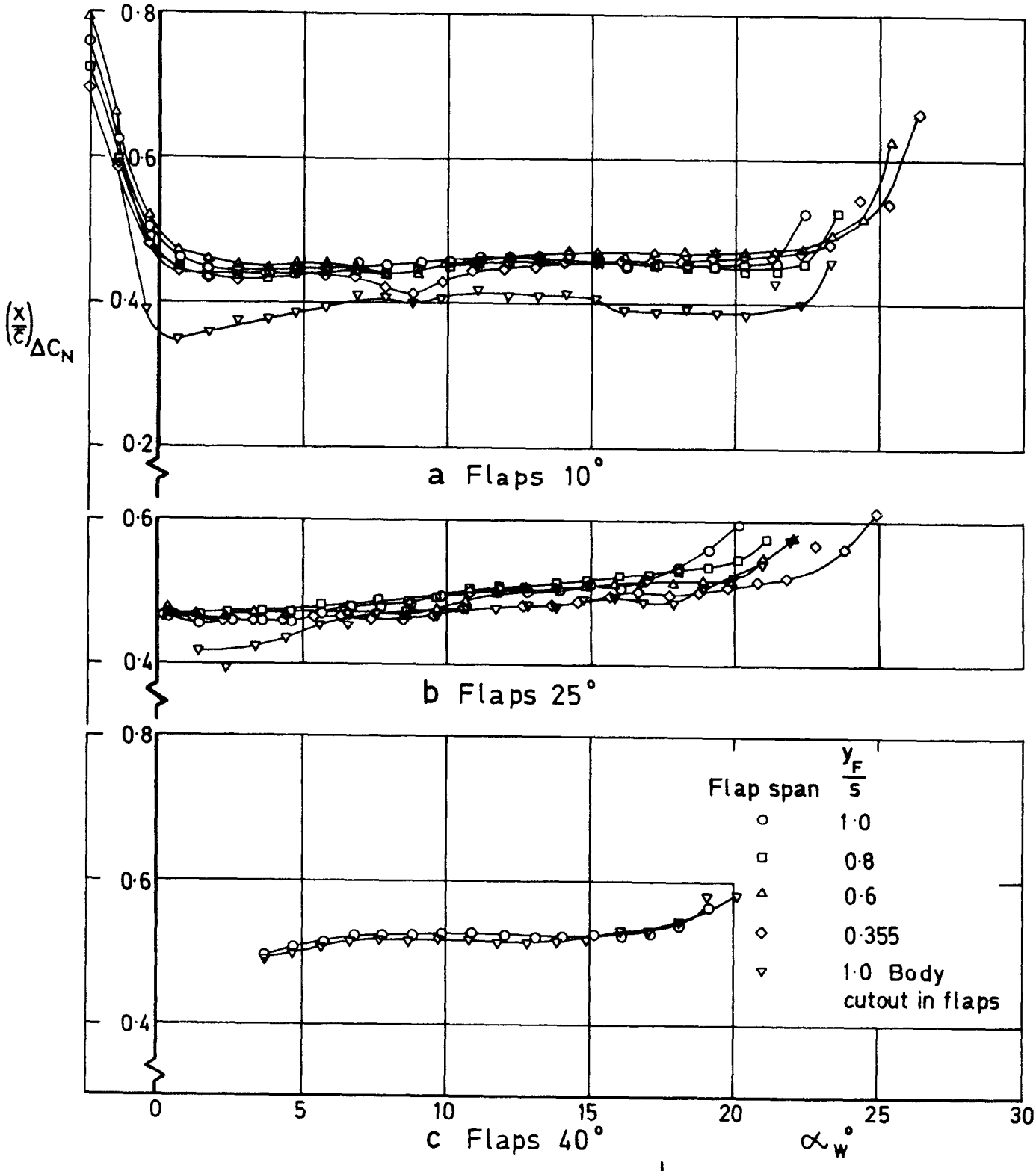

$\left(\frac{x}{\bar{c}}\right)_{\Delta C_N}$ = Distance forward of the flap mean $\frac{1}{4}$ chord at which the flap load acts

Fig. 75 a - c Variation of the position of the load due to flap deflection with incidence.
Basic wing, slats deflected 25°

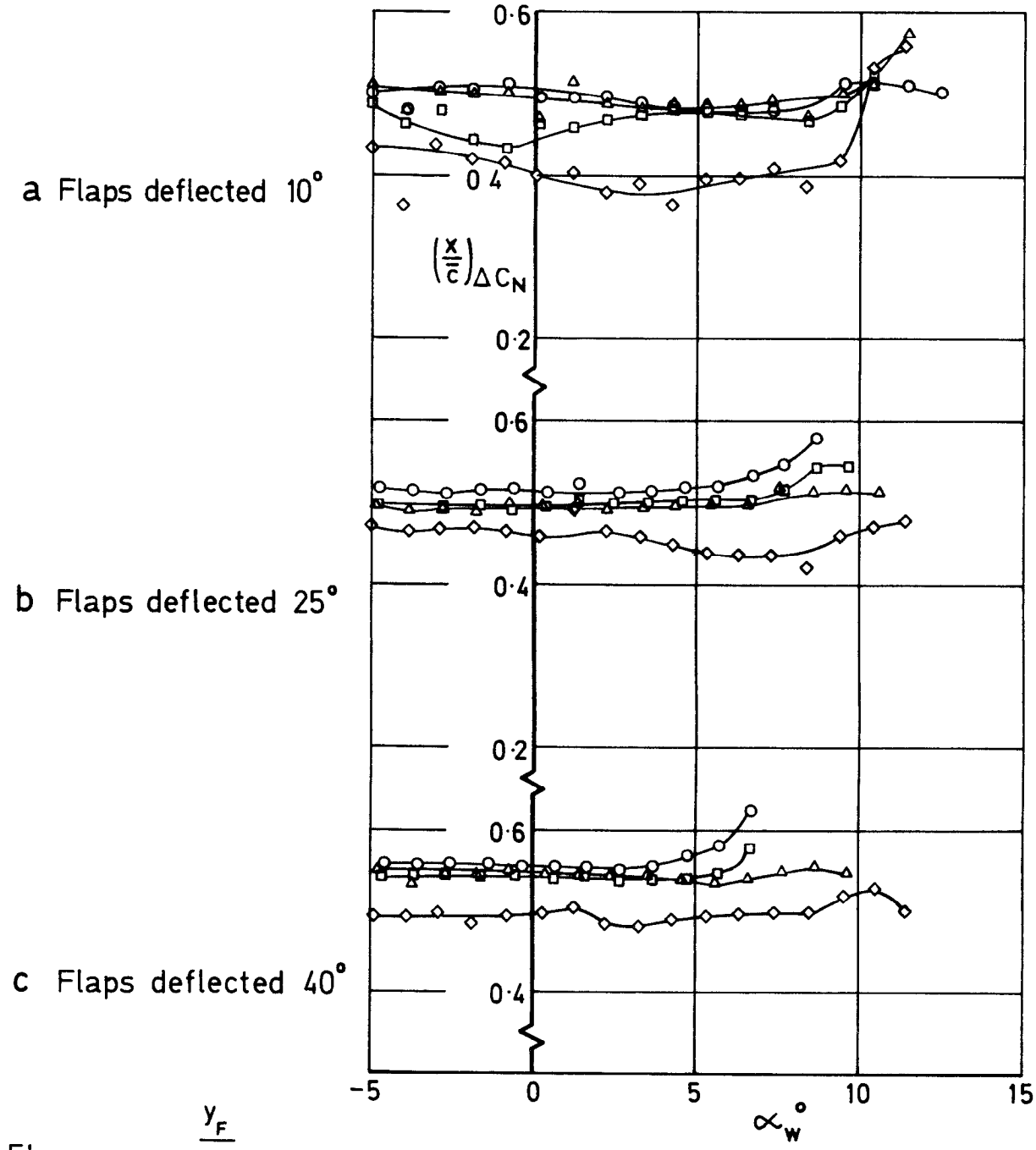

Fig.76 a - c Variation of the position of the load due to flap deflection with incidence.
Basic wing+body, slats retracted

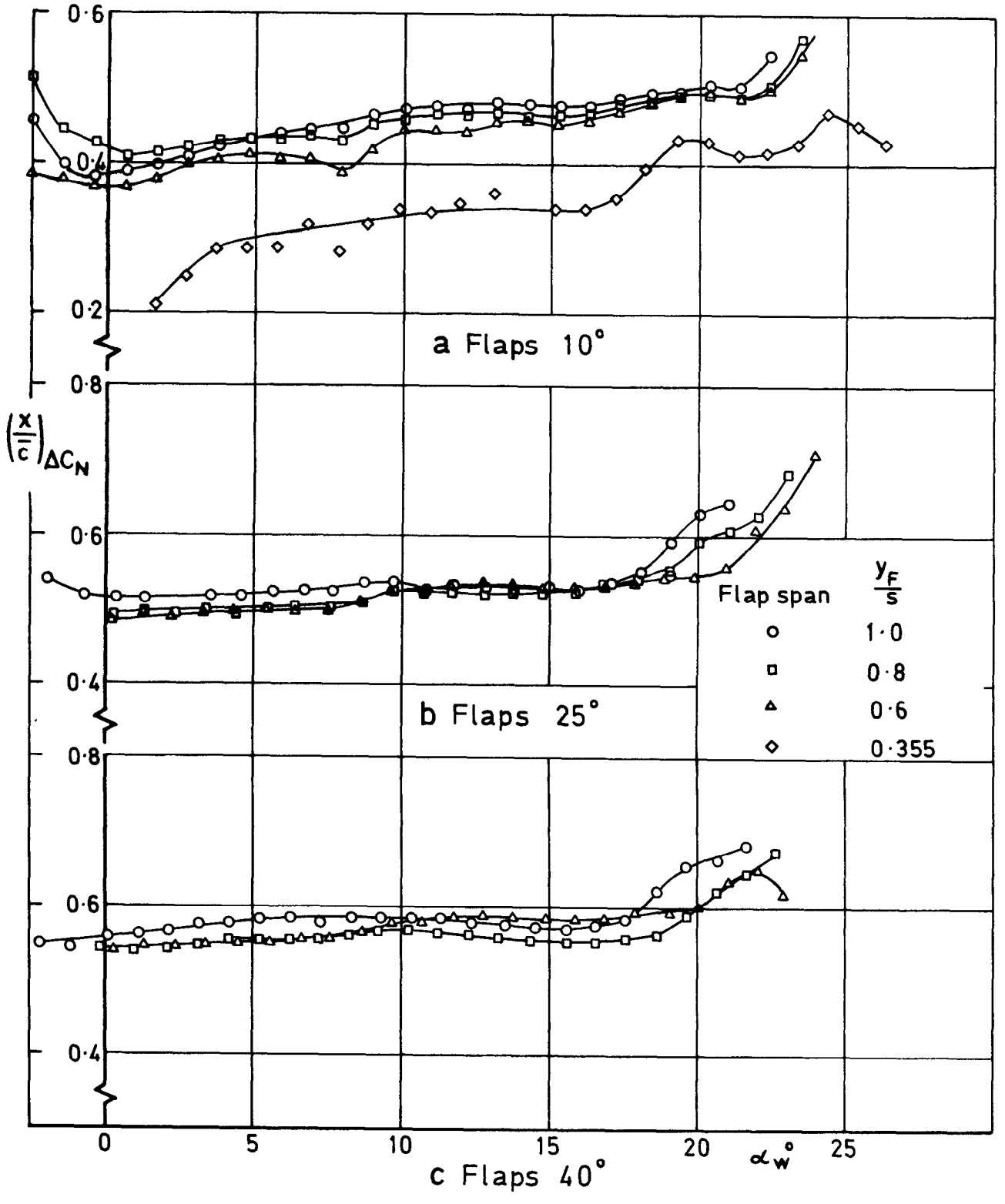

$\left(\frac{x}{c}\right)_{\Delta C_N}$ = Distance forward of the flap mean $\frac{1}{4}$ chord at which the flap load acts

Fig.77a - c Variation of the position of the load due to flap deflection with incidence.
Basic wing + body, slats deflected 25°

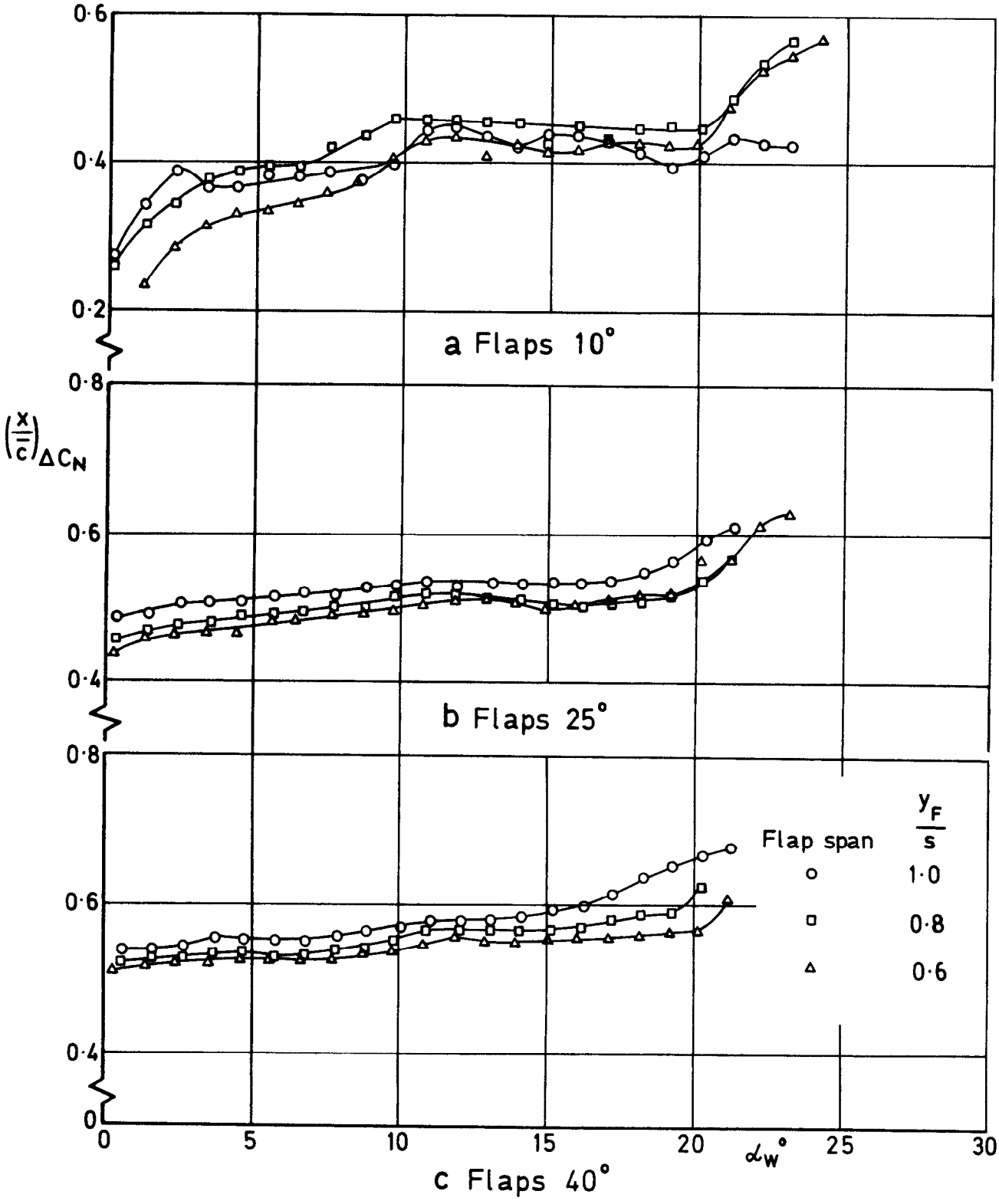

$\left(\frac{x}{c}\right)_{\Delta C_N}$ = Distance forward of the flap mean $\frac{1}{4}$ chord at which the flap load acts

Fig.78a - c Variation of the position of the load due to flap deflection with incidence.
Extended wing + body, slats deflected 25°

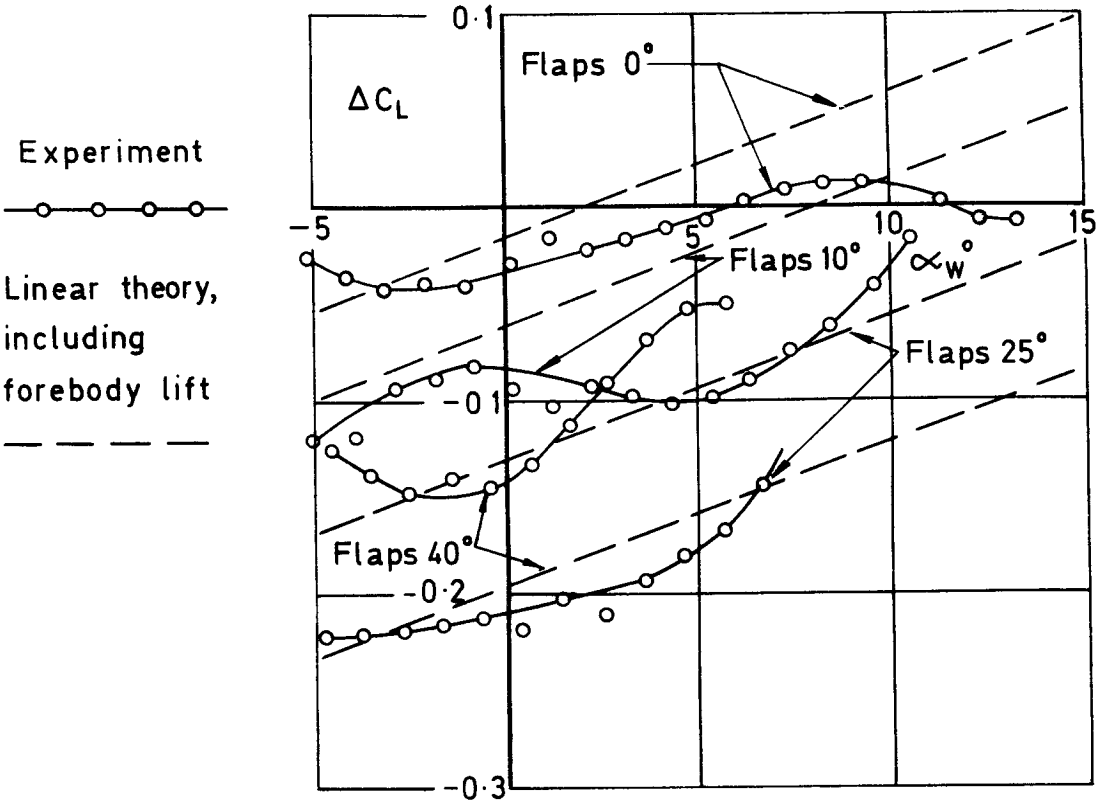

a Slats retracted

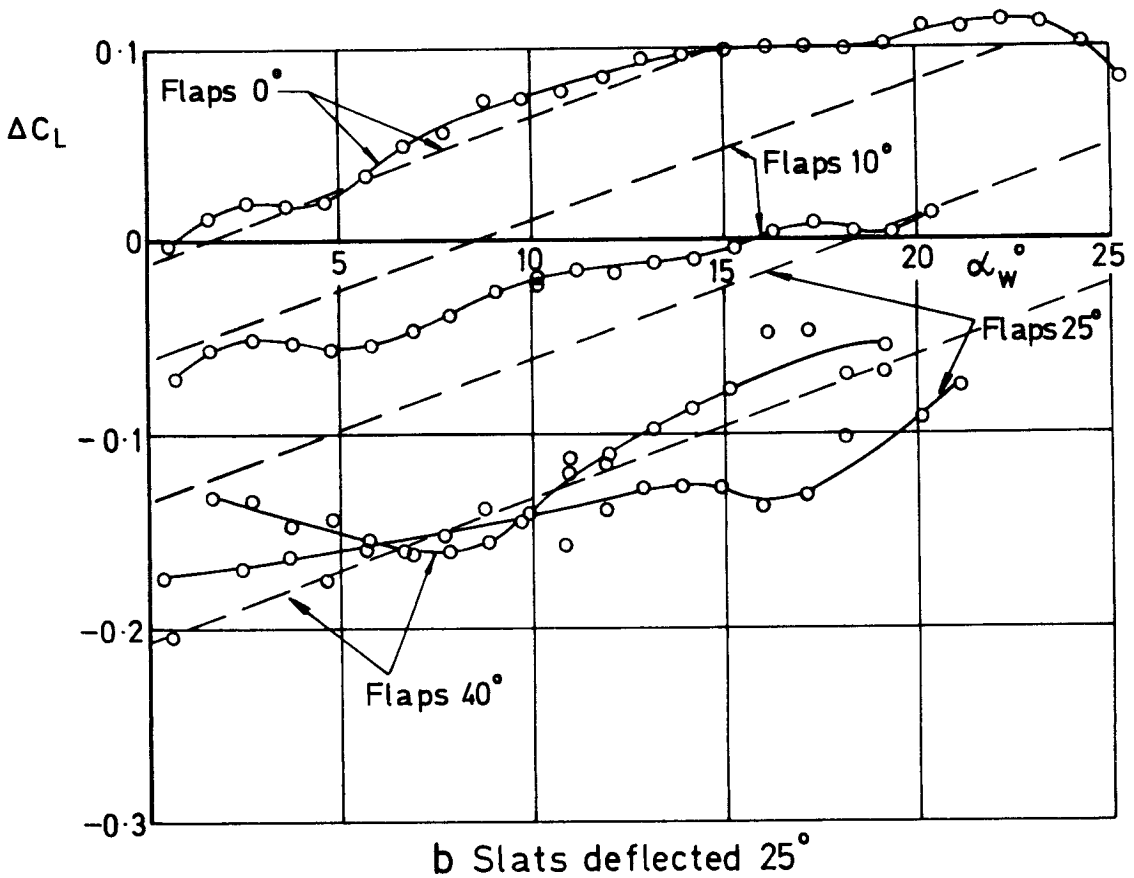

b Slats deflected 25°

$$\Delta C_L = C_{L_{\text{wing+body}}} - C_{L_{\text{wing alone}}}$$

Fig.79 a & b Effect of flap deflection angle on the variation with incidence of the lift increment due to the body. Basic wing planform

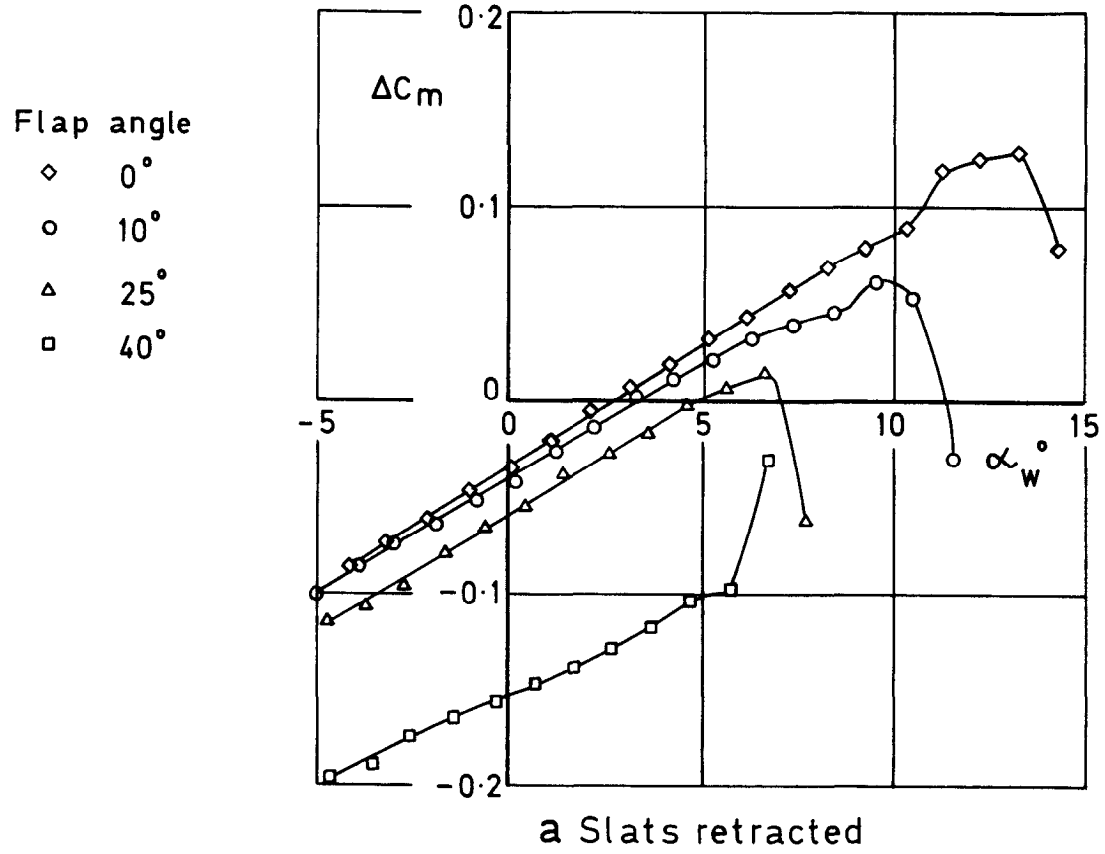

a Slats retracted

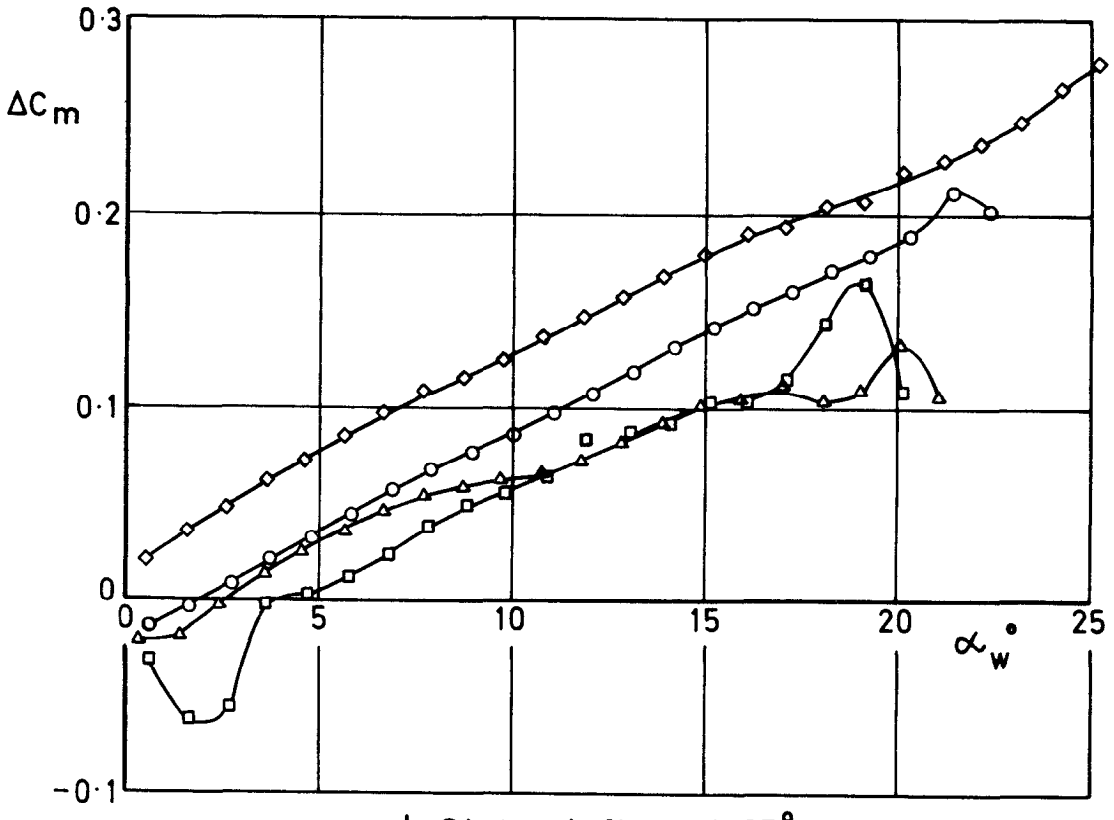

b Slats deflected 25°

$$\Delta C_m = C_{m\,\text{wing + body}} - C_{m\,\text{wing alone}}$$

Fig. 80 a & b Effect of flap deflection angle on the variation with incidence of the pitching moment increment due to the body.
Basic wing planform

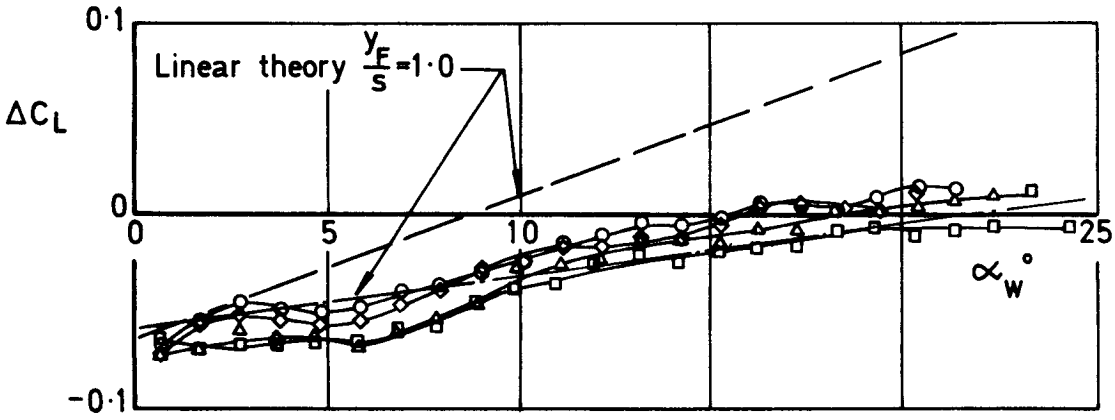

Fig.81 Effect of flap span on the lift increment due to the body. Basic wing, slats deflected 25°, flaps deflected 10°

Flap span	$\frac{y_F}{s}$
◇	1·0
○	0·8
△	0·6
□	0·355

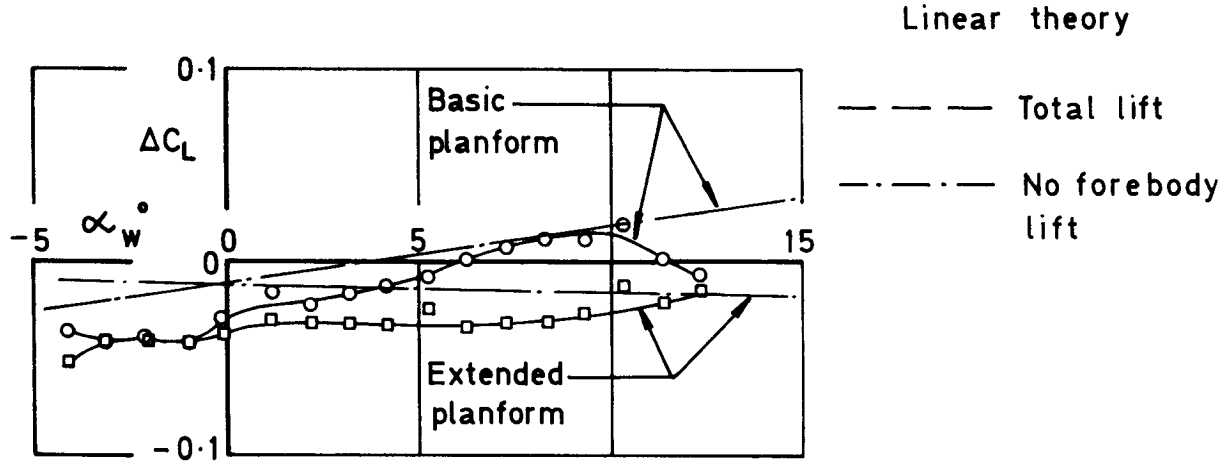

$$\Delta C_L = C_{L_{\text{wing + body}}} - C_{L_{\text{wing alone}}}$$

Fig.82 Effect of planform on the lift increment due to the body. Slats and flaps retracted

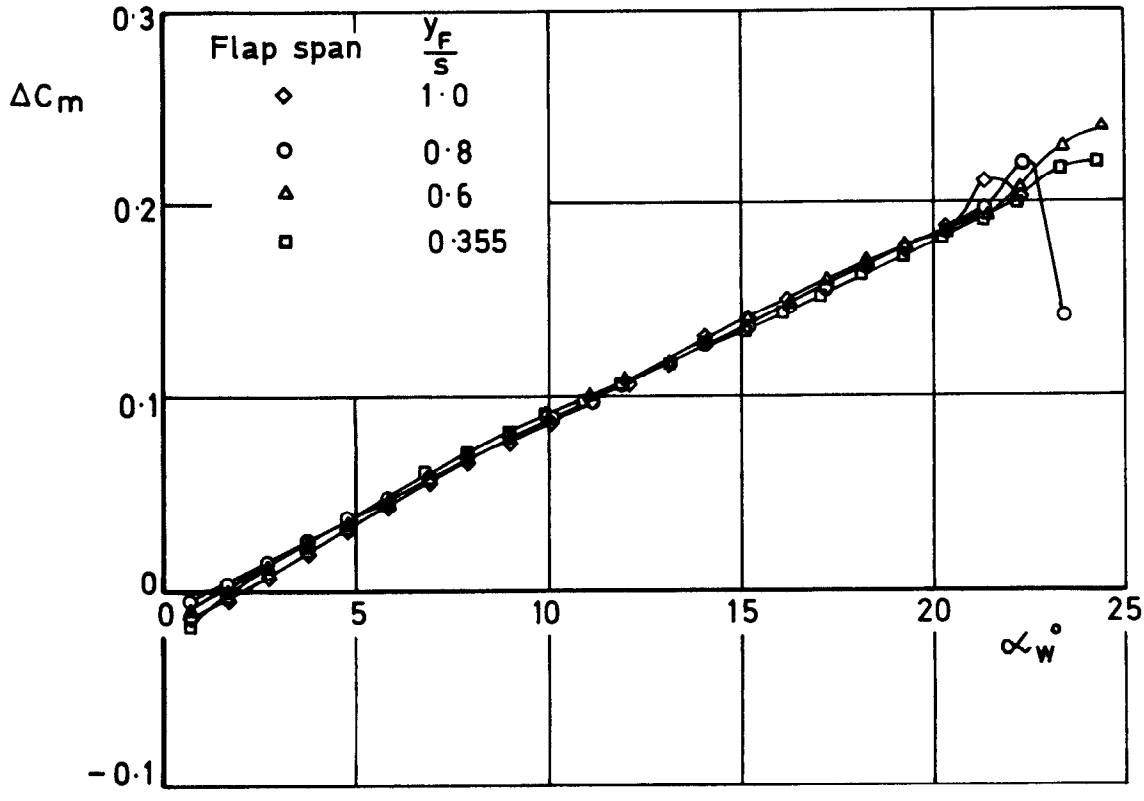

Fig.83 Effect of flap span on the pitching moment increment due to the body. Basic wing, slats deflected 25°, flaps deflected 10°

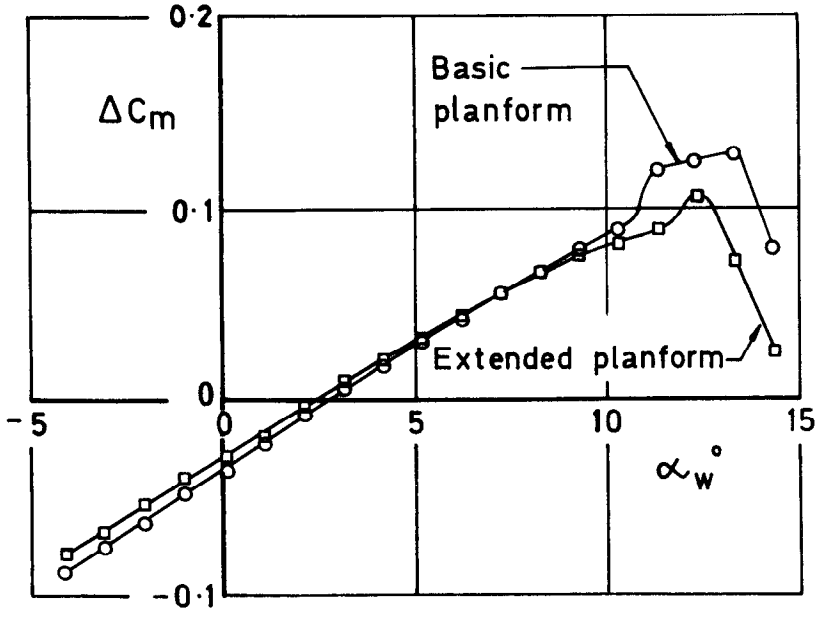

$$\Delta C_m = C_{m_{wing+body}} - C_{m_{wing\ alone}}$$

Fig.84 Effect of planform on the pitching moment increment due to the body. Slats and flaps retracted

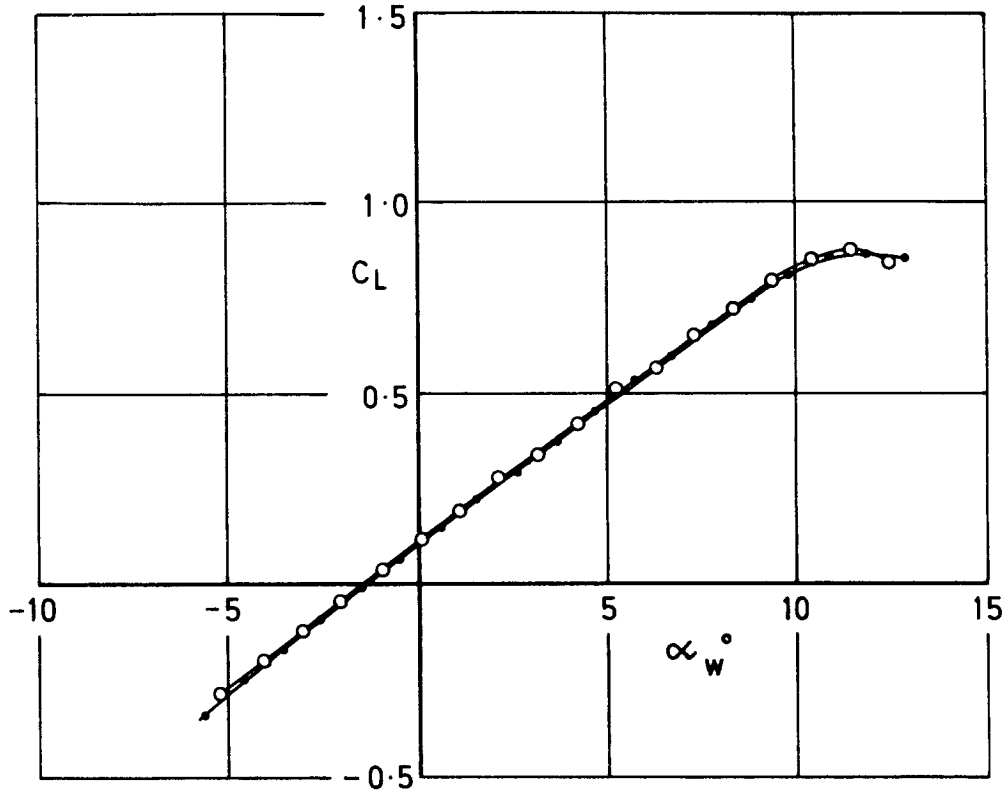

a C_L vs $\alpha_w°$

Basic planform

Extended planform

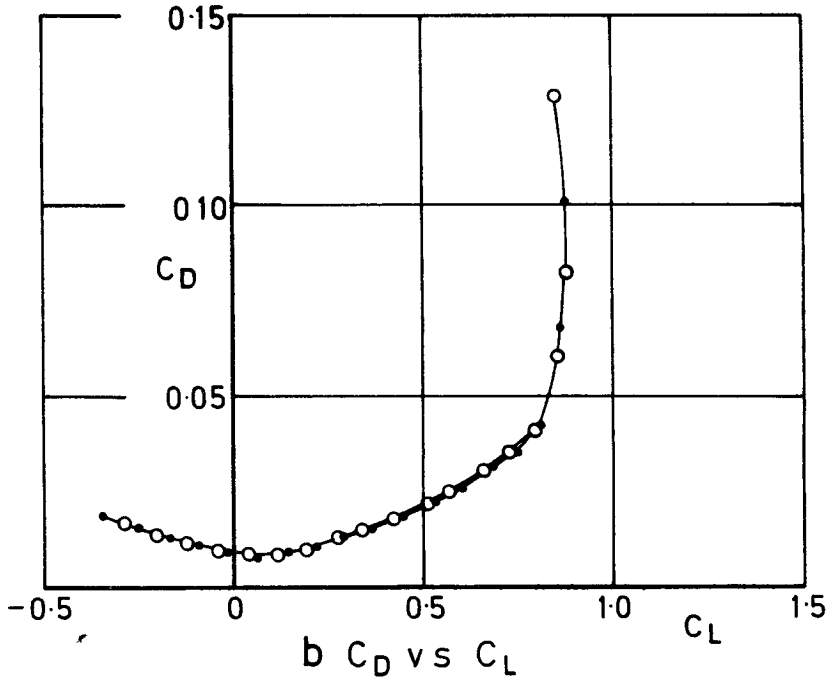

b C_D vs C_L

N B All coefficients are referred to the actual wing planform area

Fig.85 a & b Comparison of wing planforms.
Basic wing, slats and flaps retracted

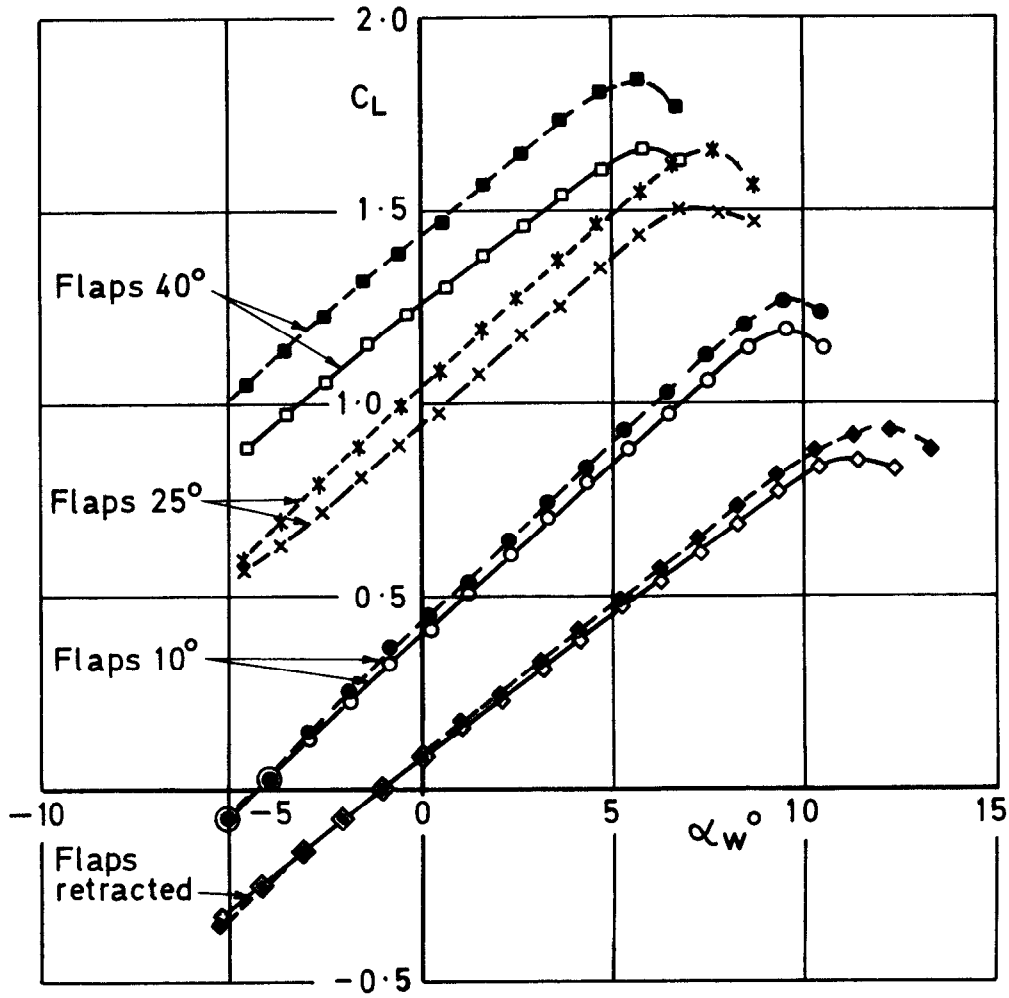

– – – – – – Basic planform

——————— Extended planform

NB All coefficients are referred to the actual wing planform area

Fig. 86 Comparison of planforms, wing + body
Slats retracted C_L vs $\alpha_w°$

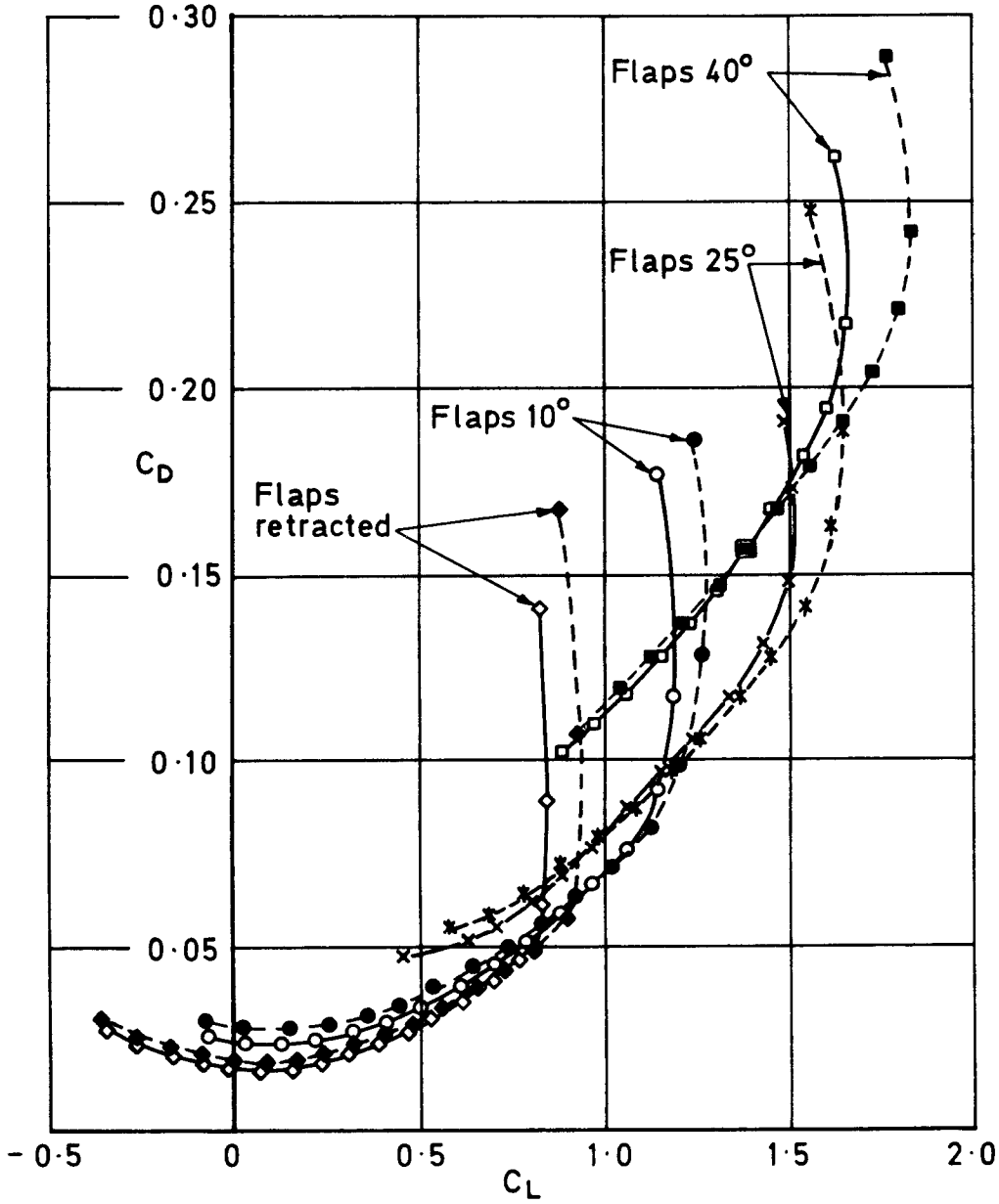

------ Basic planform

——— Extended planform

NB All coefficients are referred to the actual wing planform area

Fig.87 Comparison of planforms, wing + body.
Slats retracted, C_D vs C_L

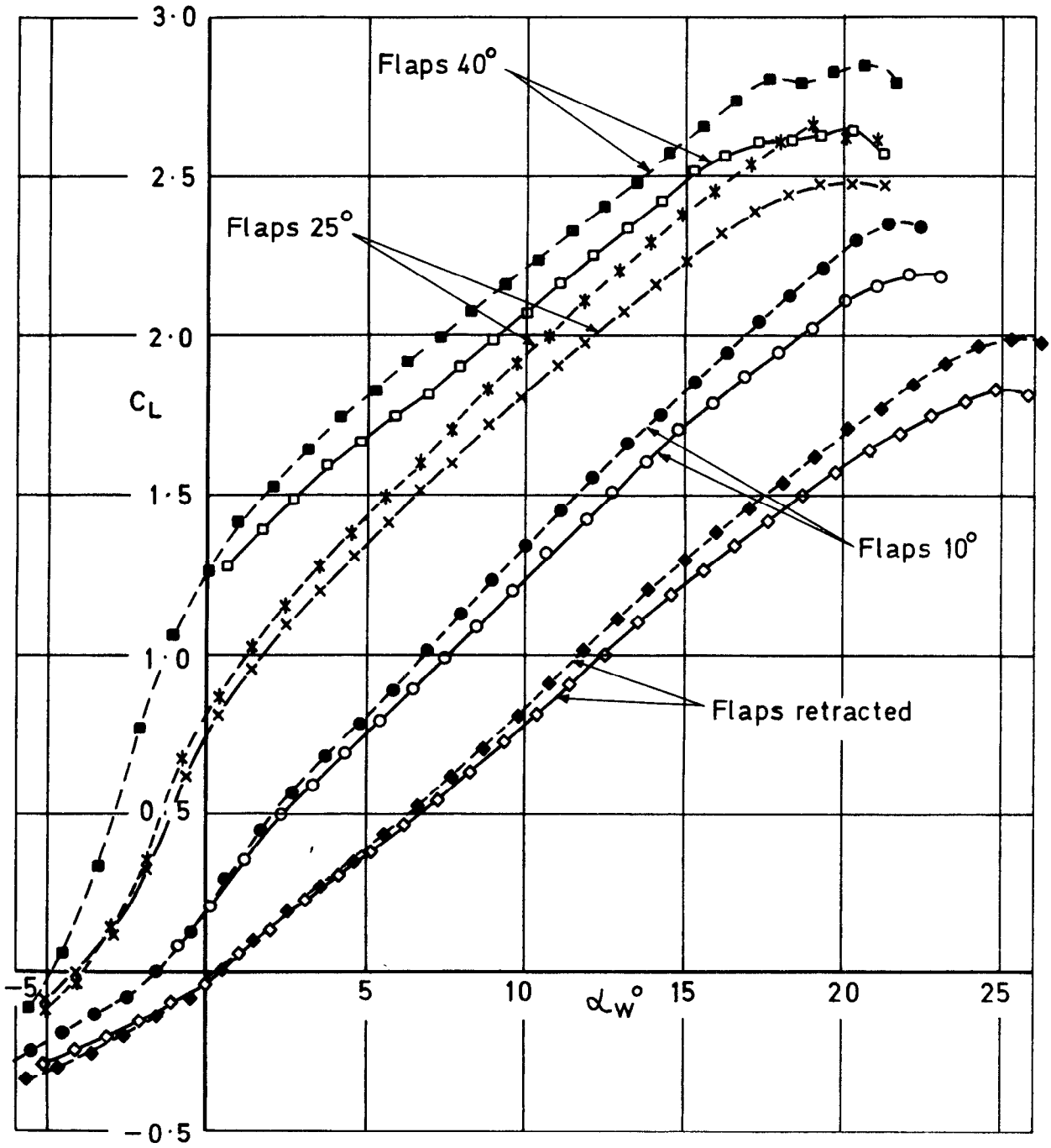

------ Basic planform

——— Extended planform

NB All coefficients are referred to the actual wing planform area

Fig. 88 Comparison of planforms, wing + body
Slats deflected 25°. C_L vs α_W°

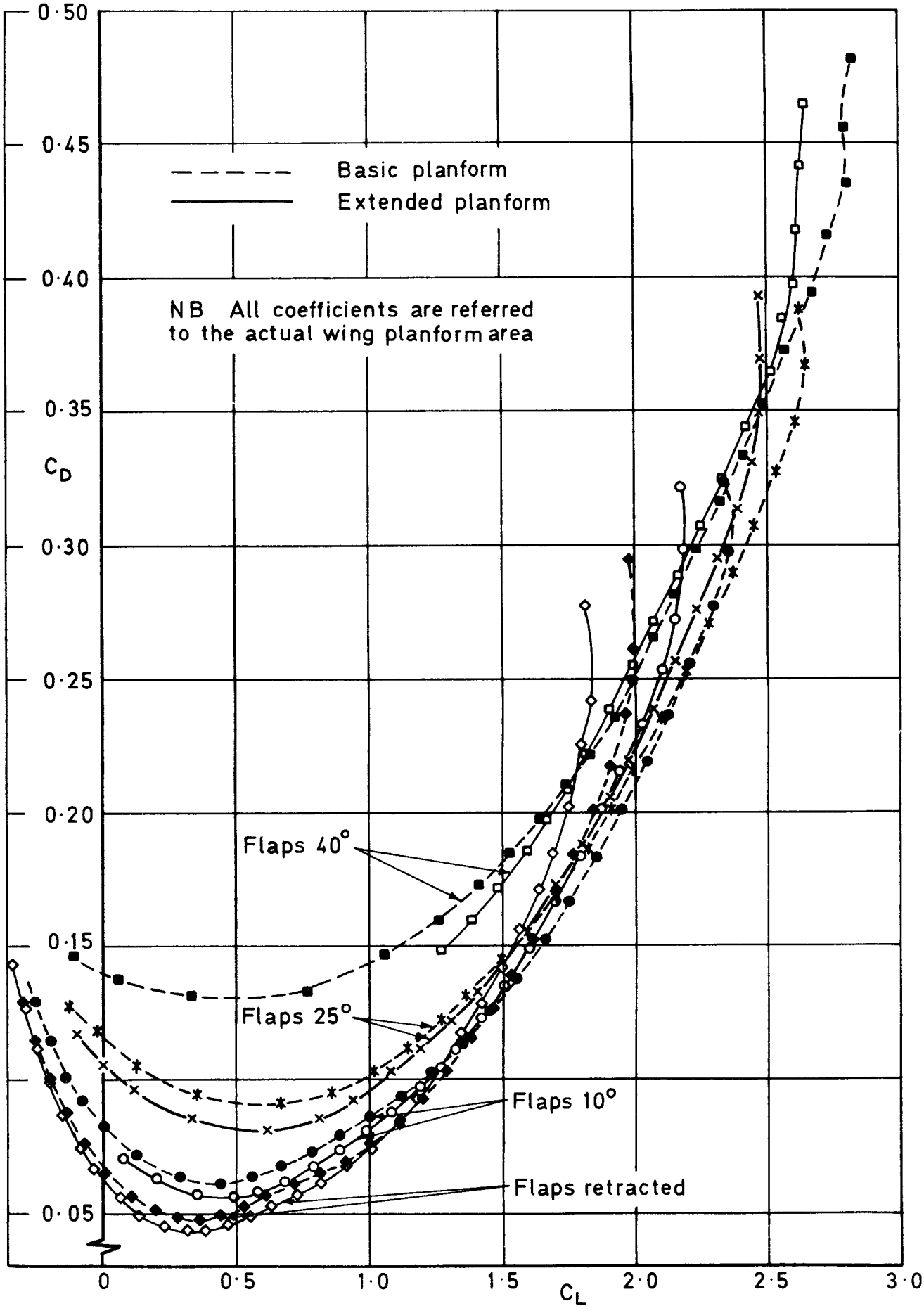

Fig. 89 Comparison of planforms, wing + body.
Slats deflected 25°, C_D vs C_L

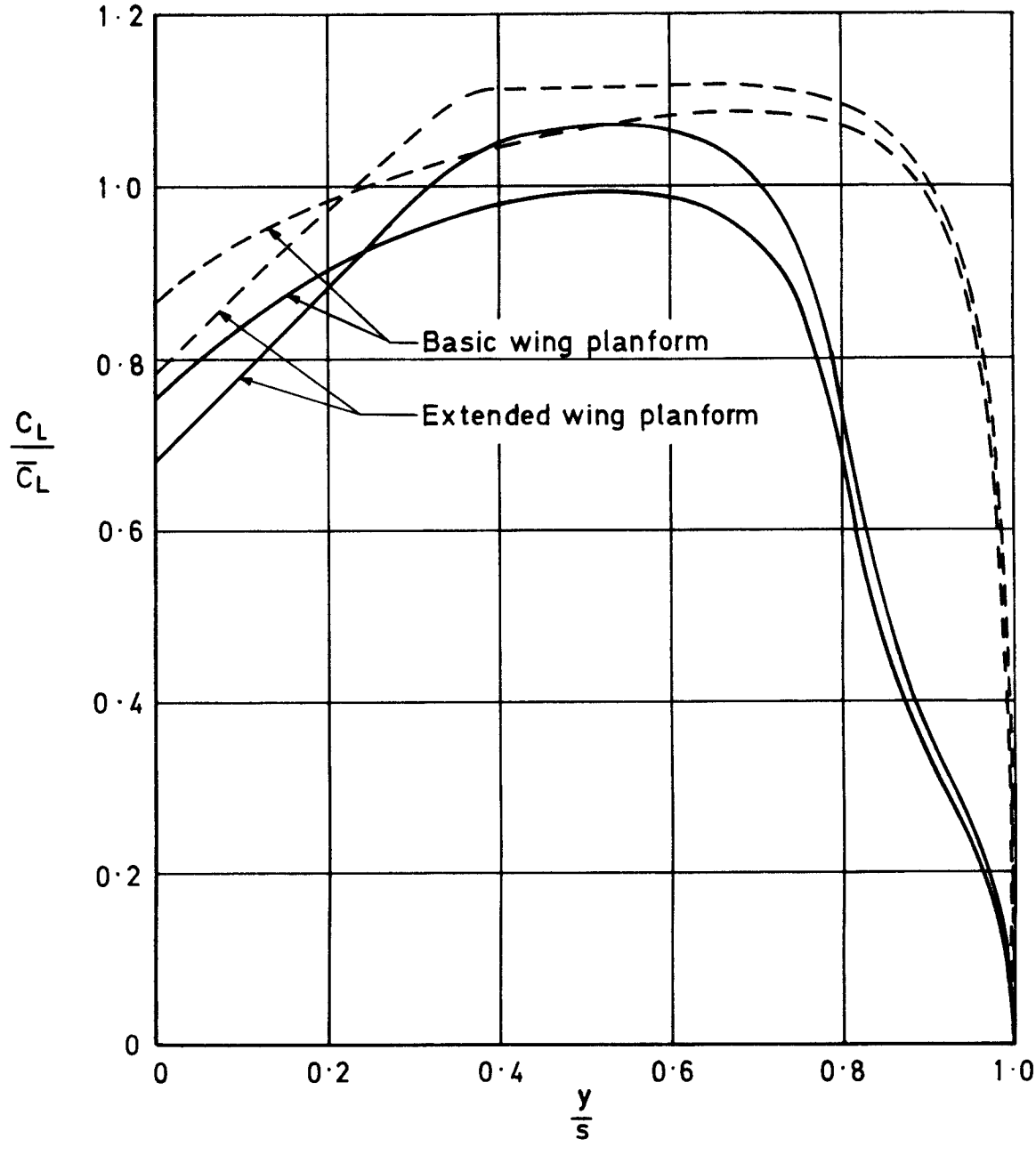

----- Slats and flaps retracted, $\alpha_W = 10^\circ$

——— Slats deflected 25°, flaps deflected 25°, $\frac{y_F}{s} = 0{\cdot}8$, $\alpha_W = 0^\circ$

Fig. 90 Effect of planform modification on the spanwise loading. Linear theory calculation

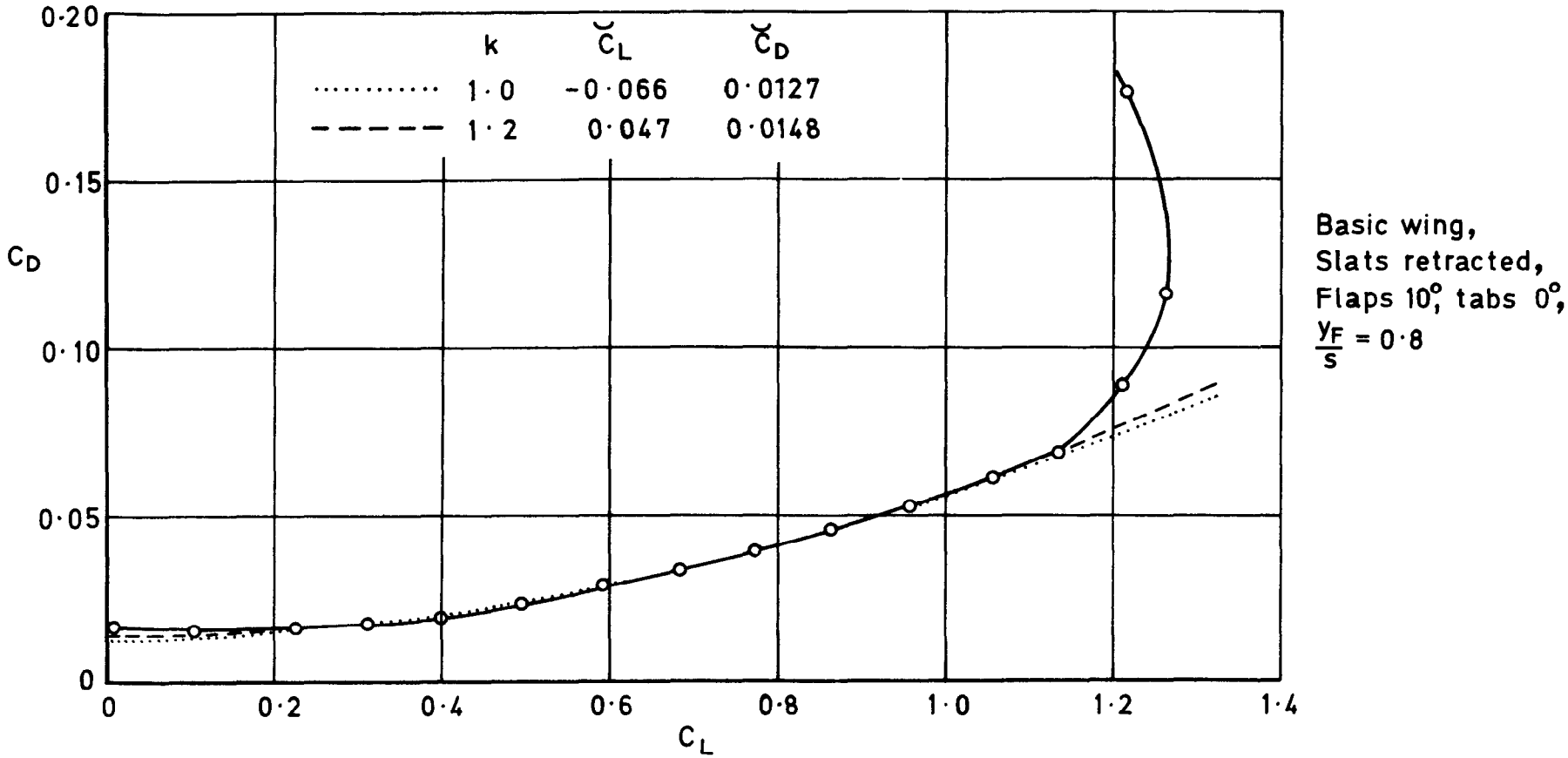

Fig.91 Example of the method of drag analysis, Slats retracted

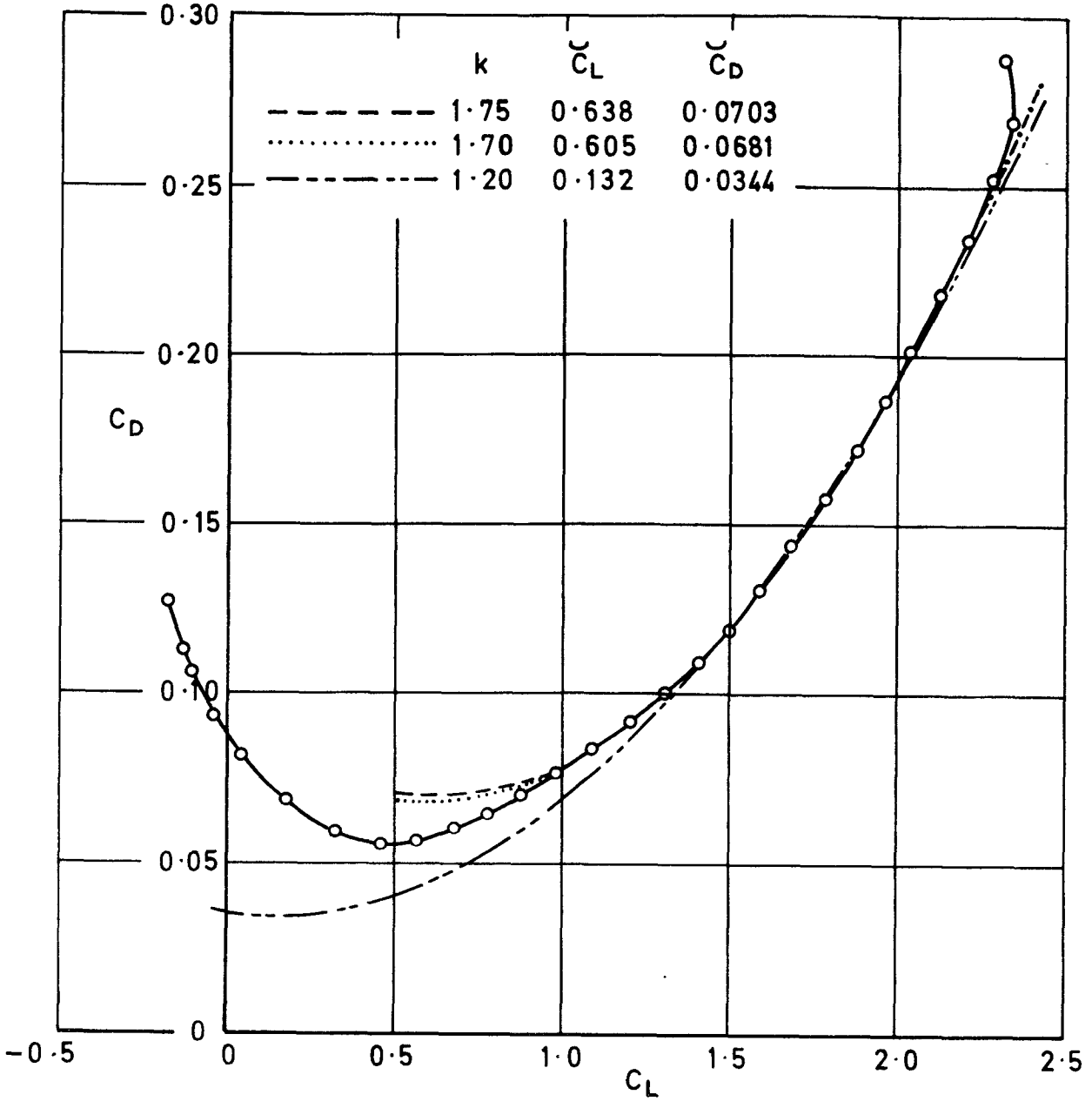

Basic wing,
Slats deflected 25°,
Flaps 10°, tabs 0°, $\frac{y_F}{s} = 0·8$

Fig.92 Example of the method of drag analysis. Slats deflected 25°

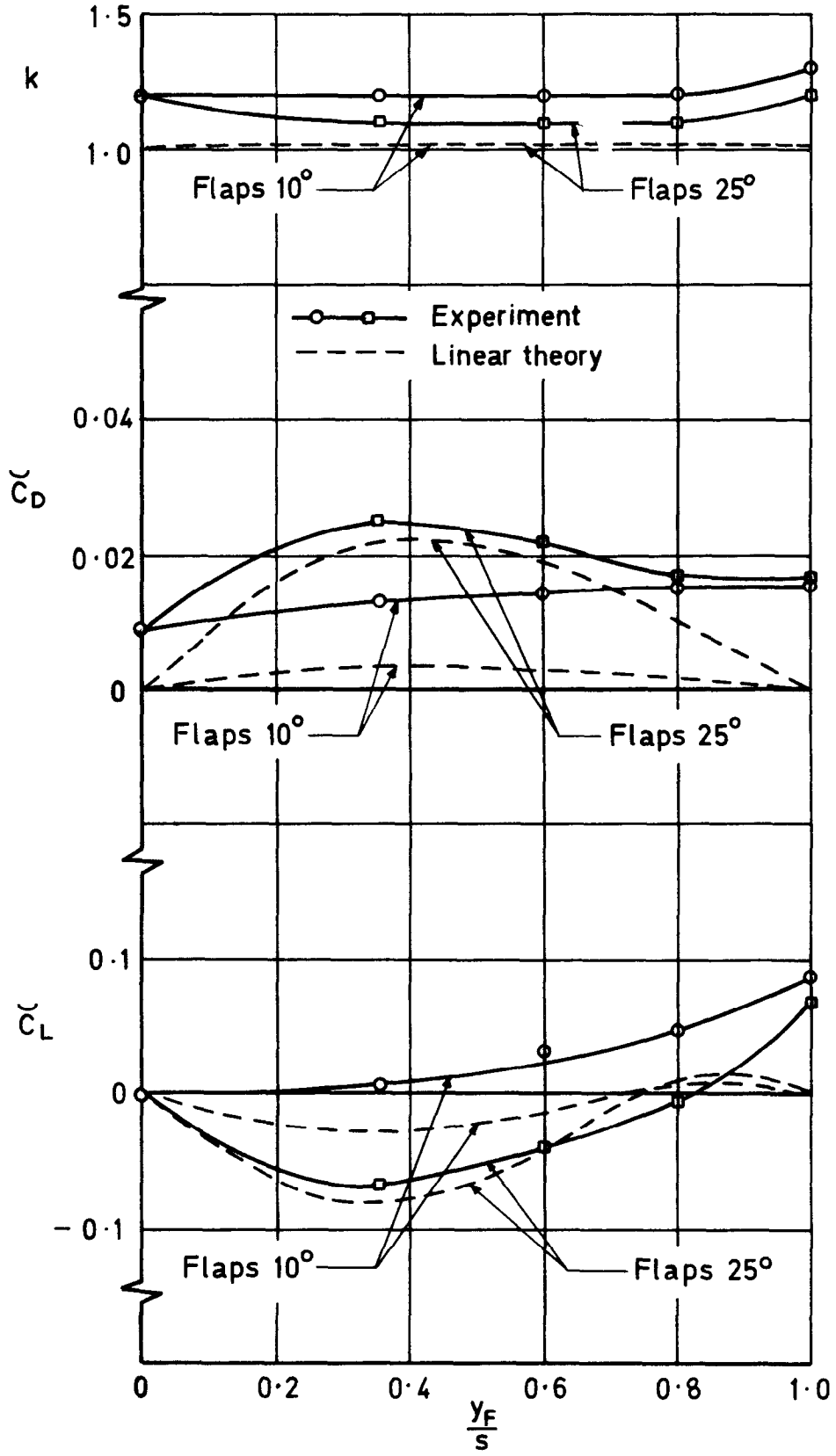

Fig. 93 Drag analysis for the basic wing with slats retracted

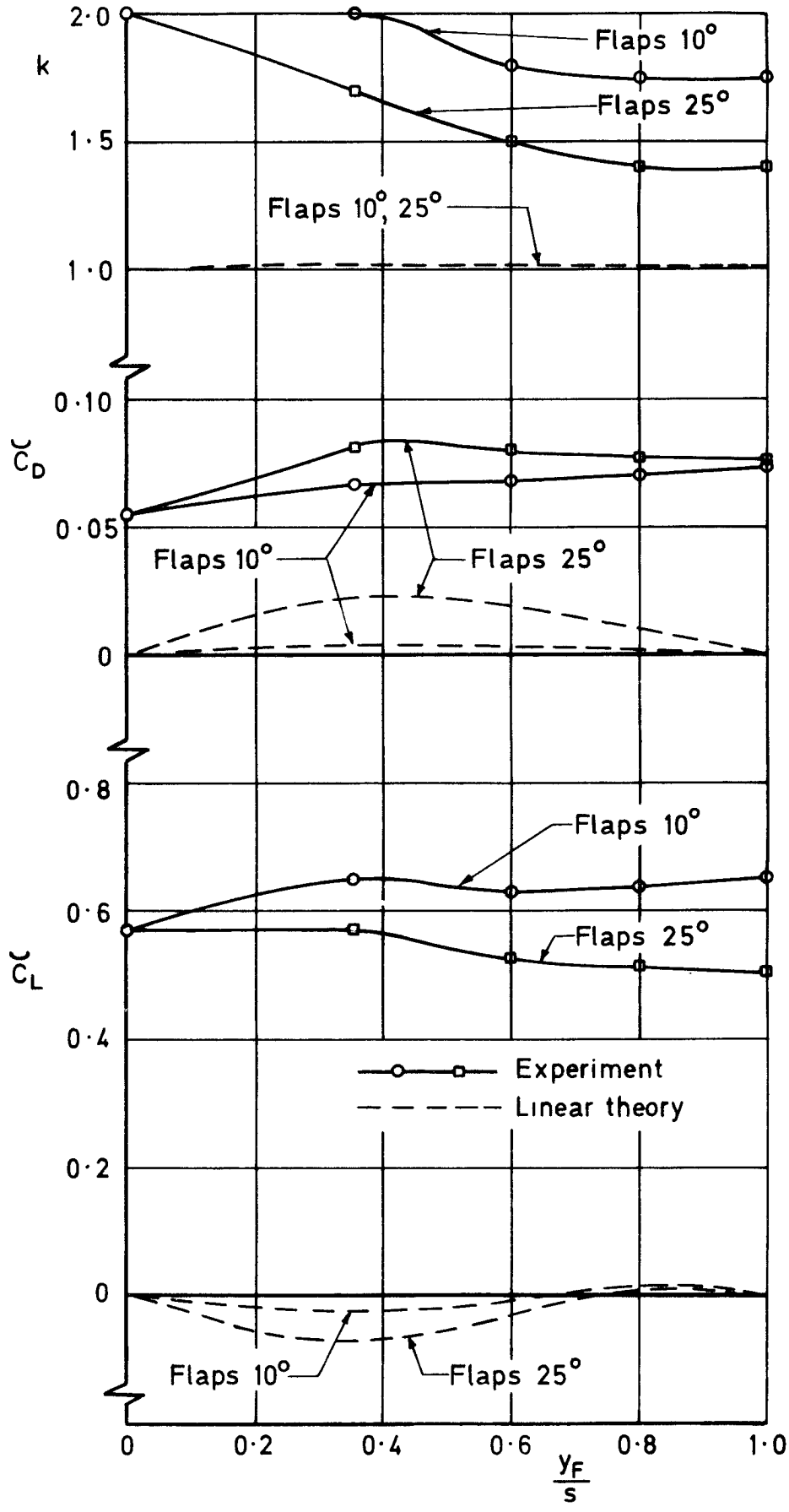

Fig. 94 Drag analysis for the basic wing with slats deflected 25°

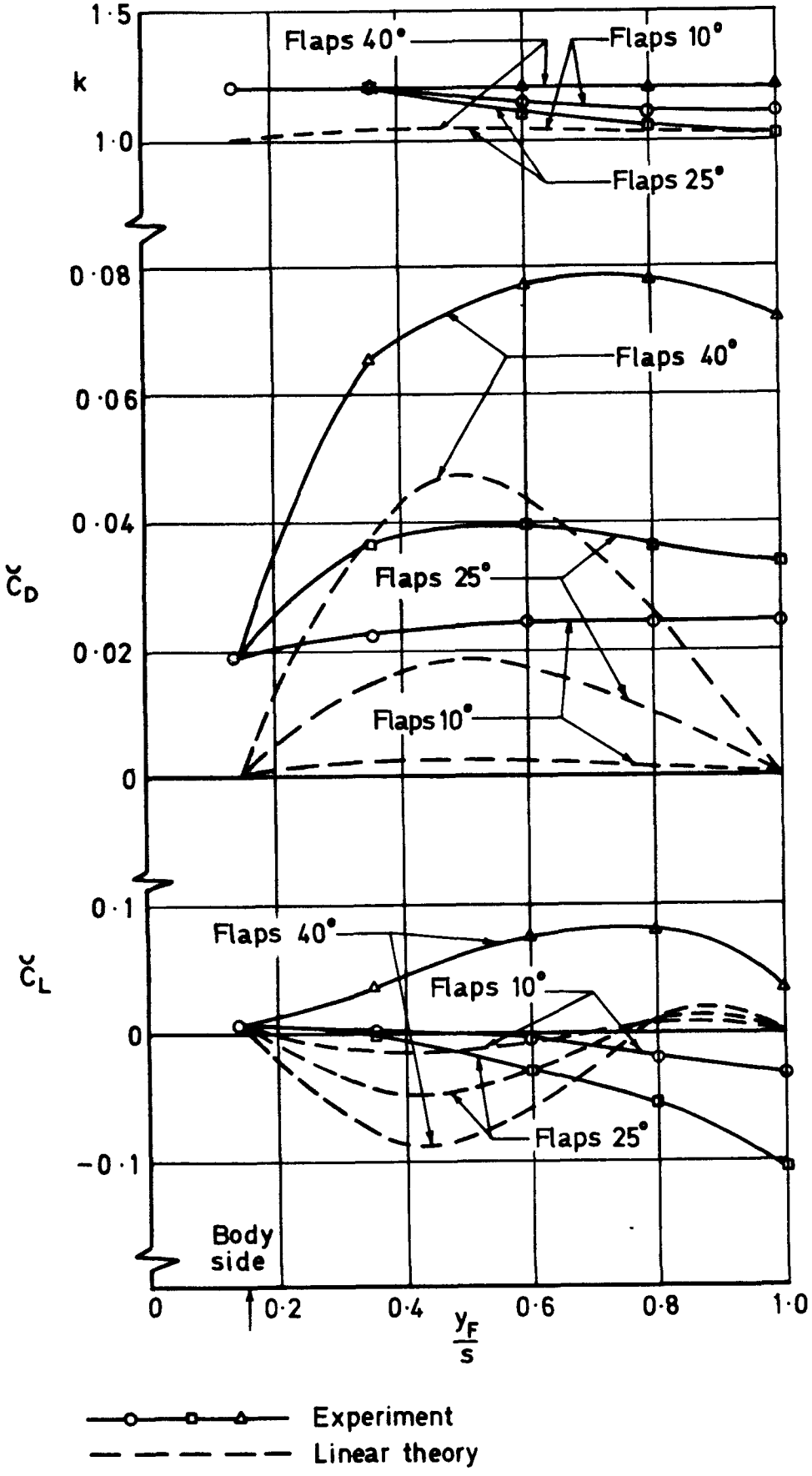

Fig. 95 Drag analysis for the basic wing + body, slats retracted

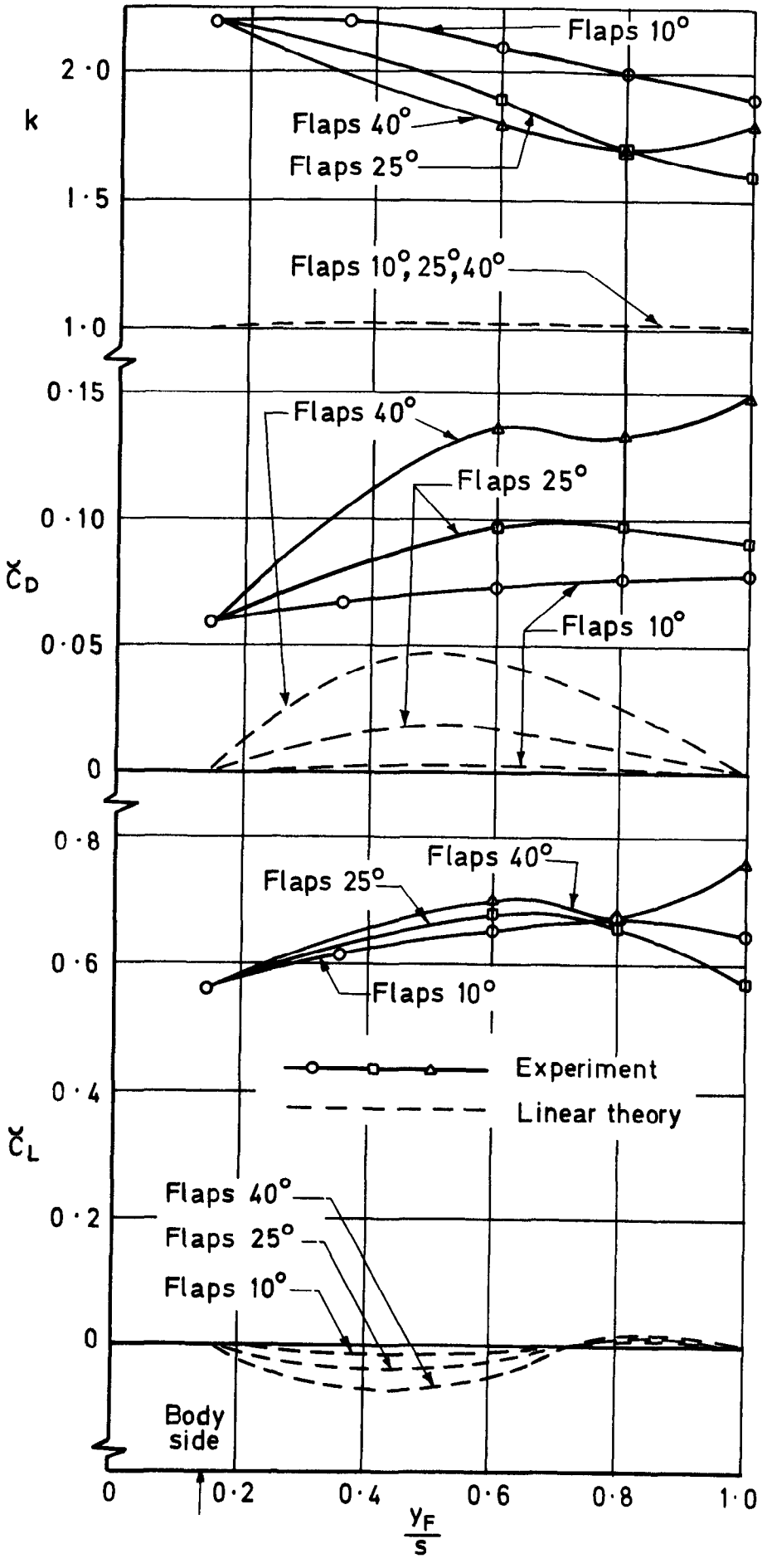

Fig. 96 Drag analysis for the basic wing + body, slats deflected 25°

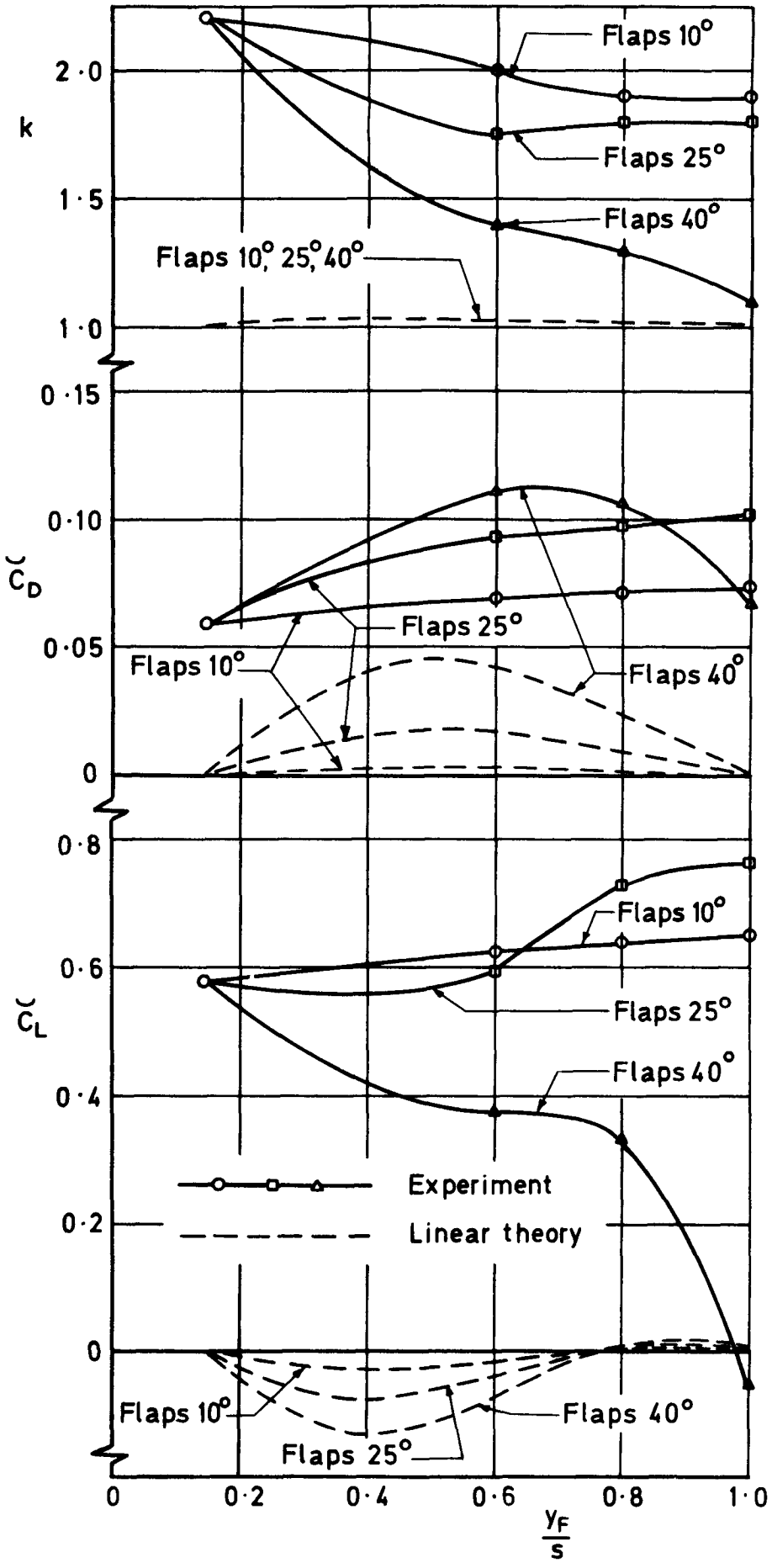

Fig.97 Drag analysis for the extended wing + body, slats deflected 25°

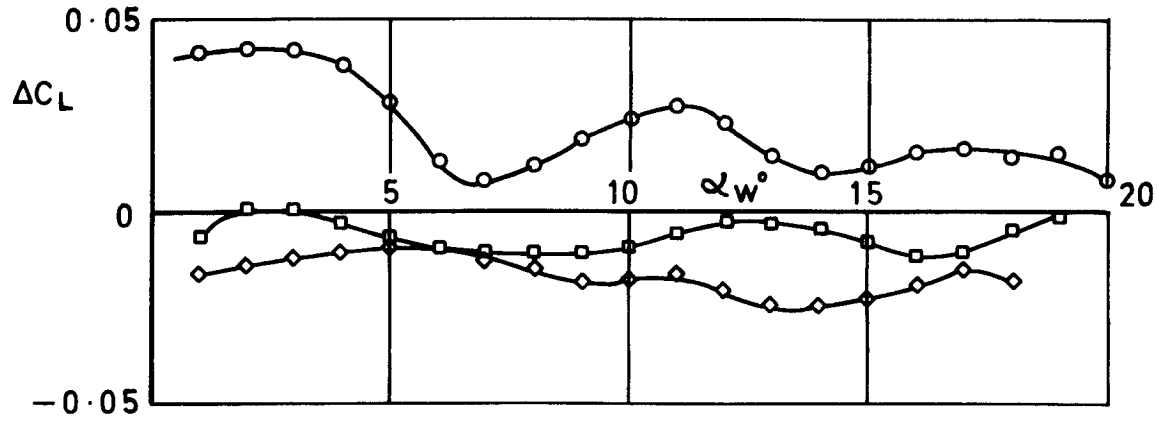

a Lift increment

Flaps 10° ○
Flaps 25° □
Flaps 40° ◇

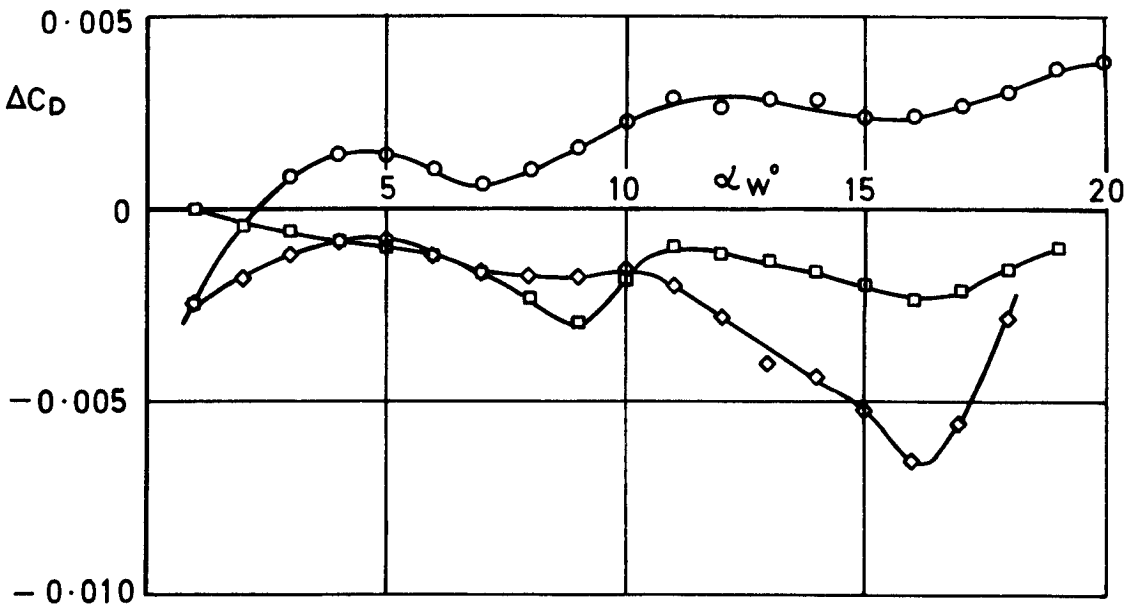

b Drag increment

Fig.98 a & b Effect of an additional flap bracket at $\frac{y}{s} = 0{\cdot}237$
Extended wing + body, slats deflected 25°, $\frac{y_F}{s} = 0{\cdot}8$

	$\Delta\alpha_w^\circ$ derived from	
	C_L vs α_w°	C_D vs α_w°
Flaps 10°	○	●
Flaps 25°	□	■
Flaps 40°	◇	◆

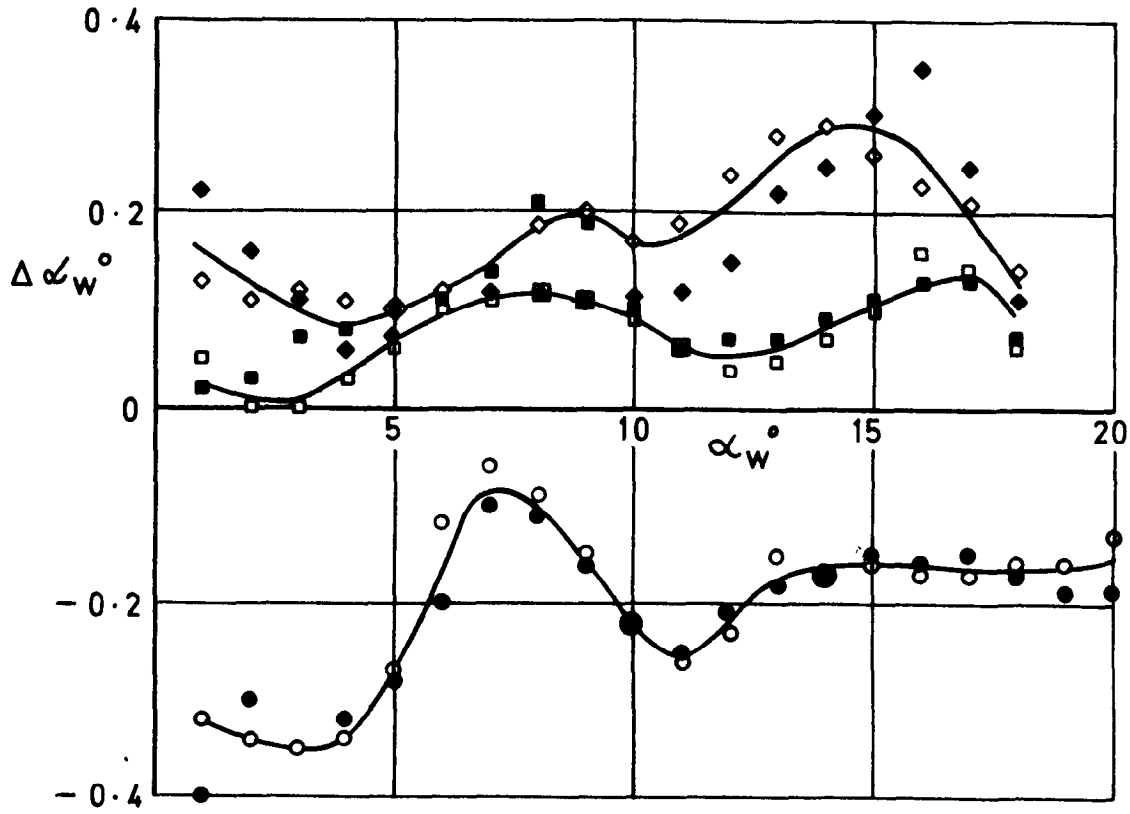

$\Delta\alpha_w^\circ$ = Effective increase of angle of incidence required to collapse the lift and drag curves when the extra flap bracket is added

Fig.99 Effective increase in wing incidence required when the extra flap bracket is added

Printed in England for Her Majesty's Stationery Office by the Royal Aircraft Establishment, Farnborough. Dd. 290279 K5 3/77.

ARC CP No.1372
March 1976

Lovell, D. A.

A WIND-TUNNEL INVESTIGATION OF THE EFFECTS OF FLAP SPAN AND DEFLECTION ANGLE, WING PLANFORM AND A BODY ON THE HIGH-LIFT PERFORMANCE OF A 28° SWEPT WING

533.693.1 :
533.695.12 :
533.694.2 :
533.6.013.13 :
533.6.013.644
533.6.013.66

Lift, drag and pitching moment have been measured over an extensive range of configurations of the high-lift system on a wing of basic aspect ratio 8.35 and with a trailing-edge planform extension and a body added The results were analysed and compared with two linear-theory prediction methods. The measured increments in lift generated by the various elements of the high-lift system were lower than the predicted levels. An exploratory analysis of the drag results showed that the lift-dependent drag factor was considerably underestimated by linear theory, particularly when the slat was deployed. The limitations of the planar vortex sheet used in the theory and the neglect of viscous effects are suggested as the principal reasons for the differences between experiment and theory.

(Over)

ARC CP No.1372
March 1976

Lovell, D. A.

A WIND-TUNNEL INVESTIGATION OF THE EFFECTS OF FLAP SPAN AND DEFLECTION ANGLE, WING PLANFORM AND A BODY ON THE HIGH-LIFT PERFORMANCE OF A 28° SWEPT WING

533.693.1 .
533.695.12 :
533.694.2 :
533.6.013.13 :
533.6.013.644
533.6.013.66

Lift, drag and pitching moment have been measured over an extensive range of configurations of the high-lift system on a wing of basic aspect ratio 8.35 and with a trailing-edge planform extension and a body added. The results were analysed and compared with two linear-theory prediction methods. The measured increments in lift generated by the various elements of the high-lift system were lower than the predicted levels. An exploratory analysis of the drag results showed that the lift-dependent drag factor was considerably underestimated by linear theory, particularly when the slat was deployed. The limitations of the planar vortex sheet used in the theory and the neglect of viscous effects are suggested as the principal reasons for the differences between experiment and theory.

(Over)

Cut here

ARC CP No.1372
March 1976

Lovell, D A

A WIND-TUNNEL INVESTIGATION OF THE EFFECTS OF FLAP SPAN AND DEFLECTION ANGLE, WING PLANFORM AND A BODY ON THE HIGH-LIFT PERFORMANCE OF A 28° SWEPT WING

533.693.1 :
533.695.12 :
533.694.2 :
533.6.013.13 :
533.6.013.644 :
533.6.013.66

Lift, drag and pitching moment have been measured over an extensive range of configurations of the high-lift system on a wing of basic aspect ratio 8.35 and with a trailing-edge planform extension and a body added. The results were analysed and compared with two linear-theory prediction methods. The measured increments in lift generated by the various elements of the high-lift system were lower than the predicted levels. An exploratory analysis of the drag results showed that the lift-dependent drag factor was considerably underestimated by linear theory, particularly when the slat was deployed. The limitations of the planar vortex sheet used in the theory and the neglect of viscous effects are suggested as the principal reasons for the differences between experiment and theory

(Over)

ARC CP No.1372
March 1976

Lovell, D A.

A WIND-TUNNEL INVESTIGATION OF THE EFFECTS OF FLAP SPAN AND DEFLECTION ANGLE, WING PLANFORM AND A BODY ON THE HIGH-LIFT PERFORMANCE OF A 28° SWEPT WING

533.693.1 .
533.695.12 :
533.694.2 :
533.6.013.13 :
533.6.013.644 :
533.6.013.66

Lift, drag and pitching moment have been measured over an extensive range of configurations of the high-lift system on a wing of basic aspect ratio 8.35 and with a trailing-edge planform extension and a body added. The results were analysed and compared with two linear-theory prediction methods. The measured increments in lift generated by the various elements of the high-lift system were lower than the predicted levels. An exploratory analysis of the drag results showed that the lift-dependent drag factor was considerably underestimated by linear theory, particularly when the slat was deployed. The limitations of the planar vortex sheet used in the theory and the neglect of viscous effects are suggested as the principal reasons for the differences between experiment and theory.

(Over)

Cut here

DETACHABLE ABSTRACT CARDS

DETACHABLE ABSTRACT CARDS

Deflection of the flap produced a load, which acted at a distance forward of the mean quarter chord of the flap, that was practically independent of incidence and flap span. The wing/body interference effect was insensitive to flap span and there was some evidence of a download being generated on the rear body when the high-lift system was deployed. The performance of the high-lift system was downgraded when the wing planform was extended in the root region and this was attributed to the greater non-uniformity of the spanwise loading.

Deflection of the flap produced a load, which acted at a distance forward of the mean quarter chord of the flap, that was practically independent of incidence and flap span. The wing/body interference effect was insensitive to flap span and there was some evidence of a download being generated on the rear body when the high-lift system was deployed. The performance of the high-lift system was downgraded when the wing planform was extended in the root region and this was attributed to the greater non-uniformity of the spanwise loading.

Deflection of the flap produced a load, which acted at a distance forward of the mean quarter chord of the flap, that was practically independent of incidence and flap span. The wing/body interference effect was insensitive to flap span and there was some evidence of a download being generated on the rear body when the high-lift system was deployed. The performance of the high-lift system was downgraded when the wing planform was extended in the root region and this was attributed to the greater non-uniformity of the spanwise loading.

Deflection of the flap produced a load, which acted at a distance forward of the mean quarter chord of the flap, that was practically independent of incidence and flap span. The wing/body interference effect was insensitive to flap span and there was some evidence of a download being generated on the rear body when the high-lift system was deployed. The performance of the high-lift system was downgraded when the wing planform was extended in the root region and this was attributed to the greater non-uniformity of the spanwise loading.

DETACHABLE ABSTRACT CARDS

DETACHABLE ABSTRACT CARDS

© *Crown copyright*

1977

Published by
HER MAJESTY'S STATIONERY OFFICE

Government Bookshops
49 High Holborn, London WC1V 6HB
13a Castle Street, Edinburgh EH2 3AR
41 The Hayes, Cardiff CF1 1JW
Brazennose Street, Manchester M60 8AS
Southey House, Wine Street, Bristol BS1 2BQ
258 Broad Street, Birmingham B1 2HE
80 Chichester Street, Belfast BT1 4JY
Government Publications are also available through booksellers

C.P. No. 1372

ISBN 011 471118 6